EXPERIMENTAL AND COMPUTATIONAL STUDIES OF CORROSION IN HIBITION POTENTIAL OF SELECTED PLANT EXTRACTS ON CORROSION OF MILD STEEL AND ALUMINIUM IN ACID MEDIUM

BY

FEMI EMMANUEL AWE

DEPARTMENT OF CHEMISTRY,
FACULTY OF SCIENCE,
AHMADU BELLO UNIVERSITY,
ZARIA, NIGERIA

NOVEMBER, 2015

EXPERIMENTAL AND COMPUTATIONAL STUDIES OF CORROSION IN HIBITION POTENTIAL OF SELECTED PLANT EXTRACTS ON CORROSION OF MILD STEEL AND ALUMINIUM IN ACID MEDIUM

BY

Femi Emmanuel AWE
B.Sc. (Hons) M.Sc. (ABU)
Ph.D / SCIEN / 35066 / 2012-2013

A THESIS SUBMITTED TO THE SCHOOL OF POSTGRADUATE STUDIES, AHMADU BELLO UNIVERSITY, ZARIA.

IN PARTIAL FULFILLMENT OF THE REQUIREMENTS FOR THE AWARD OF DOCTOR OF PHILOSOPHY IN PHYSICAL CHEMISTRY

DEPARTMENT OF CHEMISTRY,
FACULTY OF SCIENCE,
AHMADU BELLO UNIVERSITY,
ZARIA, NIGERIA

NOVEMBER, 2015

Declaration

I declare that the work in this thesis entitled **'**EXPERIMENTAL AND COMPUTATIONAL STUDIES OF CORROSION INHIBITION POTENTIAL OF SELECTED PLANT EXTRACTS ON CORROSION OF MILD STEEL AND ALUMINIUM IN ACID MEDIUM**'** was performed by me in the Department of Chemistry, under the supervision of Dr. S. O. Idris, Dr. M. Abdulwahab and Prof. E. E. Oguzie. The information derived from the literature has been duly acknowledged in the text and a list of references provided. No part of this thesis has been previously presented for another Degree or Diploma in any Institution.

Femi Emmanuel AWE ---------- ----------

Signature Date

Certification

This thesis entitled **'EXPERIMENTAL AND COMPUTATIONAL STUDIES OF CORROSION INHIBITION POTENTIAL OF SELECTED PLANT EXTRACTS ON CORROSION OF MILD STEEL AND ALUMINIUM IN ACID MEDIUM'** by Femi Emmanuel AWE, meets the regulations governing the award of Doctor of Philosophy (PhD) in Physical Chemistry of Ahmadu Bello University, and is approved for its contribution to knowledge and literary presentation.

Dr. S. O. Idris Chairman, Supervisory Committee	Signature	Date
Dr. M. Abdulwahab Member, Supervisory Committee	Signature	Date
Prof. E. E. Oguzie Member, Supervisory Committee	Signature	Date
Prof. V. O. Ajibola Head of Department	Signature	Date
Prof. K. Bala Dean, School of Postgraduate Studies	Signature	Date

Dedication

This work is dedicated to Jehovah, Jesus Christ the author and finisher of my faith. “And now shall mine head be lifted up above mine enemies round about me: therefore will I offer in his tabernacle sacrifices of joy; I will sing, yea, I will sing praises unto the Lord”. Ps 27:5

Acknowledgements

My utmost appreciation goes to the Almighty God, the Father of all flesh and spirits for uncommon favour, grace, strength and divine supplies in the course of this research.

I am most grateful to my supervisors, Dr. S. O. Idris and Dr. M. Abdulwahab, of Department of Chemistry and Department of Metallurgical and Materials Engineering, Ahmadu Bello University Zaria respectively as well as Prof. E.E. Oguzie of the Department of Chemistry (Electrochemistry and Material Science Research Unit), Federal University of Technology (FUTO), Owerri, for their guidance and effective supervision. I acknowledge the support of the Chief Technologists viz: Dr. (Mrs) O. R. A. Iyun and Mr. C. A. Ochigbo a Senior Technologist and the other members of staff of the Department of Chemistry, Ahmadu Bello University Zaria.

I am much indebted to Prof. G. I. Ndukwe, Prof. C. E. Gimba, and Dr O. J. Okunola, for their valuable advice and suggestions. I sincerely want to appreciate my lovely and wonderful wife, Mrs. Oluwatoyin Awe, for her understanding throughout my studies. To my brother Michael Awe, I must also say big thank you for your support throughout my studies. I also like to thank Mr. D. Zang for his valuable contribution and Mr. Y. Suleiman of Mechanical Engineering workshop is specially acknowledged for cutting the metal sheets into coupons.

My special gratitude goes to the Tertiary Educational Trust Fund (TETFUND), Federal University Dutsin-ma for providing financial support for this work. I am indebted to my colleaques in the Department of Applied Chemistry, Federal University Dutsin-ma for holding the fort while I was on study leave. I am grateful to the Dean Faculty of Science and Education, Prof. J. A. Fatokun and the Head of Department Applied Chemistry, Prof. E. J. Ekanem for their valuable advice and support. I wish to thank my spiritual Father Sup. Evang. I. P. Lawal for his prayers during the course of my program. To my relatives, friends and well-wishers too many to mention, I am grateful and may God bless them.

Abstract

In this thesis, the ethanol extracts of some plant namely: *Phyllanthus amarus* (PA)*; Paullina pinnata* (PP)*; Parinari polyandra* (PP1)*; and Boscia senegalensis* (BS) were investigated for their corrosion inhibition potential on mild steel and aluminium in HCl (1.0 M) and H_2SO_4 (0.5 M) respectively using gravimetric and linear polarization methods. The influence of extract concentrations (0.1g/l to 0.5g/l) and temperatures (303K to 323K) on corrosion and corrosion inhibition was assessed. The results obtained showed that PP, PA, BS and PP1 decreased the corrosion rate of mild steel and aluminium in the acid media. The rate generally decreased with increasing extract concentration in the order: PP> PP1> BS> PA and PP> BS> PP1> PA in HCl and H_2SO_4 respectively for aluminium; PP> PA> PP1> BS and BS> PP> PP1> PA in HCl and H_2SO_4 respectively for mild steel at 303 K. The corresponding maximum inhibition efficiencies were 73.55% and 40.00% for aluminium in HCl and H_2SO_4 respectively and 83.52% and 80.29% for mild steel. Inhibition efficiency in all the systems decreased with rise in temperature, suggesting physical adsorption of the extract constituents on the metal surfaces. Scanning electron microscopy (SEM) and infra-red (FTIR) spectroscopy analyses of the metal surfaces in the presence and absence of the inhibitors confirmed the presence of adsorbed protective layers. Linear polarization studies showed that the plant extracts suppressed both the anodic and cathodic half reactions of the corrosion processes, thereby acting as mixed-type inhibitors. Langmuir isotherm was found to be the best in describing the adsorption behaviour of the extract on the surfaces of mild steel and aluminium at room temperature, whereas the adsorption property at elevated temperature was best described by the Freundlich isotherm. Calculated values of free energy of adsorption, ΔG_{ads}^{o}, on mild steel in the presence of PP, PA, BS and PP1 are as follows: -9.93 to -10.31 kJ mol^{-1} and -8.31 to -10.73 kJ mol^{-1} in HCl at 303 and 333K respectively, and -9.39 to -10.32 kJ mol^{-1} and -7.68 to -13.58 kJ mol^{-1} in H_2SO_4 at 303 and 333K respectively. The calculated ΔG_{ads}^{o} values for the corrosion of aluminium in the presence of PP, PA, BS and PP1 follows the order: -9.01 to -9.53 kJ mol^{-1} and -7.91 to -9.58 kJ mol^{-1} in HCl at 303 and 333K respectively. Corrosion activation energy (E_a) values for mild steel and aluminium in the acids solutions increased in the presence of the inhibitor and the values were found to be less than 80kJmol^{-1} supporting the proposed physiosorption of the extract constituents. Density functional theory (DFT) based molecular dynamics simulations were adopted to theoretically describe the interactions of selected extract constituents with the metal surfaces. The computed binding energy values ($E_{binding}$) for the various constituent indicate the adsorption process to be non-covalent (physiosorption).

TABLE OF CONTENT **Page**

Title page ii

Declaration iii

Certification iv

Dedication v

Acknowledgements vi

Abstract vii

Table of Contents viii

List of Figures xiii

List of Plates xix

List of Tables xx

List of Appendices xxii

Abbreviations and Symbols xxiv

CHAPTER ONE

1.0 INTRODUCTION 1

1.1 Justification of Study 3

1.2 Aim and Objectives 4

CHAPTER TWO

2.0 LITERATURE REVIEW 6

2.1 Corrosion 6

2.2 Forms of Corrosion 8

2.2.1 Uniform corrosion 8

2.2.2 Galvanic corrosion 9

2.2.3 Pitting corrosion 10

2.2.4 Crevice corrosion 11

2.2.5 Intergranular corrosion 11

2.2.6 Erosion corrosion 11

2.2.7 Cavitation corrosion 12

2.2.8 Fretting corrosion 12

2.3 Corrosion Monitoring Techniques 12

2.3.1 Gravimetric technique 13

2.3.2 Gasometric technique 14

2.3.3 Thermometric technique 14

2.3.4 Potentiodynamic polarization techniques 15

2.3.5 Linear polarization resistance 15

2.3.6 Electrochemical noise 15

2.3.7 Electrochemical impedance spectroscopy 16

2.3.8 Galvanic monitoring 16

2.4 Common Methods of Corrosion Prevention 17

2.4.1 Selection of materials and design against corrosion 18

2.4.2 Protective coatings 18

2.4.3 Cathodic protection 19

2.4.4 Anodic protection 19

2.4.5 Chemical inhibition 19

2.5 Inhibition of Corrosion 19

2.5.1 Interphase inhibitors 20

2.5.2 Passivating or oxidizing inhibitors 21

2.5.3 Non-oxidizing inhibitors 21

2.5.4 Interface inhibitions 21

2.6 Adsorption Isotherms 22

2.6.1 Langmuir adsorption isotherm 23

2.6.2 Freundlich isotherm 23

2.6.3 Temkin adsorption isotherm 24

2.6.4 Flory-Huggins adsorption isotherm 24

2.6.5 El-Awady adsorption isotherm 24

2.6.6 Frumkin adsorption isotherm 25

2.7 Corrosion Inhibitors 26

2.8 Green Corrosion Inhibitors 26

2.8.1 Green corrosion inhibitors: Plant extract 27

2.8.2 Green corrosion inhibitors: Amino acids 33

2.8.3 Triazoles and benzotriazoles derivativesas corrosion inhibitors 38

2.8.4 Dyes as corrosion inhibitors 40

2.8.5 Schiff bases as corrosion inhibitors 41

CHAPTER THREE

3.0 EXPERIMENTAL 43

3.1 Materials 43

3.2 Methods 44

3.2.1 Plant extraction 44

3.2.2 Chemical analysis 44

3.2.3 Gravimetric method 45

3.2.4 Fourier transform infrared spectrophotometry 47

3.2.5 Scanning electron microscopy 47

3.2.6 Linear polarisation resistance 48

3.3 Computational and Theoretical Consideration 49

3.3.1 Quantum chemical calculations 49

3.3.2 Molecular dynamics simulation 49

CHAPTER FOUR

4.0 RESULTS 51

4.1 Phytochemical Screening and Gas Chromatography Mass Spectrophotometry of the Plants Extract 51

4.2 Weight loss Measurement of Plant Extracts on the Corrosion of Mild steel and Aluminium 51

4.3 Effect of Temperature 68

4.4 Thermodynamic/adsorption Study 98

4.5 Electrochemical Measurement 98

4.6 Infrared Spectroscopic Study 137

4.7 Scanning Electron Microscopy Study 137

4.8 Computational and Theoretical Modelling 161

4.8.1 Quantum chemical calculations 161

4.8.2 Molecular dynamics 168

CHAPTER FIVE

5.0 DISCUSSION 179

5.1 Gas Chromatography – Mass Spectra Analysis 179

5.2 Corrosion Studies 180

5.2.1 Effect of concentration of extracts on the corrosion of mild steel and aluminium 180

5.2.2 Effect of temperature 183

5.2.3 Thermodynamic or adsorption study 185

5.3 Infrared Spectroscopic Study 188

5.4 Scanning Electron Microscopy Study 192

5.5 Linear Polarization Measurement 193

5.6 Computational and Theoretical Modelling 195

5.6.1 Quantum chemical calculations 195

5.6.2 Molecular dynamics simulations 196

CHAPTER SIX

6.0 SUMMARY, CONCLUSIONS AND RECOMMENDATIONS 198

6.1 Summary 198

6.2 Conclusions 199

6.3 Recommendations 200

REFERENCES 202

APPENDICES 217

List of Figures

Figure(s) **Page**

4.1 Variation of Weight loss with Time for Aluminium in 1.0 M HCl Containing Various Concentration of PP at 303K 60

4.2. Variation of Weight loss with Time for Aluminium in 1.0 M HCl Containing Various Concentration of PA at 303K 61

4.3. Variation of Weight loss with Time for Aluminium in 1.0 M HCl Containing Various Concentration of BS at 303K 62

4.4. Variation of Weight loss with Time for Aluminium in 1.0 M HCl Containing Various Concentration of PP1 at 303K 63

4.5. Variation of Weight loss with Time for Mild Steel in 1.0 M HCl Containing Various Concentration of PP at 303K 64

4.6. Variation of Weight loss with Time for Mild Steel in 1.0 M HCl Containing Various Concentration of PA at 303K 65

4.7. Variation of Weight loss with Time for Mild Steel in 1.0 M HCl Containing Various Concentration of BS at 303K 66

4.8. Variation of Weight loss with Time for Mild Steel in 1.0 M HCl Containing Various Concentration of PP1 at 303K 67

4.9. Variation of Weight loss with Time for Mild Steel in 0.5 M H_2SO_4 Containing Various Concentration of PP at 303K 69

4.10. Variation of Weight loss with Time for Mild Steel in 0.5 M H_2SO_4 Containing Various Concentration of PA at 303K 70

4.11. Variation of Weight loss with Time for Mild Steel in 0.5 M H_2SO_4 Containing Various Concentration of BS at 303K 71

4.12. Variation of Weight loss with Time for Mild Steel in 0.5 M H_2SO_4 Containing Various Concentration of PP1 at 303K 72

4.13. Variation of log (Corrosion Rate) with Inverse of Temperature for Aluminium in 1.0 M HCl Containing Various Concentration of (a) PP (b) PA 77

4.14. Variation of log (Corrosion Rate) with Inverse of Temperature for Aluminium in 1.0 M HCl Containing Various Concentration of (a) BS (b) PP1 78

4.15. Variation of log (Corrosion Rate) with Inverse of Temperature for Aluminium

in1.0 M HCl Containing Various Concentration of (a) PP (b) PA 79

4.16. Variation of log (Corrosion Rate) with Inverse of Temperature for Aluminium in1.0 M HCl Containing Various Concentration of (a) BS (b) PP1 80

4.17. Variation of log (Corrosion Rate) with Inverse of Temperature for Aluminium in 0.5 M H_2SO_4 Containing Various Concentration of (a) PP (b) PA 81

4.18. Variation of log (Corrosion Rate) with Inverse of Temperature for Aluminium in 0.5 M H_2SO_4 Containing Various Concentration of (a) BS (b) PP1 82

4.19. Variation of log (Corrosion Rate) with Inverse of Temperature for Mild Steel in 0.5 M H_2SO_4 Containing Various Concentration of (a) PP (b) PA 83

4.20. Variation of log (Corrosion Rate) with Inverse of Temperature for Mild Steel in 0.5 M H_2SO_4 Containing Various Concentration of (a) BS (b) PP1 84

4.21. Variation of log CR/T with Inverse of Temperature for Aluminium in 1.0 M HCl Containing Various Concentration of (a) PP (b) PA 88

4.22. Variation of log CR/T with Inverse of Temperature for Aluminium in 1.0 M HCl Containing Various Concentration of (a) BS (b) PP1 89

4.23. Variation of log CR/T with Inverse of Temperature for Mild Steel in 1.0 M HCl Containing Various Concentration of (a) PP (b) PA 90

4.24. Variation of log CR/T with Inverse of Temperature for Mild Steel in 1.0 M HCl Containing Various Concentration of (a) BS (b) PP1 91

4.25. Variation of log CR/T with Inverse of Temperature for Aluminium in 0.5 M H_2SO_4 Containing Various Concentration of (a) PP (b) PA 92

4.26. Variation of log CR/T with Inverse of Temperature for Aluminium in 0.5 M H_2SO_4 Containing Various Concentration of (a) BS (b) PP1 93

4.27. Variation of log CR/T with Inverse of Temperature for Mild Steel in 0.5 M H_2SO_4 Containing Various Concentration of (a) PP (b) PA 94

4.28. Variation of log CR/T with Inverse of Temperature for Aluminium in 0.5 M H_2SO_4 Containing Various Concentration of (a) BS (b) PP1 95

4.29. Langmuir Isotherm for PP Adsorption on Mild Steel Surface in (a) 1.0 M HCl and (b) 0.5 M H_2SO_4 Solution at Various Temperature 99

4.30. Langmuir Isotherm for PA Adsorption on Mild Steel Surface in (a) 1.0 M HCl and (b) 0.5 M H_2SO_4 Solution at Various Temperature 100

4.31. Langmuir Isotherm for BS Adsorption on Mild Steel Surface in (a) 1.0 M HCl and (b) 0.5 M H_2SO_4 Solution at Various Temperature 101

4.32. Langmuir Isotherm for PP1 Adsorption on Mild Steel Surface in (a) 1.0 M HCl and (b) 0.5 M H_2SO_4 Solution at Various Temperature 102

4.33. Langmuir Isotherm for the Adsorption of (a) PP and (b) PA on Aluminium Surface in 1.0 M HCl Solution at Various Temperature 103

4.34. Langmuir Isotherm for the Adsorption of (a) BS and (b) PP1 on Aluminium Surface in 1.0 M HCl Solution at Various Temperature 104

4.35. Freundlich Isotherm for PP Adsorption on Mild Steel Surface in (a) 1.0 M HCl and (b) 0.5 M H_2SO_4 Solution at Various Temperature 105

4.36. Freundlich Isotherm for PA Adsorption on Mild Steel Surface in (a) 1.0 M HCl and (b) 0.5M H_2SO_4 Solution at Various Temperature 106

4.37. Freundlich Isotherm for BS Adsorption on Mild Steel Surface in (a) 1.0 M HCl and (b) 0.5 M H_2SO_4 Solution at Various Temperature 107

4.38. Freundlich Isotherm for PP1 Adsorption on Mild Steel Surface in (a) 1.0 M HCl and (b) 0.5 M H_2SO_4 Solution at Various Temperature 108

4.39. Freundlich Isotherm for the Adsorption of (a) PP and (b) PA on Aluminium Surface in 1.0 M HCl Solution at Various Temperature 109

4.40. Freundlich Isotherm for the Adsorption of (a) BS and (b) PP1 on Aluminium Surface in 1.0 M HCl Solution at Various Temperature 110

4.41. Temkin Isotherm for PP Adsorption on Mild Steel Surface in (a) 1.0 M HCl and (b) 0.5 M H_2SO_4 Solution at Various Temperature 111

4.42. Temkin Isotherm for PA on Mild Steel Surface in (a) 1.0 M HCl and (b) 0.5 M H_2SO_4 Solution at Various Temperature 112

4.43. Temkin Isotherm for BS on Mild Steel Surface in (a) 1.0 M HCl and (b) 0.5 M H_2SO_4 Solution at Various Temperature 113

4.44. Temkin Isotherm for PP1 on Mild Steel Surface in (a) 1.0 M HCl and (b) 0.5 M H_2SO_4 Solution at Various Temperature 114

4.45. Temkin Isotherm for the Adsorption of (a) PP and (b) PA on Aluminium Surface in 1.0 M HCl Solution at Various Temperature 115

4.46. Temkin Isotherm for the Adsorption of (a) BS and (b) PP1 on Aluminium Surface in 1.0 M HCl Solution at Various Temperature 116

4.47. El-Awady Isotherm for PP on Mild Steel Surface in (a) 1.0 M HCl and (b) 0.5 M H_2SO_4 Solution at Various Temperature 117

4.48. El-Awady Isotherm for PA on Mild Steel Surface in (a) 1.0 M HCl and (b) 0.5 M H_2SO_4 Solution at Various Temperature 118

4.49. El-Awady Isotherm for BS on Mild Steel Surface in (a) 1.0 HCl and (b) 0.5 M H_2SO_4 Solution at Various Temperature 119

4.50. El-Awady Isotherm for PP1 on Mild Steel Surface in (a) 1.0 M HCl and (b) 0.5 M H_2SO_4 Solution at Various Temperature 120

4.51. El-Awady Isotherm for the Adsorption of (a) PP and (b) PA on Aluminium Surface in 1.0 M HCl Solution at Various Temperature 121

4.52. El-Awady Isotherm for the Adsorption of (a) BS and (b) PP1 on Aluminium Surface in 1.0 M HCl Solution at Various Temperature 122

4.53. Polarization Curve for the Corrosion of Mild Steel in 1.0 M HCl in the Absence and Presence of Various Concentration of PP at 303K 123

4.54. Polarization Curve for the Corrosion of Mild Steel in 0.5 M H_2SO_4 in the Absence and Presence of Various Concentration of PP at 303K 124

4.55. Polarization Curve for the Corrosion of Mild Steel in 1.0 M HCl in the Absence and Presence of Various Concentration of PA at 303K 125

4.56. Polarization Curve for the Corrosion of Mild Steel in 0.5 M H_2SO_4 in the Absence and Presence of Various Concentration of PA at 303K 126

4.57. Polarization Curve for the Corrosion of Mild Steel in 1.0 M HCl in the Absence and Presence of Various Concentration of BS at 303K 127

4.58. Polarization Curve for the Corrosion of Mild Steel in 0.5 M H_2SO_4 in the Absence and Presence of Various Concentration of BS at 303K 128

4.59. Polarization Curve for the Corrosion of Mild Steel in 1.0 M HCl in the Absence and Presence of Various Concentration of PP1 at 303K 129

4.60. Polarization Curve for the Corrosion of Mild Steel in 0.5 M H_2SO_4 in the Absence and Presence of Various Concentration of PP1 at 303K 130

4.61. Polarization Curve for the Corrosion of Aluminium in 1.0 M HCl in the Absence and Presence of Various Concentration of PP at 303K 131

4.62. Polarization Curve for the Corrosion of Aluminium in 1.0 M HCl in the Absence and Presence of Various Concentration of PA at 303K 132

4.63. Polarization Curve for the Corrosion of Aluminium in 1.0 M HCl in the Absence and Presence of Various Concentration of BS at 303K 133

4.64. Polarization Curve for the Corrosion of Aluminium in 1.0 M HCl in the Absence and Presence of Various Concentration of PP1 at 303K 134

4.65. Comparative Chart of Inhibitor Efficiency (IE) for Mild Steel-1 M HCl Solution of A) *Boscia senegalensis* and B) *Phyllanthus amarus* Concentration Obtained by Different Techniques 138

4.66. Comparative Chart of Inhibitor Efficiency (IE) for Mild Steel-1 M HCl Solution of A) *Paulona pinnata* and B) *Parinari polyandra* Concentration Obtained by Different Techniques 139

4.67. Comparative Chart of Inhibitor Efficiency (IE) for Mild Steel-1 M H_2SO_4 Solution of A) *Boscia senegalensis* and B) *Phyllanthus amarus* Concentration Obtained by Different Techniques 140

4.68. Comparative Chart of Inhibitor Efficiency (IE) for Mild Steel-1 M H_2SO_4 Solution of A) *Paulina pinnata* and B) *Parinari polyandra* Concentration Obtained by Different Techniques 141

4.69. Comparative Chart of Inhibitor Efficiency (IE) for Aluminium-1 M HCl Solution of A) *Boscia senegalensis* and B) *Phyllanthus amarus* Concentration Obtained by Different Techniques 142

4.70. Comparative Chart of Inhibitor Efficiency (IE) for Aluminium-1 M HCl Solution of A) *Paulina pinnata* and B) *Parinari polyandra* Concentration Obtained by Different Techniques 143

4.71. FTIR Spectrum of the Corrosion Product of Mild Steel in 1.0 M HCl 144

4.72. FTIR Spectra of (a) BS alone (b) Corrosion Product from the Corrosion of Mild Steel when 0.5g/l of BS was used as an Inhibitor in 1.0 M HCl 145

4.73. FTIR Spectra of (a) PA alone (b) Corrosion Product from the Corrosion of Mild Steel when 0.5g/l of PA was used as an Inhibitor in 1.0 M HCl 146

4.74. FTIR Spectra of (a) PP alone (b) Corrosion Product from the Corrosion of Mild Steel when 0.5g/l of PP was used as an Inhibitor in 1.0 M HCl 147

4.75. FTIR Spectrum of the Corrosion Product of Aluminium in 1.0 M HCl 148

4.76. FTIR Spectra of (a) BS alone (b) Corrosion Product from the Corrosion of Aluminium when 0.5g/l of BS was used as an Inhibitor in 1.0 M HCl 149

4.77. FTIR Spectra of (a) PA alone (b) Corrosion Product from the Corrosion of

Aluminium when 0.5g/l of PA was used as an Inhibitor in 1.0 M HCl 150

4.78. FTIR Spectra of (a) PP alone (b) Corrosion Product from the Corrosion of Aluminium when 0.5g/l of PP was used as an Inhibitor in 1.0 M HCl 151

4.79. FTIR Spectrum of the Corrosion Product from the Corrosion of Mild Steel in 0.5 M H_2SO_4 152

4.80. FTIR Spectra of (a) BS alone (b) Corrosion Product from the Corrosion of Aluminium when 0.5g/l of BS was used as an Inhibitor in 0.5 M H_2SO_4 153

4.81. FTIR Spectra of (a) PA alone (b) Corrosion Product from the Corrosion of Aluminium when 0.5g/l of PA was used as an Inhibitor in 0.5 M H_2SO_4 154

4.82. FTIR Spectra of (a) PP alone (b) Corrosion Product from the Corrosion of Aluminium when 0.5g/l of PP was used as an Inhibitor in 0.5 M H_2SO_4 155

4.83. HOMO – LUMO Orbital Diagram of Some Constituents of *Boscia senegalensis* Extract (atom legend: White = H; Light gray = C; Red = O; Blue = N) 162

4.84. HOMO – LUMO Orbital Diagram of Some Constituents of *Parinari polyandra* Extract (atom legend: White = H; Light gray = C; Red = O; Blue = N) 163

4.85. HOMO – LUMO Orbital Diagram of Some Constituents of *Paulina pinnata* Extract (atom legend: White = H; L,ight gray = C; Red = O; Blue = N) 164

4.86. HOMO – LUMO Orbital Diagram of Some Constituents of *Phyllanthus amarus* Extract (atom legend: White = H; Light gray = C; Red = O; Blue = N) 165

4.87. Adsorption of Single Molecules of BS1, BS2, BS3 and BS4 on a Fe (110) Surface 169

4.88. Adsorption of Single Molecules of PP0, PP4, PP2 and PP3 on a Fe (110) Surface 170

4.89. Adsorption of Single Molecules of PP*1, PP*2 and PP*3 on a Fe (110) Surface 171

4.90. Adsorption of Single Molecules of PA1, PA2 and PA3 on a Fe (110) Surface 172

4.91. Adsorption of Single Molecules of PA1, PA2 and PA3 on an Al (110) Surface 173

4.92. Adsorption of Single Molecules of BS1, BS2, BS3 and BS4 on an Al (110) Surface 174

4.93. Adsorption of Single Molecules of PP0, PP2, PP3 and PP4 on an Al (110) Surface 175

4.94. Adsorption of Single Molecules of PP*1, PP*2 and PP*3 on an Al (110) Surface 176

List of Plates

Plate(s) **Page**

4.1. SEM Micrographs of Polished A) Aluminium Sheet and B) Mild Steel alone 156

4.2. SEM Micrographs of Mild Steel as Corroded in 1.0 M HCl Solution for 7 days
(a) Mild Steel alone and in the Presence of (b) BS (c) PA (d) PP (x 5000) 157

4.3. SEM Micrographs of Aluminium as Corroded in 1.0 M HCl Solution for 7 days
(a) Aluminium alone and in the Presence of (b) BS (c) PA (d) PP (x 5000) 158

4.4. SEM Micrographs of Mild Steel as Corroded in 0.5 M H_2SO_4 Solution for 7 days
(a) Mild Steel alone and in the Presence of (b) BS (c) PA (d) PP (x 5000) 159

4.5. SEM Micrographs of Aluminium as Corroded in 0.5 M H_2SO_4 Solution for 7 days
(a) Aluminium and in the Presence of (b) BS (c) PA (d) PP (x 5000) 160

List of Tables

Table(s)	Page
3.1: Nominal Elemental Composition of Aluminium Sheet	43
3.2: Nominal Elemental Composition of Mild Steel Sheet	43
4.1: Phytochemcial Screening of the Various Plant Extract	52
4.2: Characterization of Peaks Obtained from GC-MS Spectrum of Ethanol Extract of *Paulina pinnata*	53
4.3: Characterization of Peaks Obtained from GC-MS spectrum of Ethanol Extract of *Parinari polyandra*	55
4.4: Characterization of Peaks Obtained from GC-MS Spectrum of Ethanol Extract of *Phyllanthus amarus*	57
4.5: Characterization of Peaks Obtained from GC-MS Spectrum of Ethanol Extract of *Boscia senegalensis*	59
4.6: Corrosion Rate of Aluminium and Inhibition Efficiencies of the Various Inhibitors in 1.0 M HCl	73
4.7: Corrosion Rate of Aluminium and Inhibition Efficiencies of the Various Inhibitors in 0.5 M H_2SO_4	74
4.8: Corrosion Rate of Mild Steel and Inhibition Efficiencies of the Various Inhibitors in1.0 M HCl	75
4.9: Corrosion Rate of Mild Steel and Inhibition Efficiencies of the Various Inhibitors in 0.5 M H_2SO_4	76
4.10: Thermodynamic Parameters for the Adsorption of Various Concentration of the Inhibitor on Aluminium Surface in 1.0 M HCl	85
4.11: Thermodynamic Parameters for the Adsorption of Various Concentration of the Inhibitor on Mild Steel Surface in 1.0 M HCl	86
4.12: Thermodynamic Parameters for the Adsorption of Various Concentration of the Inhibitor on Aluminium and Mild Steel Surface in 1.0 M HCl	87
4.13: Thermodynamic Parameters for the Enthalpy and Entropy of Activation of Various Concentration of the Inhibitor on Mild Steel and Aluminium Surface in 1.0 M HCl	96

4.14: Thermodynamic Parameters for the Enthalpy and Entropy of Activation of Various Concentration of the Inhibitor on Mild Steel and Aluminium Surface in 0.5 M H_2SO_4 97

4.15: Tafel Polarization Parameters Obtained at Various Concentration of Inhibitors on Mild Steel Surface in Acidic Media 135

4.16. Linear Polarization Resistant Data for BS, PA, PP and PP1 in Various Acidic Media 136

4.17: Computed Quantum Chemical Parameters of the Studied Compounds 166

4.18: Fukui Indices Calculated with DND 167

4.19: Calculated Binding Energies of the Adsorption of Various Molecules of the Plant Extracts using Forcite Quench Molecular Dynamics 177

List of Appendices

Appendix **Page**

I: Adsorption Isotherm Parameters Obtained from the Corrosion Data of Mild Steel in 1.0 M HCl Containing Various Concentration of Inhibitors 217

II: Adsorption Parameters Obtained from the Corrosion Data of Mild Steel in 1.0 M HCl Containing Various Concentrations of Inhibitors 218

III: Adsorption Isotherm Parameters Obtained from the Corrosion Data of Mild Steel in 0.5 M H_2SO_4 Containing Various Concentrations of Inhibitors 219

IV: Adsorption Isotherm Parameters Obtained from the Corrosion Data of Mild Steel in 0.5 M H_2SO_4 Containing Various Concentration of Inhibitors 220

V: Adsorption Isotherm Parameters Obtained from the Corrosion Data of Aluminium in 1.0 M HCl Containing Various Concentration of Inhibitors 221

VI: Adsorption Isotherm Parameters Obtained from the Corrosion Data of Aluminium in 1.0 M HCl Containing Various Concentration of Inhibitors 222

VII: Frequencies and Peaks of IR Adsorption by BS and the Corrosion Product of Mild Steel in HCl 223

VIII: Frequencies and Peaks of IR Adsorption by PA and the Corrosion Product of Mild Steel in HCl 224

IX: Frequencies and Peaks of IR Adsorption by PP and the Corrosion Product of Mild Steel in HCl 225

X: Frequencies and Peaks of IR Adsorption by BS and the Corrosion Product of Aluminium in HCl 226

XI: Frequencies and Peaks of IR Adsorption by PA and the Corrosion Product of Aluminium in HCl 227

XII: Frequencies and Peaks of IR Adsorption by PP and the Corrosion Product of Aluminium in HCl 228

XIII: Frequencies and Peaks of IR Adsorption by BS and the Corrosion Product of Aluminium in H_2SO_4 229

XIV: Frequencies and Peaks of IR Adsorption by PA and the Corrosion Product of Aluminium in H_2SO_4 230

XV: Frequencies and Peaks of IR Adsorption by PP and the Corrosion Product of

Aluminium in H_2SO_4 231

XVI: Inhibitive and Adsorptive Effect of *Parinari polyandra* on Mild Steel Corrosion in Aqueous Sulphuric Acid 232

XVII: Theoretical and experimental inhibitive properties of mild steel in HCl by ethanolic extract of *Boscia senegalensis* 243

Abbreviations and Symbols

Abbreviation	
mV	millivolts
mV/s	millivolts per sec
ps	pico second
fs	femto second
E_{corr}	Corrosion potential
I_{corr}	Corrosion current density
IE%	Inhibition efficiency in percentage
R^2	Regression coefficient
A/cm^2	Ampere per centimetre square
SCE	Saturated Calomel Electrode
ASTM	American Society for Testing Materials
NACE	National Association of Corrosion Engineers
$DMOl^3$	A unification of density functional calculations on molecules (DMol)
DFT	Density Functional Theory
DND	Double-Numerical + d-orbital
COMPASS	Condensed-phase Optimised Molecular Potentials for atomistic Simulation Studies
Inh	Inhibitor
NVE	Microcanonical Ensemble
Å	Angstrom

Fe (1 1 0)	A plane in the Fe lattice that intersects the x-axis at a distance **'a'** from the origin, the y-axis at a distance **'b'**, and the z-axis at **infinity**.
Al (1 1 0)	A plane in the Al lattice that intersects the x-axis at a distance **'a'** from the origin, the y-axis at a distance **'b'**, and the z-axis at **infinity**.
PA1	1, 2, 3-Benzaetriol
PA2	linolenic acid (*Phyllanthus amarus*)
PA3	ethanone
BS1	Methyllinositol (*Boscia senegalensis*)
BS2	1, 2, 3-Benzaetriol
BS3	Hydroquinone
BS4	3, 5-bis(1,1-dimethylethyl)-phenol
PP0	Methyllinositol (*Paulina pinnata*)
PP2	β-sitosterol
PP3	Cis-alpha-Bisabolene
PP4	Squalene
PP*1	linolenic acid (*Parinari polyandra*)
PP*2	9-oxabicyclo [3.3.1]nona-3, 6-dien-2-one
PP*3	Gama Tocophenol

CHAPTER ONE

1.0 INTRODUCTION

Industrial development is vital in the history of any developed country. Most industries use various types of metals including their alloy for the construction or fabrication of their plants and other installations. In most cases, contact between the metal and aggressive medium (such as acid, base and salt) is unavoidable (Eddy *et al.*, 2009a, 2009b). Corrosion is defined as an electrochemical process that tends to returns the metal to its original state (Eddy *et al*., 2010).

In view of the above, industrial facilities exposed to corrosion are often protected against corrosion by adopting several options including painting, oiling, cathodic and anodic protections, etc. However, the use of inhibitors has been found to be one of the best options available for the protection of metals against corrosion (Okafor *et al*., 2007; Oguzie *et al*., 2006; and Abdallah, 2004a).

Inhibitors are compounds that tend to retard the rate of corrosion of metals by being on the surface of the metal either through the transfer of charge from charge inhibitor molecule to charged metal surface (physical adsorption) or by electron transfer from the inhibitor's molecule to the vacant orbital (mostly d-orbital) of the metal (Eddy *et al.,* 2015). Numerous studies have been carried out on the corrosion of metals in different environments and their inhibition and most of the well-known inhibitors suitable for the inhibition of the corrosion of metals in acidic medium are heterocyclic compounds (Eddy *et al*., 2015, 2010; Elayyoubi *et al*., 2004; Ita, 2004a, b; Ita and Offiong, 1997; Khavasfar and Iran, 2006; and Okafor *et al*., 2007). For these compounds, their adsorption on the metal

surface is the initial step of inhibition (El Ashry *et al.,* 2006a, 2006b). The adsorption of inhibitor is linked to the presence of heteroatoms such as N, O, P, and S and long carbon chain length as well as triple bond or aromatic ring in their molecular structure (Emregul *et al.,* 2006; Umoren *et al.,* 2006). Generally, a strong coordination bond causes higher inhibition efficiency.

Most inhibitors are organic compounds whose inhibition potentials can be correlated with their chemical structure. However, some of them are toxic, non-degradable and are not eco-friendly (Ita, 2004a). On the other hand green corrosion inhibitors are biodegradable and do not contain heavy metals or other toxic compounds. The successful use of naturally occurring substances to inhibit the corrosion of metals in acidic and alkaline environment have been reported by some research groups (Oguzie *et al*., 2004, 2007; Umoren *et al*., 2006 and Okafor *et al*., 2007).

Researchers generally agree that most of these plants are green inhibitors because they are biodegradable, less toxic and do not contain heavy metals (Okafor *et al*.; 2007). In the light of these, several plants extract have been reported and their corrosion inhibition properties are often attributed to their phytochemical constituents (Umoren and Ebenso, 2008).

The active phytochemicals in plants that are effective for corrosion inhibition can be regarded as those with heteroatom(s) in their aromatic or long chain, possession of π-electrons or suitable groups may also facilitate the transfer of charge from the inhibitors' molecule to charge metal surface (physical adsorption) or the transfer of electron from the inhibitors molecule to vacant d-orbital of the metal (chemical adsorption). Therefore in

order to identify the active constituent of plant extract involved in corrosion inhibition, explicit knowledge of the chemical structures of its phytochemicals is required. Therefore, the present study is aimed at elucidating the chemical structures of the ethanol extracts of four (4) plants waste and to investigate their corrosion potentials for mild steel and aluminium in acid media.

1.1 Justification of Study

In spite of the broad spectrum of naturally/synthesized inhibitors used for the inhibition of the corrosion of metals including mild steel and aluminium, it has been found that most inhibitors are toxic thereby posing a problem to the environment. In order to overcome the challenges poised by toxic inhibitors, there is need to focus future research on the use of eco-friendly corrosion inhibitors. Plant extracts are products of naturally occurring substance, they are cheap and can be readily produced and are readily available in our immediate environment as waste product which cause environmental pollution. Therefore, the present study shall attempt to explore the possibility of using some plant extracts for the inhibition of the corrosion of mild steel and aluminium in HCl and H_2SO_4 solution. It has also been found that the inhibition potentials of any inhibitor are also affected by electronic and structural parameters. Therefore, quantum chemical studies shall be considered in finding possible relationship between microscopic and macroscopic behaviour of the inhibitors. However, most corrosion inhibitors are not environmentally friendly, hence this study is designed to investigate the corrosion inhibition potential of some plants extract which are environmentally friendly.

1.2 Aim and Objectives

The present study is aimed at investigating corrosion inhibition potentials and mechanisms of inhibition of the ethanol extracts of *Phyllanthus amarus* (PA)*; Paullina pinnata* (PP)*; Parinari polyandra* (PP1)*; and Boscia senegalensis* (BS) on mild steel and aluminium in HCl and H_2SO_4 solutions at 303K, 313K, 323K and 333K using experimental and theoretical approaches. The aim of the research shall be achieved through the following objectives:

(i) To perform phytochemical screening on the ethanol extract of the plants and identify structures of the active constituents using gas chromatography-mass spectrometry (GCMS).

(ii) To study corrosion rates of the aluminium and mild steel in uninhibited and inhibited acid (HCl and H_2SO_4) at various temperatures using gravimetric and Linear polarisation techniques.

(iii) To evaluate the inhibition efficiencies of the extracts for the corrosion of mild steel and aluminium in the different media.

(iv) To investigate the effect of temperature and thermodynamic properties of the inhibitors on the metals in the various acid media

(v) To study the adsorption characteristics of the inhibitors by fitting adsorption data into different adsorption isotherms.

(vi) To examined the surface of the metals and corrosion morphology using scanning electron microscopy (SEM).

(vii) To identify the functional groups present in both the extracts as well as corrosion product using Infrared Spectroscopic (FTIR).

(viii) To obtain the electronic structures of the selected constituents of the extracts by means of quantum chemical computations as well as obtain their stable adsorption structures on the different metal surfaces and the corresponding adsorption energies using molecular dynamics simulations.

CHAPTER TWO

2.0 LITERATURE REVIEW

2.1 Corrosion

Corrosion is the degradation of materials due to interactions with their environments. It is an electrochemical process which involves transfer of electrons between a metal surface and an aqueous solution. When metal atoms are exposed to an aggressive medium such as water, they can loose electrons, becoming themselves positively charged ions provided electrical circuits are completed. One of the most familiar corrosion processes is oxidation of iron (rusting). Iron oxidizes in the presence of oxygen and aqueous electrolyte solution. Physical strains such as scratches, dents, etc, on the iron are more easily oxidized than other areas. The result is that these regions are anodic (oxidation occurs) and simultaneously a different region are cathodic (reduction occurs). When this occurs, iron atom gives up two electrons to form Fe^{2+} as illustrated in equation 2.1

2.1

The electrons released during the above reaction (equation 2.1) flow through the iron metal to the cathodic region leading to a reduction.

$O_2 + 2H_2O(l) + 4e^-$ $4OH^-(aq)$ 2.2

Combination of equation 2.1 and 2.2 gives equation 2.3:

$2Fe + O_2 + 2H_2O$ $2Fe^{2+} + 4OH^-$ 2.3

A typical experience of this process occur in car fenders were Fe^{2+} is eventually oxidized further to Fe^{3+}, in iron (III) oxide compounds (rust).

$2Fe^{2+} + O_2 + 4H_2O(l)$ $2Fe_2O_3(s) + 8H^+(aq) + 4e^-$ 2.4

Corrosion can often be predictable or it can be totally unpredictable and catastrophic, as exemplified by the hydrogen embrittlement or stress corrosion of critical structural members and pressure vessels in the aerospace and chemical processing industries. However, thermodynamic principles can be applied to determine which processes can occur and the tendency for the changes to take place (El Ashry *et al*., 2006a, b; Cardoso *et al*., 2006; and Eddy and Odoemelam, 2008a, b).

The great impact of corrosion of metals in the oil, metallurgical and other industries has been widely acknowledged and several researches have been carried out on the protection of metals against corrosion. Results obtained showed that one of the best methods involves the use of inhibitors. However, owing to strict environmental regulations, such as toxic nature of some of the inhibitors, organic compounds are preferred to inorganic compounds especially heavy metals derivatives, as corrosion inhibitors. Organic compounds containing hetero atoms such as N, S, P or O in conjugated or aromatic systems have been reported to be effective corrosion inhibitors (Abdallah, 2004a, b; Ashassi-Sorkhabi *et al.*, 2006; and Umoren and Ebenso, 2008). The presence of polar functional groups such as $–NH_2$, -COOH and –OH, as well as π-electrons facilitates the adsorption of the inhibitor on the surface of the metal (Ebenso *et al*., 2008; Eddy, 2008; and Obot *et al.*, 2009a). Also studies on the use of green corrosion inhibitors have been intensified. These inhibitors are biodegradeable and do not contain heavy metals or other toxic compounds (Eddy and Ebenso, 2008). The successful use of these substances to inhibit the corrosion of metals in acidic and alkaline environment has been reported by some group of researchers (Abiola *et al*., 2007; Abdallah, 2004a, b; and Bendahou *et al*., 2006). The adsorption bond strength is dependent on the composition of the metal and that of the corrodent, inhibitor

structure and concentration as well as temperature. Despite the broad spectrum of organic compounds, the final choice of appropriate inhibitors for a particular application is restricted by several factors which include toxicity, cost, ease of availability etc.

In the absence of adequate information on corrosion rate (metal weight loss/unit area/unit time) and various methods of protecting a metal, over-design (e.g. thicker tube wall, leading to greater power requirements for moving parts), lower efficiency of equipment, contaminations, plants shut down, loss of production and loss of equipment will be inevitable.

2.2 Forms of Corrosion

Basically, there are eight forms of corrosion which are classified based on appearance of the corroded metal. Some of these eight forms are unique and distinct but all of them are to varying degrees interrelated. These are:-

2.2.1 Uniform corrosion

Uniform corrosion is the attack of a metal at essentially the same rate at all exposed areas of its surface. It is characterized by laterally constant speed of corrosion. For example, in the atmospheric corrosion of galvanized steel, the speed of corrosion depends on the thickness of the steel, as such, the thicker the steel coating, the longer the service life of the metal. Uniform attack is the most common type of corrosion and causes the greatest destruction of metals on a weight basis (Moore, 1990). It is often expressed in terms of depth of penetration or as weight loss. The units often quoted in literature are ipy (inches penetrating per year), ipm (inches of penetration per month), mdd (mg per dm^3 per day) and $mmyr^{-1}$ (millimetres penetration per year). However, the SI unit is $mmyr^{-1}$ and the conversion factor is given by equations 2.5, 2.6 and 2.7 respectively.

$$mdd = 10 \times gm^{-2}d^{-1} \quad (2.5)$$

$$mmyr^{-1} = 36.52 \times mdd \times 1/\rho \quad (2.6)$$

$$mdd = \rho \times ipy \times 1/1.44 \quad (2.7)$$

where ρ is the density of the metal (kgm^{-3})

2.2.2 Galvanic Corrosion

Galvanic corrosion also known as bimetallic corrosion is a localised mechanism by which metals can be preferentially corroded. When two dissimilar metals are in contact with each other or otherwise electrically connected and exposed to a corrosive liquid or conductive solution, a potential is set up between these two metals and a current flows. Corrosion of one metal is often accelerated and the other reduced, as compared to the behaviour of these metals when they are not in contact. Because of the electric currents and dissimilar metals involved, this form of corrosion is called "galvanic" or "two-metal" corrosion. Consequently, the more active metal oxidizes more quickly in the galvanic arrangement while an inert or noble metal will essentially be unaffected. The extent of galvanic corrosion increases with the potential difference of the metal. The relative size of the anode or cathode significantly affects the relationship between the active and inert metals. Therefore a small anode in the presence of a large cathode corrodes more quickly and vice versa. This form of corrosion can be prevented by keeping dissimilar metals apart or by the provision of insulating materials between the metals in order to interrupt current flow (Oldfield, 1988; Baboian *et al*., 1990; Eddy, 2008; and Oguzie *et al*., 2012a).

2.2.3 Pitting corrosion

It results from galvanic action where the metal surface appears to have pinhole. The pinhole represent the anode while the surrounding surface as the cathode (Jones, 1982; Moniz, 1986; and Clark and Varney, 1987). It may occur as a result of one of the following:

a. a change in the acidity of the pit area;
b. differential aeration may also be a contributing factor to the increase in pit because most solutions are in contact with air and because of convection, transportation of oxygen through the solution leads to areas of high or low oxygen concentration. Therefore, it may cause the area with the higher oxygen concentration to become a cathode while an area of lower oxygen concentration becomes anode resulting in localized attacked;
c. depletion of inhibitor will also cause pits to form. In most cases, naturally formed oxides on the metal surface act as inhibitors and protect the substrate from pits (Jones, 1982; Moniz, 1986; and Clark and Varney, 1987).

The real pitting initiates as localized breakdown of protective films on the metal. This breakdown is followed by rapid film repair but if the damaging condition persists long enough, the film may not be able to reform itself and a pit is initiated. After initiation, the mechanism of the propagation is just the same as that for crevice corrosion. In essence, the pitted metal has created its own crevice. The cathode reactant becomes depleted in the pit while the anode reaction continues. Migration of chlorides and other reactive ions into the pit permits metal salts to be formed or hydrolyzed, making the solution in the pit very

acidic. As the acidity and the concentration of the chloride inside the pit increase with time, the maximum pit depth (D) often obeys equation 2.8.

$$D = kt^n \qquad 2.8$$

where k is the absorption equilibrium constant and n is the number of water molecule absorb and t is the time

2.2.4 Crevice corrosion

Crevices are present in all equipment. They occur naturally around bolts, rivets etc. They are also created by scratches on the metal surface. The corrosion absorbs and draws solution toward the reactive area. It is also influence by the same factors affecting pitting corrosion and is indeed a specific form of pitting corrosion (Clark and Varney, 1987).

2.2.5 Intergranular corrosion

Intergranular corrosion occurs by localized attack at grain boundaries, which behave as anode to the larger surrounding cathode grains (Moore, 1990). Metals usually are not homogeneous. Impurities or alloying elements may segregate into grain boundaries. Heat treatment or localized heating by welding may provoke change in composition localized in or near grain boundaries.

2.2.6 Erosion corrosion

Almost all corrosive media can bring about erosion-corrosion and nearly all metals and alloys are susceptible to this except those metals or alloys that are capable of forming hard, dense, adherent and continuous surface film (Moore, 1990). The extent of this corrosion increases with increase in the velocity of the corroding medium. In some cases,

the high velocity increases the supply of oxygen or other gases at the metal surface, which may depolarize the cathodic reaction and consequently increase the corrosion rate (Atkins, 2002).

2.2.7 Cavitation corrosion

Formation and collapse of tiny gas bubbles in a liquid stream called cavitations may mechanically destroy any protective layer, causing localized corrosion called cavitation corrosion (Moore, 1990). Similarly when an object such as propeller rotates in water, the pressure on the trailing surface of the blade fluctuates continually. At some points, very low pressures are produced which create tensile forces high enough to exceed the inter-atomic binding forces of the liquid.

2.2.8 Fretting corrosion

Fretting corrosion is a combination of mechanical wear and atmospheric oxidation which frequently occurs between close fitting metal components (Moore, 1990). Corrosion occurring at contact regions between materials under load subjected to slip and vibration can be termed Fretting. Such friction oxidation can occur in engine and automotive parts.

2.3 Corrosion Monitoring Techniques

Corrosion measurement is the quantitative way by which the effectiveness of corrosion control and prevention techniques can be evaluated and provides the feedback to enable corrosion control and prevention methods to be optimized. In any corrosion monitoring system, it is common to find two or more of the techniques combined to provide a wide base for data gathering. The exact techniques which can be used depend on

the actual environment, alloy system, and operating parameters. The various method of measuring corrosion as described below.

2.3.1 Gravimetric technique

The weight loss technique is the simplest, and the longest-established method of estimating corrosion losses in plants and equipment. A weighed sample (coupon) of the metal or alloy under consideration is introduced into a medium, and later removed after a reasonable time interval. The coupon is then cleaned of all corrosion products and weighed. The weight loss is converted to an average corrosion rate using proper conversion equations. The basic measurement which is determined from corrosion coupons is weight loss; the weight loss over the period of exposure being expressed as corrosion rate (Oguzie, 2005; Eddy *et al*., 2010; Olasehinde *et al*., 2012; and Adejo *et al*., 2012).

The technique is extremely versatile, since weight loss coupons can be fabricated from any commercially available alloy. Also, using appropriate geometric designs, a wide variety of corrosion phenomena can be studied. These include, stress-assisted corrosion; bimetallic (galvanic) attack; differential aeration; heat-affected zones but are not limited to these methods.

This technique is mostly widely used because of it numerous advantages which include: applicability to all environments (gases, liquids, solids/particulate flow), visual inspection can be undertaken, corrosion deposits can be observed and analyzed, weight loss can be readily determined and corrosion rate easily calculated, localized corrosion can be identified, inhibitor performance are easily assessed.

The disadvantage of the coupon technique is that, if a corrosion upset occurs during the period of exposure, the coupon alone will not be able to identify the time of occurrence

of the upset (NACE, 1999; Dean, 2003). Therefore, coupon monitoring is most useful in environments where corrosion rates do not significantly change over long time periods. However, they can provide a useful correlation with other techniques such as potentiodynamic polarization technique (Oguzie *et al.,* 2012a, b).

2.3.2 Gasometric technique

The gasometric assembly is essentially an apparatus which measures the rate of gas evolution during a corrosion reaction. In an acid medium, the volume of hydrogen gas evolved is directly proportional to the rate of corrosion of the metal (Umoren *et al*., 2009). It consists of a graduated burette which is connected to a flask containing paraffin oil. The burette is surrounded with a glass jacket with a water inlet and outlet to regulate the temperature of the gas evolved. A reaction vessel is connected to the gas burette through a delivery tube with a tap for incoming gas and another to expel the gas when the burette is full or at the end of the reaction. The reaction vessel is a three-necked flask consisting of an inlet for the metallic coupon, another one for the thermometer and the last leading to the gas burette (Umoren *et al*., 2009).

2.3.3 Thermometric technique

The reaction vessel is a well lagged, three-necked round bottom flask consisting of an inlet for the metallic coupon, another one for the thermometer and the last for introducing the test solution.

The flask is well lagged to prevent heat losses. In the thermometric technique, the progress of the corrosion reaction is monitored by determining changes in temperature with time using a thermometer (0 - 100°C) (Eddy and Ebenso, 2008; Obot *et al*., 2009a).

2.3.4 Potentiodynamic polarization techniques

Polarization techniques such as potentiodynamic polarization, potentiostaircase and cyclic voltammetry are often used for laboratory corrosion testing. These techniques can provide significant useful information regarding the corrosion mechanisms, corrosion rate and susceptibility of specific materials to corrosion in designated environments. Polarization methods involve changing the potential of the working electrode and monitoring the current which is produced as a function of time or potential. It is probably the most commonly used polarization testing method for measuring corrosion resistance and is used for a wide variety of functions (Van, 1998; Khaled, 2010a, 2010b).

2.3.5 Linear polarization resistance

The polarization resistance of a material is defined as the slope of the potential-current density ($\Delta Ecorr/\Delta icorr$) curve at the free corrosion potential, yielding the polarization resistance Rp that can be related (for reactions under activation control) to the corrosion current by the Stern-Geary equation (ASTM, 2001; Dean, 2003).

2.3.6 Electrochemical noise

The non-intrusive use of electrochemical noise (EN) for corrosion monitoring is very attractive examples are found in aircraft corrosion and gas scrubbing tower monitoring. Fluctuations of potential or current of a corroding metallic specimen are and are well known. The extensive development in the sensitivity of the equipment for studying electrochemical systems has rendered the study of oscillations in electrochemical processes that translate into measurable electrochemical noise, EN, increasingly accessible. No other technique, electrochemical or otherwise is remotely as sensitive as EN to system changes and upsets (Sastri, 2011).

2.3.7 Electrochemical impedance spectroscopy (EIS)

Electrochemical impedance spectroscopy also called AC impedance or impedance spectroscopy is usually measured by applying an AC potential to an electrochemical cell and measuring the current through the cell. A small amplitude signal, usually a voltage between 5 to 50mV, is applied to a specimen over a range of frequency of 0.001 to 100,000Hz. The EIS instrument records the real and imaginary components of the impedance response of the system. Depending upon the shape of the EIS spectrum, a circuit model or circuit description code and initial circuit parameters are assumed and analyzed (Oguzie *et al.,* 2012a, b).

An important advantage of EIS over other laboratory techniques is the possibility of using very small amplitude signals without significantly disturbing the properties being measured. It is a non-destructive technique and can provide time dependent information about the properties and also about ongoing processes such as corrosion. However, expensive and complex data analysis is required for quantification (NACE, 1999; Sastri, 2011).

2.3.8 Galvanic monitoring

The galvanic monitoring technique, also known as Zero Resistance Ammetry (ZRA) is another electrochemical measuring technique. With ZRA probes, two electrodes of dissimilar metals are exposed to the process fluid. When immersed in solution, a natural voltage (potential) difference exits between the electrodes. The current generated due to this potential difference relates to the rate of corrosion occurring on the most active of the electrode couple. This method is applicable to bimetallic corrosion, crevice and pitting attack, corrosion assisted cracking, corrosion by highly oxidizing species and weld decay.

Galvanic current measurement has found widest applications in water injection systems where dissolved oxygen concentrations are of primary concern. Oxygen leaking into such systems greatly increases galvanic currents and thus the rate of corrosion of steel process components. The monitoring systems are used to provide an indication that oxygen may be invading injection waters through leaking gaskets or deaeration systems.

In any corrosion monitoring system, it is common to find two or more techniques combined to provide a wide base for data gathering. The exact techniques which can be used depend on the actual process fluid, alloy system, and operating parameters. Corrosion monitoring offers an answer to the question of whether more corrosion is occurring today compared to yesterday. Using this information, it is possible to identify the cause of corrosion and quantify its effect. Corrosion monitoring remains a valuable weapon in the fight against corrosion, thereby providing substantial economic benefit to the user (ASTM, 2001).

2.4 Common Methods of Corrosion Prevention

In most industrial processes, it is virtually impossible to prevent corrosion. The general strategy is to use measures that reduce the corrosion rate to an economically sustainable level. The most important corrosion mitigation procedure involves selection of materials and design against corrosion, cathodic protection, anodic protection, protective coatings, change of environment and chemical inhibitors (Sastri, 1998, 2011; Danny, 2004).

2.4.1 Selection of materials and design against corrosion

Materials for a particular working environment (composition, temperature, velocity) are selected taking into account mechanical and physical properties, availability, method of fabrication and overall cost of component or structure. Geometrical configurations that facilitate corrosive conditions should be avoided which includes:

a. features that trap dust, air and water
b. designs with inaccessible areas that cannot be re-protected, e.g., by maintenance painting
c. designs that lead to heterogeneity in the metal or in the environment

Also, metal-metal or metal-non metallic contacting materials that facilitate corrosion such as bimetallic couples, a metal in contact with absorbent materials that maintain constantly wet conditions and contact with substances that give off corrosive vapours, should be avoided (Sastri, 1998; 2011).

2.4.2 Protective coatings

Basically, a protective coating should provide a complete barrier and exclude the corrosive environment from having contact with the metal which it is designed to protect. This can be achieved by the following techniques (Sastri, 1998; 2011):

a. using inorganic coatings, e.g., vitreous enamel, glasses, ceramics
b. application of organic coatings, e.g., paints, plastics, greases
c. generating metallic coatings that form protective barriers (Ni, Cr) or protect the substrate by sacrificial action (Zn, Al, Cd on steel).

2.4.3 Cathodic protection

Cathodic protection is achieved by lowering the potential of the metal being protected by connecting the metal to a corrosion cell were the protected metal forms the cathode and another anodic reaction (the oxidation) instead takes place away from the metal. Two principal means are used to achieved such a corrosion cell; sacrificial anode and impressed current. Sacrificial anode utilizes a less noble metal electrically connected to the metal being protected to form a corrosion cell were the sacrificial anode corrodes preferentially thus protecting the cathode from corrosion. Impressed- current method instead uses an external power source to produce a corrosion cell were the metal being protected is connected as the cathode (Sastri, 1998; 2011).

2.4.4 Anodic protection

Anodic protection is achieved by raising the potential of the metal being protected. The higher potential alters the corrosion product formed to create a protective surface keeping the metal in a passive region where the corrosion current is reduced.

2.4.5 Chemical inhibition

Chemical corrosion inhibitors generally prevent corrosion by forming or promoting the formation of an adsorption layer on the metal surface thus separating the metal surface and the electrolyte containing water. The inhibitor can function either by limiting the anodic reaction (anodic inhibitor), the cathodic reaction (cathodic inhibitor) or both (mixed inhibitor) (Umoren *et al*., 2009; Eddy *et al*., 2010; Akalezi *et al*., 2012).

2.5 Inhibition of corrosion

Hosseini *et al*. (2007) reported that, corrosion can be controlled by addition of chemical substances called inhibitors into acid media. By definition, an inhibitor is a

chemical compound which when added in small amounts to the corrosive environment alters the cathodic and or anodic reaction and subsequently reduces the corrosion rate. This implies that inhibitors can be classified as anodic or cathodic depending on the process (Akpan, 1994). Inhibitors can also be classified as organic or inorganic depending on their constituent and their redox characteristics. However, one of the most widely applied classification systems for inhibitor is that proposed by Kelly *et al*. (2003). However, he describe inhibitors base on three different forms namely:

a. Adsorption inhibitors: These are inhibitors which are adsorbed on the metal surface and form protective barrier films. Adsorption inhibitors function by limiting the diffusion of oxygen to the corrosion surface, trapping the metal ion on the surface, stabilizing the double layer and reducing the rate of dissolution.
b. Passivation inhibitors: passivating inhibitors function by inducing and maintaining a passive film (consisting of metal oxide) on the surface.
c. Surface reaction product inhibitors: these are inhibitors that form sparingly soluble compounds other than an oxide layer. Surface reaction product inhibitors cannot form a protective oxide layer because they are not oxidizing agents but interact with metal on the surface to form insoluble compounds which plug in pores and inhibit corrosion.

2.5.1 Interphase inhibitors

Interphase inhibitors function by facilitating the formation of a 3-D layer which acts as a barrier between the corroding substrate and the electrolyte. The protective film could be a solid film on the surface of the metal or a liquid film adjacent to it. The solid film may be an oxide layer, corrosion product, metallic or non-metallic coating or inhibitor forming a porous layer or non-porous film (Mercer, 1990; Monika *et al*., 2005). However, the liquid

film is the electrolyte in the interphase which differs from the bulk of the solution in its chemical or physical properties. Based on this model, the inhibition of metal corrosion is governed by the properties of the layer such as its porosity and stability.

2.5.2 Passivating or oxidizing inhibitors

Pourbaix (1981) stated that iron polarizes anodically in the presence of oxidizing inhibitors and passivates as the open circuit potential shifts to more positive potential. It is also possible that the inhibitors are reduced and the reduction product is deposited on the weak points of the films to improve its protective effect. An oxidizing inhibitor functions by inducing and maintaining a passive surface layer on the metal surface. These inhibitors are effective at certain concentrations (Critical concentration, Ccrit). At concentrations below the critical concentration, corrosion is enhanced but at very high concentrations of the inhibitor, increase in the anodic current density is observed.

2.5.3 Non-oxidizing inhibitors

Non-oxidizing inhibitors are also capable of passivating metals electrochemically. They include compounds such as NaOH and the salts of weak acids and strong bases such as Na_3PO_4, Na_2HPO_4, Na_2CO_3, $NaBO_3$ and $Na_2B_4O_7$ (Tarvassoli-Salardini, 2004).

2.5.4 Interface inhibitions

Interface inhibition occurs due to a strong interaction between the corroding metal and the inhibitor. The adsorption of the inhibitor depends on the potential of the electrode as well as the charge on the adsorbate molecule. The protective film is a 2-D adsorbate, which can affect the corrosion reaction by one of the following mechanisms (Tavassoli-Salardini, 2004):

a. geometric blocking: In this case, an inert inhibitor blocks the surface of the metal at a high degree of coverage and forms a diffusion barrier which restricts

the access of reactants to the metal surface for example, inhibition provided by proteins,polysaccharides or compounds with hydrocarbon chains.

b. deactivation coverage: In this process, instead of the complete coverage of the metallic surface, only the active sites are covered by an inert adsorbate and the rates of the reactions (cathodic and anodic) are reduced in proportion to the extent of coverage of the reactive sites.

c. Reactive coverage: In this case, the adsorbate undergoes electrochemical reaction and primary or secondary inhibition occurs either by the adsorbate or its reaction product respectively.

Adsorption inhibition is observed when a bare metal is in contact with the adsorbate (inhibitor) and this is usually the case in acidic solutions where the condition is not favourable to oxide formation (Mansfeld, 1987). According to Tarvassolo-Salardini (2004), majority of the very effective interface inhibitors are organic compounds containing nitrogen, sulphur and oxygen. It has been found that some interface inhibitors after initial adsorption onto the metal surface, can be reduced and the reduction product may also posses some inhibitive properties.

2.6 Adsorption Isotherms

Adsorption isotherms are very important in understanding the mechanism of inhibition of corrosion of metals and alloys. The most frequently used adsorption isotherms are Langmuir, Freundlich, Temkin, Flory-Huggins and Frumkin isotherms. All these isotherms can be generalized based on equation 2.9 (Oguzie *et al.*, 2012b):

$$f(\theta, x)\exp(-2a\theta) = kC \qquad 2.9$$

where *f(θ, x)* is the configuration factor which depends upon the physical model and the assumptions underlying the derivation of the isotherm, θ is the degree of surface coverage, *C* is the inhibitor concentration in the electrolyte, *x* is the size ratio, a is the molecular interaction parameter and *k* is the equilibrium constant of the adsorption process (Ebenso *et al*., 2008; Oguzie *et al*., 2012b).

2.6.1 Langmuir adsorption isotherm

The isotherm assumes monolayer adsorption onto a surface containing a finite number of identical sites and absence of lateral interactions between the adsorbed species. It can be represented by equation 2.11:

$$C/\theta = 1/k + C \qquad 2.11$$

where *k* is the adsorption equilibrium constant, C is the concentration of the inhibitor and θ is the degree of surface coverage of the inhibitor. By plotting values of *C/θ* versus values of *C*, straight line graphs are obtained (Eddy and Ebenso, 2010; Akalezi *et al.*, 2012).

2.6.2 Freundlich isotherm

Freundlich suggested an empirical equation which describes adsorption on heterogeneous surfaces. This isotherm is based on the assumption that adsorption sites are distributed exponentially with respect to energy of adsorption and that the surface sites are subdivided into several types, each possessing a characteristic heat of adsorption (Odoemelam *et al*., 2009). This equation is presented by equation 2.12:

$$\log\theta = logk + nlogC \qquad 2.12$$

where θ is the degree of surface coverage, C is the concentration of inhibitor in solution, k is the adsorption equilibrium constant and n is the Freundlich isotherm constant (with 0 < n

< 1). By plotting values of logθ against logC, straight line graphs are obtained with slope 'n' and intercept logk.

2.6.3 Temkin adsorption isotherm

According to Temkin adsorption isotherm, the degree of surface coverage *(θ)* is related to the inhibitor's concentration *(C)* in the bulk electrolyte according to equation 2.13:

$$\exp(-2 \propto \theta) = kC \qquad 2.13$$

where *k* is the equilibrium constant of adsorption, *θ* and '*α*' is the molecular interaction parameter. Rearranging and taking logarithm of both sides gives equations 2.14:

$$\theta = -2.303log\,{}^{k}/_{2\propto} - 2.303log\,{}^{C}/_{2\propto} \qquad 2.14$$

a plot of *θ* versus *log C* gives a linear plot provided the Temkin isotherm is obeyed (Eddy and Ebenso, 2010; Adejo *et al.*, 2012).

2.6.4 Flory-Huggins adsorption isotherm

The assumptions of Flory-Huggins adsorption isotherm can be expressed as equation 2.15:

$$log\,{}^{\theta}/_{C} = logk + xlog(1-\theta) \qquad 2.15$$

where '*x*' is the number of inhibitor molecules occupying one site (or the number of water molecules replaced by one molecule of the inhibitor). A plot of *log(θ/C)* versus *log(1- θ)* is linear confirming the application of Flory-Huggins (Eddy and Ita, 2010).

2.6.5 El-Awady adsorption isotherm

The El-awady model can be expressed by equation 2.16:

$$\log\left({}^{\theta}/_{1-\theta}\right) = logK' + ylogC \qquad 2.16$$

where K is a constant related to the adsorption equilibrium constant expressed as:

$k = K'^{(1/y)}$ 2.17

where *y* is the number of the inhibitor molecules occupying one active site and *1/y = x* which is the number of active sites of the surface occupied by one molecule of the inhibitor. It has been found that values of *x* greater than unity indicates that a given inhibitor molecule would occupy more than one active site. Also, values of y > 1 imply the formation of multi-layers of inhibitor on the surface of the metal, while y < 1 indicates that a given inhibitor molecule occupy more than one active site (Noor, 2009; Li *et al.*, 2010; Adejo *et al.*, 2012).

2.6.6 Frumkin adsorption isotherm

The assumptions of Frumkin isotherm can be expressed as equation 2.18:

$$\log\left(\theta/_{1-\theta}\right) = 2.303 log k + 2 \propto \theta \quad 2.18$$

where *k* is the adsorption equilibrium constant and α is the lateral interaction term describing the molecular interaction in the adsorbed layer. When α is positive, it indicates the attractive behaviour of the surface of the metal (Eddy and Odiongenyi, 2010).

The equilibrium constant of adsorption *k*, of an inhibitor on the surface of a metal is related to the free energy of adsorption ΔGads°as according to equation 2.19:

$$k = {}^{1}/_{55.5} \exp\left(-\frac{\Delta G_{ads}}{RT}\right) \quad 2.19$$

where R is the molar gas constant, T is the absolute temperature and 55.5 is the concentration of water in solution expressed in M.

Generally, ΔG_{ads} values with magnitude much less than 40 kJ mol^{-1} have typically been correlated with the electrostatic interactions between organic molecules and charged metal surface (physiosorption), whilst those of magnitude in the order of 40 kJ mol^{-1} and above are associated with charge sharing or transfer from the organic molecules to the

metal surface (chemisorption) (Popova *et al*., 2003; Eddy and Ita, 2010; Oguzie *et al.*, 2012b).

2.7 Corrosion Inhibitors

Corrosion inhibitors are defined compounds that can reduce the rate of corrosion process of any metal through the mechanism of adsorption, which can be physical (i.e, involving the transfer of charges from charged inhibitor to a charged metal surface) or a chemical adsorption (which usually involves the transfer of electrons from the inhibitor to the vacant d-orbital of the metal).

Most corrosion inhibitors have been observed to posses one or more of the following properties (Eddy *et al*., 2010; Oguzie *et al*., 2012a, b):

a. possession of an hetero atoms in aromatic rings or long chain carbon
b. possession of polar functional groups such as –COOH, -NH_2, etc as well as π-electrons.

2.8 Green corrosion inhibitors

Eddy and Ebenso (2008) reported that green corrosion inhibitors are gotten from plant and animals which are non-toxic because they do not contain heavy metals, relatively cheap and are biodegradable. Most green corrosion inhibitors are extracts (ethanol, aqueous, methanol, etc) of plants and animal products. The use of green inhibitors is preferred because of their eco-friendly nature. In view of these, several extracts of plants have been successfully utilized for the inhibition of the corrosion of metals in acidic, neutral or alkaline media.

2.8.1 Green corrosion inhibitors: Plant extract

Eddy *et al*. (2009c) study the inhibition potentials of ethanol extract of *Lasianthera africana* for the corrosion of mild steel H_2SO_4 using gasometric, thermometric, gravimetric and FTIR methods. The inhibitive properties of the extract were attributed to enhancement in adsorption of the inhibitor on mild-steel surface by saponin, alkaloid, tannin, flavanoid, cardiac glycoside, and anthraquinone in the extract. Also, adsorption of the inhibitor was found to be exothermic, spontaneous, and supported the Langmuir and Temkin adsorption models. Synergistic study indicated that of the investigated halides (KBr, KCl and KI), only KCl enhanced the adsorption of the inhibitor while (KBr and KI) antagonized its adsorption. Based on the decrease in efficiency of the inhibitor with temperature, with values of activation energy and free energy of adsorption below the threshold values of -40 and 80 kJ mol^{-1}, respectively, a physical adsorption mechanism was proposed for the adsorption. Alkaloid extract of *Annona squamosa* plant has been studied by Lebrini *et al*. (2010) as possible corrosion inhibitor for C38 steel in 1 M HCl using potentiodynamic polarization and AC impedance methods. Inhibition efficiency was found to increase with extract concentration. Polarization studies showed that *Annona squamosa* extract was a mixed type inhibitor, it indicated that the extract was temperature dependent and its addition led to an increase in the activation energy showing a physical adsorption between the metal surface and the extract.

Okafor *et al.* (2012) investigated the action of ethanol, acid and toluene extracts from *Artemisia annua* and *Artemisinim* on mild steel corrosion in H_2SO_4 solutions using gravimetric and gasometric techniques. The extracts functioned as good inhibitors, and their inhibition efficiencies followed the trend EEAA > AEAA > TEAA. Inhibition

efficiency was also found to increase with increase in inhibitor concentration and decreased with increase in temperature. The adsorption of the inhibitors was consistent with Langmuir isotherm. Uwah *et al*., (2013) also investigated the inhibitive performance of ethanol extracts of *Andrographis paniculata* (King bitter) EEAP and *Vernonia amygdalina* (bitter leaf), EEVA on the corrosion of mild steel in 2 M HCl solution at 30, 40, 50 and 60^0C using weight loss and hydrogen evolution techniques. The results indicated that both plant extracts inhibit the corrosion of mild steel in the acid solution by adsorption. EEAP exhibited higher maximum inhibition efficiency 89.7% than EEVA 76.9% at 4.0g/l inhibition efficiency was found to increase with temperature. Adsorption of both plant extracts on the mild steel coupon was found to obey Langmuir adsorption isotherm.

Ebenso *et al*. (2008) in there study reported on the corrosion inhibition of mild steel by ethanol extract of *Piper guinensis* (EEPG) using gravimetric, gasometric and thermometric methods. The results of the study indicated that various concentrations of ethanol extract of *Piper guinensis* (EEPG) inhibit mild steel corrosion. Inhibition efficiency of the extract is found to vary with concentration, temperature and period of immersion. Values of activation energy of the inhibited corrosion reaction of mild steel are greater than the value obtained for the blank. Thermodynamic consideration indicated that the adsorption of *P. guinensis* extract (EEPG) on mild steel surface is spontaneous and occurs according to Langmuir adsorption isotherm. Physical adsorption mechanism was proposed for the adsorption of the inhibitor from the trend of the inhibition efficiency with temperature and the values of some kinetic and thermodynamic parameters obtained.

Eddy *et al*. (2009e), also study the inhibitive and adsorptive characteristics of ethanol extract of *Gnetum africana* for the corrosion of mild steel in H_2SO_4 using weight

loss, gasometric, thermometric, and IR methods of monitoring corrosion and found that ethanol extract of *Gnetum africana* is a good adsorption inhibitor for the corrosion of mild steel in H_2SO_4. The inhibitive property of the extract was attributed to the presence of alkaloid, saponin, tannin, terpene, anthraquinone, cardiac glycoside, and alkaloid in the extract. The adsorption of the inhibitor on mild steel surface was exothermic, spontaneous and is consistent with the mechanism of physical adsorption. In addition, Langmuir and Temkin adsorption isotherms best described the adsorption characteristics of the inhibitor. Efforts to improve the adsorption of the inhibitor through synergistic combinations with halides indicated that only KCl may enhance the efficiency of the inhibitor. The study provides information on the use of ethanol extract of *Gnetum africana* as a corrosion inhibitor for mild steel.

Odiongenyi *et al*. (2009) investigated the inhibitive and adsorption properties of ethanol extract of *Vernonia amygdalina* for the corrosion of mild steel in H_2SO_4 using weight loss, thermometric, gasometric and IR methods of monitoring corrosion. The results obtained revealed that ethanol extract of *Vernonia amygdalina* inhibited the corrosion of mild steel. The inhibition efficiency of the extract increased as the concentration of the extract increases. The inhibitor was found to function by being adsorbed on the surface of mild steel. The adsorption of the inhibitor followed the Langmuir adsorption isotherm. IR spectra of the corrosion product (without inhibitor), the extract and the corrosion product (with the inhibitor) confirmed that ethanol extract of V*ernonia amygdalina* is an adsorption inhibitor. Phytochemical studies also showed that ethanol extract of *Vernonia amygdalina* contains tannin, saponnins, flavanoid and anthraquinone, all of them contributing to the

corrosion inhibition. Physical adsorption mechanism was proposed from the values of some of the thermodynamic parameters obtained.

Eddy and Mamza (2009) studied the corrosion of mild steel in H_2SO_4 using gravimetric, gasometric and IR methods. The results indicated that the rate of corrosion of mild steel in H_2SO_4 increases with increase in the concentration of the acid and that ethanol extracts of the seeds and leaves of *Azadirachta indica* inhibited the corrosion of mild steel in H_2SO_4. Inhibition efficiencies of the leaves and seeds extract ranged from 82.62 to 94.24% and from 60.55 to 84.78%, respectively. The inhibition potentials of these extracts were attributed to the presence of tannin, saponin, glycoside, anthraquinone, flavonone and other phytochemical constituents in the extracts. IR study indicated that the inhibitors are adsorptive in nature and that the adsorption of the inhibitors on mild steel surface is exothermic, spontaneous and consistent with the assumptions of Flory-Huggins adsorption isotherm. Based on the values of the activation, free energy of adsorption and the variation of inhibition efficiency with temperature, a physical adsorption mechanism was proposed for the adsorption of ethanol extract of leaves and seeds of *Azadirachta indica* on the surface of mild steel. Eddy *et al*. (2009d) also study the inhibitive and adsorption properties of ethanol extract of *Terminalia catappa* for the corrosion of mild steel in H_2SO_4 using weight loss, hydrogen evolution, and infra red methods. Ethanol extract of *T. catappa* was found to be a good adsorption inhibitor for the corrosion of mild steel in H_2SO_4. The inhibition efficiency of the inhibitor increased with increasing concentration but decreased with increasing temperature. The inhibition potential of ethanol extract of *T. catappa* was attributed to the presence of saponnin, tannin, phlobatin, anthraquinone, cardiac glycosides, flavanoid, terpene, and alkaloid in the extract. The adsorption of the inhibitor on mild steel

surface was exothermic, spontaneous and was best described by Langmuir adsorption model. From the calculated values of activation energy, free energy of adsorption and the trend in the variation of inhibition efficiency with temperature, the mechanism of adsorption of the inhibitor was physical adsorption.

Saratha and Vasudha (2010), investigated the corrosion inhibition efficiency of acid extract of dry *Emblicaofficinalis* leaves on mild steel in HCl using weight loss, Potentiodynamic polarization and impedance studies. The results indicated that the leaves of *Emblicaofficinalis* was found to be good corrosion inhibitors of mixed type and having good inhibition efficiency of 87.9% at 2% v/v inhibitor concentration. Corrosion inhibition was due to the spontaneous adsorption from the free gibbs energy value, it was also found that the experimental data fitted the Langmuir, Temkim, Freundlich and Flory-Huggins adsorption isotherms.

Oguzie (2008) studied the inhibitory potentials of calyx extract of *Hibiscus sabdariffa* for the corrosion of mild steel in HCl and H_2SO_4 solutions, using gasometric method and found that the inhibition efficiency of the inhibitor increased with increasing concentration of the inhibitor. The adsorption of the inhibitor on mild steel surface followed the Langmuir adsorption model and supported the mechanism of physical adsorption. Eddy and Odoemelam (2009) used FTIR, gravimetric and thermometric methods to study the inhibitive properties of ethanol extract of *Aloe vera* and reported inhibition efficiencies ranging from 65.08 to 89.67 %. The adsorption of the inhibitor on mild steel surface was spontaneous and supported the mechanism of physical adsorption.

Noor (2009) studied the inhibitory potentials of aqueous extract of *Hibiscus sabdariffa* leaves for the corrosion of mild steel in 0.5 M NaOH using chemical and electrochemical techniques. Electrochemical measurements indicated that aqueous extract of *Hibiscus sabdariffa* acted as a mixed inhibitor and the adsorption of the inhibitor on aluminum surface supported the mechanism of physical adsorption and was best explained by the Langmuir and Dubinin–Radushkevich adsorption isotherms. Hazwan-Hussin and Jain-Kassim **(**2011) analyzed the inhibitive effect of the ethyl acetate extract of *Uncaria gambir* on the corrosion of mild steel in 1M HCl solution by weight loss measurement, potentiodynamic polarization and electrochemical impedance spectroscopy techniques. The presence of this catechin-containing extract reduces remarkably the corrosion rate of mild steel in acidic solution. The results from this corrosion test clearly revealed that the extract behaves as a mixed type corrosion inhibitor with the highest inhibition at 1000 ppm. Akalezi *et al* (2012) reported on the assessment of the inhibitive action of *Petersianthus macrocarpus leave* extract on corrosion of mild steel in 1 M HCl and 0.5 M H_2SO_4 solutions was done using gravimetric, electrochemical impedance and potentiodynamic methods. The inhibition efficiency of the inhibitor increased with increasing extract concentration. Results indicated that the extracts functioned as a good inhibitor in both corrodent solutions. Temperature studies in the range 313 - 333K reveal increase in inhibition efficiency of the extract with rise in temperature. The authors proposed a mechanism of chemical adsorption. The adsorption characteristics of the inhibitor were found to obey Langmuir isotherm and supported chemiosorption.

Ilomaeke *et al.* (2013), studied the effectiveness of leaves extract of *Emilia sonchifolia* and *Vitex doniana* as corrosion inhibitors of mild steel in 2.5 M HCl medium

using gasometric method at 30°C and 60°C**.** Adsorption of *Emilia sonchifolia* leaves extract on the surface of the mild steel followed Langmuir, Temkin and Freundlich adsorption isotherm while adsorption of *Vitex donania* leaves extract on the surface of the mild steel obeyed Langmuir and Temkin adsorption isotherm. The adsorption of the inhibitor was through physical means.

Apart from the above listed studies, other researchers have successfully used different plant exracts as corrosion inhibitors (Nwosu *et al.*, 2013; Onuegbu *et al.*, 2013; Patel *et al.*, 2013; Achebe *et al*., 2012; Abiola *et al*., 2007; Abdallah, 2004a; Bendahou *et al.*, 2006; Bouyanzer and Hammouti, 2004; Chetouani *et al*., 2004; Ebenso *et al*., 2008, 2004; Ajayi, 2003; Ebenso and Ekpe, 1996; Eddy and Ebenso, 2008; Ekpe *et al*., 1994; El-Etre, 1998, 2003, 2006; El-Etre and Abdallah, 2002; Kliskic *et al*., 2000; Krajewka *et al*., 2002; Oguzie, 2005,2006, 2007; Oguzie *et al*., 2006, 2007; Okafor *et al*., 2005, 2007, 2008; Okafor and Ebenso, 2007; Umoren *et al*., 2006a, 2008a, 2008b; Umoren and Ebenso, 2008, 2007; Sethuraman *et al.*, 2005*;* Rajendran *et al*., 2005 ; Zucchi and Omar, 1985; Zucchi *et al*., 1978).

2.8.2 Green corrosion inhibitors: Amino acids

Some amino acids have been found to be good inhibitors for the corrosion of mild steel in HCl. Amino acids are molecules that contain both amino and carboxylic acid functional groups. The acids are non toxic, contain $–NH_2$ and COOH functional groups and completely soluble in aqueous media and can be produced with high purity at reduced costs. They are therefore expected to be good inhibitors for the corrosion of mild steel in H_2SO_4 solutions.

Badawy *et al*. (2006), studied the corrosion inhibition of Cu–Ni alloys in aqueous chloride solutions using amino acids which are environmentally friendly materials. The corrosion rate was calculated in the absence and presence of the corrosion inhibitor using polarization and impedance techniques. The inhibition efficiency of the different amino acids was also calculated. The experimental results have shown that a simple amino acid like glycine can be used as an efficient corrosion inhibitor for the Cu–Ni alloys in neutral chloride solutions. An inhibition efficiency of about 85% was achieved at very low concentrations of the amino acid (0.1 mM). For low Ni content alloy (Cu–Ni), 2.0 mM cysteine showed a remarkable high (~96%) corrosion inhibition efficiency. The experimental impedance data were fitted to theoretical data according to a proposed equivalent circuit model for the electrode/electrolyte interface, and the mechanism of the corrosion inhibition process was suggested. Different adsorption isotherms were tested and the corrosion inhibition process was found to depend on the adsorption of the amino acid molecules and/or the deposition of corrosion products on the alloy surface. The adsorption free energy of cysteine on Cu–Ni (-37.81 kJ mol^{-1}) indicated a strong physical adsorption of the inhibitor on the alloy surface. Olivares-Xometl *et al*. (2008) investigated the potentials of new compounds of alkylamides derived from -amino acids were tested as corrosion inhibitors for carbon steel in an aqueous solution of hydrochloric acid. Electrochemical testing was carried out using polarization scans and weight loss measurements. Polarization scans indicated that the compounds acted as mixed corrosion inhibitors with an efficiency of 80–90% when dissolved in the testing solution at ≥50 ppm, whereas gravimetric results displayed a similar tendency. Microtox testing indicated a correlation with the molecular structure of inhibitors. Apparently, a long aliphatic chain (C

> 12) promoted not only higher corrosion efficiency, but also a higher toxicity. The higher efficiency of dodecyl amine of tyrosine was apparently derived from its longer aliphatic chain, with some contribution from its phenyl ring, which reinforces the molecular interactions of type bonding to the d orbital metal favouring film formation.

Aksot and Bilgic (1992) investigated the inhibitory effect of thirteen different amino acids on the corrosion of nickel in sulphuric acid medium. Corrosion current densities were determined by the extrapolation of the cathodic Tafel region to the corrosion potential. The effect of the amino acids on the passivity of nickel was examined by anodic current-potential curves. It was shown that some amino acids are inhibitors Ni corrosion to various degrees while others were found to accelerate corrosion rate. El-Rabiee *et al*. (2008) studied the electrochemical behavior of vanadium in amino acid using open-circuit potential measurements, polarization techniques and electrochemical impedance spectroscopy (EIS). The effect of chloride ion on the corrosion inhibition efficiency especially in acid solutions was investigated. In neutral and basic solutions, the presence of amino acids increases the corrosion resistance of the metal. The electrochemical behavior of V before and after the corrosion inhibition process has shown that some amino acids like glutamic acid and histidine have promising corrosion inhibition efficiency at low concentration (~= 25 mM). The inhibition efficiency (η) was found to depend on the structure of the amino acid and the constituents of the corrosive medium. The corrosion inhibition process was based on the adsorption of the amino acid molecules on the metal surface and the adsorption process follows the Freundlich isotherm. The adsorption free energy for valine on V in acidic solutions was found to be −9.4 kJ/mol which shows strong physical adsorption of the amino acid molecules on the vanadium surface. Zhang *et al*.

(2008) investigated the inhibition effect of four amino acids such as aspartic acid (Asp), glutamic acid (Glu), asparagines (Asn), and glutamine (Gln) towards the corrosion of copper in 0.5 M hydrochloric acid solution using potentiodynamic polarization and EIS methods. The measurements indicated that these compounds have some protective effect against copper corrosion in 0.5M HCl solution. The inhibition efficiency of these compounds was found to increases in the order Gln > Asn > Glu > Asp and tend to increase with increase in the concentration of the inhibitors. Addition of iodide ions into 10mM glutamine solution increases the protection efficiency, reaching a maximum value of 93.74% for 5mM KI. The mechanism of physical adsorption was proposed for these reactions and was consistent with the Langmuir adsorption model. Spah *et al*. (2009) used electromotive force measurements to study the inhibition potentials of some amino acids and obtained results which indicated that the acids are potential corrosion inhibitors.

Asshassi-Sorkhabi *et al*. (2004) investigated the inhibitory effect of three amino acids (alanine (Ala), glycine (Gly) and leucine (Leu)) against steel corrosion in HCl solutions using potentiodynamic polarization method. Corrosion data such as corrosion rate, corrosion potential (Ecorr) and corrosion resistance (Rp) were determined by extrapolation of the cathodic and anodic Tafel region. Adsorption isotherm was investigated by weight loss measurement. The effect of inhibitor concentration and acid concentration against inhibitor action was investigated. The inhibition efficiency depends on the type of amino acid and its concentration. The inhibition effect ranged from 28 to 91%. The amino acids acted as a corrosion inhibitor in HCl solution through adsorption on the steel surface and the adsorption also supported the Langmuir adsorption isotherm. Barouni *et al*. (2008) also investigated the inhibition effect of five amino acids such as

valine (Val), glycine (Gly), lysine (Lys), arginine (Arg) and cysteine (Cys) on the corrosion of copper in molar nitric solution using weight loss and electrochemical polarization measurements. The results obtained indicated that valine and Glycine accelerated the corrosion process; but Arginine, Lysine and cysteine inhibited the corrosion phenomenon. Cysteine was found to be the best inhibitor. Correlation between the quantum chemical calculations and inhibition efficiency was discussed using semi-empirical methods (AM1 and MNDO).

The inhibition effect of three amino acids namely: proline (Pro), methionine (Met) and trytophane (Trp) towards the corrosion of Pb–Sb–Se–As alloy in H_2SO_4 solution was study using linear polarization and weight loss measurements methods(Ghasemi and Tizpar, 2006). The effect of inhibitor concentration and temperature against inhibitor action was investigated. It was found that these inhibitors acted as good inhibitors for the corrosion of lead alloy in H_2SO_4 solution. Increasing inhibitor concentration increases the inhibition efficiency. It was found that adsorption of the amino acids on lead alloy surface follows Langmuir isotherm. Asshassi-Sorkhabi *et al*. (2005) also determined the inhibition effect of alanine, leucine, valine, proline, methionine, and tryptophan towards the corrosion of aluminum in 1 M HCl + 1 M H_2SO_4 solution using weight loss measurement, linear polarization and SEM techniques. The results of these techniques were comparable. The effect of inhibitor concentration and temperature against inhibitor action was established. It was found that these amino acids acted as good inhibitors for the corrosion of aluminum in 1 M HCl + 1 M H_2SO_4 solution. Increasing inhibitor concentration increases the inhibition efficiency and with increasing temperature the inhibition efficiency decreases. It was also found that adsorption process followed Langmuir and Frumkin isotherms.

Moretti *et al*. (2004) also study the inhibition effects of tryptamine (TA) on the corrosion behaviour of ARMCO iron in 0.5 M deaerated H_2SO_4 using potentiodynamic curves (PCM) and electrochemical impedance spectroscopy (EIS). TA was found to be an effective ARMCO iron inhibitor, even at higher temperature and for long term exposure. Inhibition efficiencies, calculated by PCM and EIS, ranged from 90% to 99% and did not diminish over time and as the temperature increased. TA adsorption followed Bockris–Swinkels adsorption isotherm. Silva *et al*. (2006) also deetermine the effect of cysteine on the corrosion of 304L stainless steel in 1 M H_2SO_4 using open-circuit potential measurements, anodic polarization curves, electrochemical impedance spectroscopy (EIS) and scanning electron microscopy (SEM). The results obtained indicated that the effect of cysteine was concentration dependent. Other studies are those reported by Kiani *et al*. (2008) and Zerfaoui *et al*. (2004). Goa and Liang (2007) evaluated the electrochemical performance of 1-diethylamino-propan-2-ol (EAP) and 1, 3-bis-diethylamino-propan-2-ol (DEAP) for brass in simulated atmospheric water using potentiodynamic curves and electrochemical impedance spectroscopy (EIS). The experimental results indicated that the investigated compounds retarded the anodic dissolution of brass. The experimental data was partly supported by density functional theoretical (DFT) and quantum chemical analysis.

2.8.3 Triazoles and benzotriazoles derivatives as corrosion inhibitors

Selvi *et al*. (2003) also synthesized some benzotriazole derivatives (N-[1-(benzotriazolo-1-yl)-alkyl] aryl amine (BTMA), N-[1-(benzotriazolo-1-yl)aryl] aryl amine (BTBA), and 1-hydroxy methyl benzotriazole (HBTA) and found that these compounds possess excellent inhibition properties of corrosion of mild steel in 0.5 M H_2SO_4 at room

temperature using potentiodynamic polarization and AC impedance methods. These compounds were found to act as mixed type inhibitors. Among the compounds, HBTA exhibited the best inhibiting performance giving more than 95% IE. Also, Rct values were found to have increased while those of Cdl decrease with increase in the concentration of benzotriazole. The observed trend was attributed to the adsorption of benzotriazole on the metal surface. Gopi *et al.* (2007) studied the corrosion inhibition of mild steel by means of newly synthesized triazole phosphonates 3-vanilidene amino 1, 2, 4-triazole phosphonate (VATP), 3-anisalidene amino 1, 2, 4-triazole phosphonate (AATP) and 3-paranitro benzylidene amino 1, 2, 4-triazole phosphonate (PBATP) together with cetyl trimethyl ammonium bromide (CTAB) in natural aqueous environment using weight loss, potentiodynamic polarisation and AC impedance measurements. Addition of molybdate was noticed to increase the inhibition efficiency of triazole in a synergistic manner. Results from experimental observations indicated VATP as a better corrosion inhibitor for mild steel in aqueous solution. Additionally the formulation consisting of VATP, sodium molybdate and CTAB offered good corrosion inhibition efficiency. Khadom *et al*. (2009) investigated the adsorption of 4-amino-5-phenyl-4H-1, 2, 4-triazole-3-thiol (APTT) as a corrosion inhibitor for mild steel in hydrochloric acid (HCl) solution using the weight loss technique. The degree of surface coverage by APTT was used to calculate the free energy of adsorption, using Bockris-Swinkels isotherm. The dependence of free energy of adsorption, on the surface coverage, was ascribed to the surface heterogeneity of the adsorbent. The adsorption of APTT molecules on the surface occurred without modifying the kinetics of the corrosion process.

Matheswaran and Ramasamy (2010) studied benzotriazole as an inhibitor for the corrosion inhibition of mild steel in 1 N citric acid using weight loss method. The results obtained indicated that the corrosion inhibition efficiency of the benzotriazole varied with the temperature and acid concentrations. Also, it was found that the corrosion inhibition behaviour of benzotriazole was better when the concentration of inhibitor was increased. Kinetic treatment of the results showed first order kinetics. Li *et al*. (2011) synthesized two triazole derivatives [1-phenyl-2-(5-(1,2,4) triazol-1-ylmethyl-(1,3,4) oxadizaol-2-ylsulphanyl)-ethanone (PTOE) and 2-(4-tert-butyl-benzylsulphanyl)-5-(1,2,4) triazol-1-ylmethyl-(1,3,4) oxadiazole (TBTO)] as new corrosion inhibitors for the corrosion of mild steel in 1 M hydrochloric acid. The inhibition efficiencies of the different inhibitors were evaluated using weight loss and electrochemical techniques such as electrochemical impedance spectroscopy (EIS) and polarization curves. The results obtained from electrochemical investigation revealed that these compounds acted as mixed-type inhibitors retarding the anodic and cathodic corrosion reactions and did not change the mechanism of either hydrogen evolution reaction or mild steel dissolution. The adsorption of the inhibitors obeyed the Langmuir adsorption model. The effect of molecular structure on the inhibition efficiency of the inhibitors was investigated using *ab initio* calculations while electronic properties such as the energy of the highest occupied molecular orbital (HOMO), the energy of the lowest unoccupied molecular orbital (LUMO), dipole moment (μ) and molecular orbital densities were also calculated.

2.8.4 Dyes as corrosion inhibitors

Oguzie *et al*. (2004) to study the inhibitory properties of congo red (CR) dye for the corrosion of mild steel in aerated sulphuric acid solution between 30-60°C. The effect of

addition of halide salts such as KCl, KBr and KI was also investigated. Inhibition efficiency was found to increase with increase in the concentration of CR but decreased with increase in temperature. Corrosion activation energies of 82.98 and 96.92 kJ mol^{-1} were observed in the absence and presence of CR, respectively. The observed corrosion data suggested that inhibition of mild steel corrosion is due to physical adsorption of the CR molecules on the metal surface. The adsorption of CR obeyed Flory–Huggins isotherm. Inhibition antagonism and synergism (KCl < KBr <KI) were observed at 30 and 60°C respectively on addition of halide salts to inhibited systems containing CR. The inhibition efficiency of CR in the presence of halides increased with rise in temperature but corrosion activation energy in these systems decreased from 96.92 to 40.63 kJ mol^{-1}. These observations indicate a chemical adsorption mechanism, thus suggesting that the halide ions reversed the mechanism of CR adsorption over the concentration range studied. The calculated values of heat of adsorption confirm physisorption and chemisorption mechanisms respectively for CR adsorption in the absence and presence of halides.The inhibitive properties of some organic dyes have been investigated by some researchers. Abdeli *et al.* (2009) studied the inhibiting behaviour of nile blue and indigo carmine organic dyes on corrosion of mild steel in 1 M HCl, using weight loss, potentiodynamic polarization and electrochemical impedance spectroscopy techniques. Polarization curves indicated that both inhibitors are mixed anodic–cathodic in nature, and Langmuir isotherm was found to be the best isotherm that described the adsorption behaviour.

2.8.5 Schiff bases as corrosion inhibitors

Weight loss and thermometric methods were used by Upadhyay *et al.* (2007) to study the inhibitory effect of synthesised Schiff's bases (including:N-(furfurilidine) – 4-methoxy aniline (SB1), N-(furfurilidine) – 4- methylaniline (SB2), N- (salicylidine) – 4-

methoxy aniline (SB3), N-(cinnamalidine) – 4 –methoxy aniline (SB4) and N-(cinnamalidine) - 2-methylaniline (SB5)) for the corrosion of mild steel in sulphuric acid solutions. The results obtained by both methods were in good agreement with each other and that the inhibition efficiency depended upon the concentration of inhibitor and that of the acid. Maximum inhibition efficiency was shown at highest concentration of Schiff's bases at the highest concentration of acid. The corrosion inhibition of mild steel in 0.5 M sulphuric acid by two newly synthesized Schiff bases namely 4-X-2-{[2-(2-pyridin-2-yl-ethylsulfanyl) ethylimino] and methyl}-phenol [X = $–NO_2$ and –OMe] have been investigated in the temperature range 298 – 318K using Tafel polarization and electrochemical impedance spectroscopy (EIS) methods (Hosseini *et al.,* 2009). The Temkin isotherm was found to provide an accurate description of the adsorption behaviour of the Schiff bases.

CHAPTER THREE

3.0 EXPERIMENTAL

3.1 Materials

Mild steel and aluminium sheet were the materials used for the study and their compositions as determined by the quantiometric method are presented in Tables 3.1 and 3.2. These materials were mechanically press-cut into different coupons, each of dimension, 3x2x0.12mm for weight loss investigation and 1cmx1cm for electrochemical study. The coupons were wet polished with different grades of SiC abrasive paper (#400 to #1200), degreased by washing with ethanol, cleaned with acetone and allowed to dry in the air before preservation in a desiccator. All reagents used for the study were analar grade and double distilled water was used for their preparation. Acid solutions of 1.0 M (HCl) and 0.5 M (H_2SO_4) were used for weight loss and polarization studies after they had been standardized, while the concentration range for the inhibitors was 0.1g/l to 0.5g/l respectively.

Table 3.1: Nominal Elemental Composition of Aluminium Sheet

Element	Mn	Fe	Si	Cu	Pb	Ti	V	Others	Al
Weight %	0.392	0.55	0.363	0.077	0.064	0.026	0.009	0.019	98.5

Table 3.2: Nominal Elemental Composition of Mild Steel Sheet

Element	Mn	Si	P	C	Fe
Weight %	0.6	0.03	0.36	0.15	98.86

3.2 Methods

3.2.1 Plants extraction

Sample leaves of *Phyllanthus amarus; Paullinia pinnata; Parinari polyandra; Boscia senegalensis* were obtained from Zango- shanu, Sabon Gari Local Government Area, Kaduna State, Nigeria. The samples were later taken to Herbarium in Department of Biological Sciences, Ahmadu Bello University Zaria Nigeria for identification and were assigned batch numbers. The 500g of the leaves were dried, ground and soaked in 5 L of ethanol solution for 48 hours. After 48 hours, the samples were filtered. The ethanol was then evaporated off. The stock of the extract so obtained were used in preparing different concentrations of the extract by dissolving 0.1, 0.2, 0.3, 0.4, and 0.5g of the extracts in 1L of various concentration of the acid (Eddy and Odoemelam, 2009; Arora *et al*., 2007).

3.2.2 Chemical analysis

Phytochemical analysis of the ethanol and aqueous extract of the sample was carried out according to the method reported by Qureshi and Eswar (2010). Frothing and Na_2CO_3 tests were used for the identification of saponin, bromine water, ferric chloride tests were used for the identification of tannin while Leberman's and Salkowski's tests (chloroform solution of the extracts with sulphuric acid and acetic acid) were used for the identification of cardiac glycodises while Dragendorf, Meyer, and Hager's reagent tests (solution of potassium bismuth iodide, potassium mercuric iodide and saturated solutions of picric acid) were used for the identification of alkaloid.

3.2.3 Gravimetric method

A previously weighed metal (mild steel) coupon was completely immersed in 250 ml of the test solution in an open beaker. The beaker was covered with aluminium foil and inserted into a water bath maintained at 303K. After every 24 hours, the corrosion product was removed by washing each coupon (withdrawn from the test solution) with solution containing 50% NaOH and 100g L^{-1} of zinc dust. The washed coupon was rinsed in acetone and air dried before re-weighing. The experiment was repeated at 313K, 323K and 333K respectively. In each case, the difference in weight for a period of 168 hours was taken as the total weight loss. From the average weight loss (mean of three replicate analysis) results, the inhibition efficiency (%I) of the inhibitor, the degree of surface coverage (θ) and the corrosion rate of the mild steel and aluminium (CR) were calculated using equations 3.1, 3.2 and 3.3 (Eddy and Ebenso, 2010);

$$\% I = \frac{W_2 - W_1}{W_2} \times 100 \qquad 3.1$$

$$\theta = {}^{\%\, I}/_{100} \qquad 3.2$$

$$CR = \Delta W / At \qquad 3.3$$

where W_2 and W_1 are the weight losses (g) for mild steel in the absence and presence of the inhibitor respectively, θ is the degree of surface coverage of the inhibitor, $\Delta W = W_2 - W_1$, A is the area of the mild steel and aluminium coupon (cm^2), t is the period of immersion (hours) and ΔW is the weight loss of mild steel and aluminium after time, t.

The effect of temperature on the corrosion of aluminium and mild steel in the absence and presence of various concentration of plants extract was investigated using the Arrhenius transition state equations 3.4 and 3.5.

$$logCR = logA - \frac{Ea}{2.303RT} \quad 3.4$$

$$\log\left(\frac{CR}{T}\right) = \left\{\log\left(\frac{R}{hN_A}\right) + \frac{\Delta Sa}{2.303R}\right\} - \frac{\Delta Ha}{2.303RT} \quad 3.5$$

where CR is the corrosion rate of the metal, A is the Arrhenius or pre-exponential factor, E_a is the activation energy (i.e. the minimum energy needed before the corrosion reaction of the metal can proceed), R is the universal gas constant, T is the temperature of the system, N_A is the avogadros gas constant, h is the plank constant, ΔS_a is the entropy of activation and ΔH_a is the enthalpy of activation (Dahmani *et al*., 2010 and Singh *et al*., 2010).

Another thermodynamic parameter which can further be used in verifying adsorption mechanism in a corrosion inhibition process is the heat of adsorption, Q_{ads}. The heat of adsorption of the inhibitors was calculated using the equation 3.6 (Eddy, 2009a, b; Oguzie *et al*., 2012b).

$$Qads = 2.303R\left\{\log\left(\frac{\theta 2}{1-\theta 2}\right) - \log\left(\frac{\theta 1}{1-\theta 1}\right)\right\}\left(\frac{T2xT1}{T1-T2}\right) kJmol^{-1} \quad 3.6$$

where R is the universal gas constant, T_2 and T_1 is the temperature of system at 333K and 303K, θ_2 and θ_1 are the degree of surface coverage at this temperature.

It is also significant to note that the value of the adsorption equilibrium constant obtained from the intercept of each adsorption isotherm is related to the free energy of adsorption according to the equation.

$$\Delta G^{o}_{ads} = -2.303RTlog(55.5k_{ads}) \quad 3.7$$

where R is the universal gas constant, T is temperature of the system, k_{ads} is the adsorption equilibrium constant and 55.5 is the molar volume of water.

3.2.4 Fourier transform infrared spectrophotometery

IR analyses of the inhibitor and that of the corrosion products (in the presence and absence of the respective inhibitors) were carried out using a SHIMADZU, FTIR-8400S Fourier Transform Infrared Spectrophotometer. Each coupon was separately dipped in 250 mL of 1.0 M (HCl) and 0.5 M (H_2SO_4) of acid-inhibitor concentration respectively for 7 days to form an adsorbed layer after which they were removed, dried and scraped with a sharp razor blade taken for analysis. The samples were prepared using KBr and the analysis was done by scanning the sample through a wave number range of 400-4500 cm^{-1} (Eddy and Odoemelam, 2008; Eddy *et al.*, 2009a; Enenebeaku, 2011; Oguzie *et al*., 2012).

3.2.5 Scanning electron microscopy

Surface morphologies of the mild steel and aluminium coupons before and after inhibition were studied using a JSM-5600 LV scanning electron microscope of JEOL, TOKYO, Japan. 1 cm x 1 cm coupons were dipped separately in each of the following: blank solutions and 1 M and 0.5 M of acid-inhibitor (HCl and H_2SO_4 respectively) solutions for 7 days. The coupons were removed, rinsed with distilled water and dried in the air. Each sample was mounted on a metal stub and sputtered with gold in order to make the sample conductive. Scanned images were taken at an accelerating voltage of 2.00 and 15.00 kV (Enenebeaku, 2011).

3.2.6 Linear polarisation resistance

Linear polarization measurement was used to determine the rate of corrosion of the metals in the presence of the inhibitor-acid solution. All the measurement was done in an Autolab frequency response analyzer (FRA) coupled to potentiostat that was connected to a computer system. A glass corrosion cell kit with a platinum counter electrode, a saturated Ag/Ag reference electrode and aluminium and mild steel sample as working electrode. The working electrodes samples were positioned at the glass corrosion cell kit, leaving 1 cm^2 surfaces in contact with the solution. Polarization test were carried out in 1.0 M HCl and 0.5 M H_2SO_4 solution at room temperature under static solution using a potentiostat (model: AuT71791 and PGSTAT 30) with a scan rate of 0.003V/sec. From the Tafel corrosion results, the inhibition efficiencies, corrosion rate and linear polarization resistance were obtained.The inhibition efficiencies were calculated using equation 3.8 and 3.9 repectively:

$$\%I = \left(1 - \frac{i_{inh}}{i_{corr}}\right) \times 100 \qquad 3.8$$

$$\%I = \frac{R_{ct(Inh)} - R_{ct}}{R_{ct(Inh)}} \times \frac{100}{1} \qquad 3.9$$

where i_{corr} and i_{inh} are the corrosion currents in the absence and presence of the inhibitor respectively and R_{ct} and $R_{ct(inh)}$ are the uninhibited and inhibited charge transfer resistance respectively (Oguzie *et al*, 2012; Quraishi *et al*., 2008; Cabot *et al*., 1991).

3.3 Computational and Theoretical Considerations

3.3.1 Quantum chemical calculations

The electronic structure of isolated compounds from the extracts, including the distribution of frontier molecular orbitals E_{HOMO} and E_{LUMO}, Fukui indices were assessed, with a view to establishing the active sites as well as local reactivity of the molecule. The simulations were performed by means of the Density Functional Theory (DFT) electronic program DMol^3 using the Mulliken population analysis in the Material Studio 7.0 software. DMol^3 permits analysis of the electronic structures and energetics of molecules, solids and surfaces using DFT. Electronic parameters for the simulations include restricted spin polarization using the DND basis set and the Perdew Wang local correlation density functional. Local reactivity of the studied compounds was analysed by means of the Fukui indices (FI) to assess site of nucleophilic and electrophilic attack (Khaled, 2010a; Enenebeaku, 2011; Oguzie *et al*., 2012c; Cardoso *et al*., 2007).

3.3.2 Molecular dynamics simulation

In order to sample many different low energy configurations and identify the low energy minima, molecular dynamics (MD) simulation of the interactions between a single molecule of interest and Fe/Al surface was performed using Forcite quench molecular dynamics in the Material Studio (MS) modelling 7.0 software. Calculations were carried out using COMPASS forcefield and Smart algorithm in a simulation box 17Å x 12 Å x 28 Å with a periodic boundary condition, to model a representative part of the Fe/Al slab and a vacuum layer of 20Å height. The Fe/Al crystal was cleaved along the (110) plane with a fractional depth of 3.0Å. The (110) plane was chosen because it is more densely packed and has the most stabilisation compared to Fe/Al (111) and Fe/Al (100) surfaces with

relatively open structures. We have left out solvent and charge effects in all our simulations and performed the calculations at the metal/vacuum interface.

The geometry of the bottom layers were constrained before optimizing the Fe/Al (110) surface which was subsequently enlarged into a 10 x 9 supercell to avoid edge effects. Temperature was fixed at 350 K which represents a trade off between a system with too much kinetic energy where the molecule desorbs from the surface and a system with kinetic energy for the molecule to move around the surface. Temperature was fixed with the NVE (microcanonical) ensemble with a time step of 1 fs and simulation time 5 ps. The system is quenched every 250 steps. Forcite optimised structures of the constituents from the plant extracts compounds and the Fe/Al surfaces were used to sample the different interactions of the molecule with the surfaces. The slab of iron and aluminium constructed for the docking were significantly bigger than the compounds docked in order to avoid edge effects (Oguzie *et al*., 2012a, b, c; Dai and Zhang, 2012; Enenebeaku, 2011; Chi and Zhao, 2009; Yurt *et al*., 2005).

The binding energy (E_{bind}) between the metal surface and the inhibitor molecules was calculated using equation 3.10 (Casewit *et al.*, 1992a and 1992b);

$$E_{bind} = E_{total} - (E_{mol} + E_{metal}) \qquad 3.10$$

where E_{mol}, E_{metal} and E_{total} correspond to the total energies of the molecule, metal (110) slab and the adsorbed molecule/metal (110) couple respectively. (metal = Fe/Al).

CHAPTER FOUR

4.0 RESULTS

4.1 Phytochemical Screening and Gas Chromatography Mass Spectrophotometry of the Plants Extract

The phytochemical composition of ethanol extract of the plants indicates the presence of saponnin, tannin, phlobatin, anthraquinone, cardiac glycosides, flavanoid, terpene, and alkaloid in most of the extracts as presented in Table 4.1, hence the inhibition efficiency of the extracts is attributed to the phytochemical constituents.

Tables 4.2 - 4.5 show the gas chromatography- mass spectrophotometry of the plants extracts which led to identification of thirteen components used for theoretical studies.

4.2 Weight loss Measurement of Plant Extracts on the Corrosion of Mild Steel and Aluminium

Figures 4.1 - 4.4 show the variation of weight loss of aluminium with time for the corrosion of aluminium in 1.0 M HCl containing various concentrations of the extracts. It is evident from the plots that weight loss of aluminium decreased with increase in concentration of the extracts but increased with increasing period of contact.

Figures 4.5 - 4.8 show the variation of weight loss of mild steel with time for the corrosion of mild steel in 1.0 M HCl containing various concentrations of the extracts. It shows from the plots that weight loss of mild steel decreased with increase in the concentration of the extracts but increased with increasing period of contact. These indicate that the corrosion rate of mild steel in HCl solution increased with increase in the period of contact but decreased with increase in the concentration of the extracts.

Table 4.1: Phytochemcial Screening of the Various Plant Extract

Sample	Tannins	Phlobatanins	Alkaloids	Cardiac Glycosides	Anthraquinones	Saponins	Flavonoids	Terpenes
Phyllanthus amarus	+	-	+	+	-	+	+	+
Paullinia pinnata	+	+	-	+	+	+	+	-
Boscia senegalensis	+	+	+	+	+	+	+	+
Parinari polyandra	+	-	+	+	+	+	+	+

+ = denote the presence of phytochemicals, - = denote the absence of phytochemicals

Table 4.2: Characterization of Peaks Obtained from GC-MS Spectrum of Ethanol Extract of *Paulina pinnata*

Line	Concentration (%)	Chemical formula	Retention time (s)	Molecular weight ($gmol^{-1}$)	Name of Compound	Fragmentation Peak
1	1.64	$C_{10}H_{16}O$	7.95	152	2,4-decadienal	27(28%), 29(32%), 39(30%), 41(40%), 55(11%), 67(20%), 81(100%), 95(10%)
2	1.70	$C_{15}H_{24}$	9.65	204	1-ethenyl-1-methyl-2,4-bis(1-methylethenyl)-cyclohexane	27(35%), 29(34%), 39(55%), 40(15%), 41(90%), 42(10%), 43(20%), 51(10%), 53(52%), 55(50%), 65(14%), 66(10%), 67(55%), 68(95%), 69(20%), 77(25%), 79(30%), 80(20%), 81(100%), 91(30%), 92(10%), 93(80%), 94(20%), 95(20%), 105(20%), 107(30%), 108(20%), 119(20%), 121(35%), 133(15%), 147(20%), 161(12%), 189(10%)
3	5.82	$C_7H_{14}O_6$	10.10	194.18	Methyllinositol	27(30%), 28(15%), 29(25%), 39(40%), 41(100%), 42915%), 51(10%), 53(20%0, 55(30%), 65(15%), 67(30%), 69(28%), 77(30%), 78(11%), 79(40%), 80(10%), 81(25%), 82(10%), 91(70%), 92(18%), 93(40%), 94(20%), 95(22%), 105(50%), 106(20%), 107(35%), 119(30%0, 120(13%), 121(15%), 122(14%), 133(23%), 147(20%), 148(17%), 161(30%), 189(10%), 194(10%)
4	2.61	$C_{15}H_{24}$	10.35	204	1,6,10-dodecatriene	41(100%), 53(20%), 55(20%), 67(20%), 68(10%), 69(80%), 77(13%), 79(20%), 81(17%), 91(17%), 93(40%), 120(20%), 133(21%), 161(11%)
5	1.89	$C_{15}H_{24}$	10.53	204	1,4,8-cycloundecatriene	41(50%), 42(20%), 53(25%), 55(18%), 65(10%), 67(20%), 77(20%), 79(20%), 80(40%), 91(21%), 92(19%), 93(100%), 94(11%), 105(12%), 107(12%), 121(22%), 147(15%)
6	3.22	$C_{14}H_{22}O$	11.03	206	3,5-bis(1,1-dimethylethyl)-phenol	41(35%), 57(100%), 73(10%), 74(20%), 91(20%), 107(10%), 115(11%), 191(55%), 206(12%)
7	2.07	$C_{15}H_{22}O$	12.13	220	5-oxatricyclo[8.2.0.0(4,6)-]dodecane	27(28%), 29(26%), 39(30%), 41(95%), 42(100%), 53(25%), 55(35%), 65(17%), 67(28%), 69(30%), 72(14%), 77(30%), 79(85%), 81(30%), 82(26%), 83(17%), 91(53%), 93(69%), 94(17%), 95(35%), 96(20%), 105(26%), 106(27%), 107(30%), 109(30%), 110(20%), 120(13%0, 121(22%), 123(14%), 135(11%)

Line	Concentration (%)	Chemical formula	Retention time (s)	Molecular weight ($gmol^{-1}$)	Name of Compound	Fragmentation Peak
8	1.11	$C_{10}H_{18}O$	13.14	154	Bicyclo(3.1.1)heptan-2-ol	39(20%), 41(60%), 43(100%), 53(12%), 55(28%), 59(12%), 67(11%), 69(30%), 71(73%), 72(10%), 80(12%), 81(35%), 83(30%), 93(50%), 96(12%), 99(73%), 111(10%0, 121(25%), 131(10%)
9	5.48	$C_{18}H_{34}$	15.16	414.72	B-sitosterol	27(14%), 29(30%), 39(12%), 41(75%), 43(90%), 53(10%), 54(22%), 55(70%), 56(20%), 57(60%), 67(70%), 68(30%), 69(40%), 70(16%), 71(14%), 81(100%), 82(52%), 83(40%), 95(52%), 96(30%), 97(22%), 414(20%)
10	2.32	$C_{13}H_{22}O$	16.59	194	5,9-undecadien-2-one	41(40%), 43(100%), 69(55%), 93(10%), 107(12%), 125(10%), 136(14%), 151(15%)
11	6.79	$C_{18}H_{36}O_2$	18.05	284	Hexadecanoic acid	41(50%), 42(10%), 43(55%), 45(10%), 55(50%), 56(11%), 57(40%), 60(13%), 67(10%), 69(18%), 70(16%), 71(18%), 73(20%), 88(100%), 89(15%), 101(70%), 143(10%), 157(11%), 284(10%)
12	26.76	$C_{20}H_{40}O$	20.04	296	2-hexadecen-1-ol	41(25%), 43(40%), 55(25%), 56(15%), 57(33%), 68(14%), 69(15%), 71(100%), 81(18%), 82(12%), 83(12%), 95(11%), 97(10%), 123(14%)
13	11.06	$C_{18}H_{31}ClO$	20.75	298	9,12-octadecadienoylchloride	27(10%), 29(20%), 39(13%), 41(80%), 43(30%), 53(10%), 54(30%), 55(100%), 56(13%), 57(14%), 67(85%), 68(20%), 69(30%), 70(10%), 79(30%), 80(20%), 81(50%), 81(22%), 82(20%), 83(14%), 91(10%), 93(13%), 94(10%), 95(30%), 96(23%), 97(20%), 98(23%), 109(16%), 110(16%), 123(10%)
14	4.66	$C_{20}H_{40}O_2$	21.08	312	Octadecanoic acid	27(12%), 28(30%), 41(31%), 43(52%), 55(38%), 57(30%), 60(10%), 61(13%), 62(15%), 69(17%), 70(16%), 71(15%), 73(18%), 88(100%), 89(13%), 101(62%), 157(10%)
15	22.85	$C_{30}H_{50}$	27.63	410	2,6,10,14,18,22-tetracosahexaene	41(50%), 55(105), 67(12%), 68(15%), 69(100%), 81(55%), 95(14%), 138(10%)

Table 4.3: Characterization of Peaks Obtained from GC-MS Spectrum of Ethanol Extract of *Parinari polyandra*

Line	Concentration (%)	Chemical formula	Retention time (s)	Molecular weight ($gmol^{-1}$)	Name of Compound	Fragmentation Peak
1.	1.08	C_6H_5ClO	6.86	128	3-Chlorophenol	37(10%), 38(13%), 39(30%), 62(10%), 63(25%), 64(26%), 65(60%), 73(10%), 100(20%), 128(100%), 130(10%)
2	0.81	$C_8H_{18}O_2$	7.86	138	9-oxa-bicyclo[3,3,1]nona-3,6-dien-2-one	27(18%), 39(19%), 50(10%), 51(12%), 53(14%), 77(60%), 78(10%), 79(50%), 94(20%), 107(100%), 108(20%)
3.	1.53	$C_{14}H_{22}O$	10.57	206	3,5-bis(1,1-dinethylethyl)-phenol	41(13%), 57(55%), 191(100%), 192(17%), 206(25%)
4	3.41	$C_{18}H_{30}O_2$	11.03	278.44	Linolenic acid	29(13%), 41(17%), 55(10%), 57(25%), 74(10%), 91(12%), 131(12%), 191(100%), 278(20%)
5	0.80	$C_{14}H_{28}$	11.98	196	1-tetradecene	27(20%), 29(50%), 39(15%), 41(92%), 42(24%), 43(100%), 54(13%), 55(80%), 56(60%), 57(65%), 67(10%), 68(10%), 69(55%), 70(50%), 71(25%), 82(10%), 83(50%), 84(25%), 85(12%), 97(30%), 98(16%), 112(10%)
6	0.99	$C_{18}H_{34}$	15.16	250	1-octadecyne	27(13%), 29(30%), 39(13%), 41(80%), 42(10%), 43(90%), 53(10%), 54(26%), 55(70%), 56(20%), 57(55%), 67(70%), 68(30%), 69(40%), 70(14%), 71(20%), 81(100%), 82(50%), 83(30%), 95(40%), 96(30%), 97(22%), 109(15%)
7	1.44	$C_{28}H_{48}O_2$	16.68	416.69	Gama Tocophenol	27(14%), 28(15%), 41(30%), 43(42%), 55(28%), 56(10%), 57(20%), 59(12%), 69(20%), 74(100%), 82(15%), 83(14%), 87(50%), 417(10%)

Line	Concentration (%)	Chemical formula	Retention time (s)	Molecular weight ($gmol^{-1}$)	Name of Compound	Fragmentation Peak
8	3.81	$C_{18}H_{36}O_2$	18.06	284	Hexadecanoic acid	41(45%), 42(10%), 43(52%), 45(10%), 55(48%), 56(10%), 57(39%), 60(14%), 61(12%), 67(10%), 69(20%), 70(14%), 71(17%), 73(20%), 83(14%), 85(10%), 88(100%), 89(14%), 97(10%), 101(70%), 157(10%)
9	6.60	$C_{19}H_{36}O_2$	19.82	296	11-octadecenoic acid	27(16%), 29(32%), 39(17%), 41(85%), 42(16%), 43(52%), 53(10%), 54(20%), 55(100%), 56(18%), 20.0357(17%), 59(20%), 67(25%), 68(10%), 69(50%), 70(10%), 74(35%), 81(18%), 82(10%), 83(16%), 84(15%), 87(20%), 98(20%), 264(10%)
10	11.07	$C_{20}H_{40}O$	20.03	296	2-hexadecen-1-ol	41(25%), 43(35%), 55(25%), 56(17%), 57(30%), 68(20%), 69(22%), 70(14%), 71(100%), 81(20%), 82(14%), 83(14%), 95(12%), 123(20%)
11	3.34	$C_{19}H_{38}O_2$	20.19	298	Octadecanoic acid	29(15%), 41(25%), 43(40%), 55(30%), 57(20%), 69(15%), 74(100%), 75(20%), 87(55%), 143(15%), 298(10%)
12	9.65	$C_{20}H_{38}O_2$	20.76	310	(E)-9-octadecenoic acid	41(80%), 42(15%), 43(70%), 54(25%), 55(100%), 56(225), 57(30%), 60(10%), 61(10%), 67(25%), 68(14%), 69(52%), 70(21%), 71(12%), 73(12%), 81(20%), 82(14%), 83(40%), 84(30%), 88(50%), 96(16%), 97(30%), 98(31%), 99(29%), 101(30%), 110(14%), 1119(13%), 123(10%), 180(10%), 222(10%), 264(20%), 265(10%)
13	55.49	$C_{29}H_{50}O_2$	24.85	430	Vitamin E	41(11%), 43(26%), 55(10%), 57(14%), 164(28%), 165(100%), 205(10%), 430(85%), 431(30%)

Table 4.4: Characterization of Peaks Obtained from GC-MS Spectrum of Ethanol Extract of *Phyllanthus amarus*

Line	Concentration (%)	Chemical formula	Retention time (s)	Molecular weight ($gmol^{-1}$)	Name of Compound	Fragmentation Peak
1	1.66	$C_{14}H_{22}O$	11.03	206	3,5-bis(1,1-dimethylethyl)-phenol	41(15%), 57(70%), 191(100%), 192(15%), 206(20%)
2	2.12	$C_{17}H_{34}O_2$	16.68	270	Pentadecanoic acid	29(12%), 41(21%), 43(45%), 55(20%), 57(17%), 69(10%), 74(100%), 75(19%), 87(60%)
3	3.06	$C_{18}H_{36}O_2$	18.05	284	Hexadecanoic acid	29(21%), 41(25%), 43(33%), 55(28%), 57(26%), 60(11%), 61(12%), 69(11%), 70(10%), 71(10%), 73(14%), 88(100%), 89(14%), 101(55%), 157(12%)
4	2.70	$C_3H_8O_2$	19.73	126.11	1, 2, 3-benzenetriol	39(14%), 41(92%), 42(10%), 43(30%), 53(12%), 54(32%), 55(72%), 59(14%), 67(100%), 68(32%), 69(305), 74(10%), 77(10%), 79(30%), 80(20%), 81(70%), 82(40%), 83(12%), 93(11%), 95(40%), 96(25%), 126(20%)
5	5.57	$C_{18}H_{30}O_2$	19.82	278.44	Linolenic acid	29(17%), 29(32%), 39(17%), 41(85%), 42(15%), 43(55%), 53(11%), 54(20%), 55(100%), 56(20%), 57(19%), 59(20%), 67(24%), 68(11%), 69(11%), 69(51%), 70(12%), 74(37%), 81(17%), 82(11%), 83(17%), 84(16%), 87(20%), 95(13%), 96(20%), 98(20%), 278(10%)
6	23.27	$C_{20}H_{40}O$	20.05	296	2-hexadecen-1-ol	41(22%), 43(35%), 55(24%), 56(16%), 57(30%), 68(20%), 69(21%), 70(15%), 71(100%), 81(19%), 82(14%), 83(15%), 95(11%), 123(20%)

Line	Concentration (%)	Chemical formula	Retention time (s)	Molecular weight ($gmol^{-1}$)	Name of Compound	Fragmentation Peak
7	2.44	$C_{19}H_{38}O_2$	20.19	298	Octadecanoic acid	29(12%), 41(27%), 43(40%), 55(25%), 57(23%), 69(11%), 74(100%), 75(20%), 87(60%), 143(13%), 298(10%)
8	5.35	$C_{20}H_{38}O_2$	20.75	310	9-Octadecenoic acid	41(80%), 42(15%), 43(70%), 54(21%), 55(100%), 56(21%), 57(28%), 67(28%), 68(15%), 69(55%), 70(20%), 71(11%), 73(11%), 81(20%), 82(14%), 83(35%), 84(30%), 88(50%), 95(185), 96(28%), 97(29%), 98(27%), 101(305), 109(10%), 110(11%), 111(11%), 123(10%), 180(10%), 222(10%), 264(17%)
9	21.62	$C_{22}H_{34}O_3$	24.46	346	Kauran-18-al	41(50%), 43(100%), 53(11%), 55(45%), 57(11%), 67(40%), 68(20%), 71(10%), 77(12%), 79(30%), 81(50%), 91(30%), 92(12%), 93(28%), 94(11%), 95(20%), 97(10%), 105(20%), 106(10%), 109(28%), 119(18%), 121(17%), 123(35%), 286(10%)
10	19.68	$C_{13}H_{22}O$	24.90	194	4-(2,2-dimethyl-6-methylenecyclohexyl)butanal	27(15%), 28(40%), 29(14%), 39(18%), 41(60%), 43(20%), 44(19%), 53(14%), 55(30%), 57(12%), 67(25%), 68(14%), 69(100%), 79(22%), 80(10%), 81(30%), 91(20%), 93(17%), 94(18%), 95(23%), 105(10%), 106(18%), 109(23%), 123(11%), 135(12%), 150(20%), 161(11%), 179(10%)
11	12.53	$C_6H_6O_2$	27.64	142.17	Thioisomaltol	41(50%), 55(10%), 67(10%), 68(13%), 69(100%), 81(55%), 95(13%), 142(10%)

Table 4.5: Characterization of Peaks Obtained from GC-MS Spectrum of Ethanol Extract of *Boscia senegalensis*

Line	Concentration (%)	Chemical formula	Retention time (s)	Molecular weight ($gmol^{-1}$)	Name of Compound	Fragmentation Peak
1	1.82	C_6H_5ClO	6.86	128	3-chlorophenol	37(10%), 38(15%), 39(29%), 62(10%), 63(16%), 64(19%), 65(50%), 73(10%), 100(18%), 128(100%), 130(10%)
2	6.86	$C_6H_6O_2$	7.82	110	Hydroquinone	27(17%), 39(18%), 53(15%), 54(10%), 55(23%), 81(30%), 82(17%), 110(100%)
3	2.75	$C_{14}H_{22}O$	11.03	206	3,5-bis(1,1-dimethylethyl)-phenol	41(14%), 57(65%), 191(100%), 192(11%), 206(21%)
4	0.80	$C_{13}H_{26}$	12.00	182	3-tridecene	27(21%), 29(40%), 39(19%), 41(100%), 42(20%), 43(60%), 54(11%), 55(65%), 56(40%), 57(40%), 67(18%), 68(10%), 69(48%), 70(35%), 71(18%), 83(25%), 84(20%), 98(12%)
5	1.17	$C_6H_6O_3$	12.78	126	1,2,3-benzenetriol	45(17%), 59(40%), 61(50%), 75(85%), 85(20%), 87(14%), 99(10%), 101(12%), 113(10%), 115(100%), 116(10%), 126(12%)
6	9.10	$C_7H_{14}O_6$	18.04	194	Methyllinositol	41(48%), 42(10%), 43(53%), 45(10%), 55(50%), 56(10%), 57(40%), 60(14%), 61(14%), 67(10%), 69(21%), 70(16%), 71(20%), 73(22%), 83(12%), 85(10%), 88(100%), 89(12%), 97(10%), 101(70%), 143(10%), 157(12%), 194(10%)
7	14.02	$C_{20}H_{40}O$	20.02	296	2-hexadecen-1-ol	41(25%), 43(35%), 55(25%), 56(17%), 57(30%), 68(20%), 69(22%), 70(15%), 71(100%), 81(20%), 82(15%), 83(15%), 95(11%), 97(10%), 123(20%)
8	34.10	$C_{18}H_{30}O_2$	20.76	278	9,12,15-Octadecatrienoic acid	27(28%), 29(32%), 39(30%), 41(100%), 43(20%), 45(10%), 53(12%), 54(12%), 55(60%), 60(14%), 65(12%), 66(12%), 67(70%), 68(17%), 69(20%), 77(20%), 78(10%), 79(80%), 80(32%), 81(32%), 82(17%), 91(22%), 93(31%), 94(20%), 95(32%), 107(10%), 108(28%), 121(10%)
9	5.67	$C_{24}H_{38}O_4$	24.76	390	Di-n-octylphthalate	27(10%), 28(14%), 29(20%), 41(30%), 43(30%), 55(20%), 56(10%), 57(50%), 70(30%), 71(30%), 84(10%), 104(10%), 113(10%), 149(100%), 150(20%), 167(30%), 2
10	23.71	$C_{30}H_{50}$	27.62	410	2,6,10,14,18,22-tetracosahexane	41(50%), 55(11%), 67(12%), 68(14%), 69(100%), 81(60%), 95(14%), 137(10%)

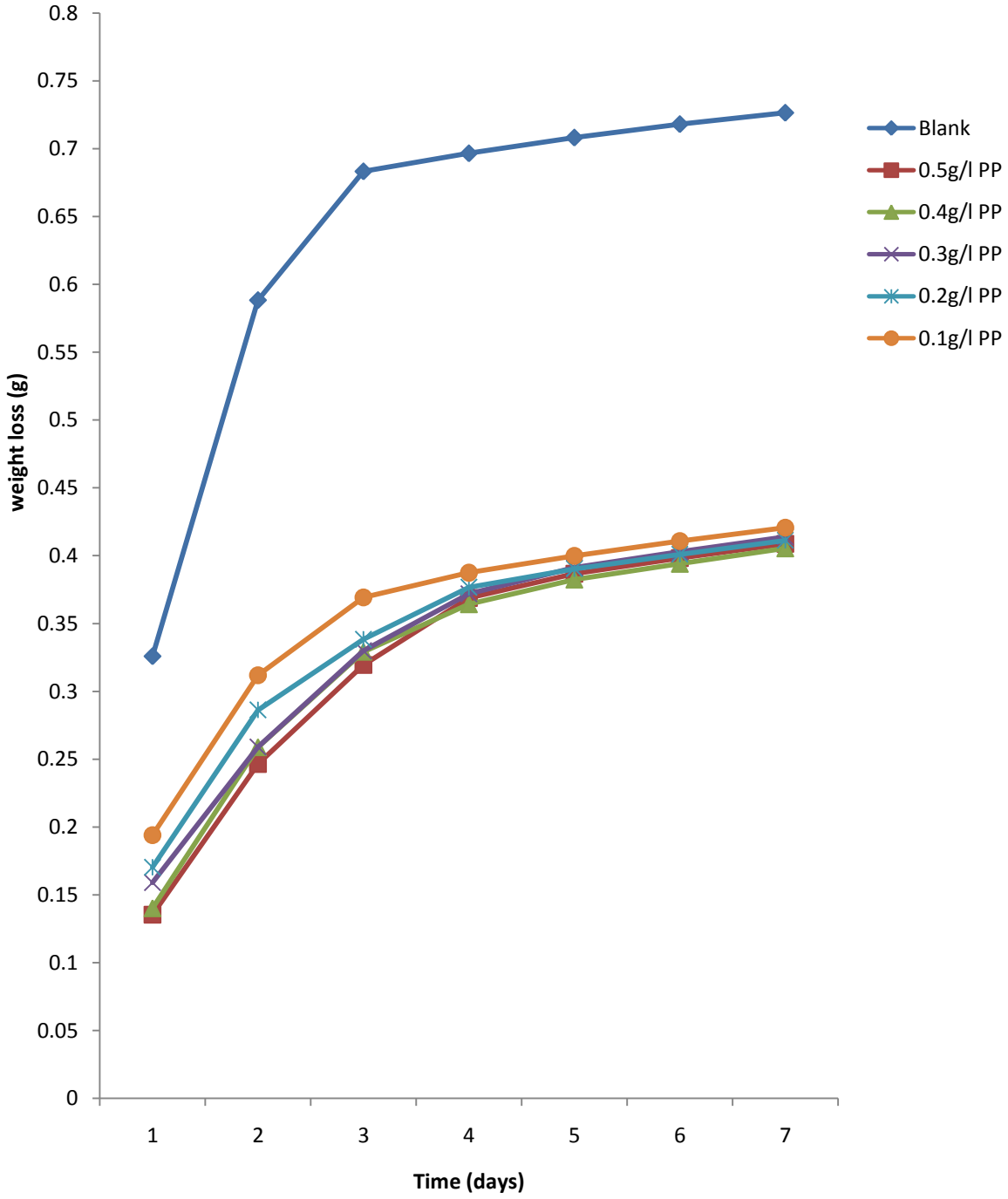


Fig. 4.1:Variation of Weight loss with Time for Aluminium in 1.0 M HCl Containing Various Concentration of *Paulina pinnata* at 303K

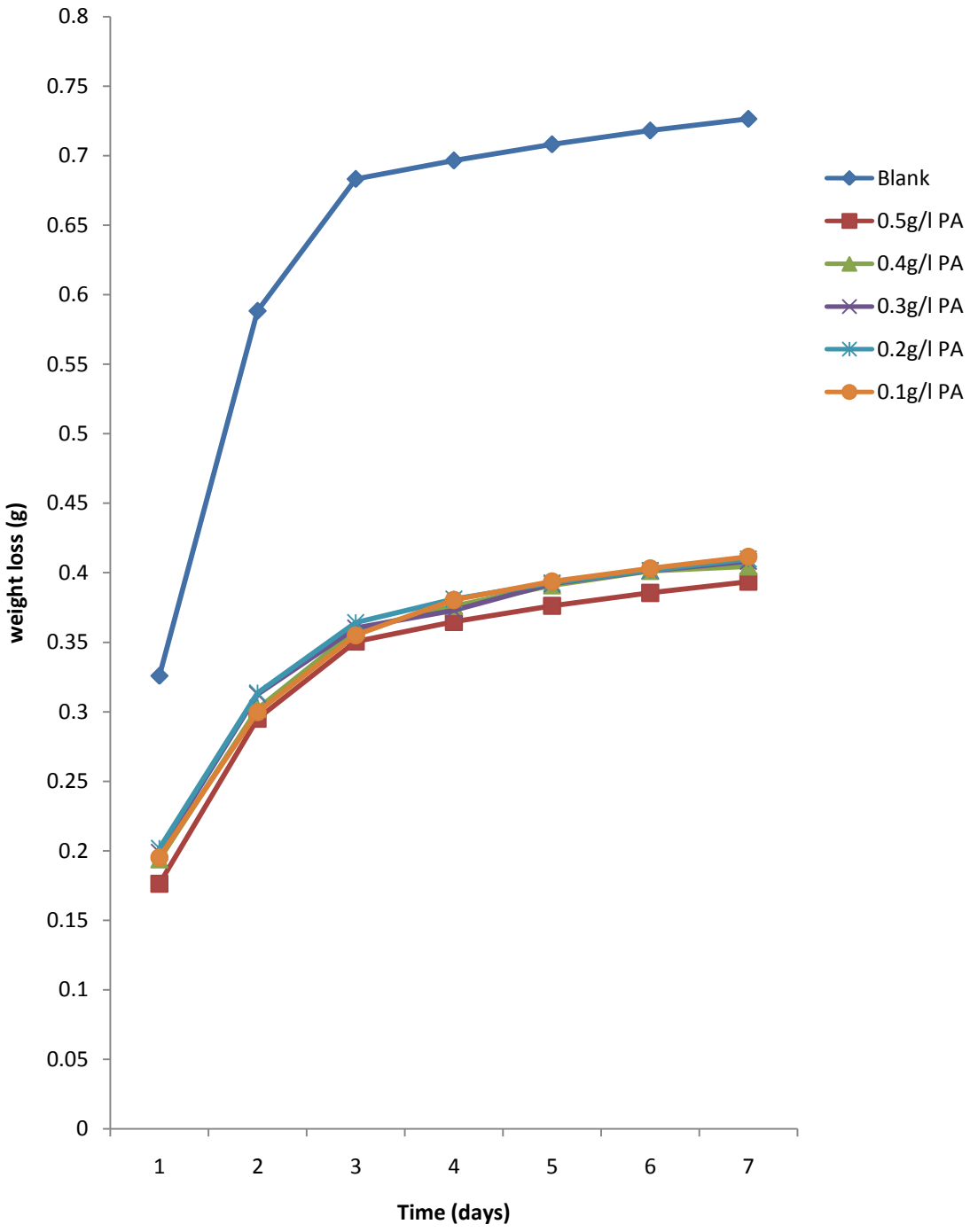


Fig. 4.2:Variation of Weight loss with Time for Aluminium in 1.0 M HCl Containing Various Concentration of *Phyllanthus amarus* at 303K

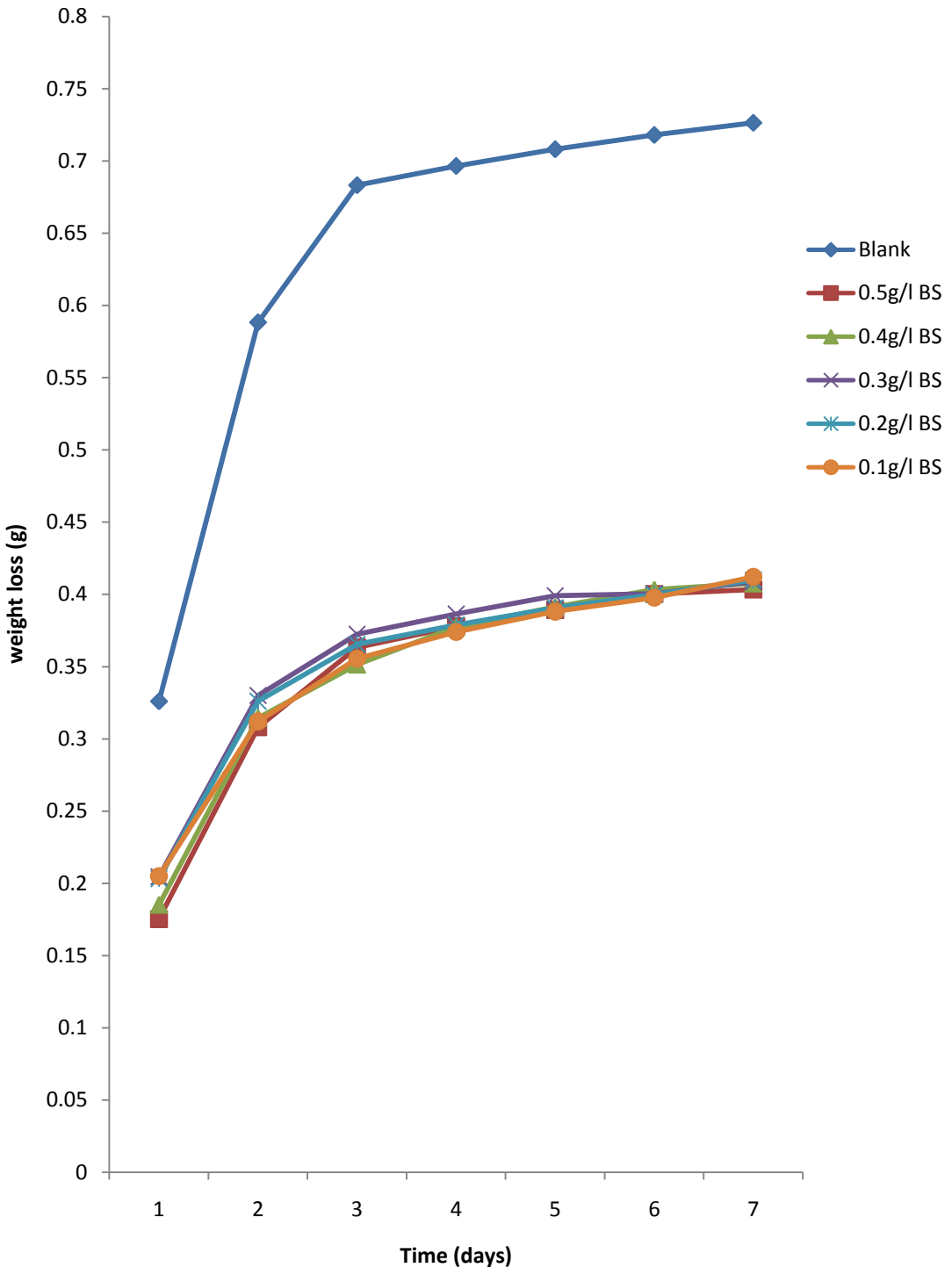


Fig. 4.3:Variation of Weight loss with Time for Aluminium in 1.0 M HCl Containing Various Concentration of *Boscia senegalensis* at 303K

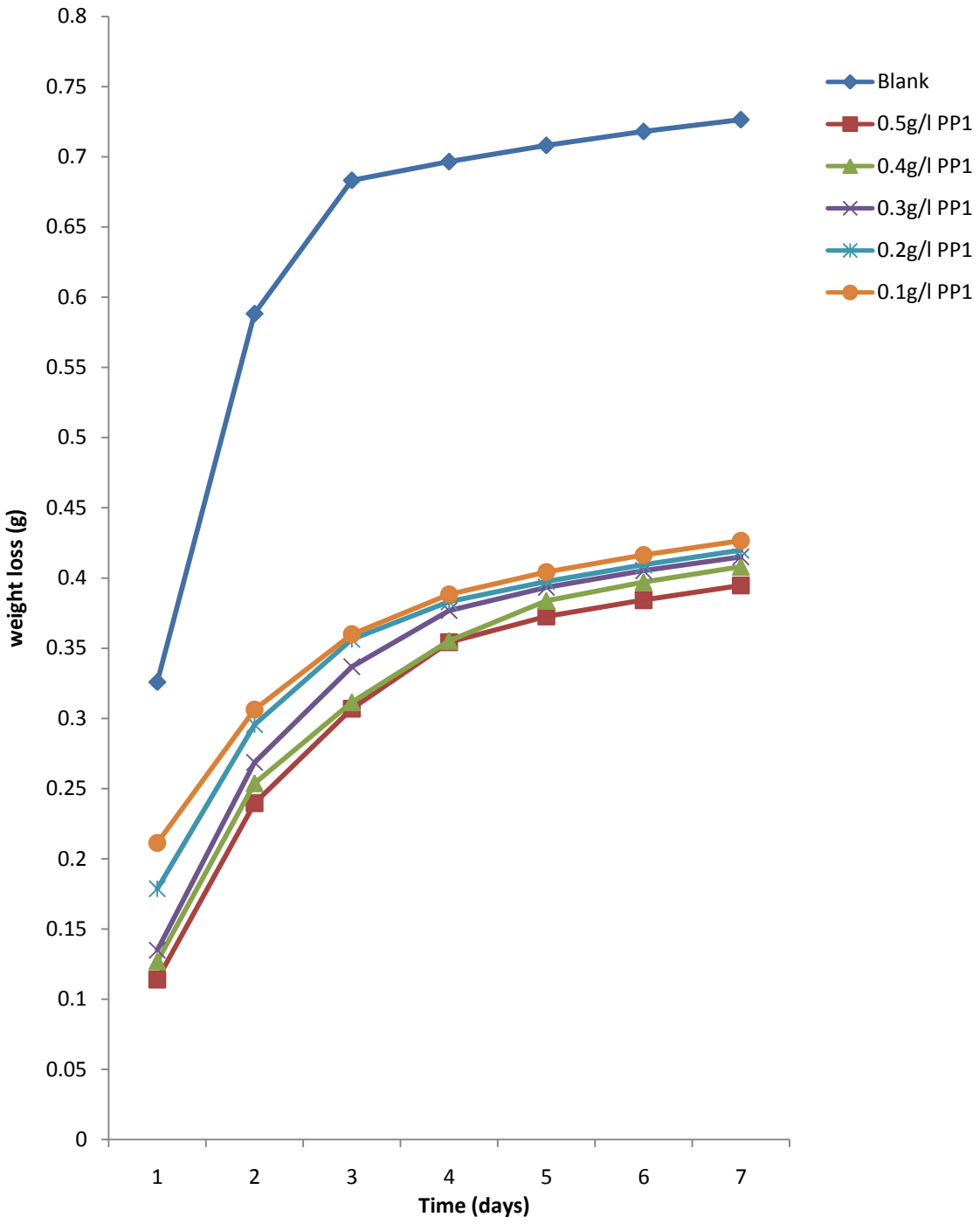


Fig. 4.4:Variation of Weight loss with Time for Aluminium in 1.0 M HCl Containing Various Concentration of *Parinari polyandra* at 303K

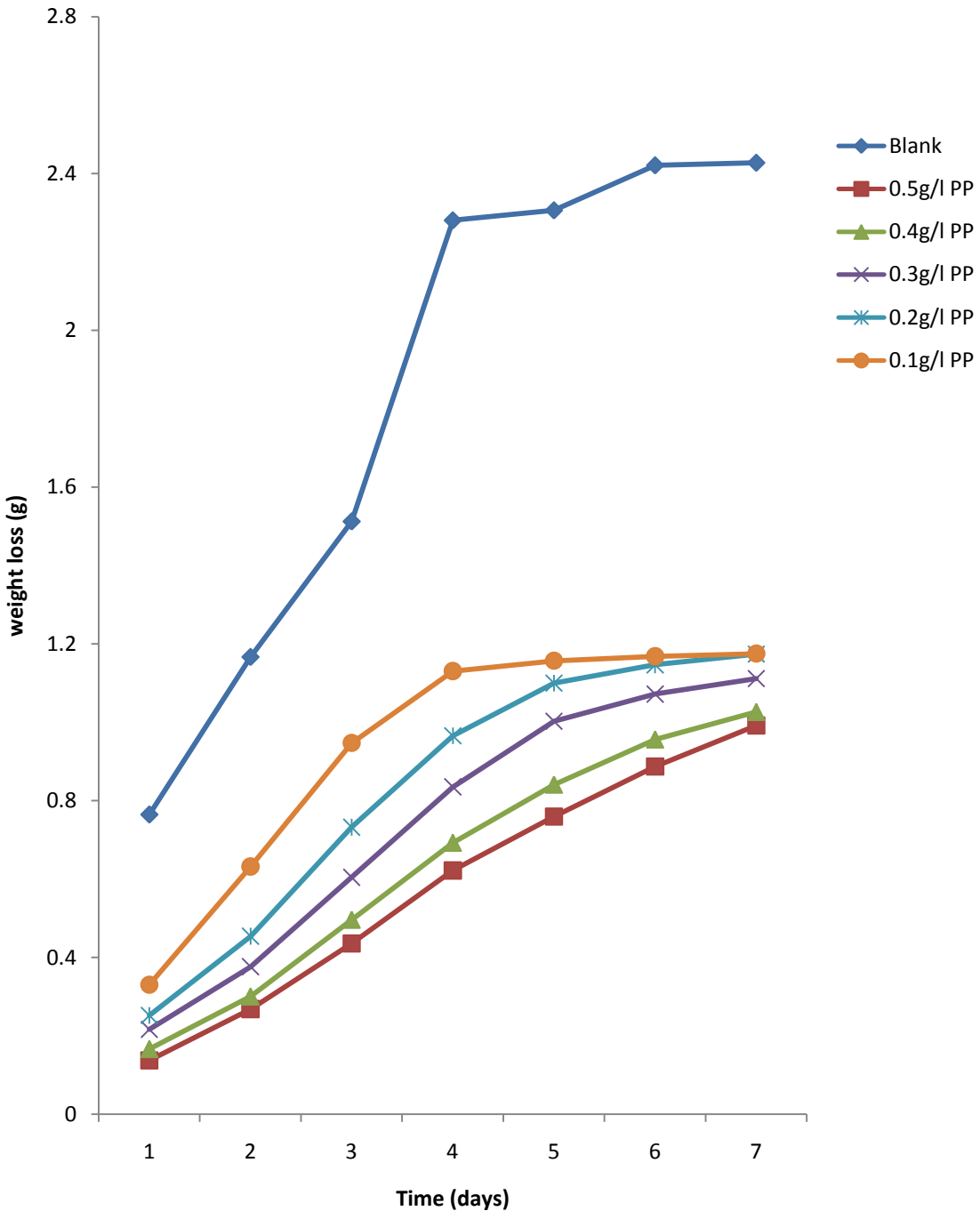


Fig. 4.5:Variation of Weight loss with Time for Mild Steel in 1.0 M HCl Containing Various Concentration of *Paulina pinnata* at 303K

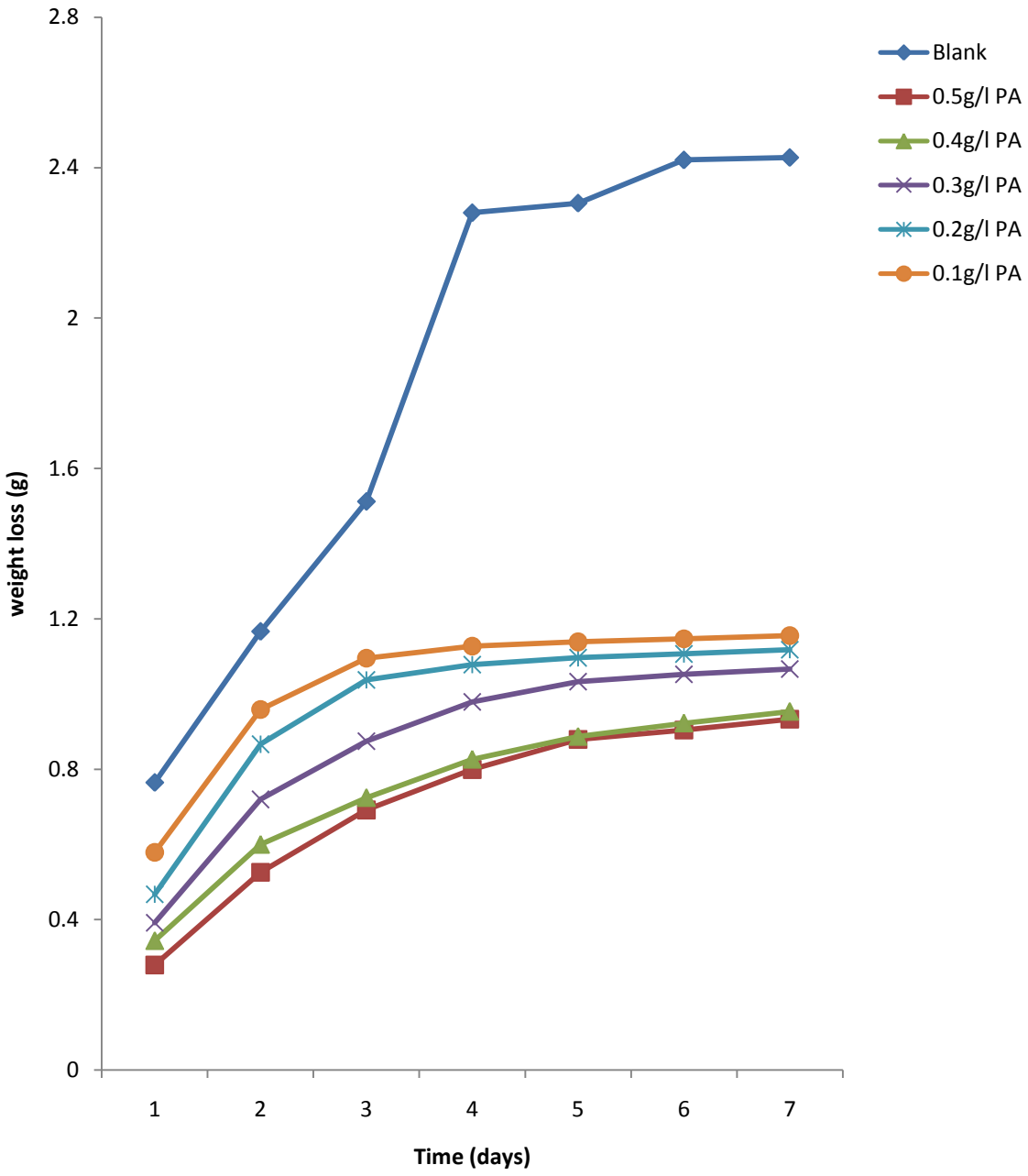


Fig. 4.6:Variation of Weight loss with Time for Mild Steel in 1.0 M HCl Containing Various Concentration of *Phyllanthus amarus* at 303K

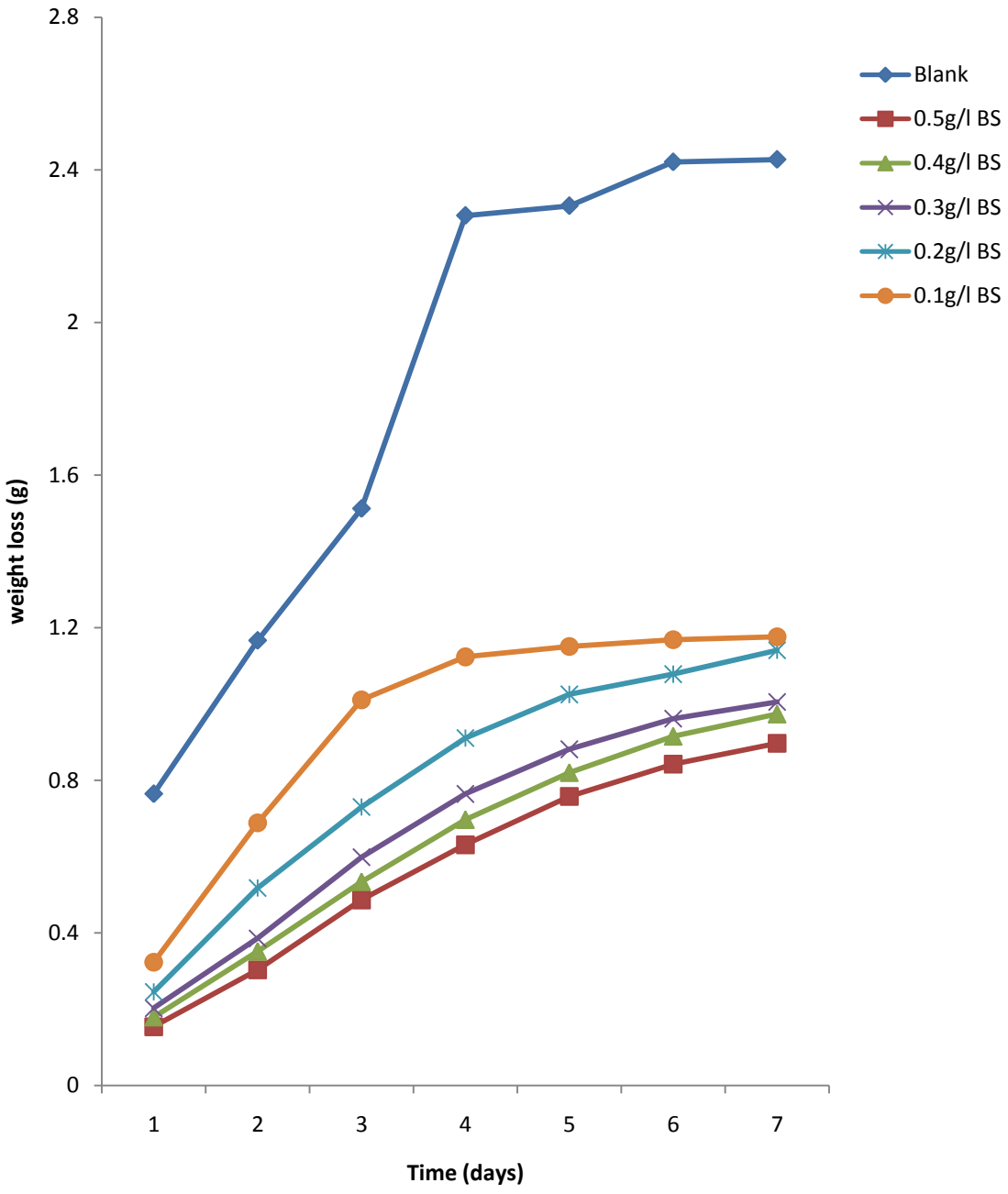


Fig. 4.7:Variation of Weight loss with Time for Mild Steel in 1.0 M HCl Containing Various Concentration of *Boscia senegalensis* at 303K

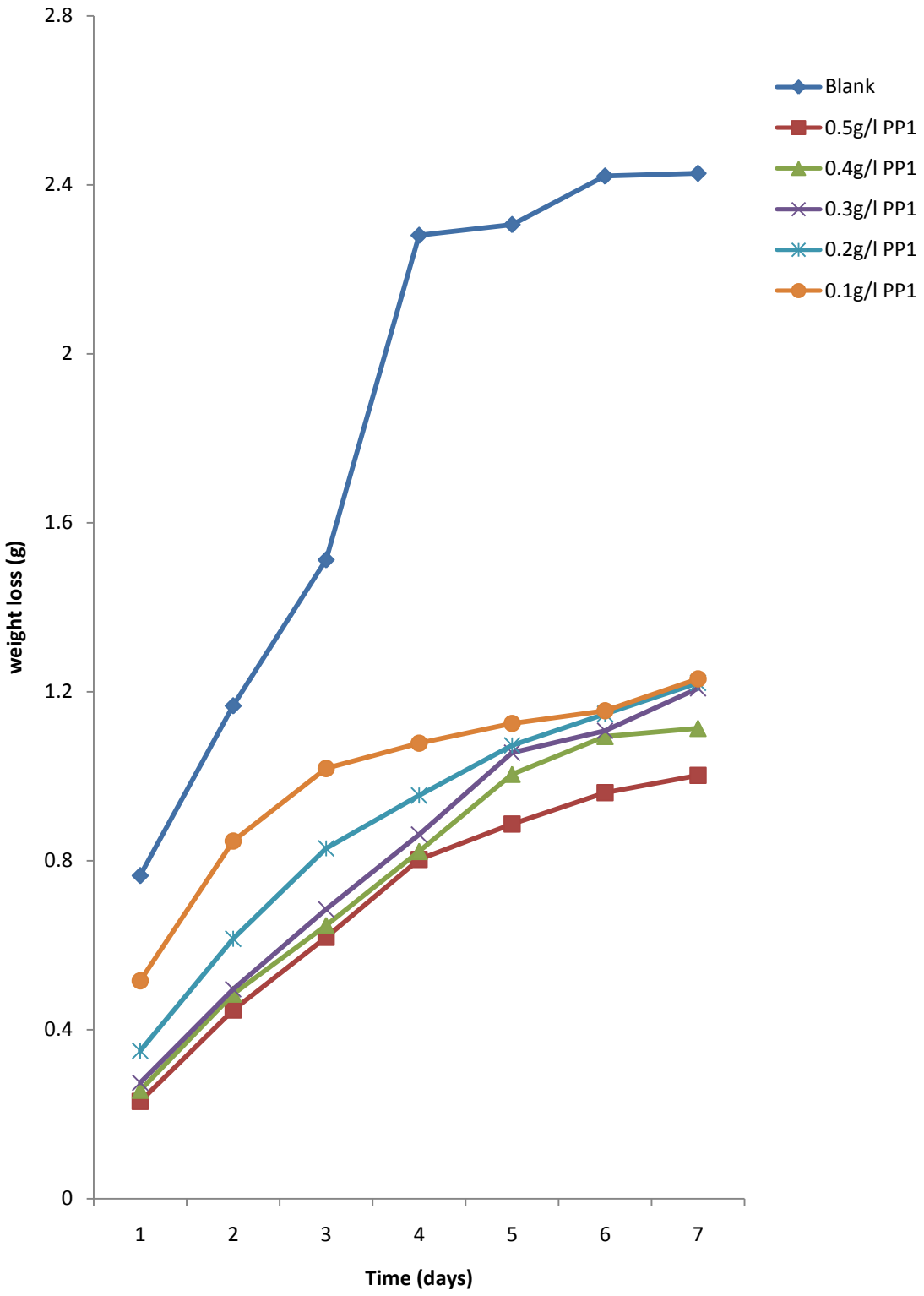


Fig. 4.8:Variation of Weight loss with Time for Mild Steel in 1.0 M HCl Containing Various Concentration of *Parinari polyandra* at 303K

Figures 4.9 - 4.12 show the variation of weight loss of mild steel with time for the corrosion of mild steel in 0.5 M H_2SO_4 containing various concentrations of the extracts. The plots shows that degradation of mild steel decreased with increased in the concentration of the studied plant extract but increases with increasing period of contact.

Tables 4.6 – 4.9 present the inhibition efficiencies and corrosion rates of mild steel and aluminium in various acid media at various temperature. These indicate that the rate of corrosion of mild steel in HCl and H_2SO_4 solution increases with increase in the period of contact but decreased with increase in the concentration of the extracts (Eddy *et al*., 2010; Oguzie *et al*., 2012a).

4.3 Effect of Temperature

Figures 4.17 - 4.24, show the plot of log CR versus reciprocal of absolute temperature, 1/T, with slope equal to $-E_a/R$, from which the activation energy for the corrosion process was calculated. The activation energy parameter is depicted in Tables 4.10 – 4.12.

Figures 4.25 - 4.32, show the plot of log CR/T versus reciprocal of absolute temperature, 1/T, with slope equal to $-\Delta H_a/2.303R$ and an intercept of $\{\log R/N_A h + \Delta S_a/2.303R\}$, from such the activation parameters were calculated and presented in Tables 4.13 – 4.14.

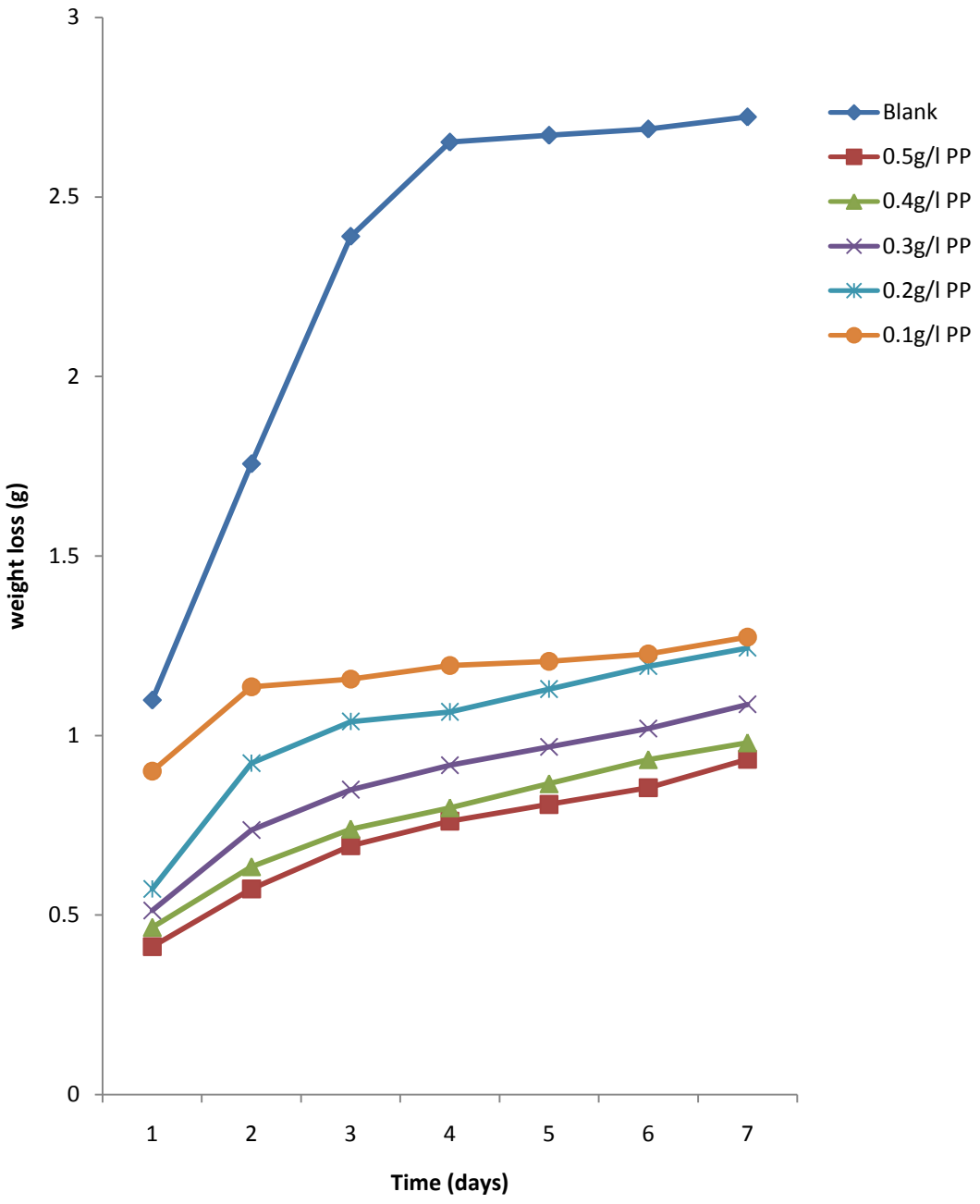


Fig. 4.9:Variation of Weight loss with Time for Mild Steel in 0.5M H_2SO_4 Containing Various Concentration of *Paulina pinnata* at 303K

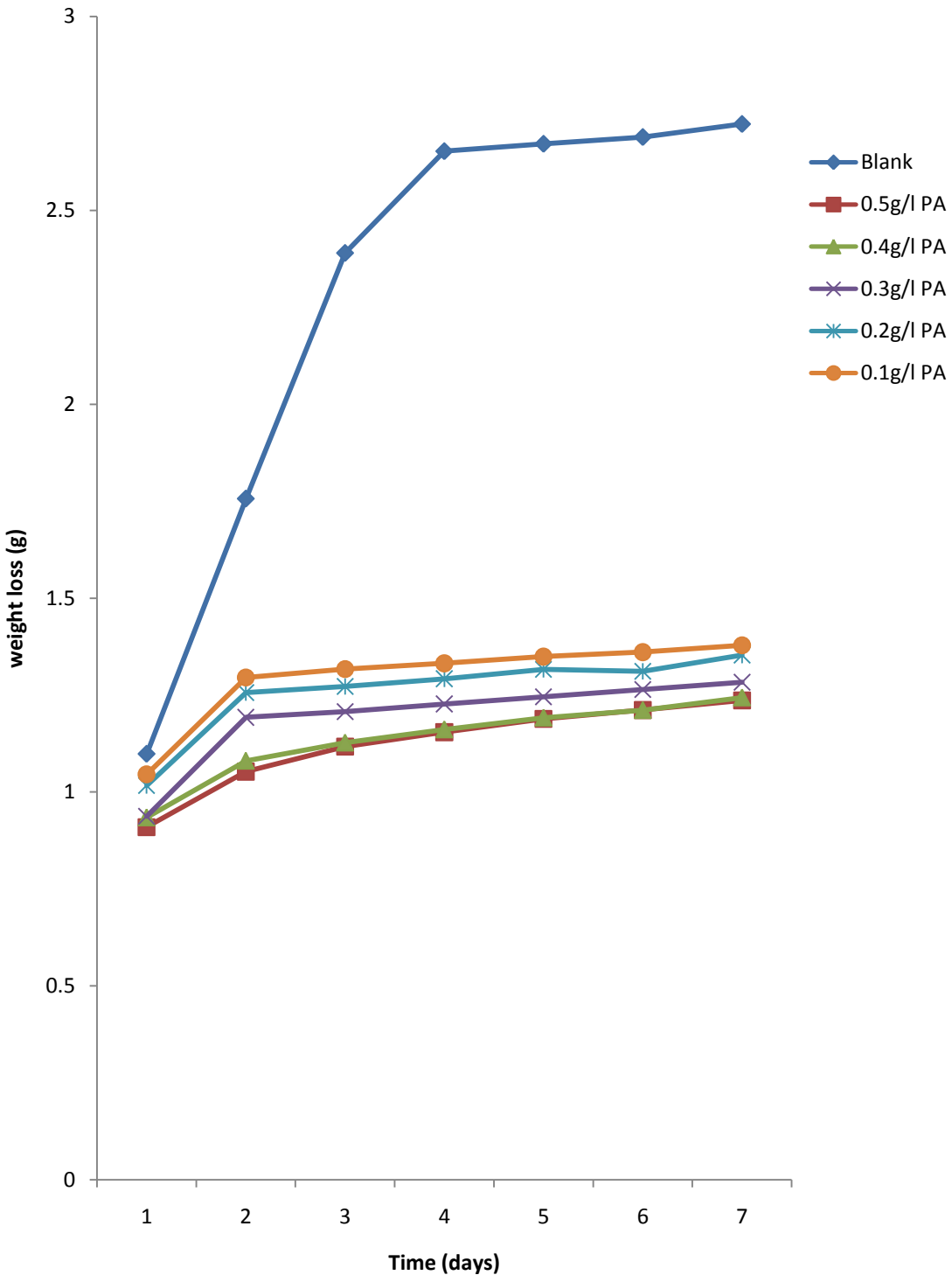


Fig. 4.10:Variation of Weight loss with Time for Mild Steel in 0.5 M H_2SO_4 Containing Various Concentration of *Phyllanthus amarus* at 303K

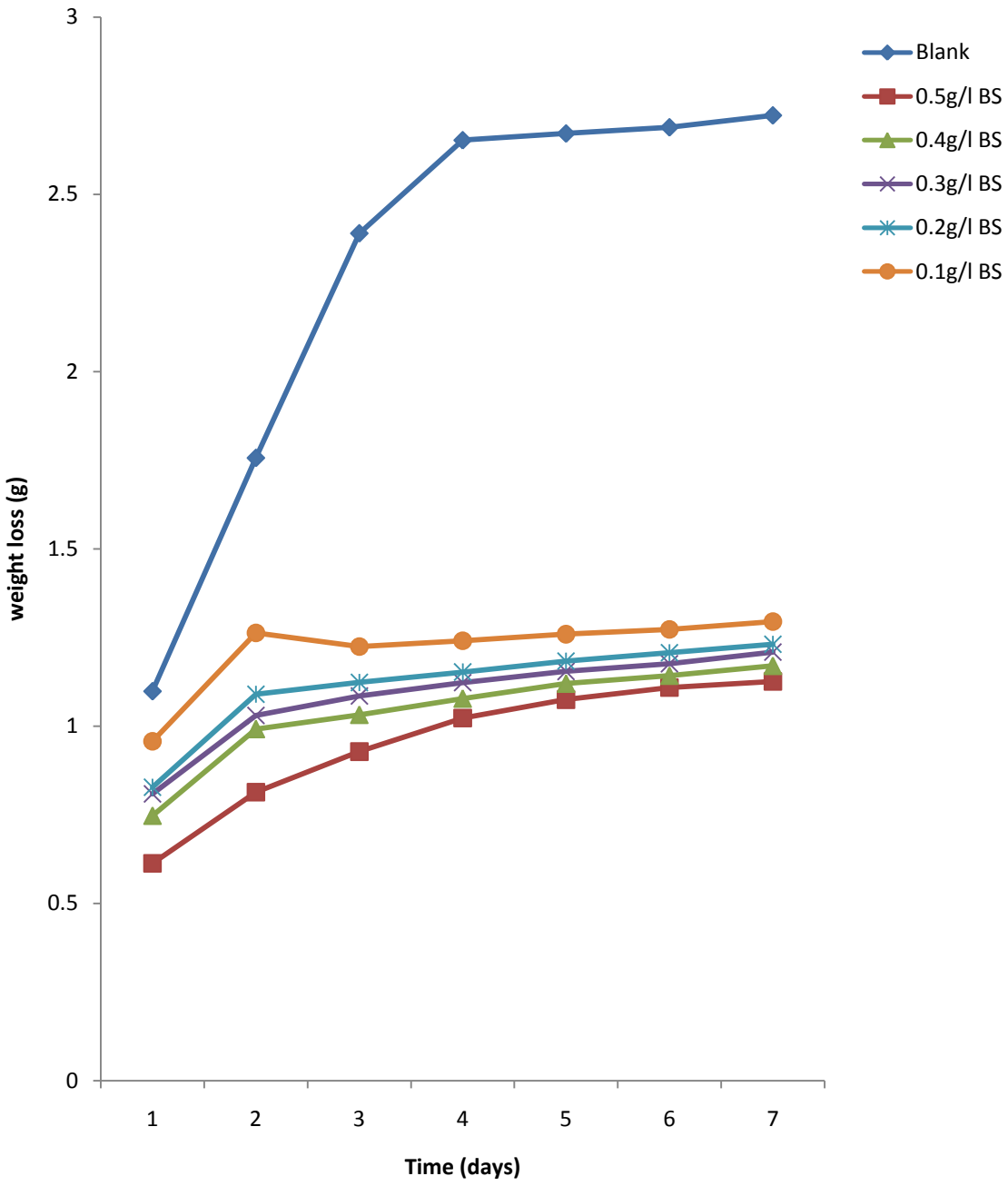


Fig. 4.11:Variation of Weight loss with Time for Mild Steel in 0.5 M H_2SO_4 Containing Various Concentration of *Boscia senegalensis* at 303K

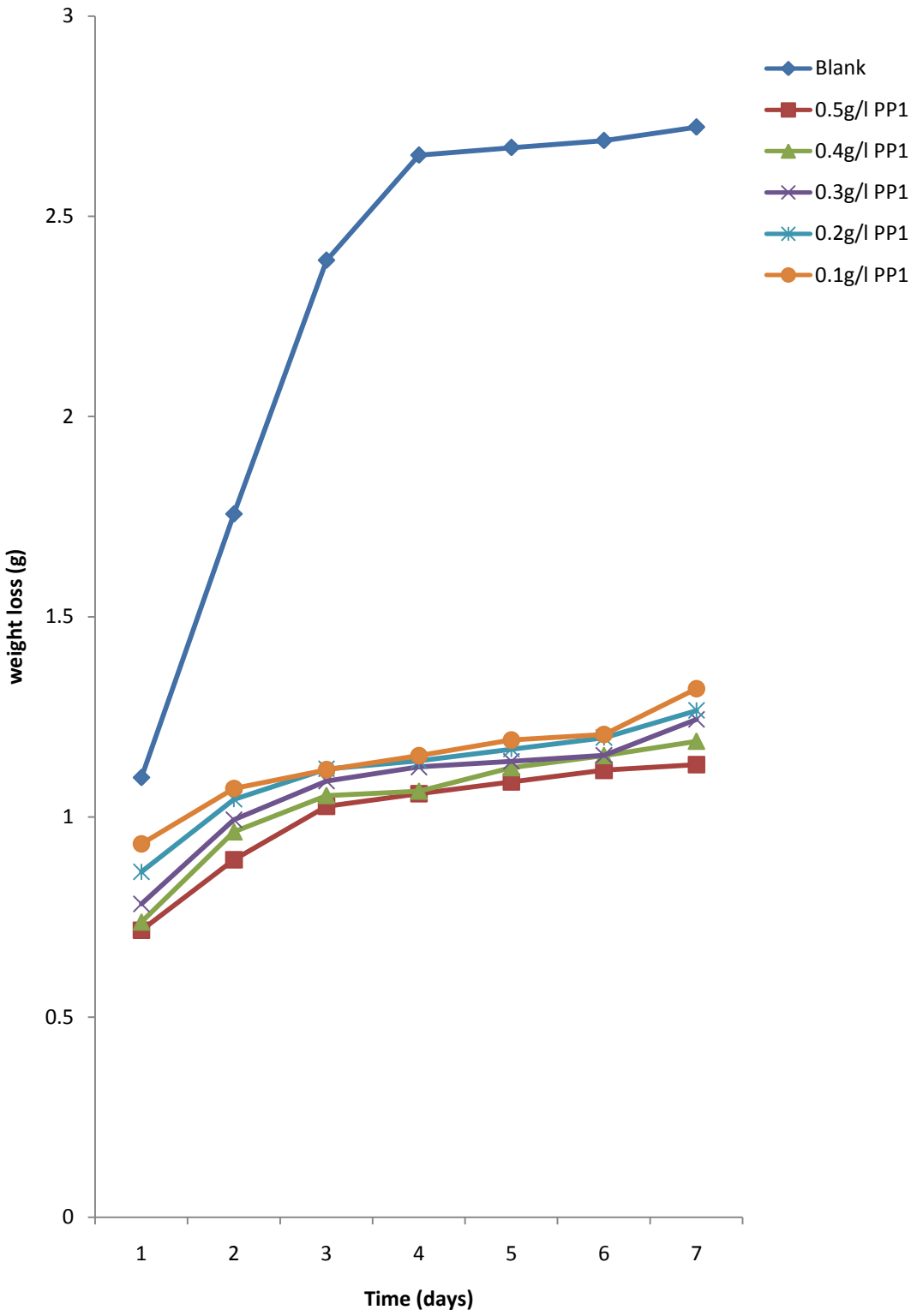


Fig. 4.12:Variation of Weight loss with Time for Mild Steel in 0.5 M H_2SO_4 Containing Various Concentration of *Parinari polyandra* at 303K

Table 4.6: Corrosion Rate of Aluminium and Inhibition Efficiencies of the Various Inhibitors in 1.0 M HCl at 303K, 313K, 323K and 333K

System	Inhibition efficiency (%)				Corrosion rate ($gh^{-1}cm^{-2}$)			
at 303K	**PP**	**PA**	**BS**	**PP1**	**PP**	**PA**	**BS**	**PP1**
Blank	-	-	-	-	0.00355	0.00355	0.00355	0.00355
0.1g/l	62.12	56.56	64.78	58.52	0.00134	0.00154	0.00125	0.00147
0.2g/l	66.66	64.63	67.76	60.71	0.00118	0.00126	0.00114	0.00139
0.3 g/l	68.85	66.19	68.85	65.72	0.00111	0.00120	0.00111	0.00122
0.4 g/l	72.61	68.85	69.01	67.60	0.00097	0.00111	0.00110	0.00115
0.5 g/l	73.55	69.17	70.10	70.57	0.00094	0.00109	0.00106	0.00104
at 313K								
Blank	-	-	-	-	0.00521	0.00521	0.00521	0.00521
0.1 g/l	34.25	47.70	40.76	56.02	0.00342	0.00272	0.00308	0.00229
0.2 g/l	45.78	52.18	42.90	59.97	0.00282	0.00249	0.00297	0.00208
0.3 g/l	54.10	54.53	45.99	64.25	0.00239	0.00237	0.00281	0.00186
0.4 g/l	58.59	54.21	47.70	66.70	0.00216	0.00238	0.00272	0.00173
0.5 g/l	62.64	59.44	51.65	69.37	0.00194	0.00211	0.00252	0.00159
at 323K								
Blank	-	-	-	-	0.01042	0.01042	0.01042	0.01042
0.1 g/l	27.57	30.56	38.82	21.38	0.00754	0.00723	0.00637	0.00819
0.2 g/l	32.16	35.94	40.96	29.12	0.00707	0.00667	0.00615	0.00738
0.3 g/l	34.45	37.17	41.70	30.50	0.00683	0.00654	0.00607	0.00724
0.4 g/l	39.78	38.98	42.08	34.77	0.00627	0.00636	0.00603	0.00679
0.5 g/l	46.98	42.08	46.66	38.45	0.00553	0.00603	0.00556	0.00641
at 333K								
Blank	-	-	-	-	0.01686	0.01686	0.01686	0.01686
0.1 g/l	26.85	26.26	12.65	07.31	0.01233	0.01243	0.01473	0.01563
0.2 g/l	30.18	33.44	17.13	07.57	0.01177	0.01122	0.01397	0.01558
0.3 g/l	32.12	35.55	21.21	21.38	0.01144	0.01087	0.01328	0.01326
0.4 g/l	35.12	36.93	22.43	23.65	0.01094	0.01063	0.01308	0.01287
0.5 g/l	45.50	40.42	22.50	30.87	0.00919	0.01004	0.01307	0.01166

Table 4.7: Corrosion Rate of Aluminium and Inhibition Efficiencies of the Various Inhibitors in 0.5 M H_2SO_4 at 303K, 313K, 323K and 333K

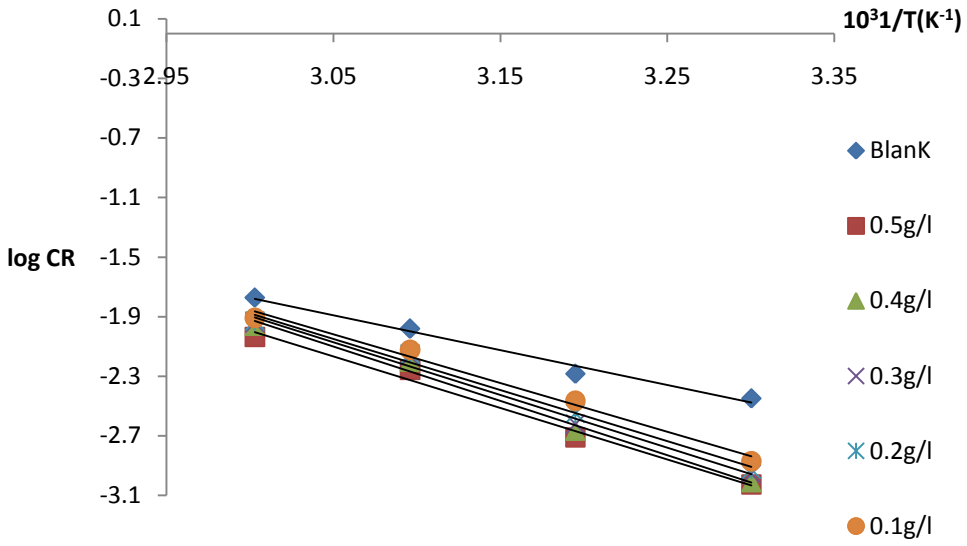
System	Inhibition efficiency (%)				Corrosion rates ($gh^{-1}cm^{-2}$)			
at 303K	**PP**	**PA**	**BS**	**PP1**	**PP**	**PA**	**BS**	**PP1**
Blank					8.33E-05	8.33E-05	8.33E-05	8.33E-05
0.1g/l	20.00	20.00	-6.66	13.33	6.67E-05	6.67E-05	8.89E-05	7.22E-05
0.2g/l	20.00	20.00	6.66	20.00	6.67E-05	6.67E-05	7.78E-05	6.67E-05
0.3g/l	20.00	20.00	6.66	20.00	6.67E-05	6.67E-05	7.78E-05	6.67E-05
0.4g/l	20.00	20.00	6.66	20.00	6.67E-05	6.67E-05	7.78E-05	6.67E-05
0.5g/l	40.00	40.00	6.66	33.33	0.00005	0.00005	7.78E-05	5.56E-05
at 313K								
Blank					0.00016	0.00016	0.00016	0.00016
0.1g/l	0.00	-3.57	-7.14	-3.57	0.00016	0.00016	0.00017	0.00016
0.2g/l	0.00	0.00	-7.14	0.00	0.00016	0.00016	0.00017	0.00016
0.3g/l	0.00	0.00	-3.57	7.14	0.00016	0.00016	0.00016	0.00014
0.4g/l	10.71	10.71	-3.57	3.57	0.00014	0.00014	0.00016	0.00015
0.5g/l	14.28	14.28	7.14	7.14	0.00013	0.00013	0.00014	0.00014
at 323K								
Blank					0.00029	0.00029	0.00029	0.00029
0.1g/l	0.00	-11.53	-11.53	-17.30	0.00029	0.00032	0.00032	0.00034
0.2g/l	0.00	-7.69	-11.53	-9.61	0.00029	0.00031	0.00032	0.00032
0.3g/l	1.92	-5.76	-3.84	-9.61	0.00028	0.00031	0.00030	0.00032
0.4g/l	1.92	0.00	-1.92	-9.61	0.00028	0.00029	0.00029	0.00032
0.5g/l	7.69	7.69	0.00	-9.61	0.00027	0.00027	0.00029	0.00032
at 333K								
Blank					0.000483	0.00016	0.000483	0.000483
0.1g/l	-5.74	-33.33	-12.64	-26.43	0.00016	0.000644	0.000544	0.000611
0.2g/l	-4.59	-33.33	-5.74	-26.43	0.00016	0.000644	0.000511	0.000611
0.3g/l	-4.59	-28.73	-3.44	-14.94	0.00016	0.000622	0.000500	0.000556
0.4g/l	-2.29	-10.34	-5.74	-14.94	0.0001	0.000533	0.000511	0.000556
0.5g/l	-1.14	-9.19	-4.59	-10.34	0.000133	0.000528	0.000506	0.000533

Table 4.8: Corrosion Rate of Mild Steel and Inhibition Efficiencies of the Various Inhibitors in 1.0 M HCl at 303K, 313K, 323K and 333K

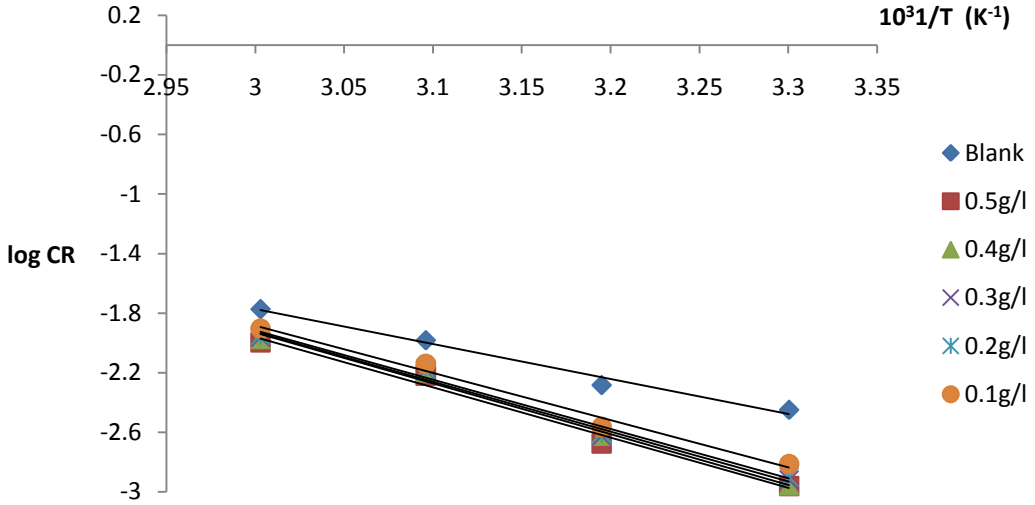
System	Inhibition efficiency (%)				Corrosion rate ($gh^{-1}cm^{-2}$)			
at 303K	**PP**	**PA**	**BS**	**PP1**	**PP**	**PA**	**BS**	**PP1**
Blank					0.00580	0.0058	0.00580	0.00580
0.1g	60.44	30.55	61.30	40.90	0.00229	0.00402	0.00224	0.00342
0.2g	69.73	43.96	70.59	50.86	0.00175	0.00325	0.00170	0.00285
0.3g	74.04	53.06	75.67	63.69	0.00150	0.00272	0.00141	0.00210
0.4g	80.07	58.71	78.54	65.03	0.00115	0.00239	0.00124	0.00202
0.5g	83.52	66.47	81.51	68.58	0.00095	0.00194	0.00107	0.00182
at 313K								
Blank					0.01190	0.01190	0.01190	0.01190
0.1g	17.40	23.01	15.21	37.33	0.00983	0.00916	0.01009	0.00746
0.2g	18.61	24.21	41.57	47.50	0.00968	0.00902	0.00695	0.00625
0.3g	41.99	27.62	54.50	62.57	0.00690	0.00861	0.00541	0.00446
0.4g	55.34	29.91	58.93	64.30	0.00531	0.00834	0.00488	0.00425
0.5g	61.03	39.80	65.05	65.32	0.00463	0.00716	0.00416	0.00413
at 323K								
Blank					0.01764	0.01764	0.01764	0.01764
0.1g	5.76	15.74	9.44	13.09	0.01663	0.01487	0.01597	0.01533
0.2g	12.21	18.35	30.41	27.20	0.01549	0.01441	0.01227	0.01284
0.3g	16.82	21.31	40.52	35.29	0.01468	0.01388	0.01049	0.01142
0.4g	23.17	28.11	43.01	40.74	0.01356	0.01268	0.01005	0.01046
0.5g	30.38	40.93	56.83	44.67	0.01228	0.01042	0.00761	0.00976
at 333K								
Blank					0.02563	0.02563	0.02563	0.02563
0.1g	4.76	12.11	6.01	0.10	0.02441	0.02252	0.02408	0.02560
0.2g	5.26	12.87	14.26	1.40	0.02428	0.022328	0.02197	0.02527
0.3g	15.73	18.46	17.64	7.54	0.02159	0.020894	0.02110	0.02369
0.4g	21.65	24.25	18.38	7.91	0.02008	0.019411	0.02091	0.02360
0.5g	23.28	32.84	18.81	10.03	0.01966	0.017211	0.02080	0.02306

Table 4.9: Corrosion Rate of Mild Steel and Inhibition Efficiencies of the Various Inhibitors in 0.5 M H_2SO_4 at 303K, 313K, 323K and 333K

System	Inhibition efficiency (%)				Corrosion rates ($gh^{-1}cm^{-2}$)			
at 303K	**PP**	**PA**	**BS**	**PP1**	**PP**	**PA**	**BS**	**PP1**
Blank					0.01384	0.01384	0.01384	0.01384
0.1g/l	51.42	28.62	41.67	37.09	0.00672	0.00988	0.00807	0.00871
0.2g/l	67.96	36.33	56.08	50.46	0.00443	0.00881	0.00608	0.00686
0.3g/l	73.34	46.96	66.84	55.92	0.00369	0.00734	0.00459	0.00610
0.4g/l	77.23	49.97	74.67	59.65	0.00315	0.00692	0.00351	0.00558
0.5g/l	79.00	55.92	80.29	65.47	0.00291	0.00610	0.00273	0.00478
at 313K								
Blank					0.01998	0.01998	0.01998	0.01998
0.1g/l	15.98	28.63	13.51	31.77	0.01679	0.01426	0.01728	0.01363
0.2g/l	16.29	31.72	29.21	45.01	0.01673	0.01364	0.01414	0.01099
0.3g/l	38.33	34.80	44.28	50.26	0.01232	0.01303	0.01113	0.00994
0.4g/l	44.75	37.89	52.93	56.43	0.01104	0.01241	0.00941	0.00871
0.5g/l	53.96	40.58	57.10	60.18	0.00920	0.01187	0.00857	0.00796
at 323K								
Blank					0.03018	0.03018	0.03018	0.03018
0.1g/l	7.69	22.06	11.87	9.88	0.02786	0.02352	0.02660	0.02720
0.2g/l	11.33	30.25	15.57	22.28	0.02676	0.02105	0.02548	0.02346
0.3g/l	16.74	34.51	27.31	30.70	0.02513	0.01977	0.02194	0.02092
0.4g/l	23.49	36.38	30.75	38.83	0.02309	0.01920	0.02090	0.01846
0.5g/l	26.24	38.43	31.51	41.08	0.02226	0.01858	0.02067	0.01778
at 333K								
Blank					0.03779	0.03779	0.03779	0.03779
0.1g/l	3.94	11.46	9.20	0.02	0.03630	0.03346	0.03431	0.00061
0.2g/l	7.04	12.27	10.48	1.59	0.03513	0.03315	0.03383	0.00061
0.3g/l	15.21	17.21	14.95	4.78	0.03204	0.03128	0.03214	0.00056
0.4g/l	20.64	23.37	17.36	5.39	0.02999	0.02896	0.03123	0.00056
0.5g/l	23.43	28.55	21.75	8.61	0.02893	0.02700	0.02957	0.00053

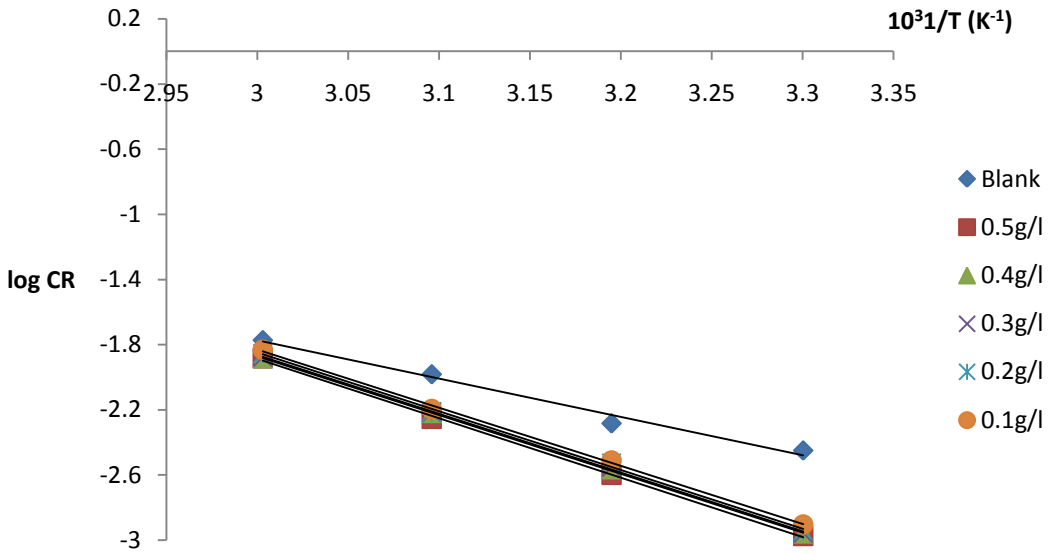


(a)

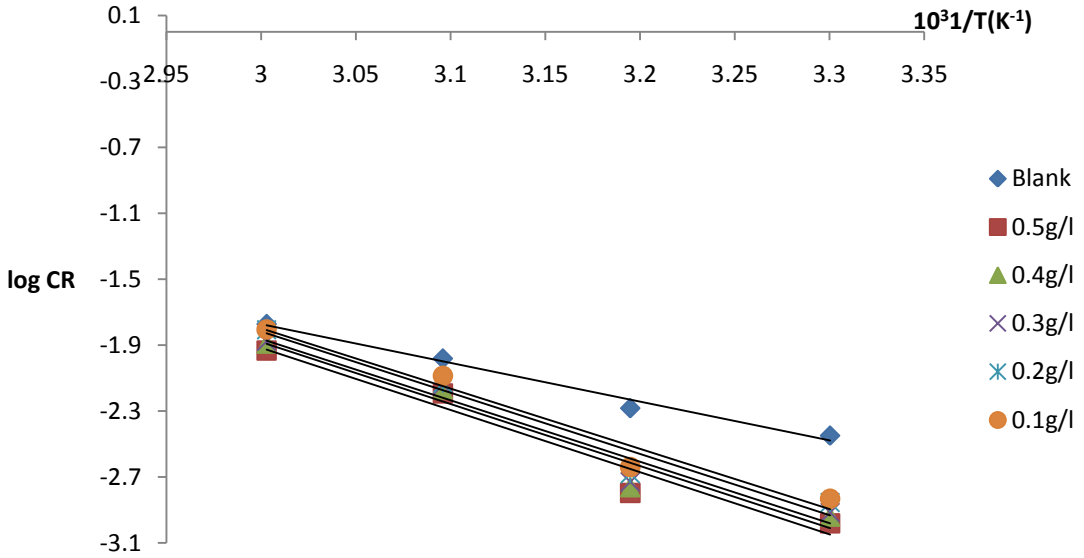


(b)

Fig. 4.13: Variation of log (Corrosion Rate) of Aluminium with Inverse Temperature in 1.0 M HCl Containing Various Concentration of (a) PP (b) PA

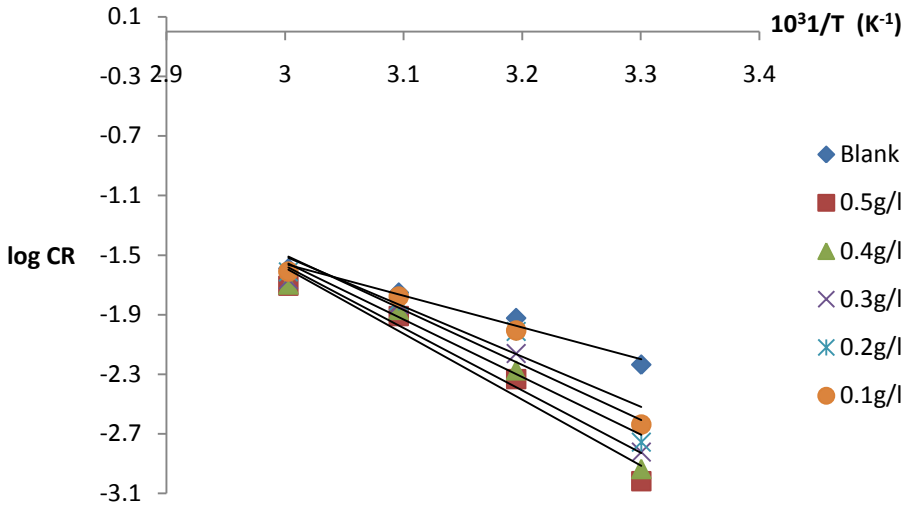


(a)

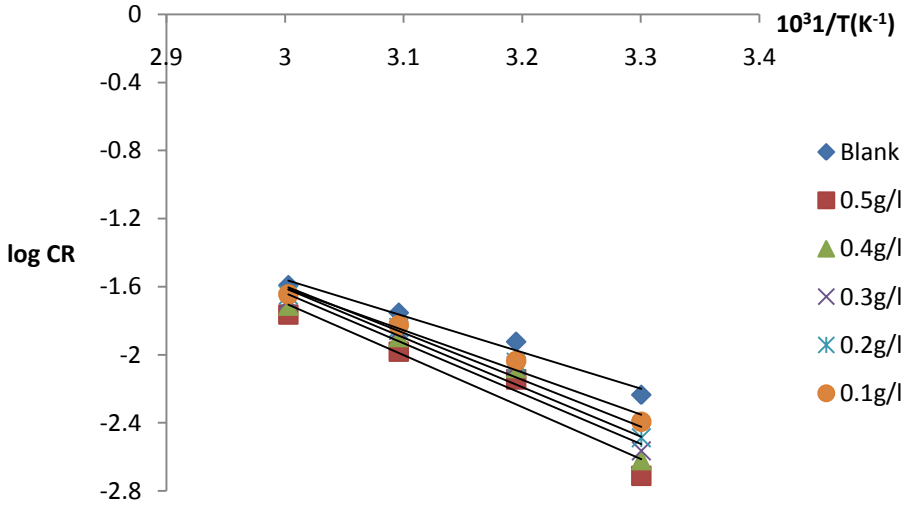


(b)

Fig. 4.14: Variation of log (Corrosion Rate) of Aluminium with Inverse Temperature in 1.0M HCl Containing Various Concentration of (a) BS (b) PP1

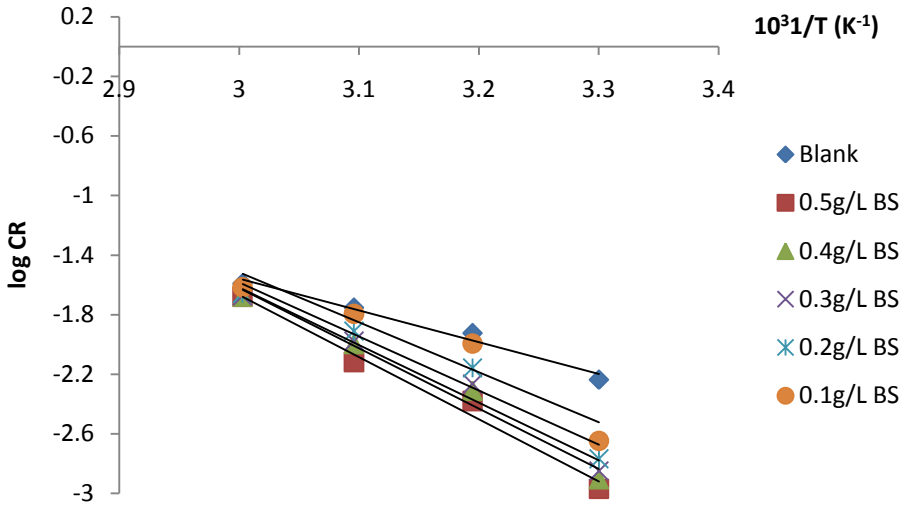


(a)

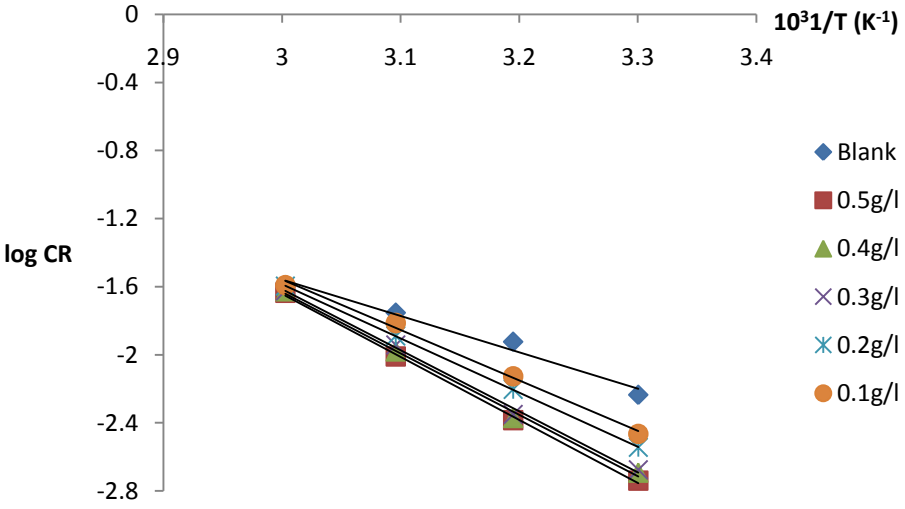


(b)

Fig. 4.15: Variation of log (Corrosion Rate) of Mild Steel with Inverse Temperature in 1.0 M HCl Containing Various Concentration of (a) PP (b) PA

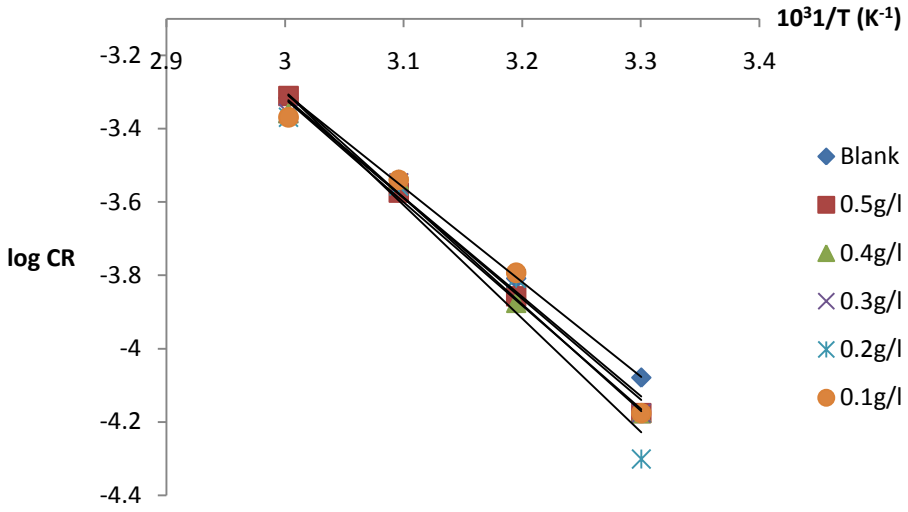


(a)

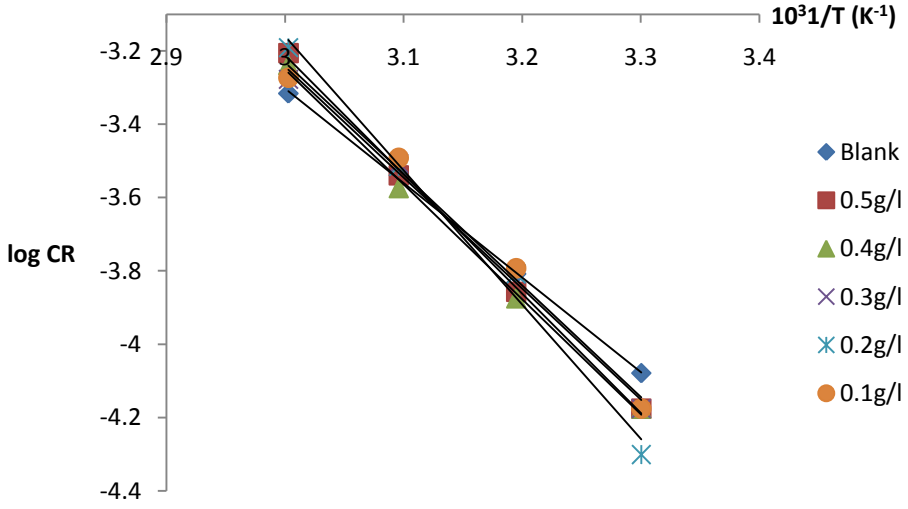


(b)

Fig. 4.16: Variation of log (Corrosion Rate) of Mild Steel with Inverse Temperature in 1.0 M HCl Containing Various Concentration of (a) BS (b) PP1

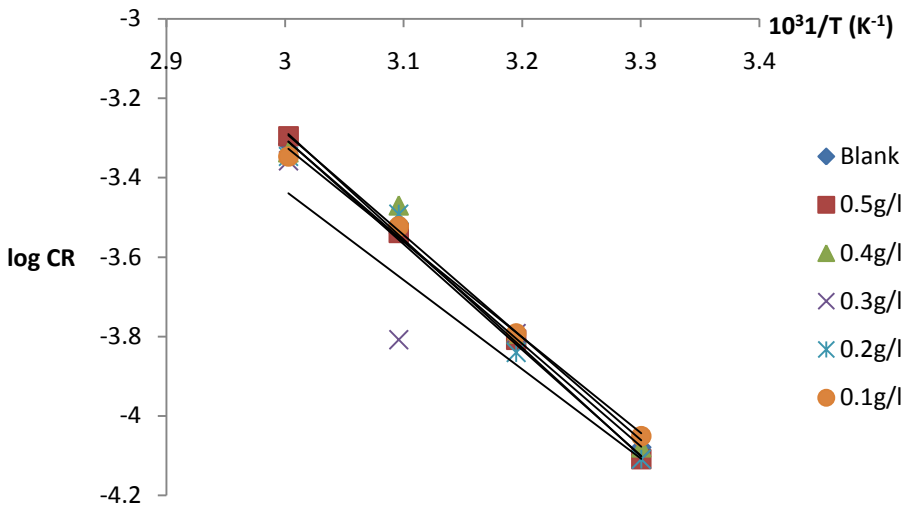


(a)

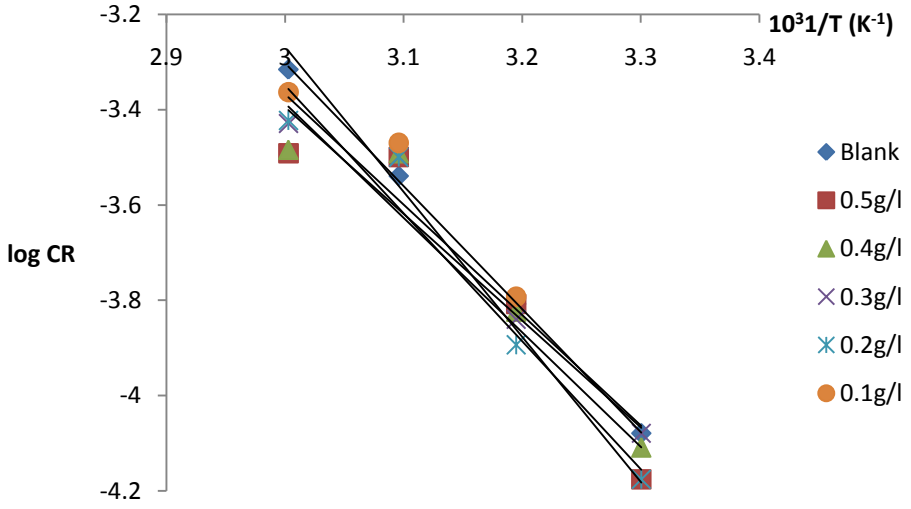


(b)

Fig. 4.17: Variation of log (Corrosion Rate) of Aluminium with Inverse Temperature in 0.5 M H_2SO_4 Containing Various Concentration of (a) PP (b) PA

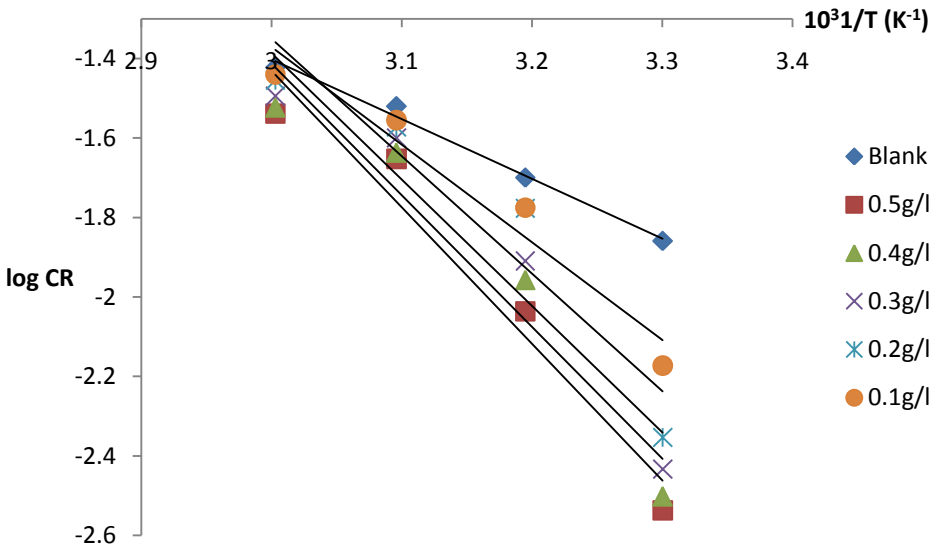


(a)

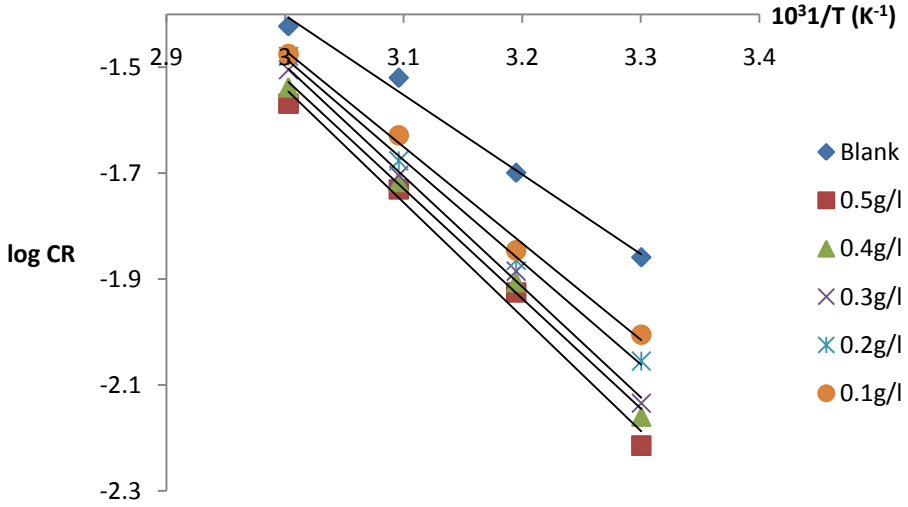


(b)

Fig. 4.18: Variation of log (Corrosion Rate) of Aluminium with Inverse Temperature in 0.5 M H_2SO_4 Containing Various Concentration of (a) BS (b) PP1

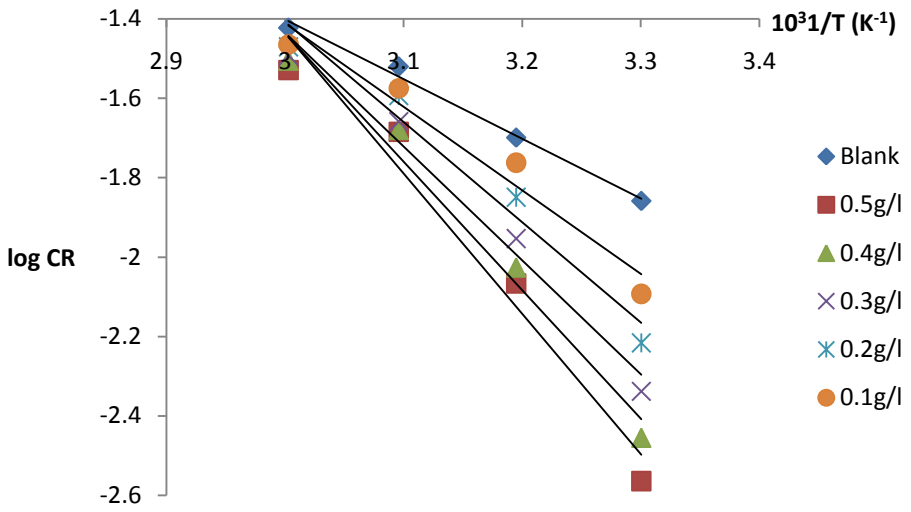


(a)

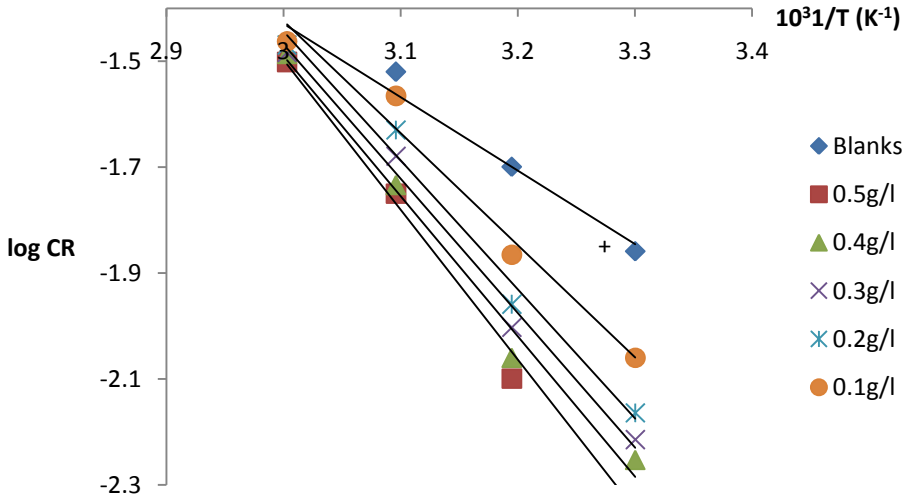


(b)

Fig. 4.19: Variation of log (Corrosion Rate) of Mild Steel with Inverse Temperature in 0.5 M H_2SO_4 Containing Various Concentration of (a) PP (b) PA



(a)



(b)

Fig. 4.20: Variation of log (Corrosion Rate) of Mild Steel with Inverse Temperature in 0.5 M H_2SO_4 containing various concentration of (a) BS (b) PP1

Table 4.10: Thermodynamic Parameters for the Adsorption of Various Concentration of the Inhibitor on Aluminium Surface in 1.0 M HCl

	System	Ea(kJmol^{-1})	Qads (kJmol^{-1})
	Blank	44.94	-
	0.1g/l	62.61	-41.87
PP Al	0.2g/l	65.67	-42.84
	0.3g/l	67.72	-39.35
	0.4g/l	69.96	-48.19
	0.5g/l	66.25	-33.65
	0.1g/l	60.75	-36.36
PA Al	0.2g/l	63.43	-36.11
	0.3g/l	64.03	-35.43
	0.4g/l	65.29	-37.15
	0.5g/l	64.64	-33.44
	0.1g/l	68.16	-71.09
BS Al	0.2g/l	69.10	-64,86
	0.3g/l	69.06	-58.88
	0.4g/l	69.01	-57.08
	0.5g/l	69.79	-58.43
	0.1g/l	69.98	-80.65
PP1 Al	0.2g/l	71.13	-82.13
	0.3g/l	71.36	-54.62
	0.4g/l	72.07	-53.34
	0.5g/l	72.24	-47.06

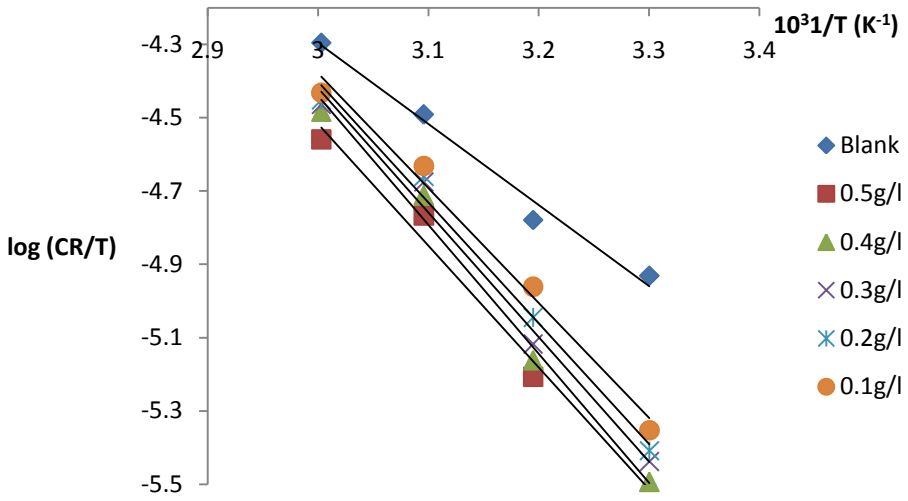
Table 4.11: Thermodynamic Parameters for the Adsorption of Various Concentration of the Inhibitor on Mild Steel Surface in 1.0 M HCl

	System	Ea (kJ/mol)	Qads (kJ/mol)
	Blank	41.55	-
	0.1g/l	66.12	-95.59
PP steel	0.2g/l	73.64	-104.15
	0.3g/l	74.49	-76.24
	0.4g/l	79.85	-74.87
	0.5g/l	84.58*	- 78.75
	0.1g/l	47.56	-32.41
PA steel	0.2g/l	52.71	-46.69
	0.3g/l	55.66	-44.96
	0.4g/l	56.58	-41.70
	0.5g/l	58.42	-39.15
	0.1g/l	64.12	-89.80
BS steel	0.2g/l	69.48	-74.65
	0.3g/l	73.93	-74.82
	0.4g/l	77.35	-77.98
	0.5g/l	79.84	-82.38
	0.1g/l	56.75	-180.62
PP1 steel	0.2g/l	60.98	-119.77
	0.3g/l	68.78	-85.81
	0.4g/l	69.24	-86.00
	0.5g/l	71.04	-83.17

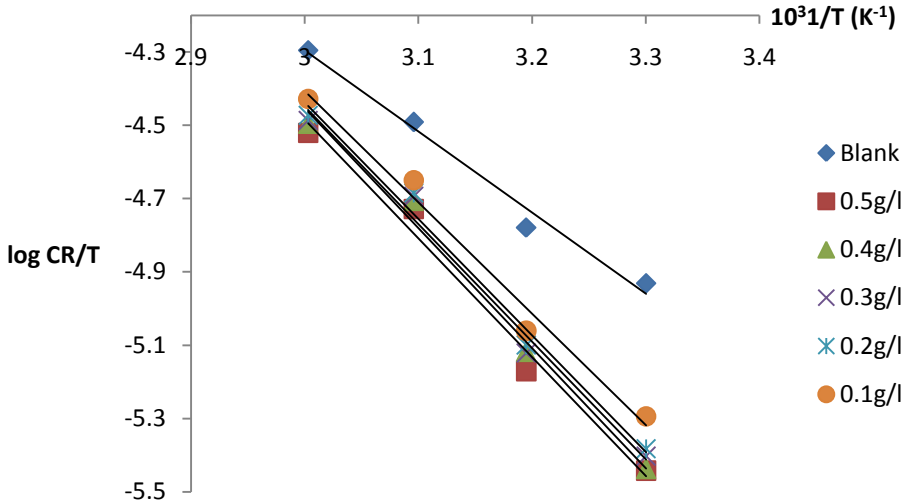
* chemisorption process

Table 4.12: Thermodynamic Parameters for the Adsorption of Various Concentration of the Inhibitor on Mild Steel and Aluminium Surface in 0.5 M H_2SO_4

		Al	Steel	
	System	**E_a(kJmol^{-1})**	**Q_{ads} (kJmol-1)**	**E_a(kJmol^{-1})**
	Blank	49.46		28.8
	0.1g/l	51.91	-90.92	47.01
	0.2g/l	59.22	-93.20	56.56
PP	0.3g/l	52.64	-76.34	60.85
	0.4g/l	54.03	-71.83	63.40
	0.5g/l	55.64	-70.17	65.69
	0.1g/l	58.32	-31.61	41.32
	0.2g/l	70.17	-39.31	39.75
PA	0.3g/l	58.02	-40.53	40.18
	0.4g/l	60.08	-33.18	36.95
	0.5g/l	62.30	-32.31	34.89
	0.1g/l	46.11	-54.61	40.29
	0.2g/l	51.03	-66.82	48.40
BS	0.3g/l	43.08	-68.22	54.91
	0.4g/l	49.44	-73.87	62.02
	0.5g/l	52.35	-75.07	67.74
	0.1g/l	58.32	-229.48	40.52
	0.2g/l	51.49	-115.81	46.64
PP1	0.3g/l	44.42	-90.30	48.60
	0.4g/l	42.93	-91.04	50.64
	0.5g/l	46.03	-83.94	54.17

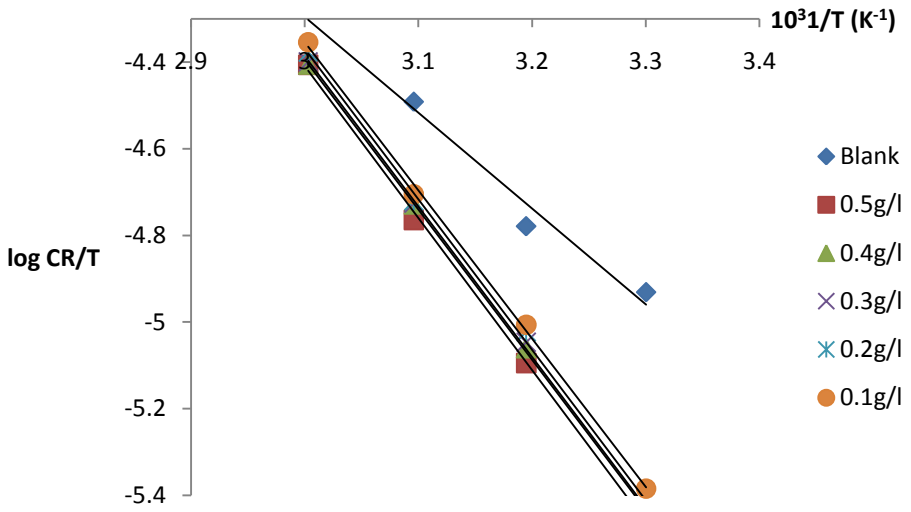


(a)

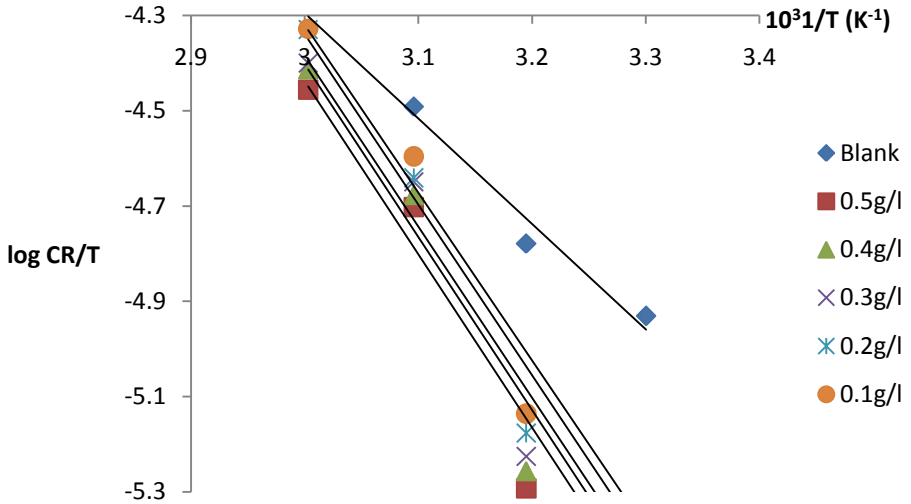


(b)

Fig. 4.21: Variation of log CR/T of Aluminium with Inverse Temperature in 1.0 M HCl Containing Various Concentration of (a) PP (b) PA

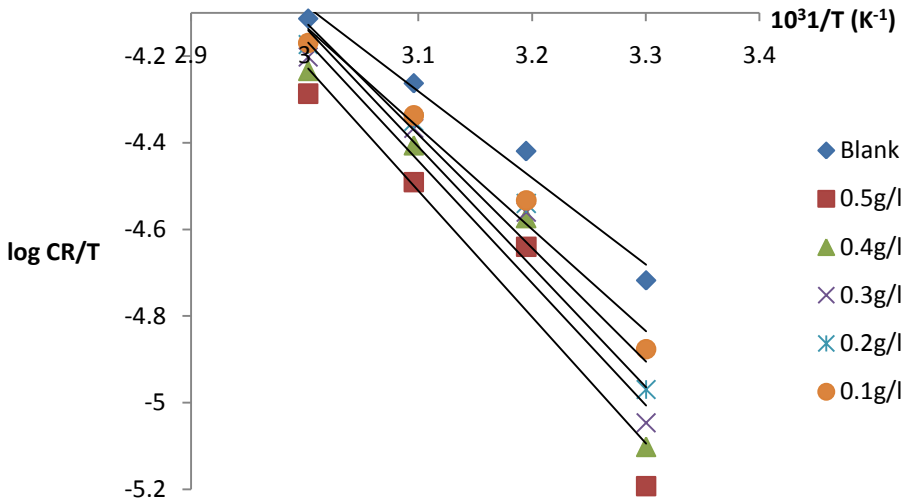


(a)

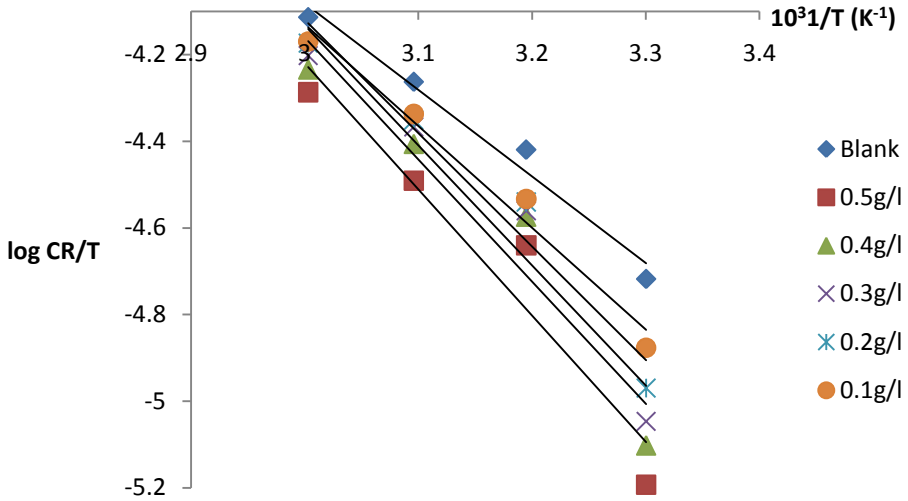


(b)

Fig. 4.22: Variation of log CR/T of Aluminium with Inverse Temperature in 1.0 M HCl Containing Various Concentration of (a) BS (b) PP1

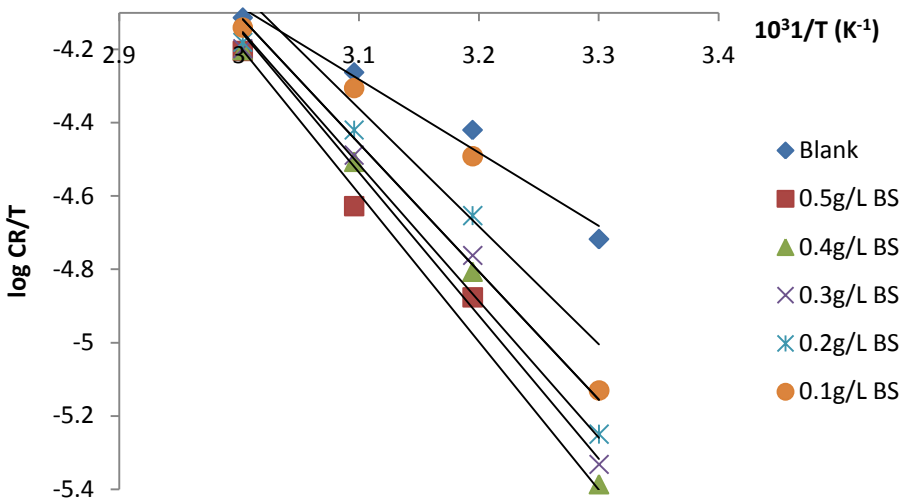


(a)

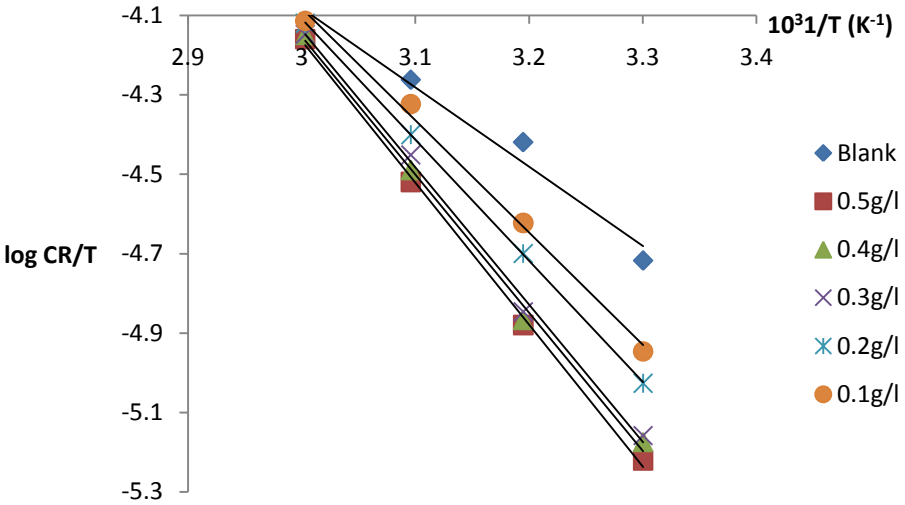


(b)

Fig. 4.23: Variation of log CR/T of Mild Steel with Inverse Temperature in 1.0 M HCl Containing Various Concentration of (a) PP (b) PA

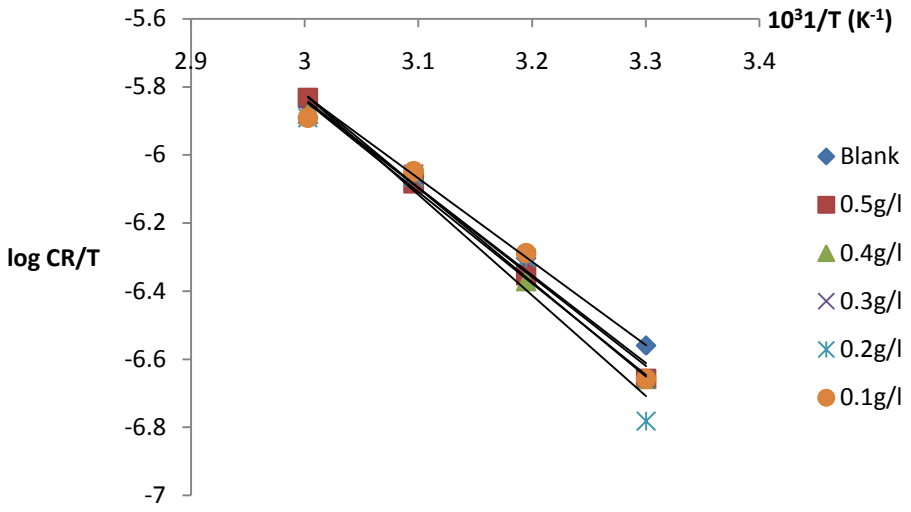


(a)

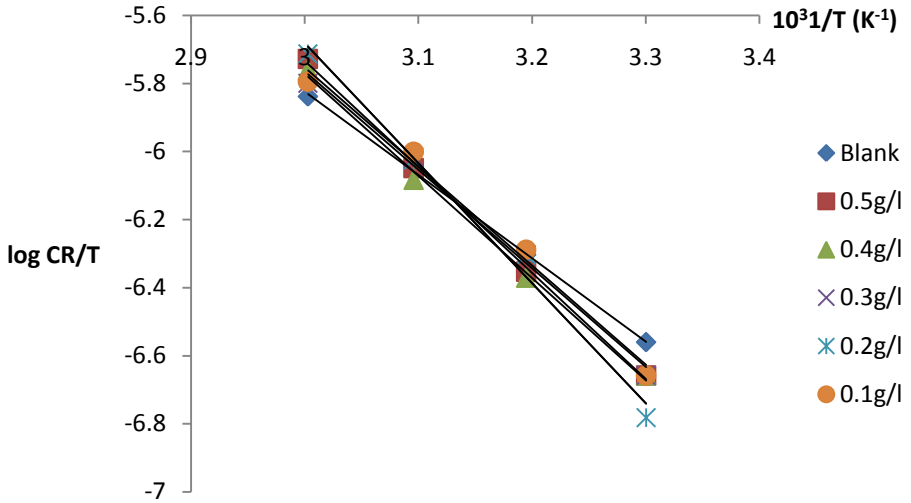


(b)

Fig. 4.24: Variation of log CR/T of Mild Steel with Inverse Temperature in 1.0 M HCl Containing Various Concentration of (a) BS (b) PP1

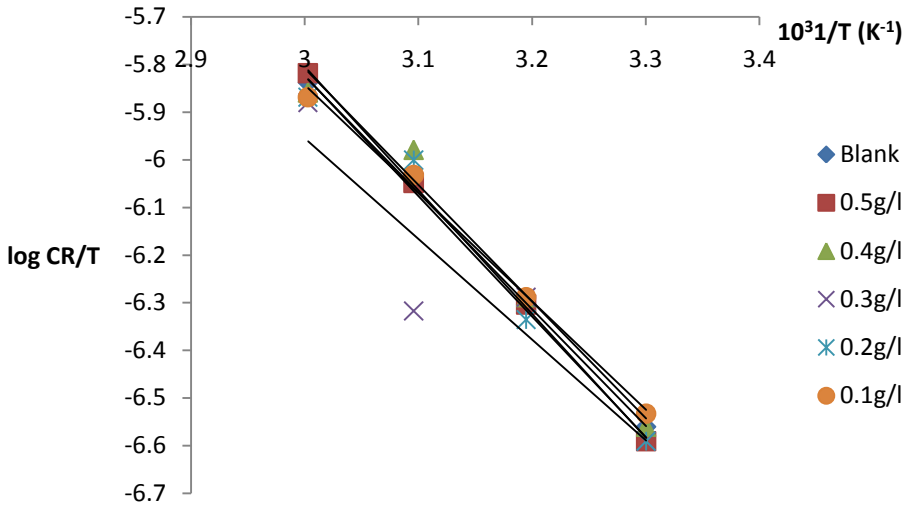


(a)

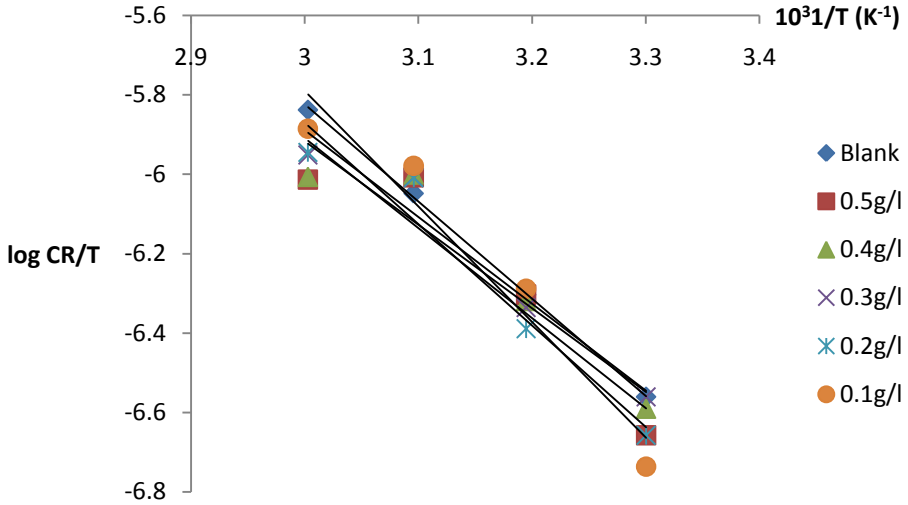


(b)

Fig. 4.25: Variation of log CR/T of Aluminium with Inverse Temperature in 0.5 M H_2SO_4 Containing Various Concentration of (a) PP (b) PA

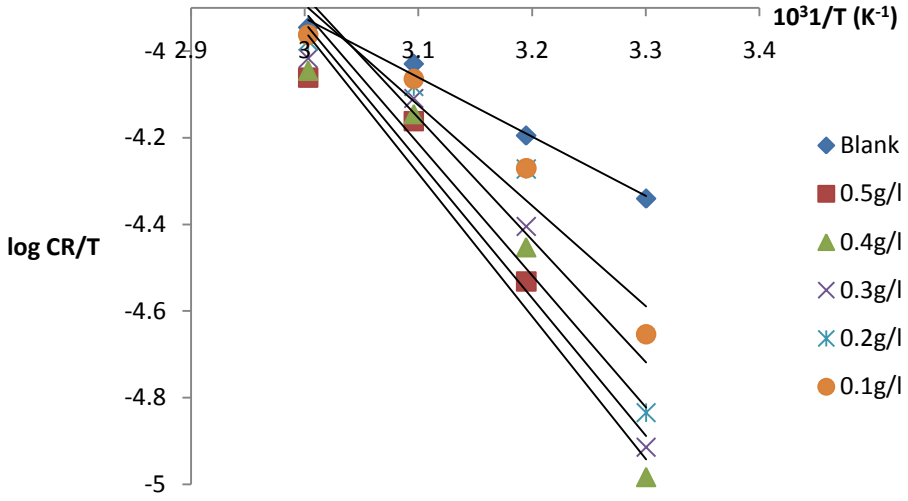


(a)

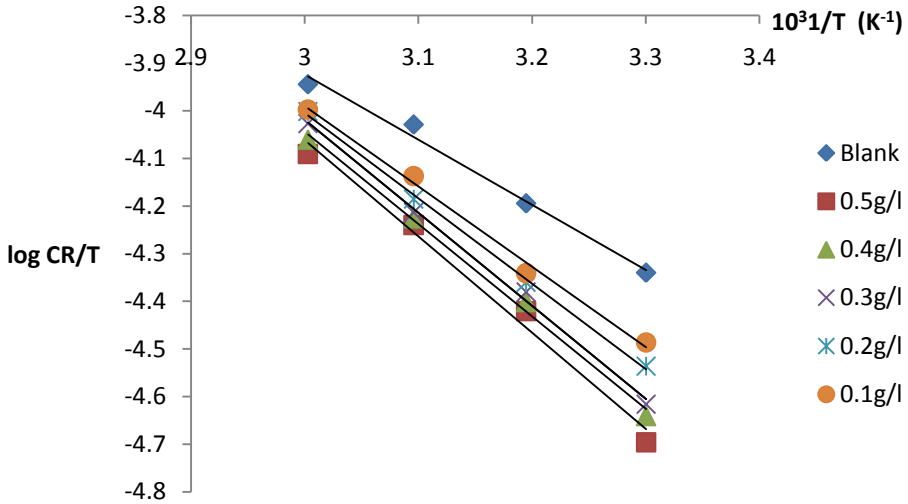


(b)

Fig. 4.26: Variation of log CR/T of Aluminium with Inverse Temperature in 0.5 M H_2SO_4 Containing Various Concentration of (a) BS (b) PP1

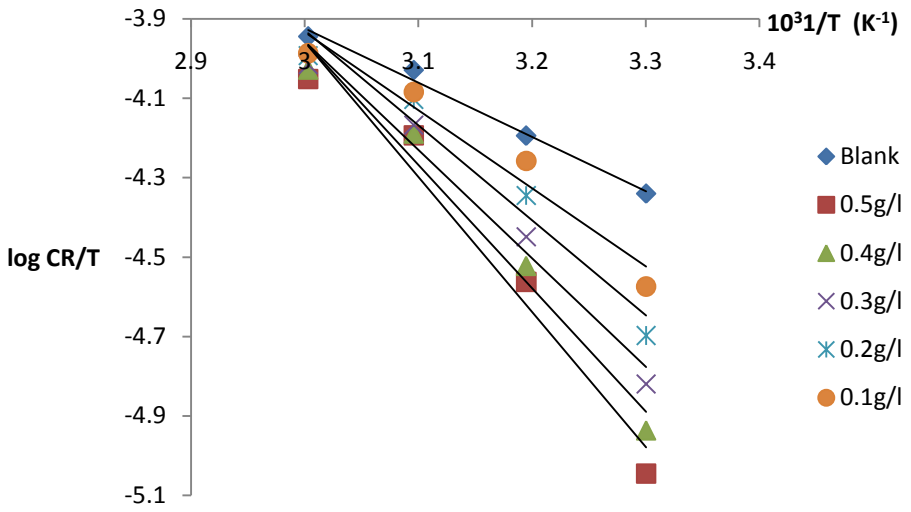


(a)

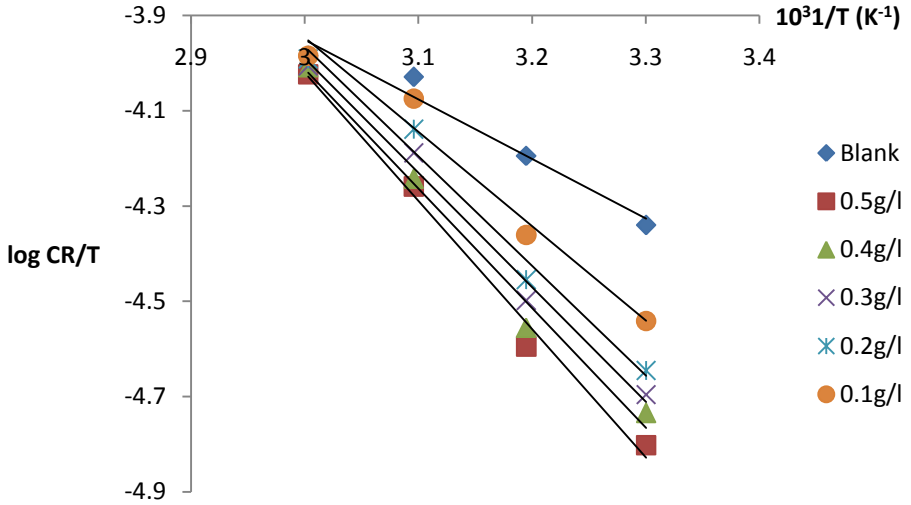


(b)

Fig. 4.27: Variation of log CR/T of Mild Steel with Inverse Temperature in 0.5 M H_2SO_4 Containing Various Concentration of (a) PP (b) PA



(a)



(b)

Fig. 4.28: Variation of log CR/T of Mild Steel with Inverse Temperature in 0.5 M H_2SO_4 Containing Various Concentration of (a) BS (b) PP1

Table 4.13: Thermodynamic Parameters for the Enthalpy and Entropy of Activation of Various Concentration of the Inhibitor on Mild Steel and Aluminium Surface in 1.0 M HCl

		Al		Steel	
		ΔH_a (kJ/mol)	ΔS_a (kJ/mol)	ΔH_a (kJ/mol)	ΔS_a(kJ/mol)
	Blank	42.32	-0.152	38.22	-0.161
	0.5g/l	63.61	-0.093	84.18*	-0.029
PP	0.4g/l	67.32	-0.081	77.62	-0.043
	0.3g/l	65.08	-0.087	71.27	-0.062
	0.2g/l	63.03	-0.093	68.03	-0.071
	0.1g/l	59.97	-0.102	61.81	-0.089
	0.5g/l	62.00	-0.097	55.78	-0.111
	0.4g/l	62.65	-0.095	53.94	-0.115
PA	0.3g/l	61.39	-0.099	53.02	-0.118
	0.2g/l	60.81	-0.100	50.07	-0.126
	0.1g/l	58.11	-0.108	44.12	-0.142
	0.5g/l	67.15	-0.081	77.22	-0.046
	0.4g/l	66.36	-0.083	74.73	-0.053
BS	0.3g/l	66.44	-0.083	71.28	-0.063
	0.2g/l	66.46	-0.082	66.84	-0.076
	0.1g/l	65.52	-0.065	61.48	-0.091
	0.5g/l	69.60	-0.074	68.39	-0.072
	0.4g/l	69.43	-0.074	66.59	-0.077
PP1	0.3g/l	68.72	-0.075	66.13	-0.078
	0.2g/l	68.49	-0.075	58.34	-0.101
	0.1g/l	67.34	-0.078	54.11	-0.113

*chemisorptions process

Table 4.14: Thermodynamic Parameters for the Enthalpy and Entropy of Activation of Various Concentration of the Inhibitor on Mild Steel and aluminium Surface in 0.5 M H_2SO_4

		Al		Steel	
		ΔH_a (kJ/mol)	ΔS_a (kJ/mol)	ΔH_a (kJ/mol)	ΔS_a(kJ/mol)
	Blank	46.81	-0.168	26.15	-0.194
	0.5g/l	53.02	-0.150	63.05	-0.084
PP	0.4g/l	51.39	-0.155	60.75	-0.091
	0.3g/l	50.01	-0.159	58.21	-0.098
	0.2g/l	56.58	-0.139	53.92	-0.110
	0.1g/l	49.27	-0.162	44.36	-0.139
	0.5g/l	59.66	-0.128	38.68	-0.159
	0.4g/l	57.44	-0.136	37.11	-0.164
PA	0.3g/l	55.37	-0.142	37.38	-0.162
	0.2g/l	67.53	-0.104	34.31	-0.171
	0.1g/l	55.68	-0.142	32.24	-0.177
	0.5g/l	49.71	-0.160	65.10	-0.078
	0.4g/l	46.81	-0.168	59.38	-0.095
BS	0.3g/l	40.44	-0.190	52.27	-0.117
	0.2g/l	48.38	-0.164	45.76	-0.136
	0.1g/l	43.46	-0.179	37.64	-0.160
	0.5g/l	43.39	-0.181	51.52	-0.120
	0.4g/l	40.29	-0.190	48.00	-0.130
PP1	0.3g/l	41.78	-0.185	45.95	-0.136
	0.2g/l	48.84	-0.164	44.00	-0.142
	0.1g/l	55.70	-0.141	37.87	-0.160

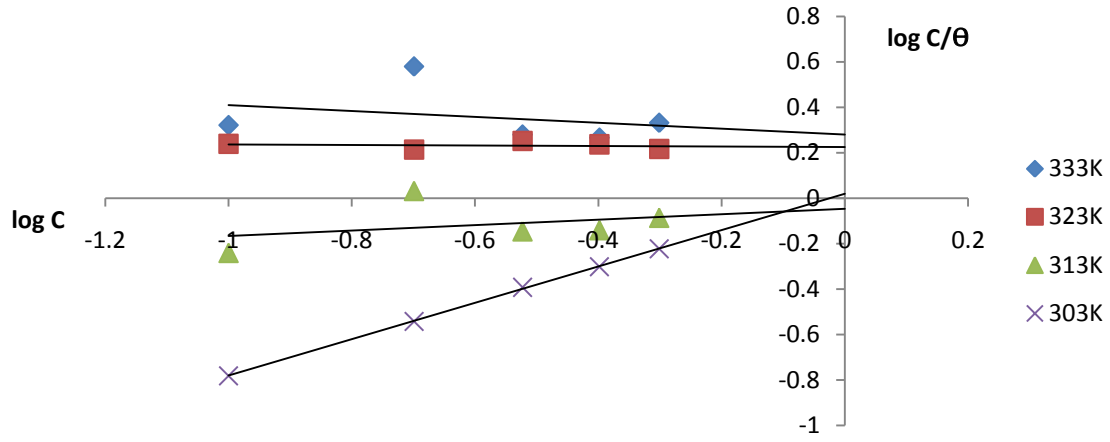
Values of Q_{ads} are also presented in Table 4.10 - 4.12. The values are negative; indicating that the adsorption of the plant extracts studied on both aluminium and mild steel surface is exothermic. It should be noted that since the corrosion reactions were carried out at constant pressure, calculated values of Q_{ads} are expected to be approximately equal to the enthalpies of adsorption.

4.4 Thermodynamic/adsorption Study

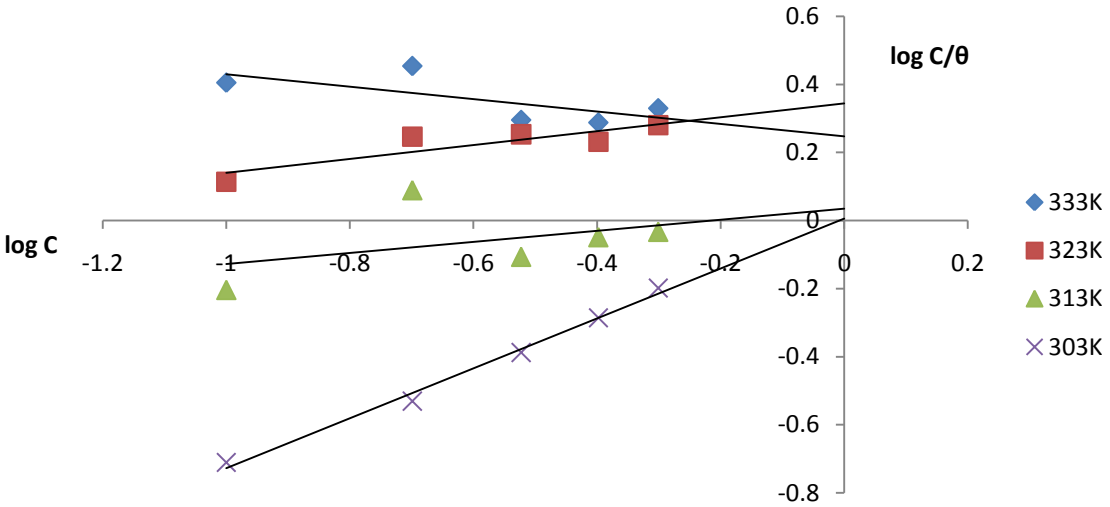
The degree of surface coverage for the various concentration of the extracts at the various temperatures were tested with four different isotherm equations and plots are presented in. Langmuir (Figures 4.29 – 4.34), Freundlich (Figures 4.35 – 4.40), Temkim (Figures 4.41 – 4.46), El-Awady (Figures 4.47 – 4.52). It is evident from the plot and values of R^2 obtianed that both aluminium and mild steel Langmuir isotherm is best fit in both acid media at room temperature while at elevated temperature mild steel is best fit for Freundlich isotherm.

4.5 Electrochemical Measurement

The results of a typical LPR (anodic and cathodic) curves for the corrosion of aluminium and mild steel in 1.0 M HCl and 0.5 M H_2SO_4 solution in the presence and absence of the various concentrations of the inhibitors are presented in Figures 4.53 - 4.64. The parameters derived from these plots are also presented in Table 4.15 and 4.16. The IE% obtained from electrochemical measurements follow similar trend as that in gravimetric method, indicating that the extracts inhibit both mild steel and aluminium.

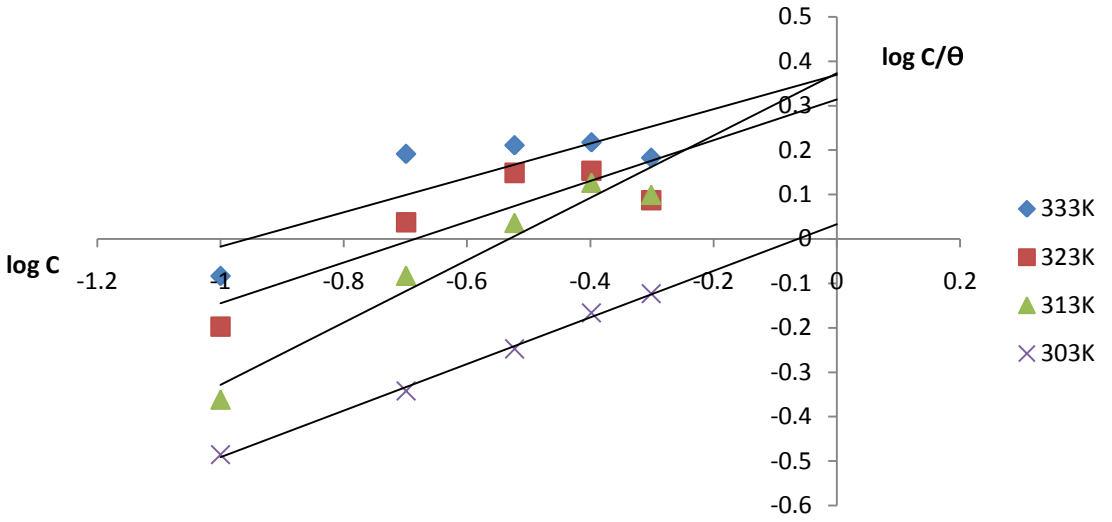


(a)

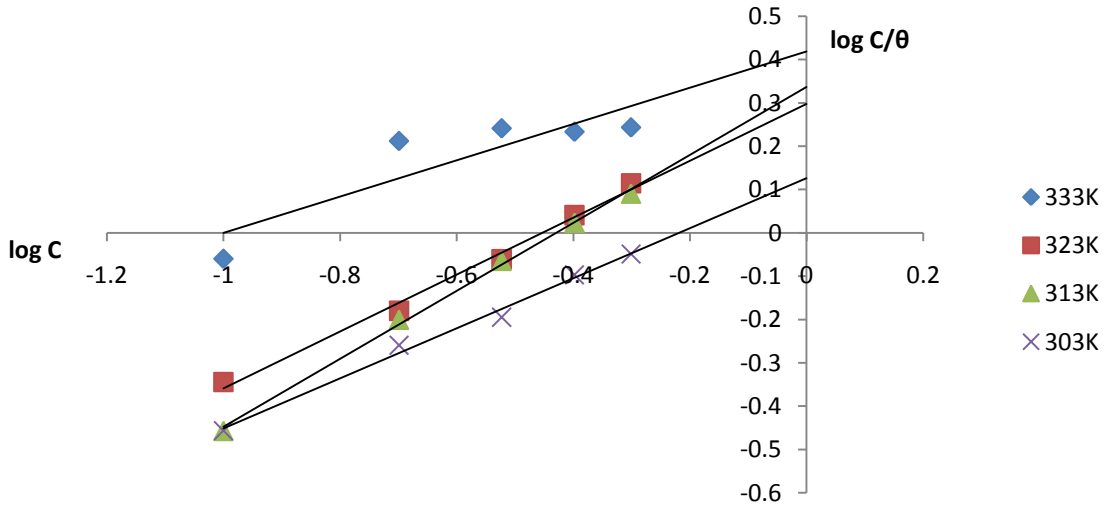


(b)

Fig. 4.29: Langmuir Isotherm for PP Adsorption on Mild Steel Surface in (a) 1.0 M HCl and (b) 0.5 M H_2SO_4 Solution at Various Temperature

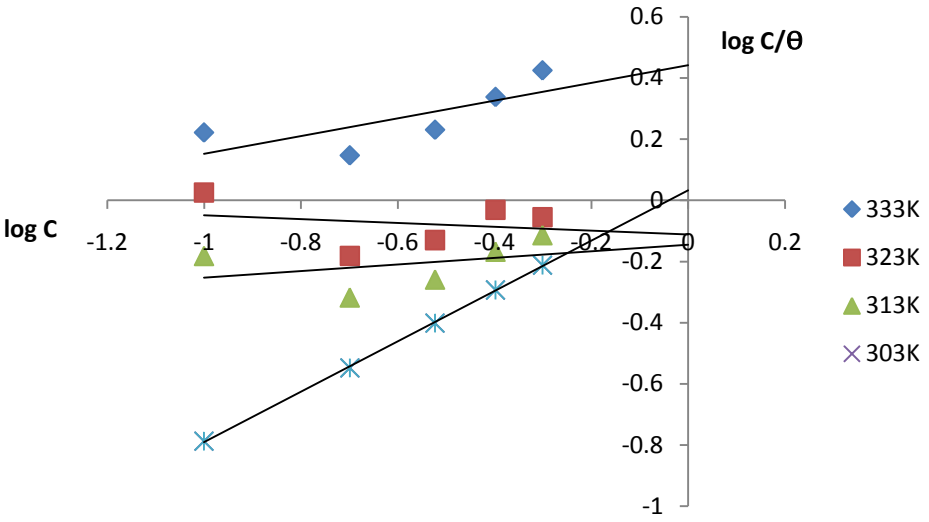


(a)

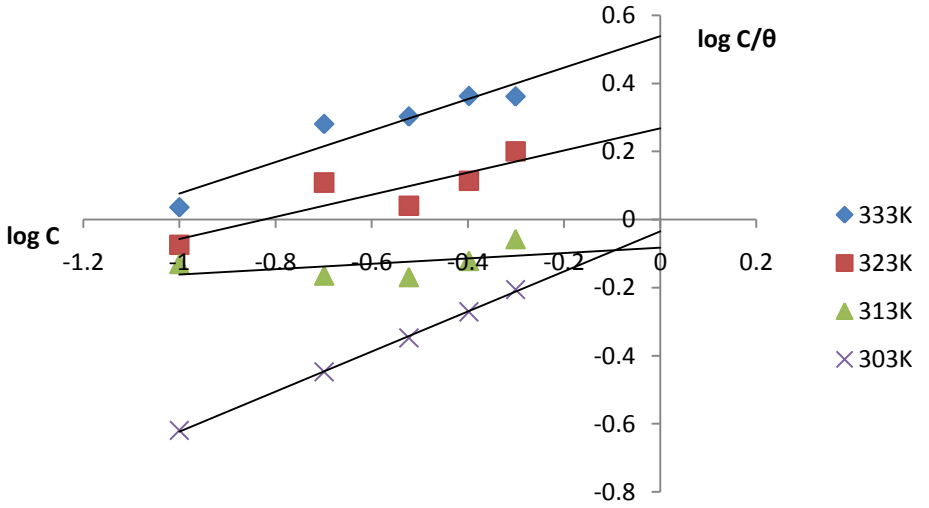


(b)

Fig. 4. 30: Langmuir Isotherm for PA Adsorption on Mild Steel Surface in (a) 1.0 M HCl and (b) 0.5 M H_2SO_4 Solutions at Various Temperature

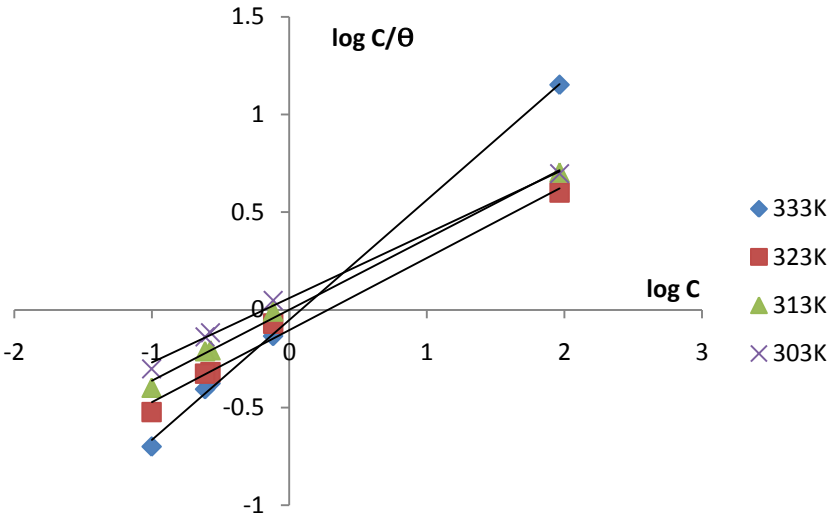


(a)

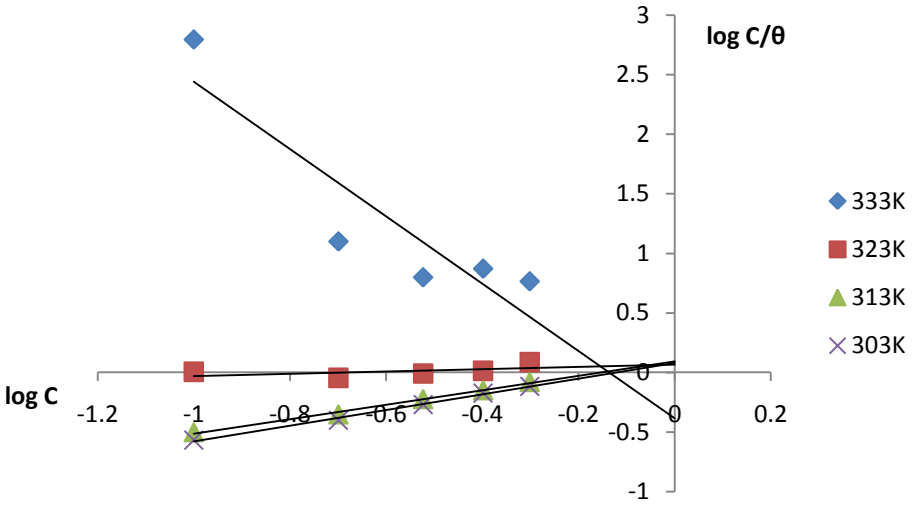


(b)

Fig. 4.31: Langmuir Isotherm for BS Adsorption on Mild Steel Surface in (a) 1.0 M HCl and (b) 0.5 M H_2SO_4 Solutions at Various Temperature

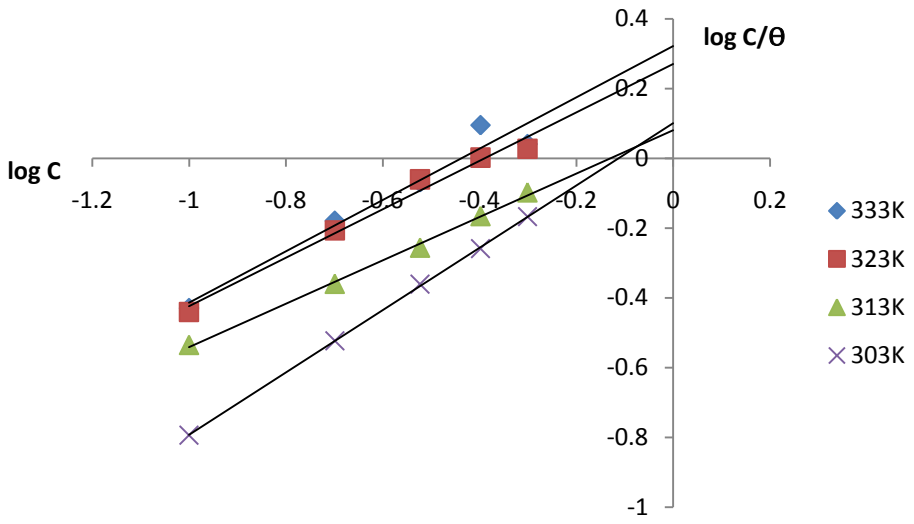


(a)

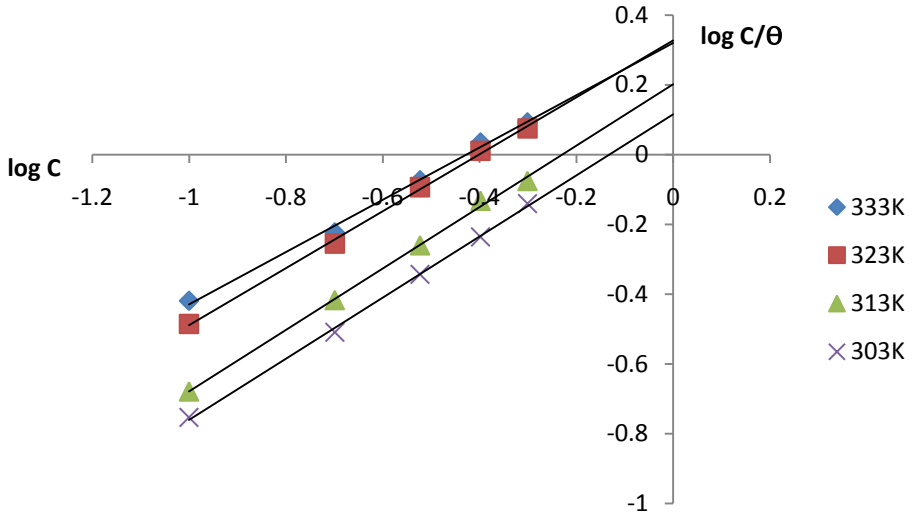


(b)

Fig. 4.32: Langmuir Isotherm for PP1 Adsorption on Mild Steel Surface in (a) 1.0 M HCl and (b) 0.5 M H_2SO_4 Solutions at Various Temperature

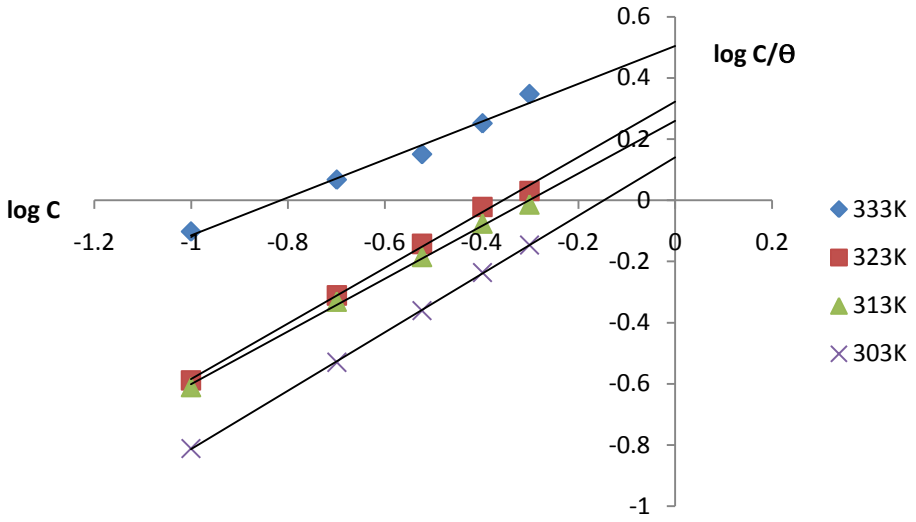


(a)

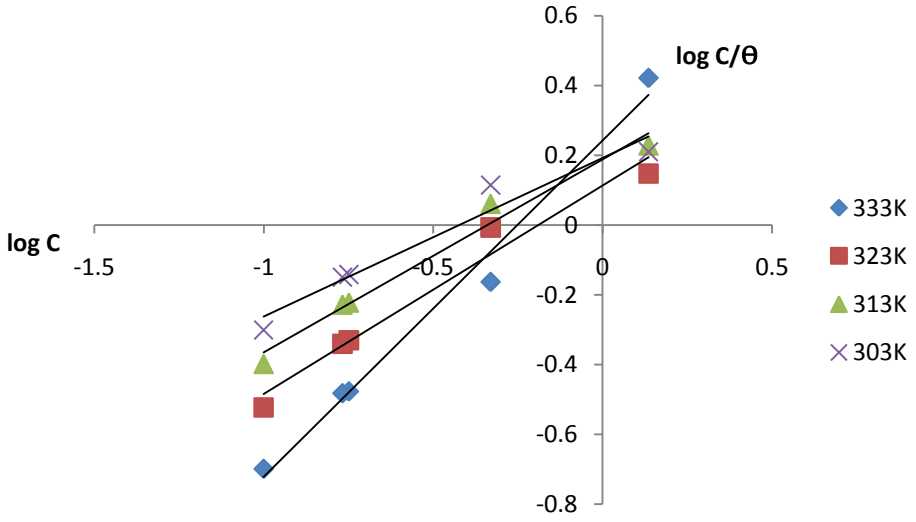


(b)

Fig. 4.33: Langmuir Isotherm for the Adsorption of (a) PP and (b) PA on Aluminium Surface in 1.0 M HCl Solution at Various Temperature

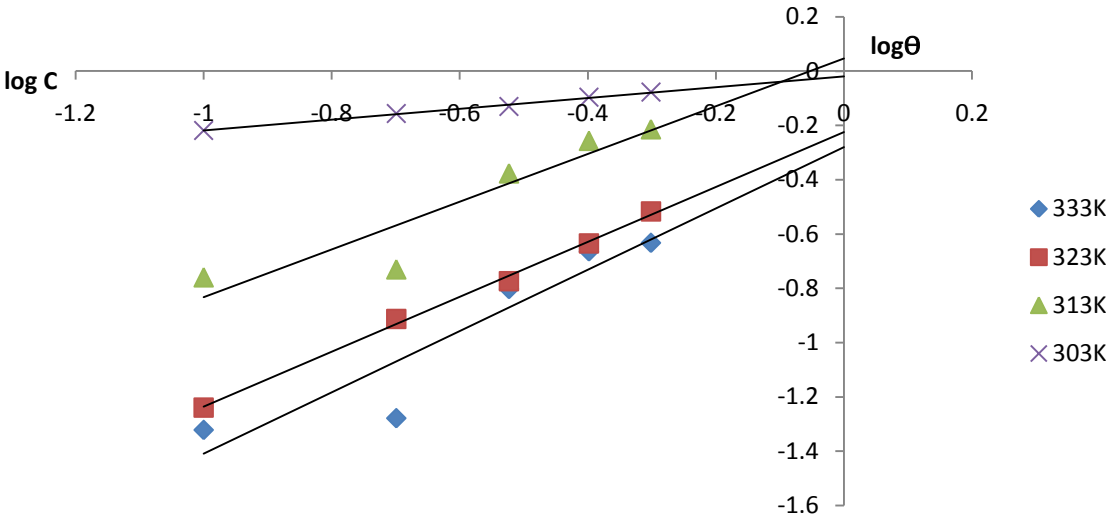


(a)

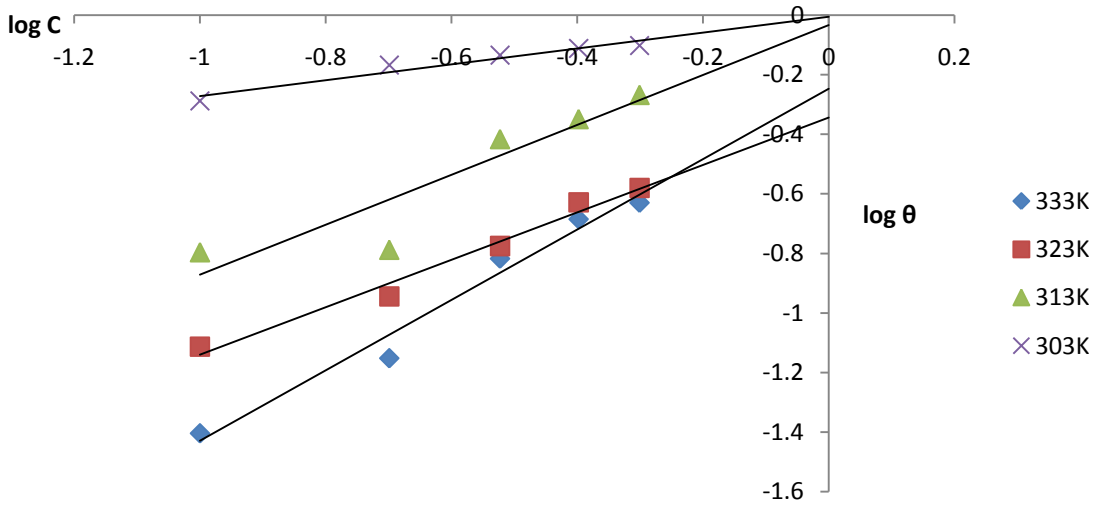


(b)

Fig. 4.34: Langmuir Isotherm for the Adsorption of (a) BS and (b) PP1 on Aluminium Surface in 1.0 M HCl Solution at Various Temperature

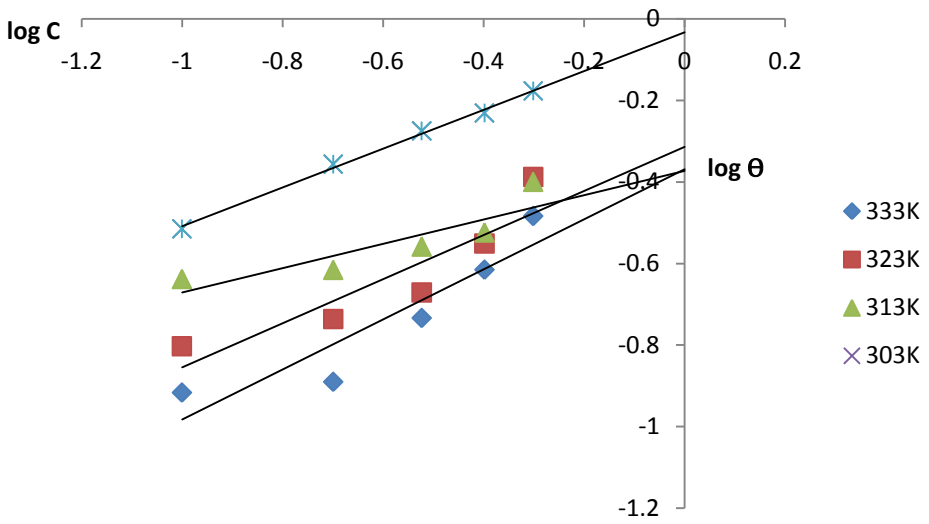


(a)

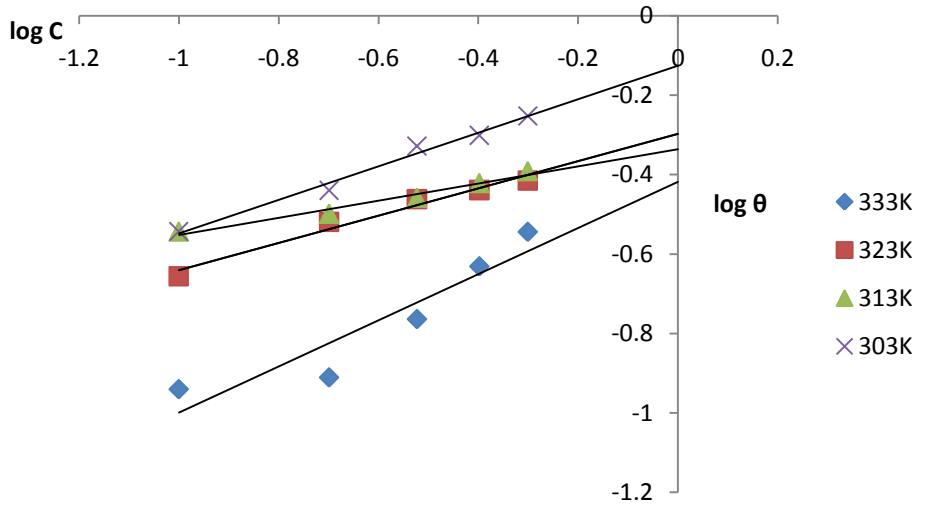


(b)

Fig. 4.35: Freundlich Isotherm for PP Adsorption on Mild Steel Surface in (a) 1.0 M HCl and (b) 0.5 M H_2SO_4 Solutions at Various Temperature

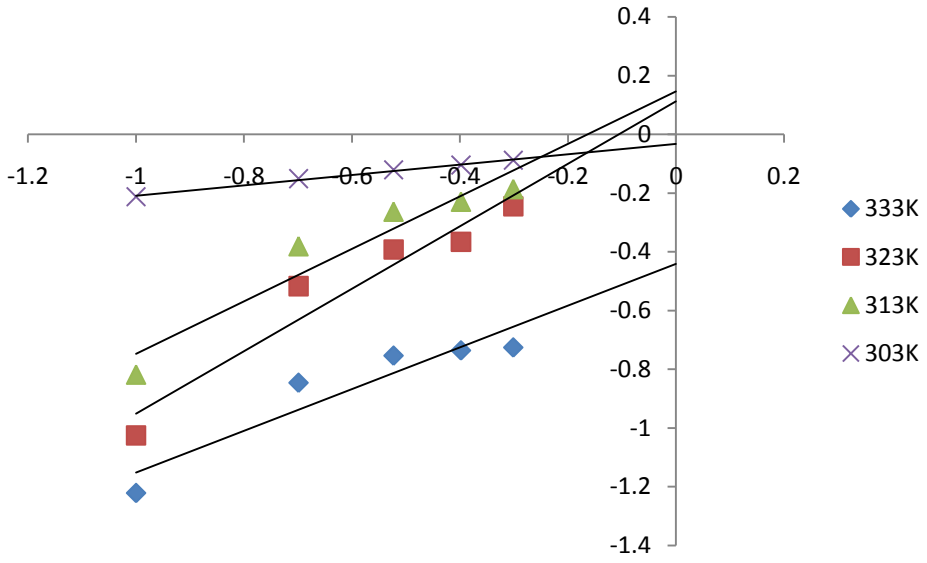


(a)

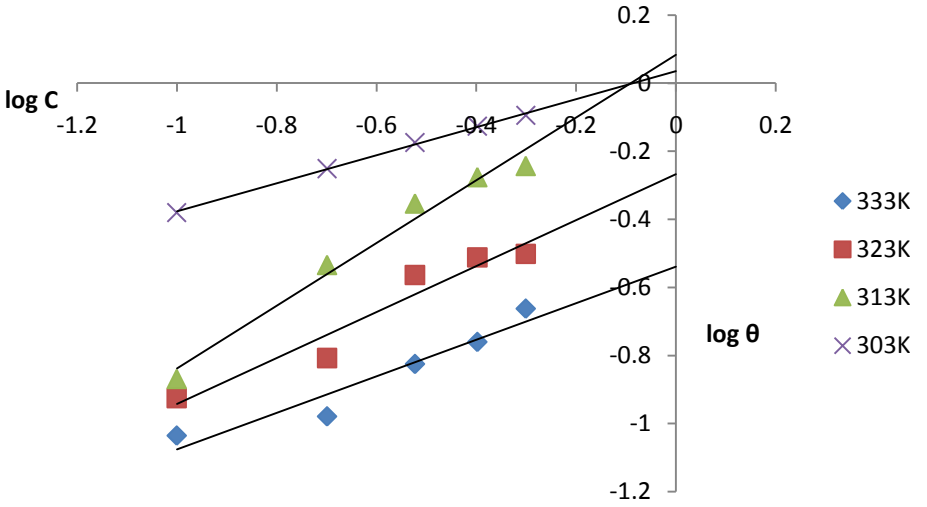


(b)

Fig. 4.36: Freundlich Isotherm for PA Adsorption on Mild Steel Surface in (a) 1.0 M HCl and (b) 0.5 M H_2SO_4 Solutions at Various Temperature

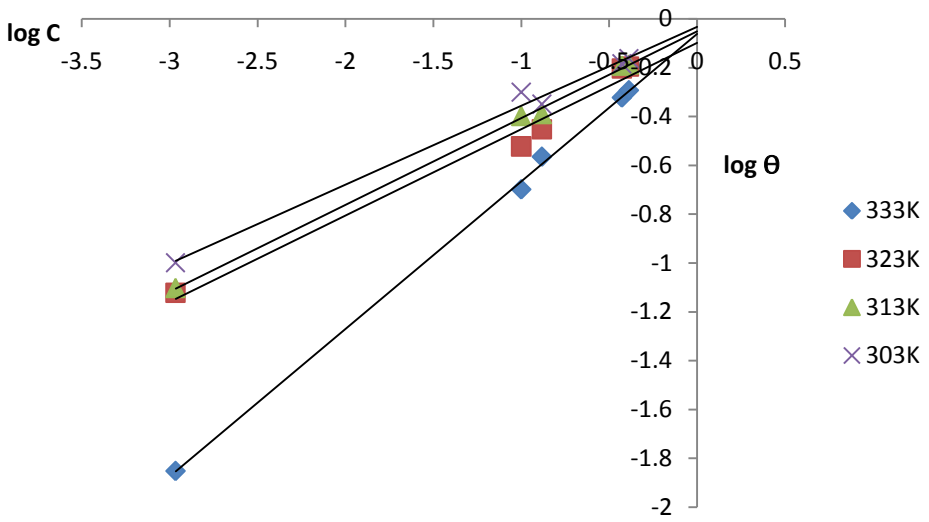


(a)

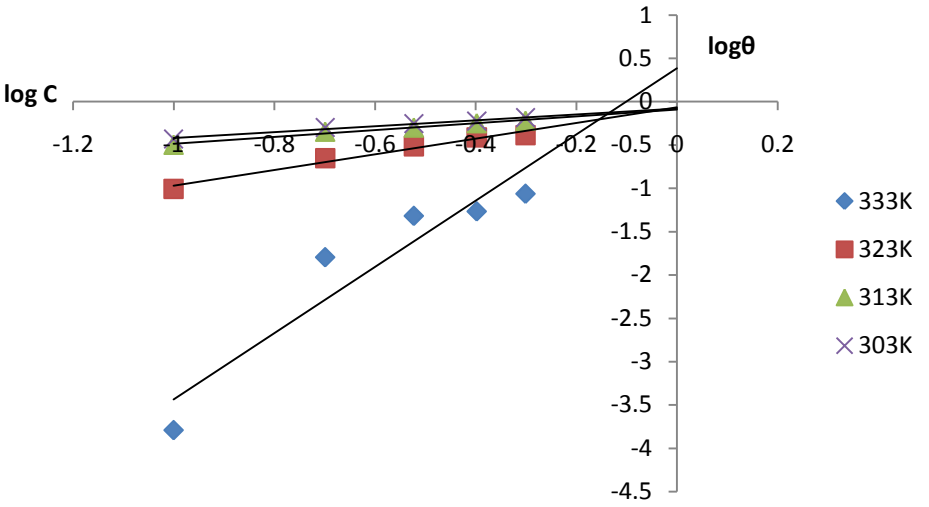


(b)

Fig. 4.37: Freundlich Isotherm for BS Adsorption on Mild Steel Surface in (a) 1.0 M HCl and (b) 0.5 M H_2SO_4 Solutions at Various Temperature

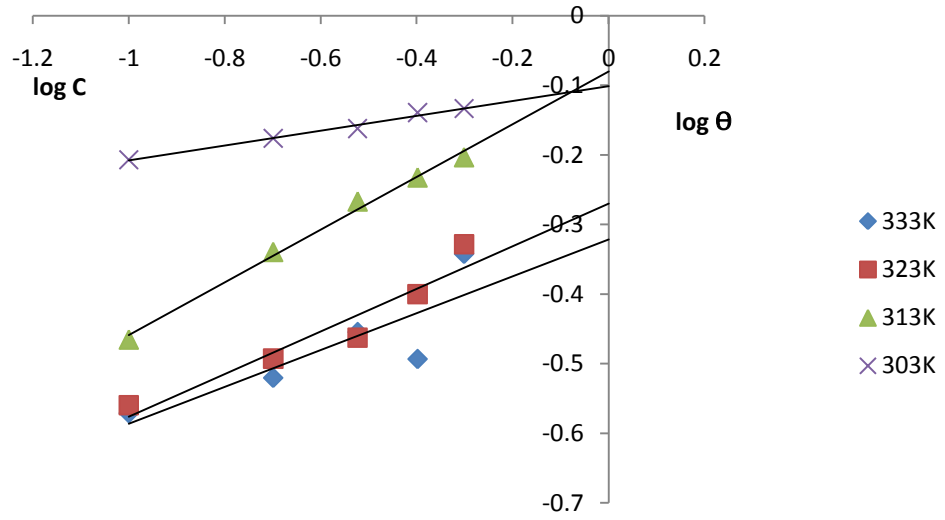


(a)

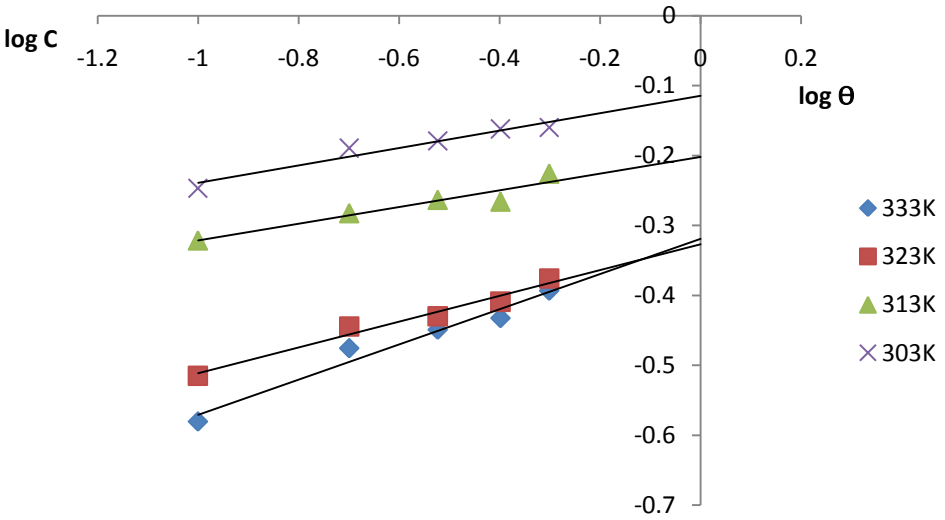


(b)

Fig. 4.38: Freundlich Isotherm for PP1 Adsorption on Mild Steel Surface in (a) 1.0 M HCl and (b) 0.5 M H_2SO_4 Solutions at Various Temperature

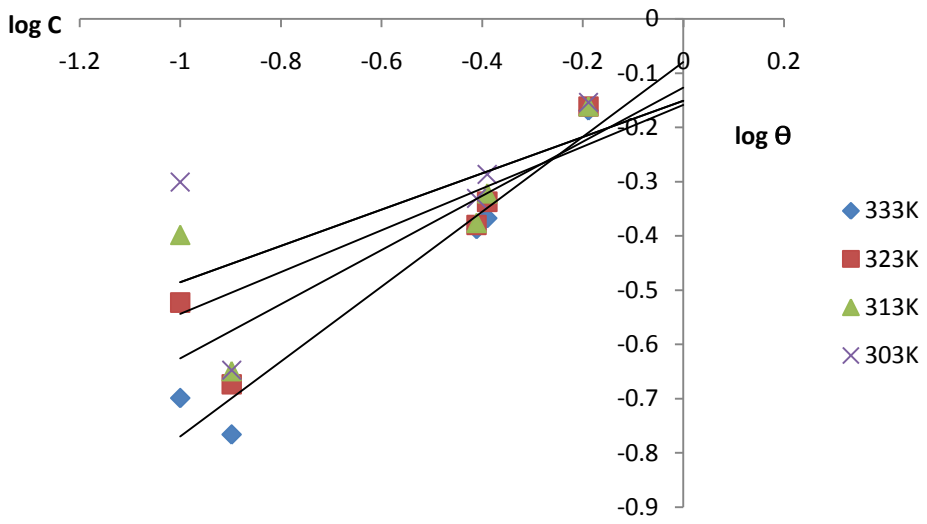


(a)

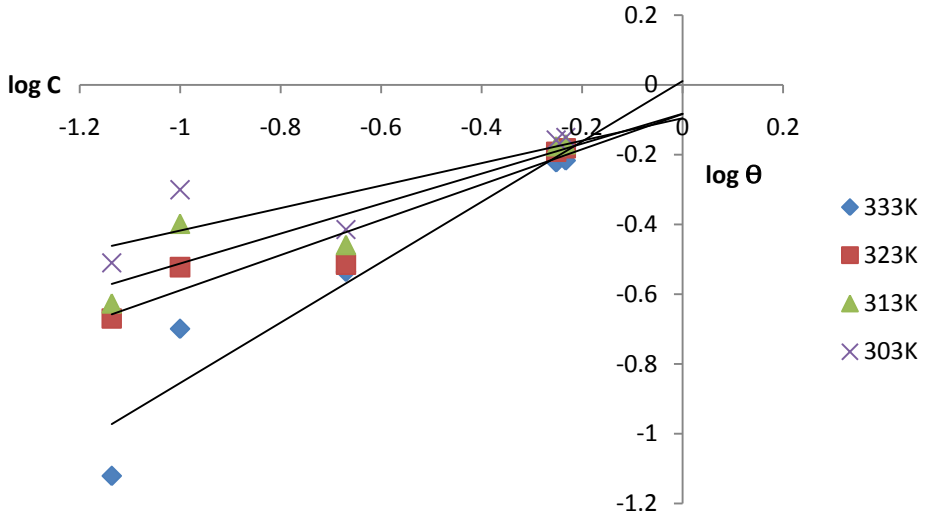


(b)

Fig. 4.39: Freundlich Isotherm for the Adsorption of a) PP and b) PA on Aluminium Surface in 1.0 M HCl Solution at Various Temperature

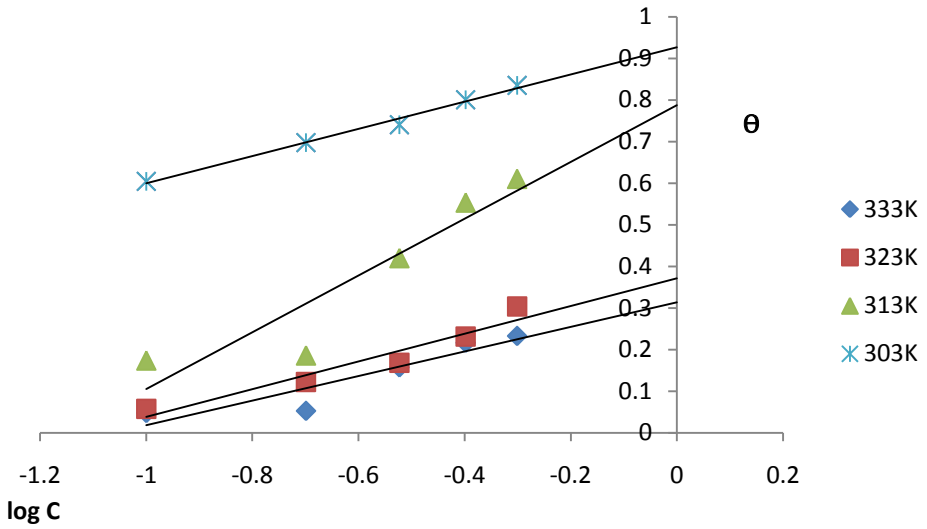


(a)

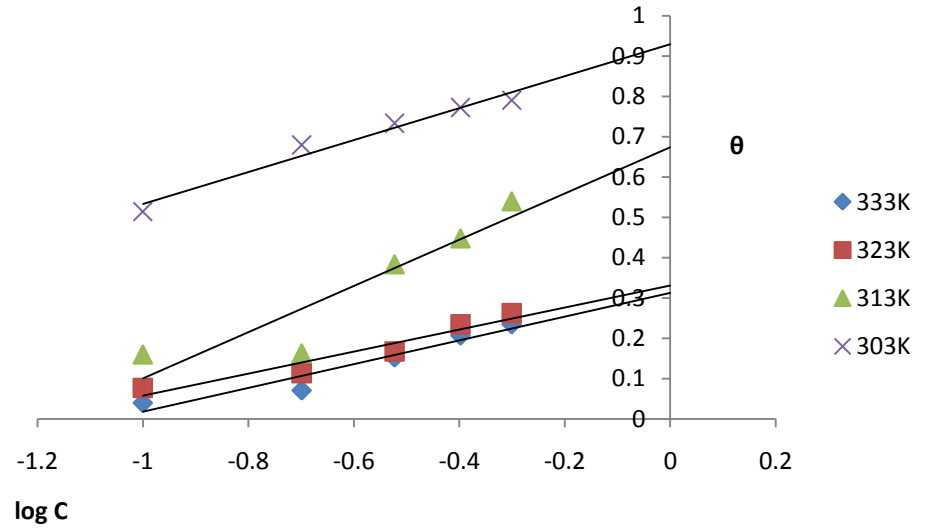


(b)

Fig. 4.40: Freundlich Isotherm for the Adsorption of (a) BS and (b) PP1 on Aluminium Surface in 1.0 M HCl Solution at Various Temperature

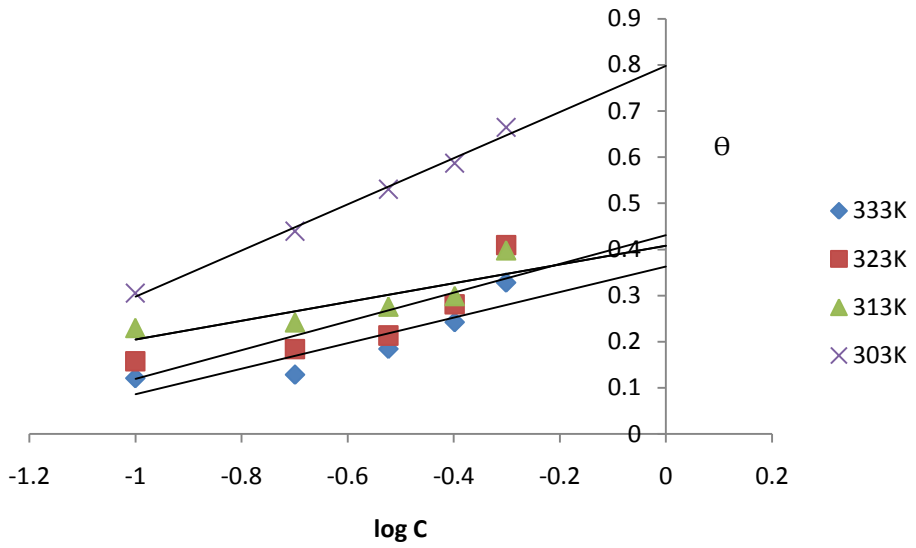


(a)

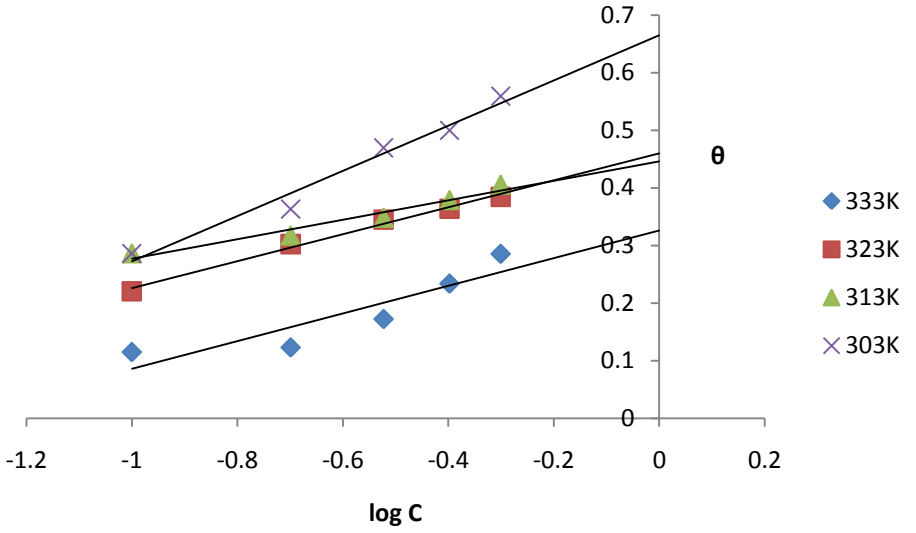


(b)

Fig. 4.41: Temkin Isotherm for PP Adsorption on Mild Steel Surface in (a) 1.0 M HCl and (b) 0.5 M H_2SO_4 Solutions at Various Temperature

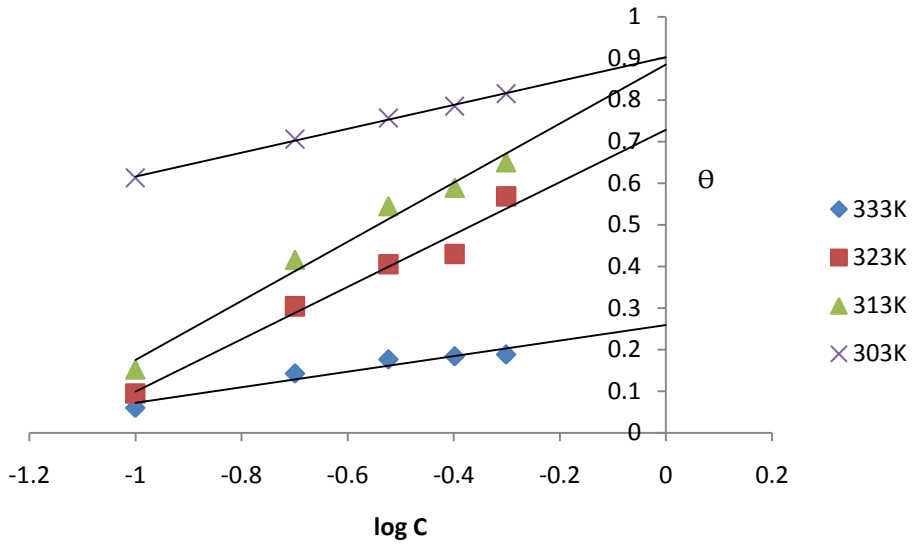


(a)

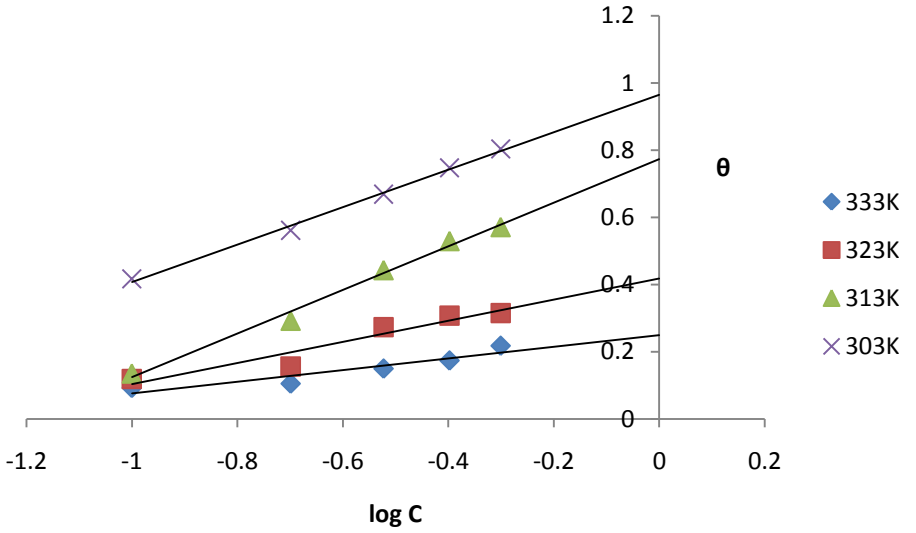


(b)

Fig. 4.42: Temkin Isotherm for PA Adsorption on Mild Steel Surface in (a) 1.0 M HCl and (b) 0.5 M H_2SO_4 Solutions at Various Temperature

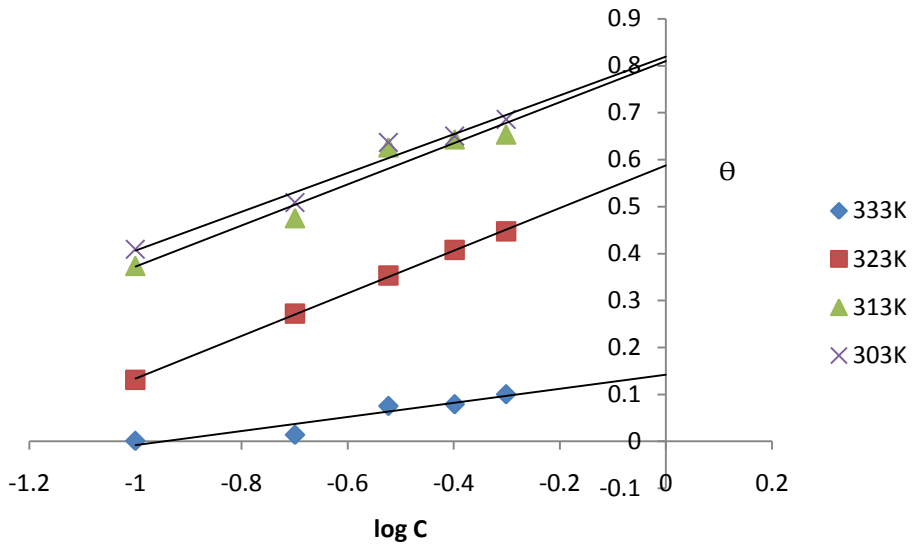


(a)

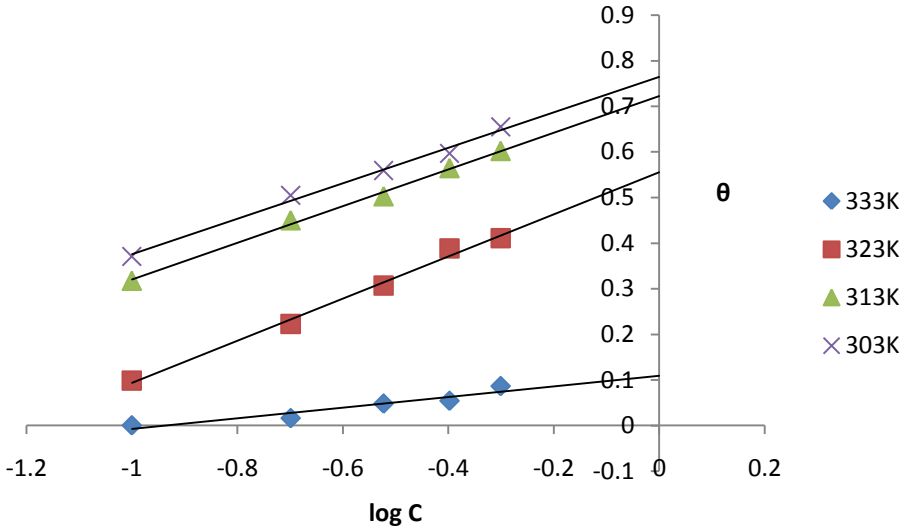


(b)

Fig. 4.43: Temkin Isotherm for BS Adsorption on Mild Steel Surface in (a) 1.0 M HCl and (b) 0.5 M H_2SO_4 Solutions at Various Temperature

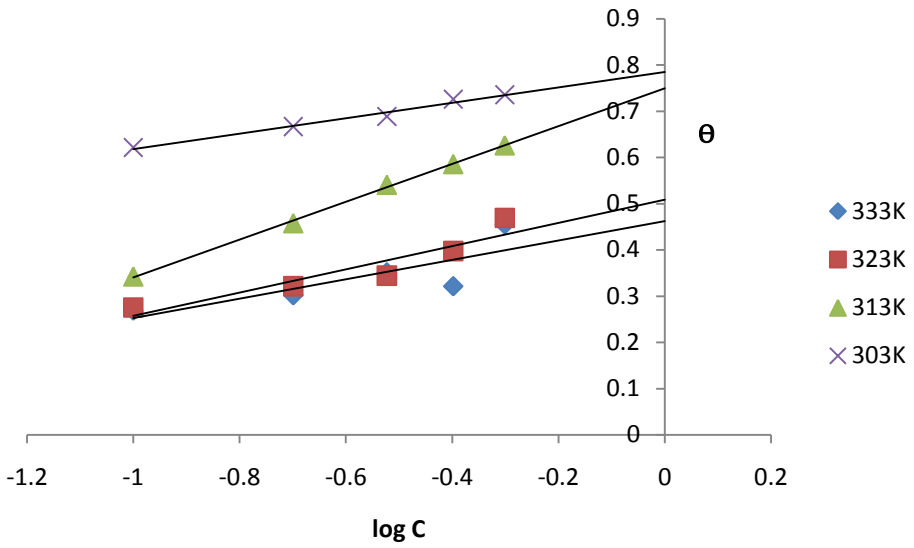


(a)

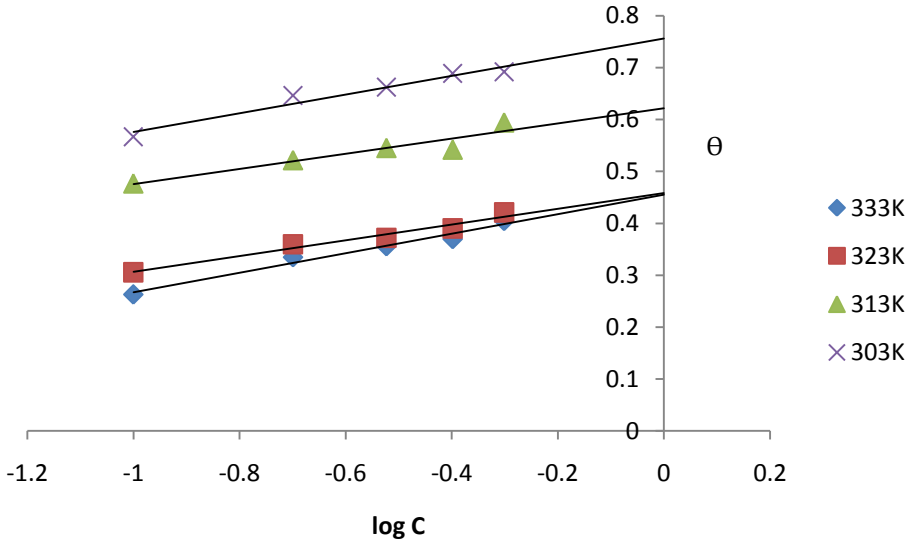


(b)

Fig. 4.44: Temkin Isotherm for PP1 Adsorption on Mild Steel Surface in (a) 1.0 M HCl and (b) 0.5 M H_2SO_4 Solutions at Various Temperature

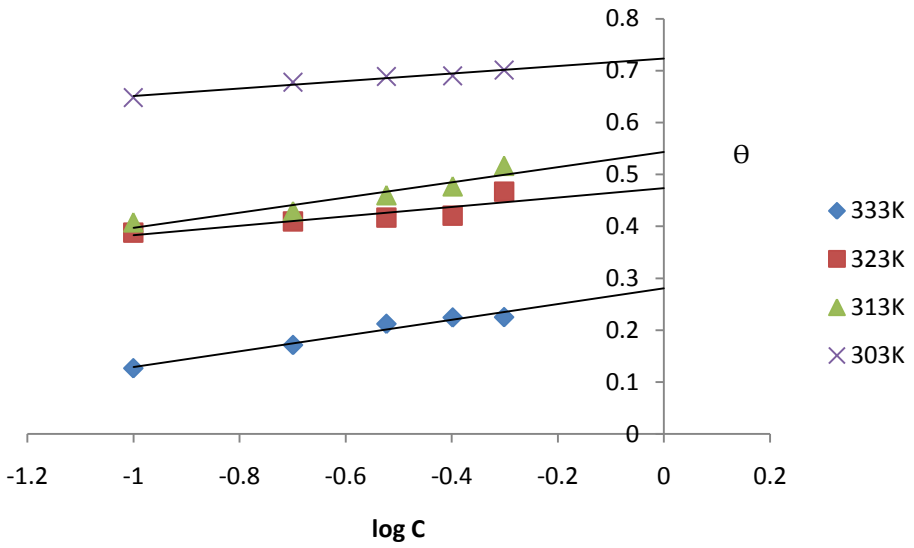


(a)

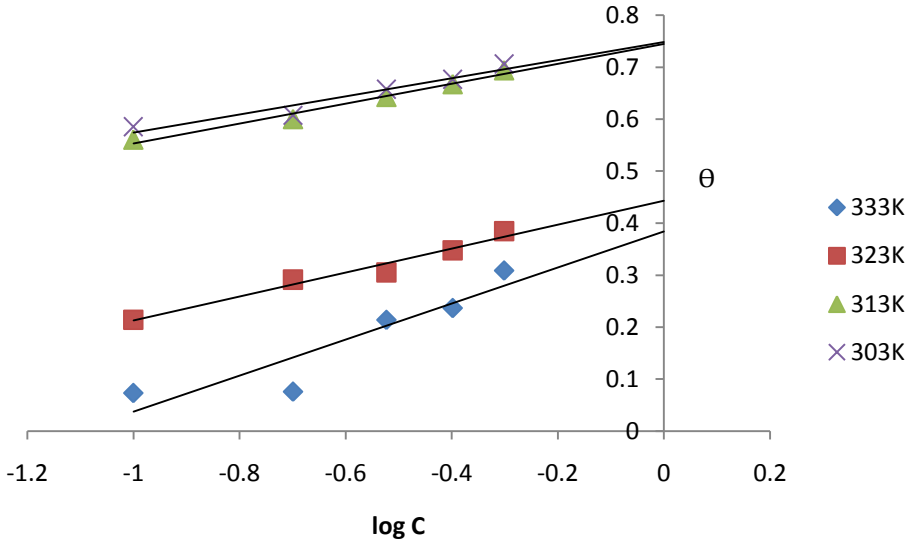


(b)

Fig. 4.45: Temkin Isotherm for the Adsorption of (a) PP and (b) PA on Aluminium Surface in 1.0 M HCl Solution at Various Temperature

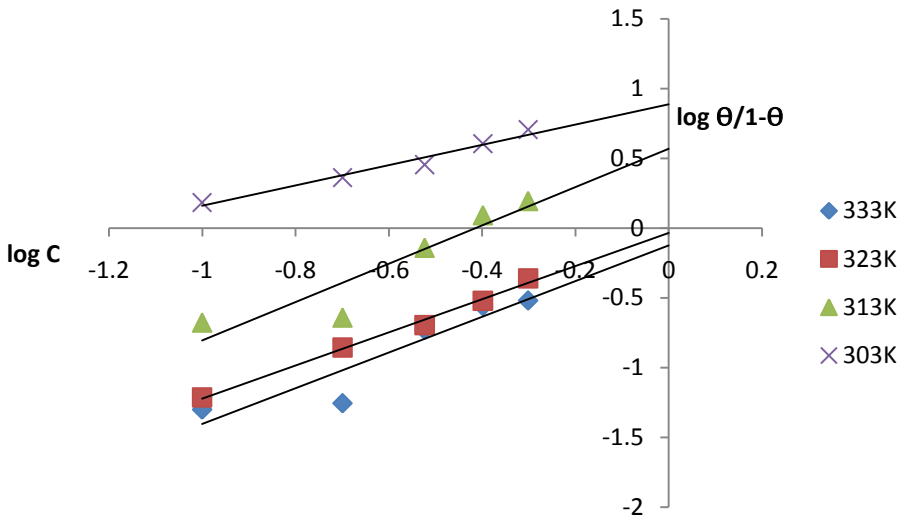


(a)

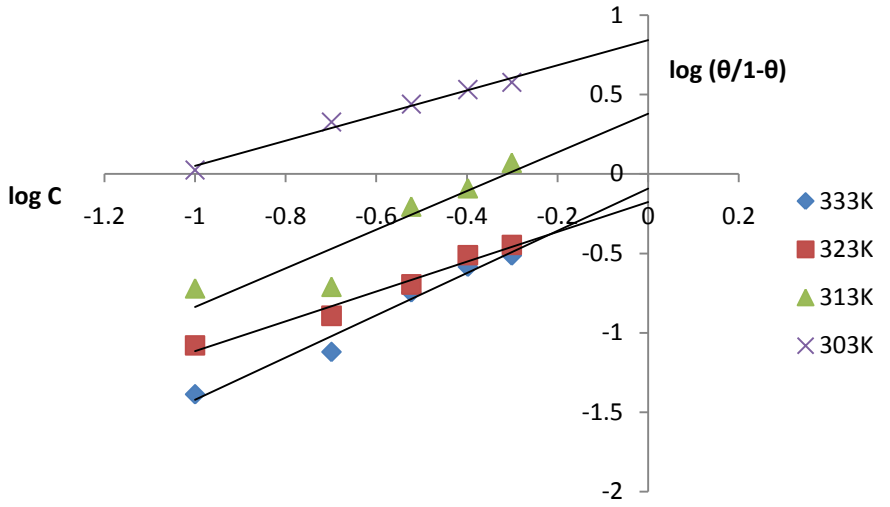


(b)

Fig. 4.46: Temkin Isotherm for the Adsorption of (a) BS and (b) PP1 on Aluminium Surface in 1.0 M HCl Solution at Various Temperature

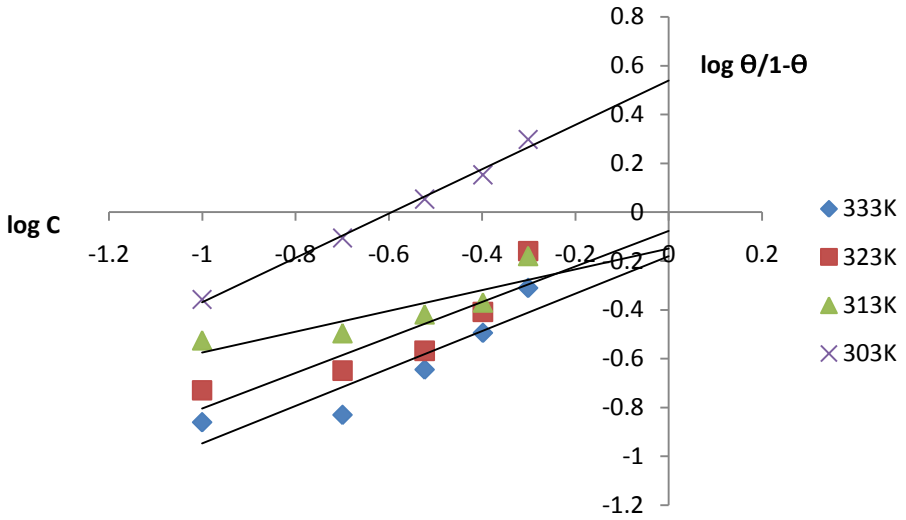


(a)

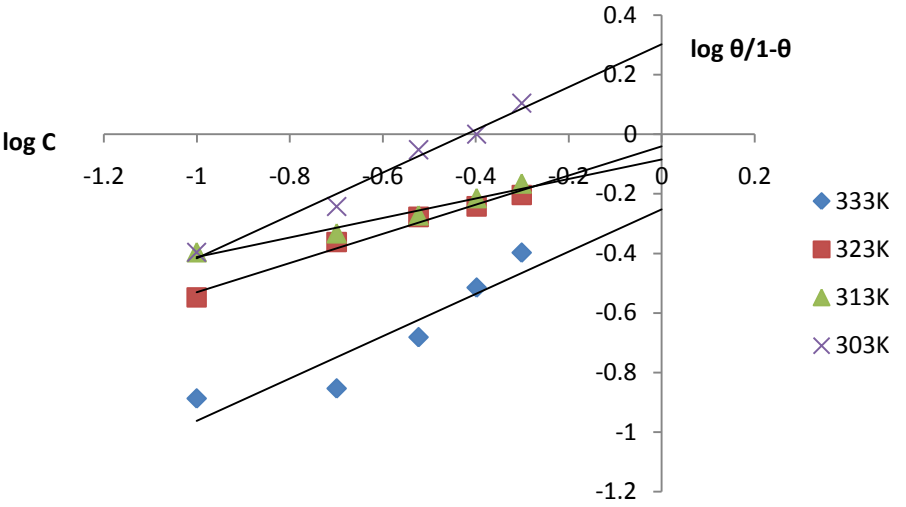


(b)

Fig. 4.47: El-Awady Isotherm for PP Adsorption on Mild Steel Surface in (a) 1.0 M HCl and (b) 0.5 M H_2SO_4 Solutions at Various Temperature

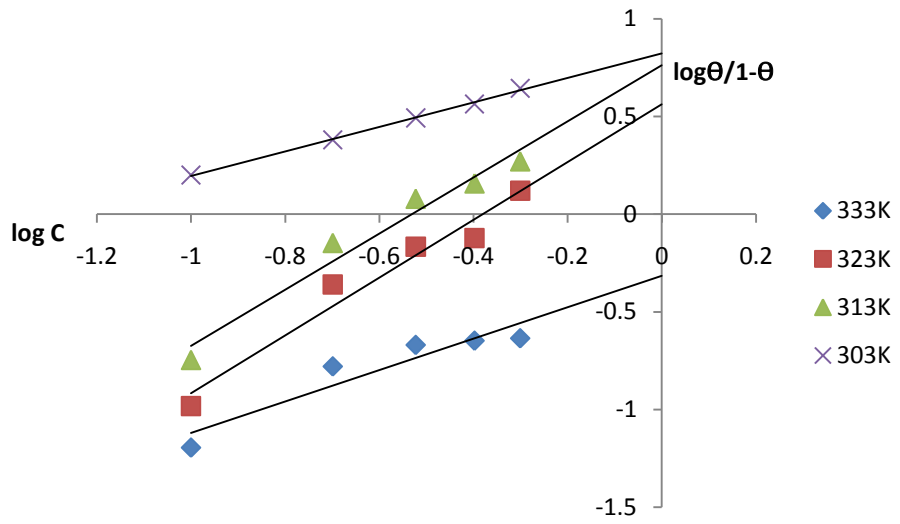


(a)

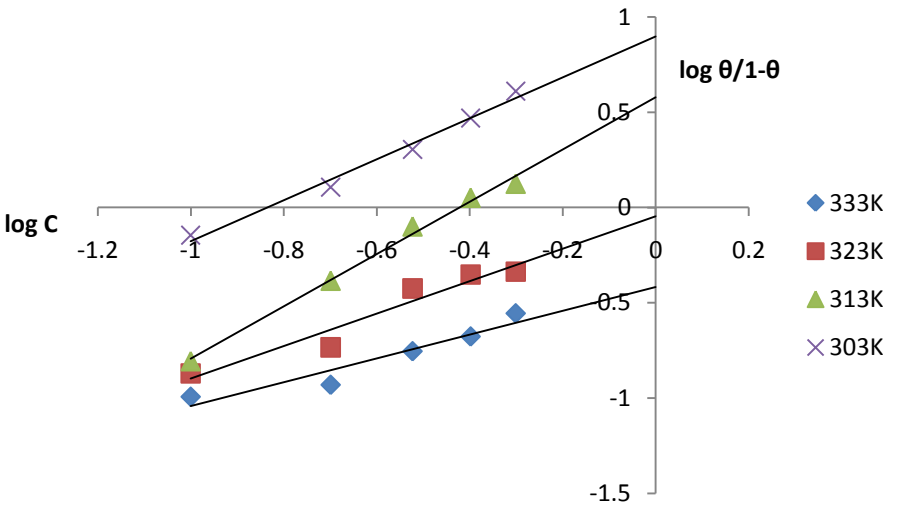


(b)

Fig. 4.48: El-Awady Isotherm for PA Adsorption on Mild Steel Surface in (a) 1.0 M HCl and (b) 0.5 M H_2SO_4 Solutions at Various Temperature

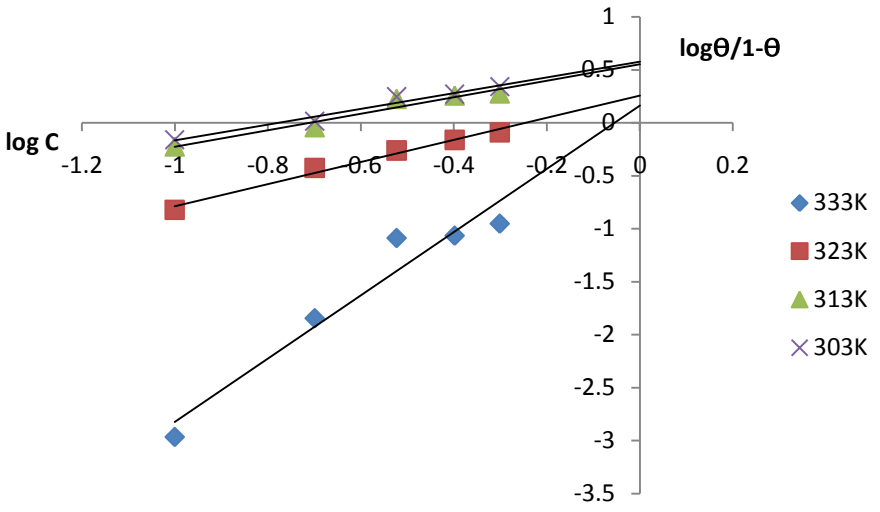


(a)

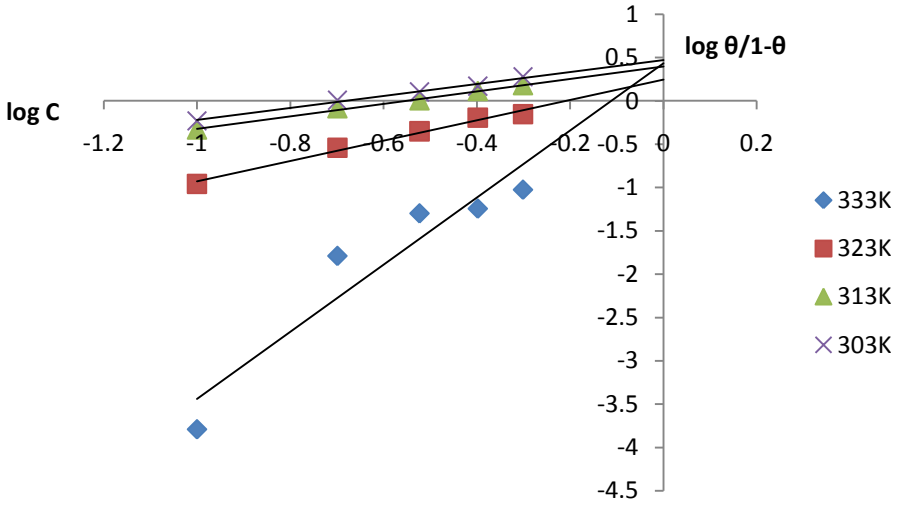


(b)

Fig. 4.49: El-Awady Isotherm for BS Adsorption on Mild Steel Surface in (a) 1.0 M HCl and (b) 0.5 M H_2SO_4 Solutions at Various Temperature

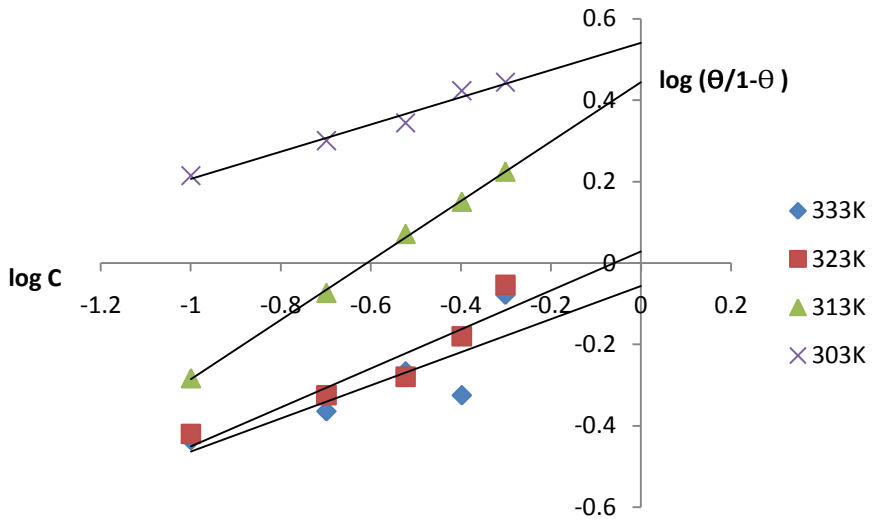


(a)

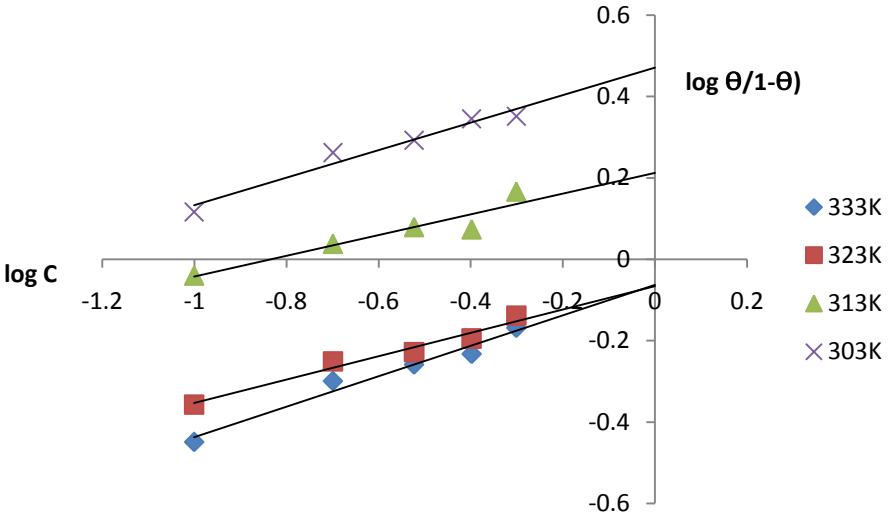


(b)

Fig. 4.50: El-Awady Isotherm for PP1 Adsorption on Mild Steel Surface in (a) 1.0 M HCl and (b) 0.5 M H_2SO_4 Solutions at Various Temperature

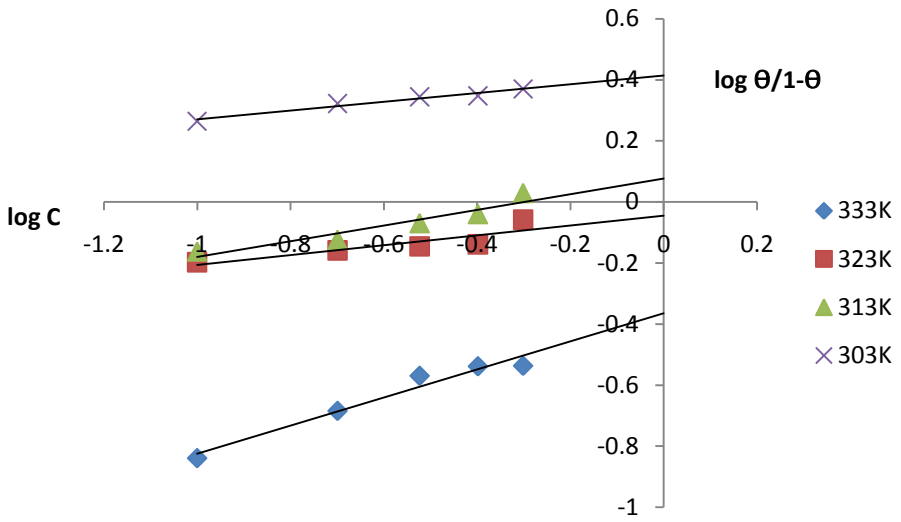


(a)

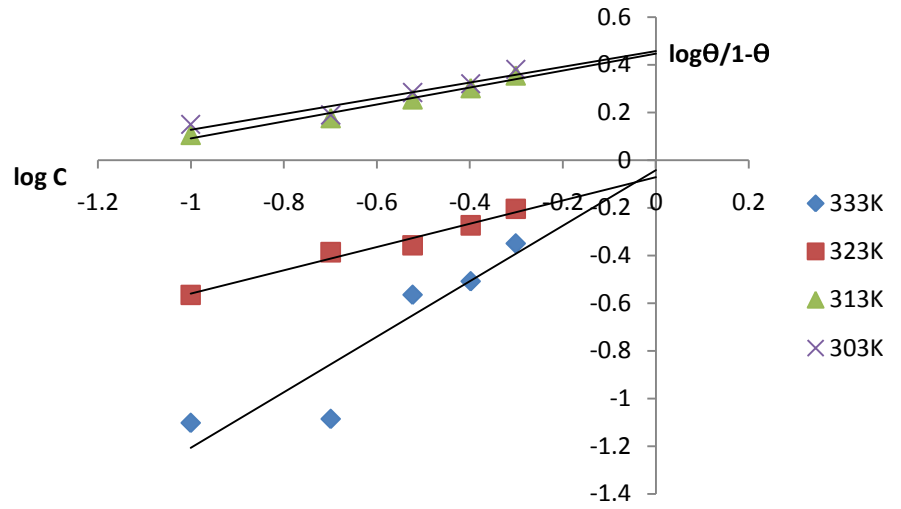


(b)

Fig. 4.51: El-Awady Isotherm for the Adsorption of (a) PP and (b) PA on Aluminium Surface in 1.0 M HCl Solution at Various Temperature



(a)



(b)

Fig. 4.52: El-Awady Isotherm for the Adsorption of (a) BS and (b) PP1 on Aluminium Surface in 1.0 M HCl Solution at Various Temperature

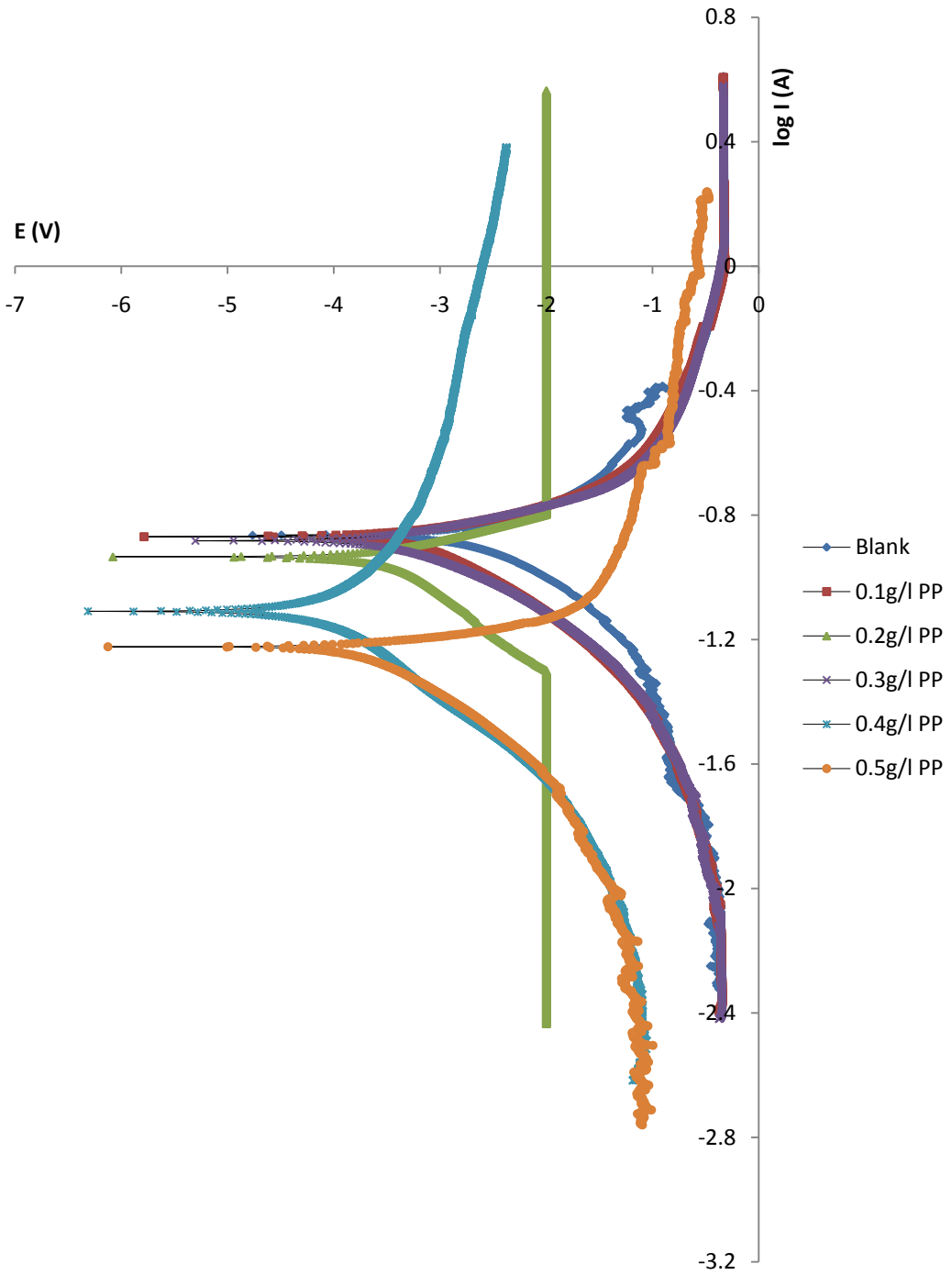


Fig. 4.53: Polarization Curve for the Corrosion of Mild Steel in 1.0 M HCl in the Presence and Absence of Various Concentrations of PP at 303K

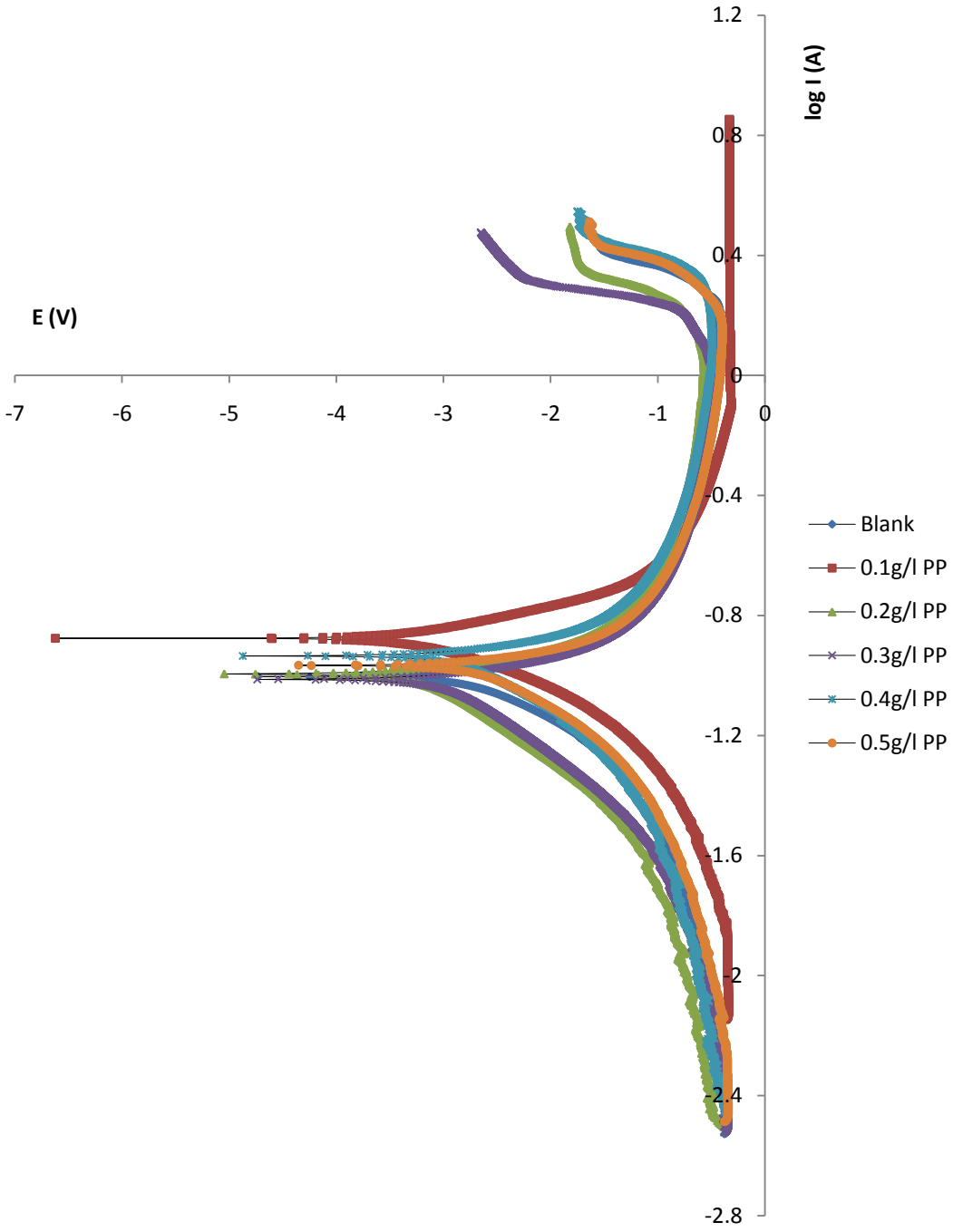


Fig. 4.54: Polarization Curve for the Corrosion of Mild Steel in 0.5 M H_2SO_4 in the Presence and Absence of Various Concentrations of PP at 303K

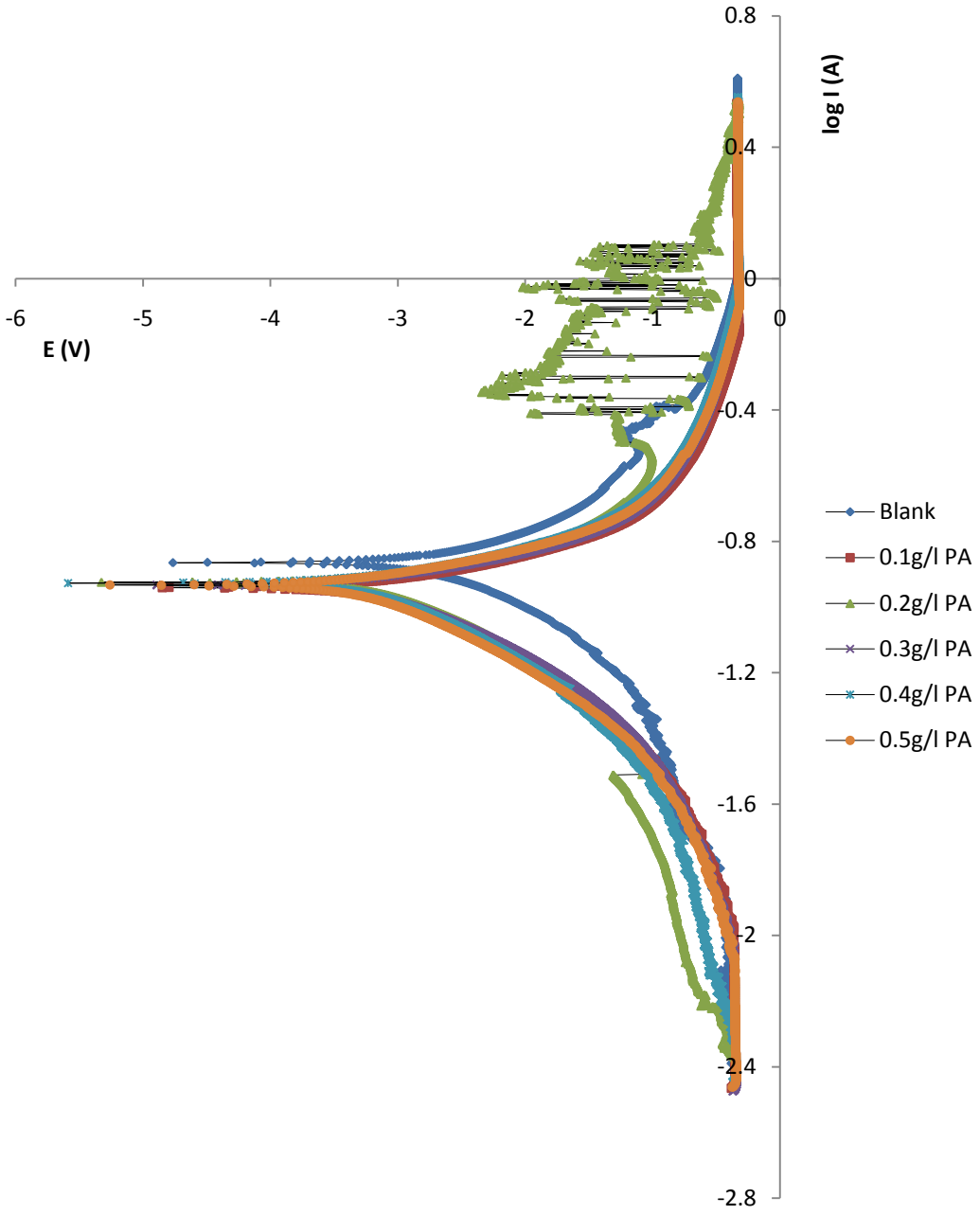


Fig. 4.55: Polarization Curve for the Corrosion of Mild Steel in 1.0 M HCl in the Presence and Absence of Various Concentrations of PA at 303K

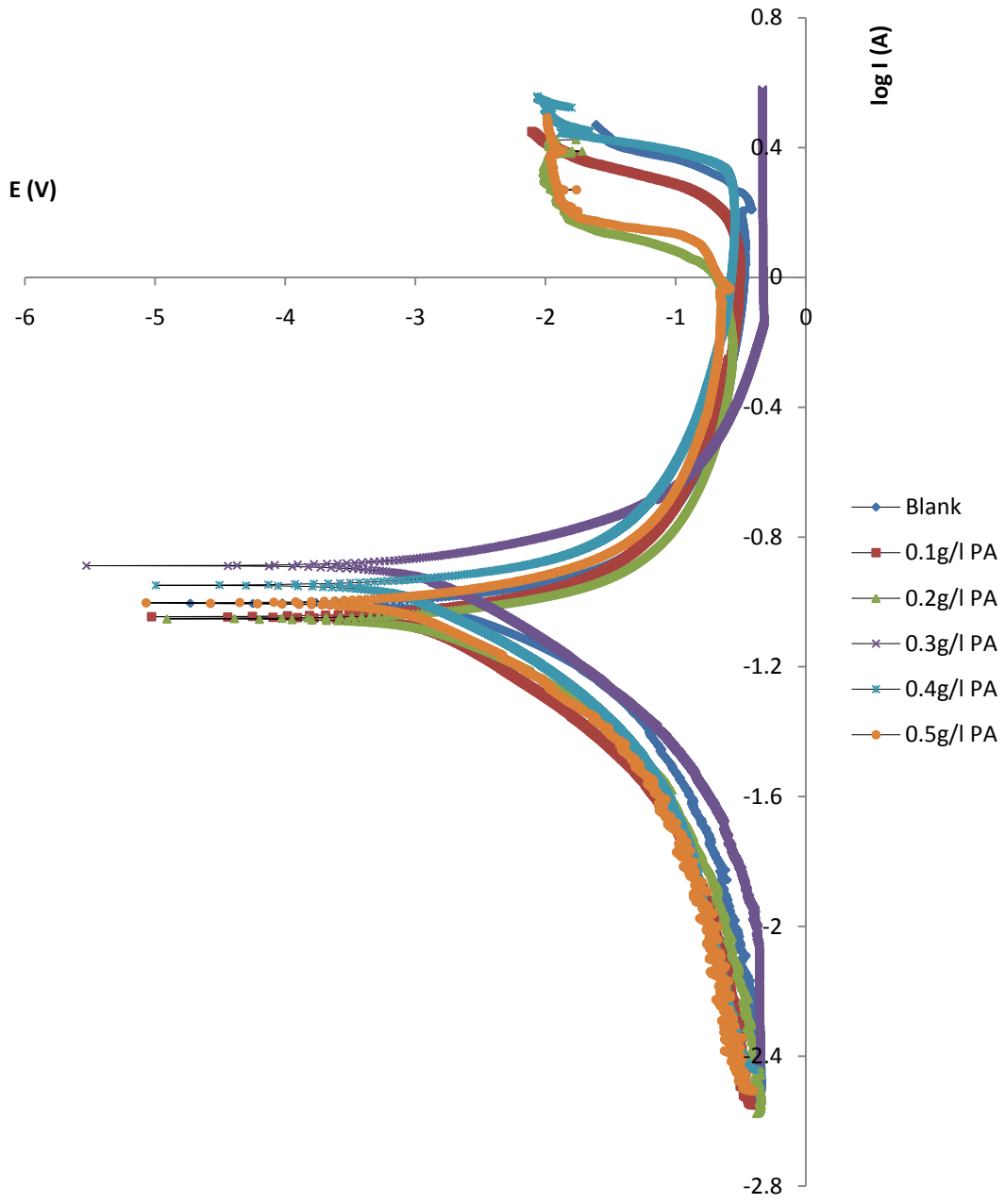


Fig. 4.56: Polarization Curve for the Corrosion of Mild Steel in 0.5 M H_2SO_4 in the Presence and Absence of Various Concentrations of PA at 303K

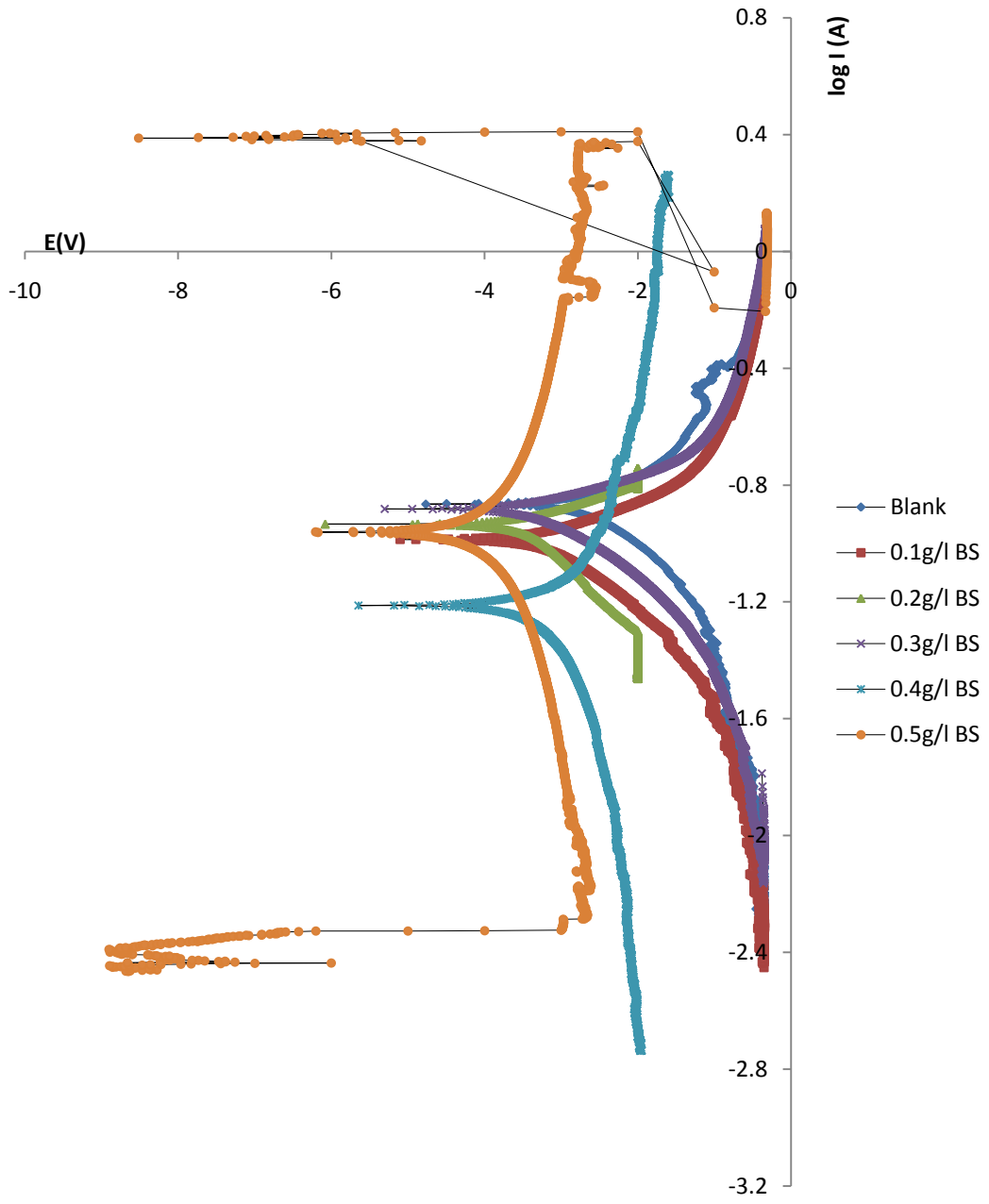


Fig. 4.57: Polarization Curve for the Corrosion of Mild Steel in 1.0 M HCl in the Presence and Absence of Various Concentrations of BS at 303K

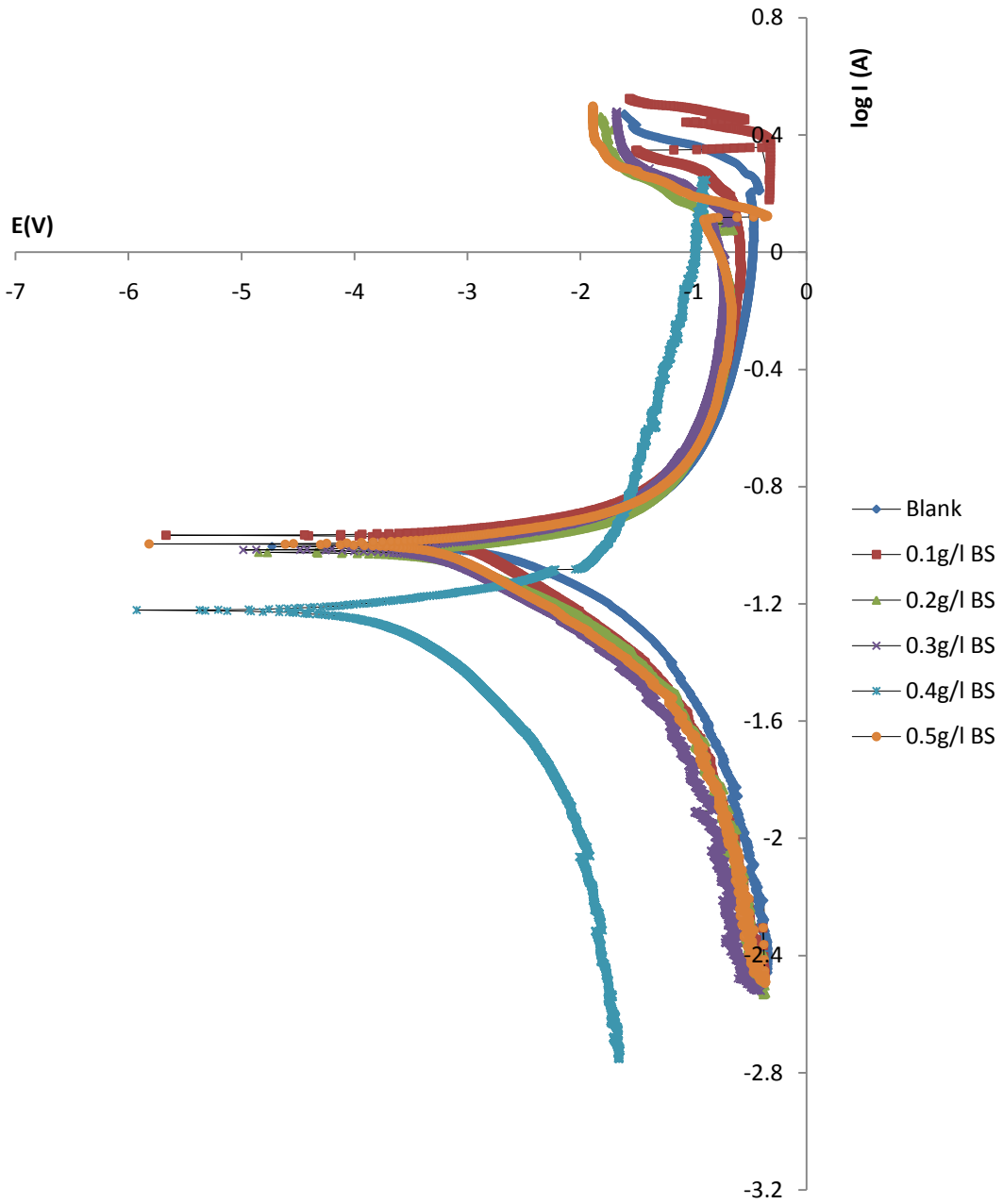


Fig. 4.58: Polarization Curve for the Corrosion of Mild Steel in 0.5 M H_2SO_4 in the Presence and Absence of Various Concentrations of BS at 303K

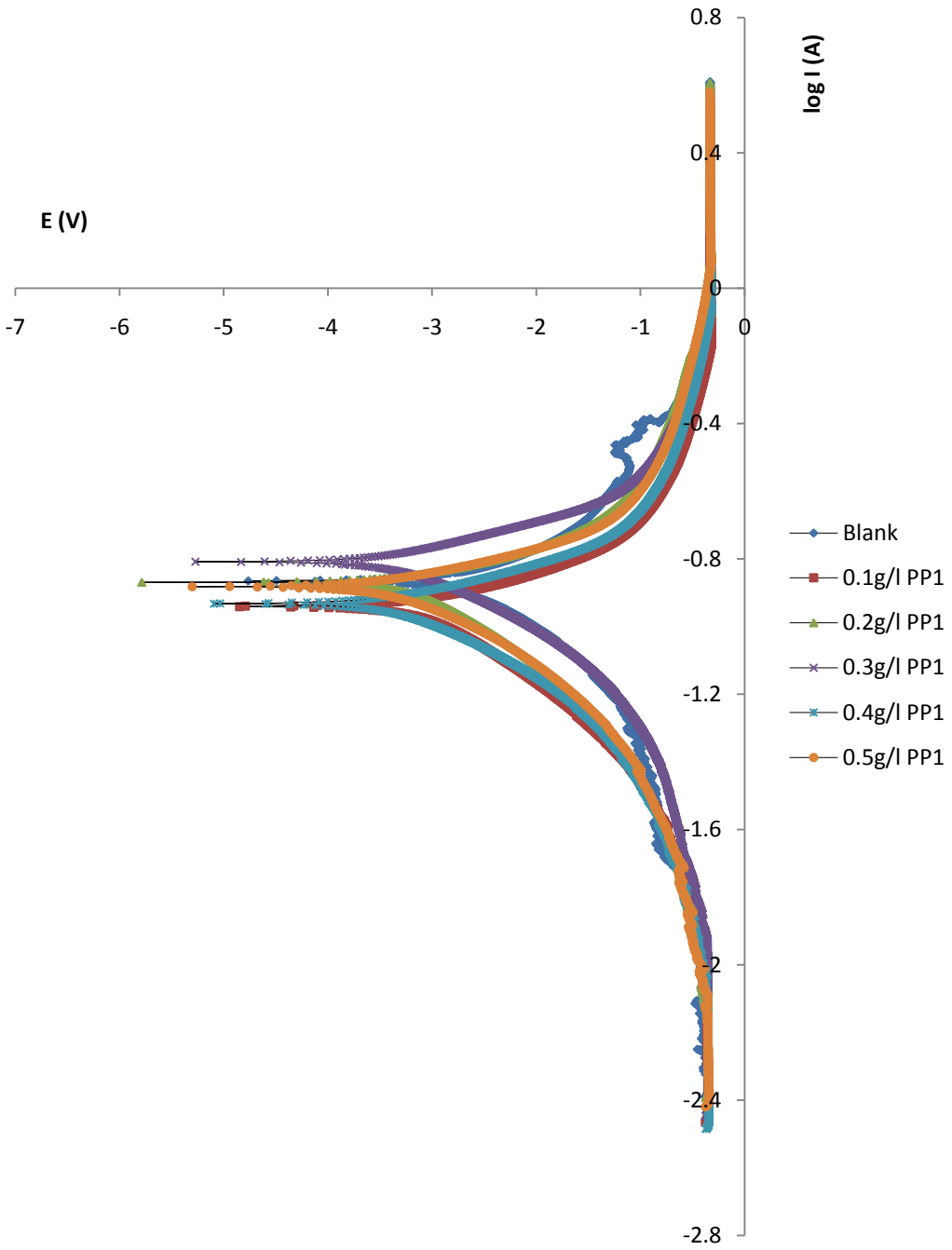


Fig. 4.59: Polarization Curve for the Corrosion of Mild Steel in 1.0 M HCl in the Presence and Absence of Various Concentrations of PP1 at 303K

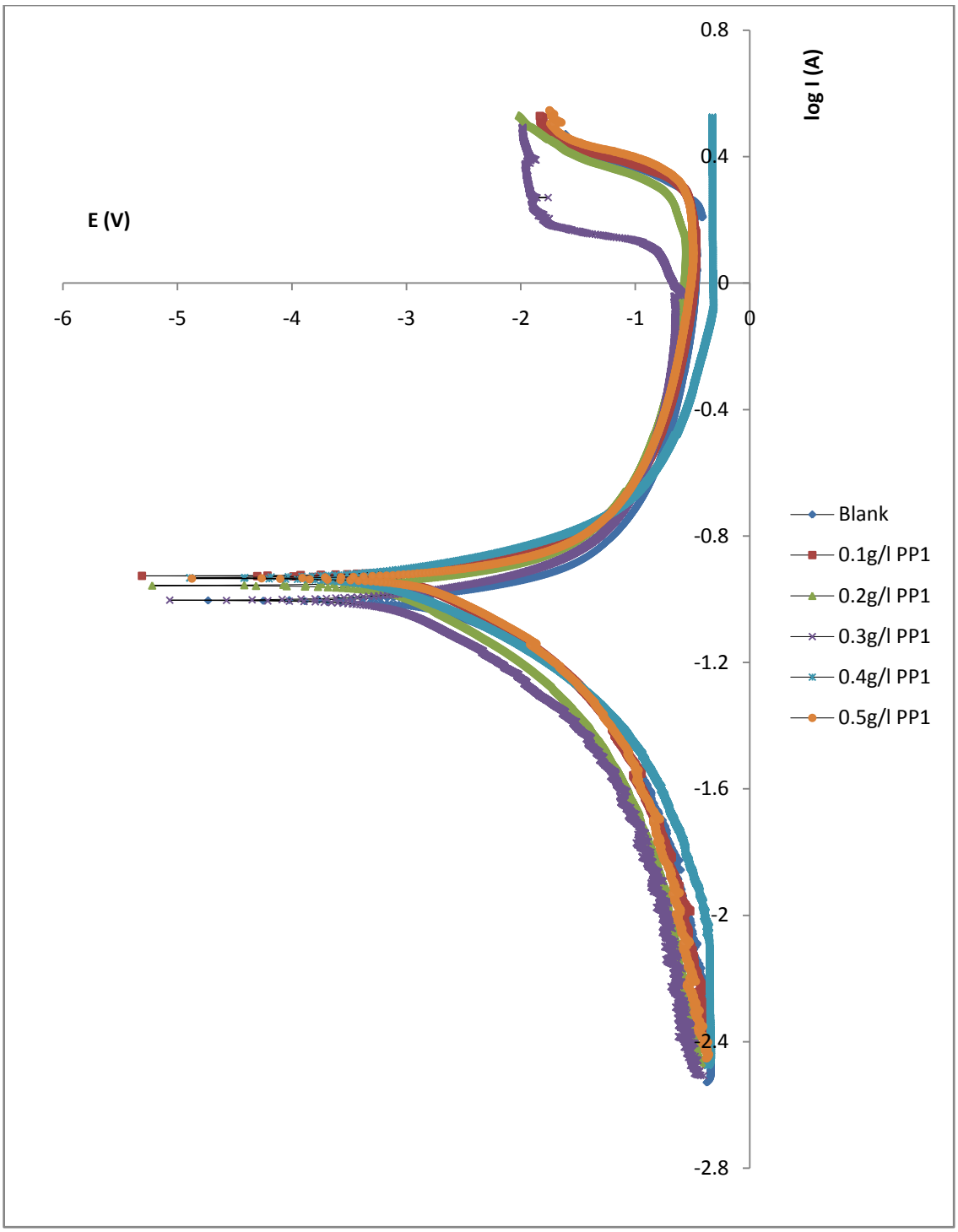


Fig. 4.60: Polarization Curve for the Corrosion of Mild Steel in 0.5 M H_2SO_4 in the Presence and Absence of Various Concentrations of PP1 at 303K

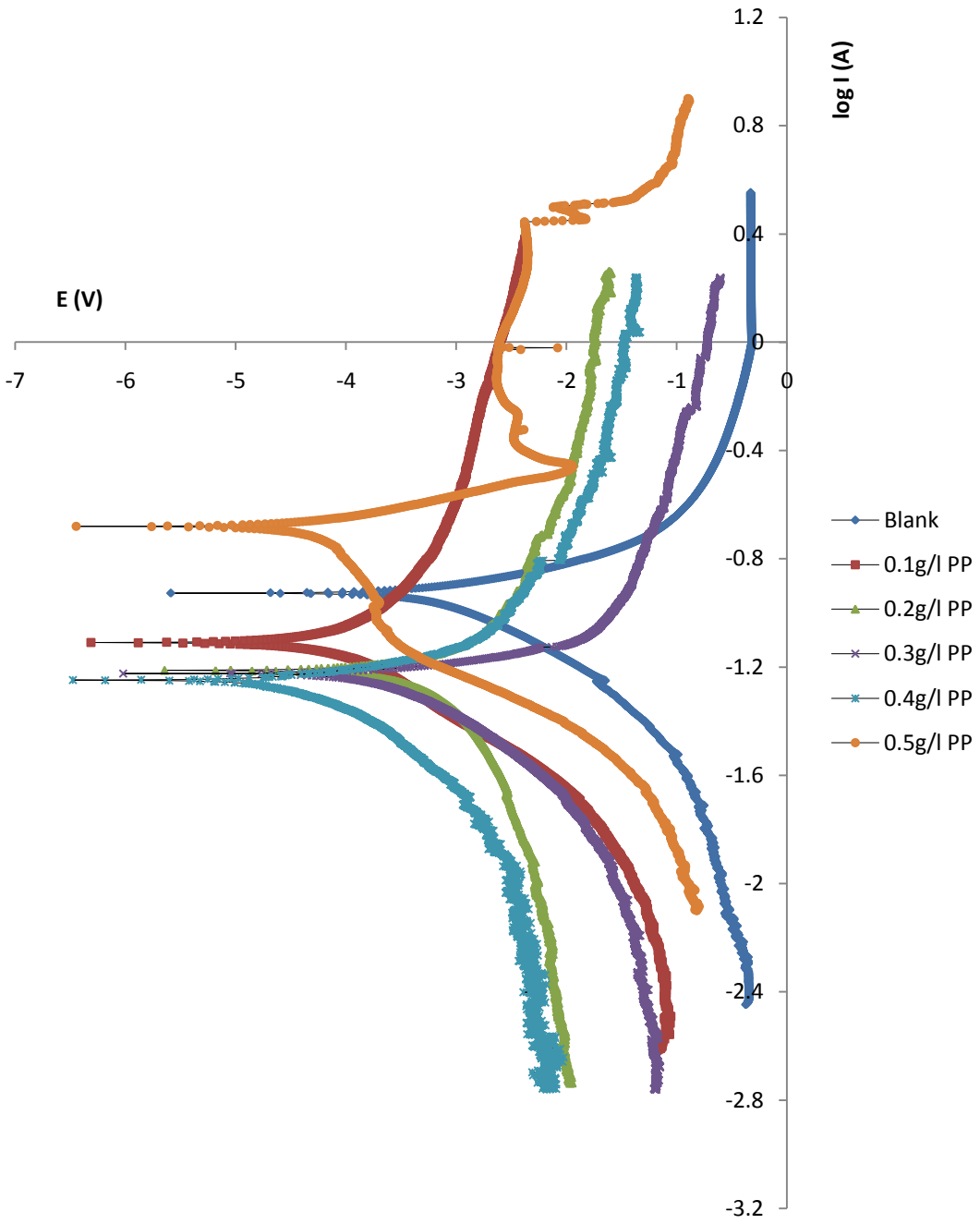


Fig. 4.61: Polarization Curve for the Corrosion of Aluminium in 1.0 M HCl in the Presence and Absence of Various Concentrations of PP at 303K

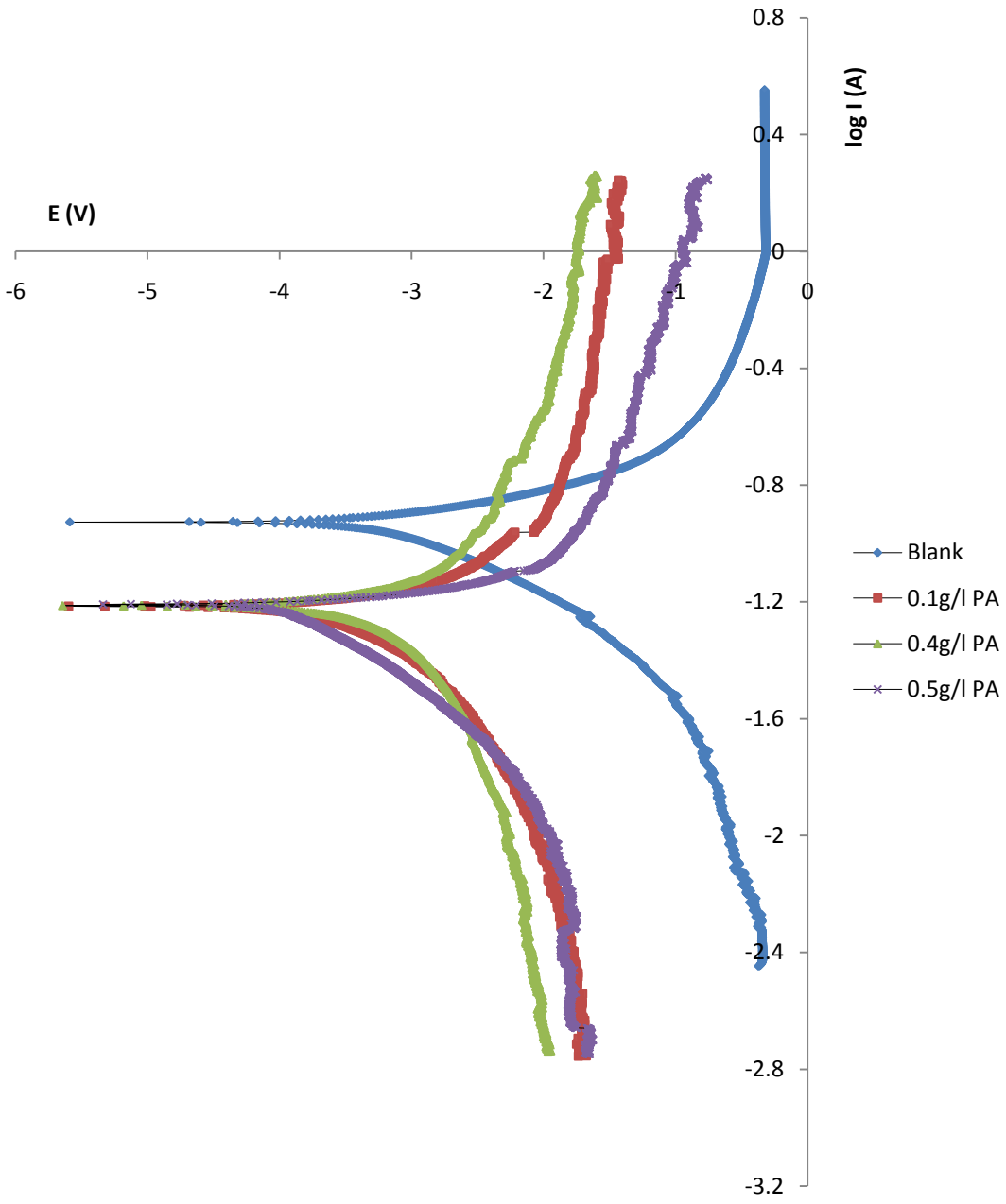


Fig. 4.62: Polarization Curve for the Corrosion of Aluminium in 1.0 M HCl in the Presence and Absence of Various Concentrations of PA at 303K

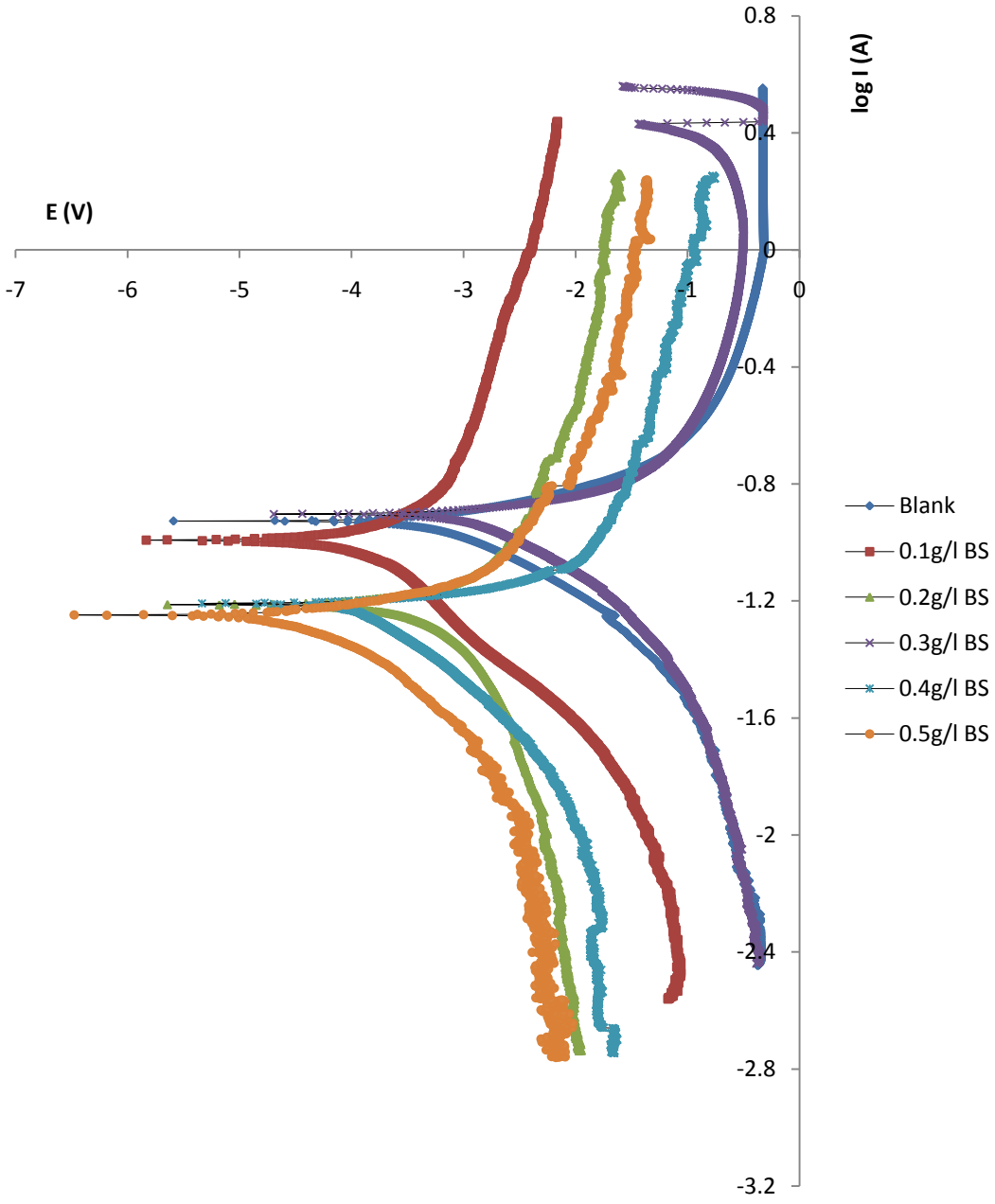


Fig. 4.63: Polarization Curve for the Corrosion of Aluminium in 1.0 M HCl in the Presence and Absence of Various Concentrations of BS at 303K

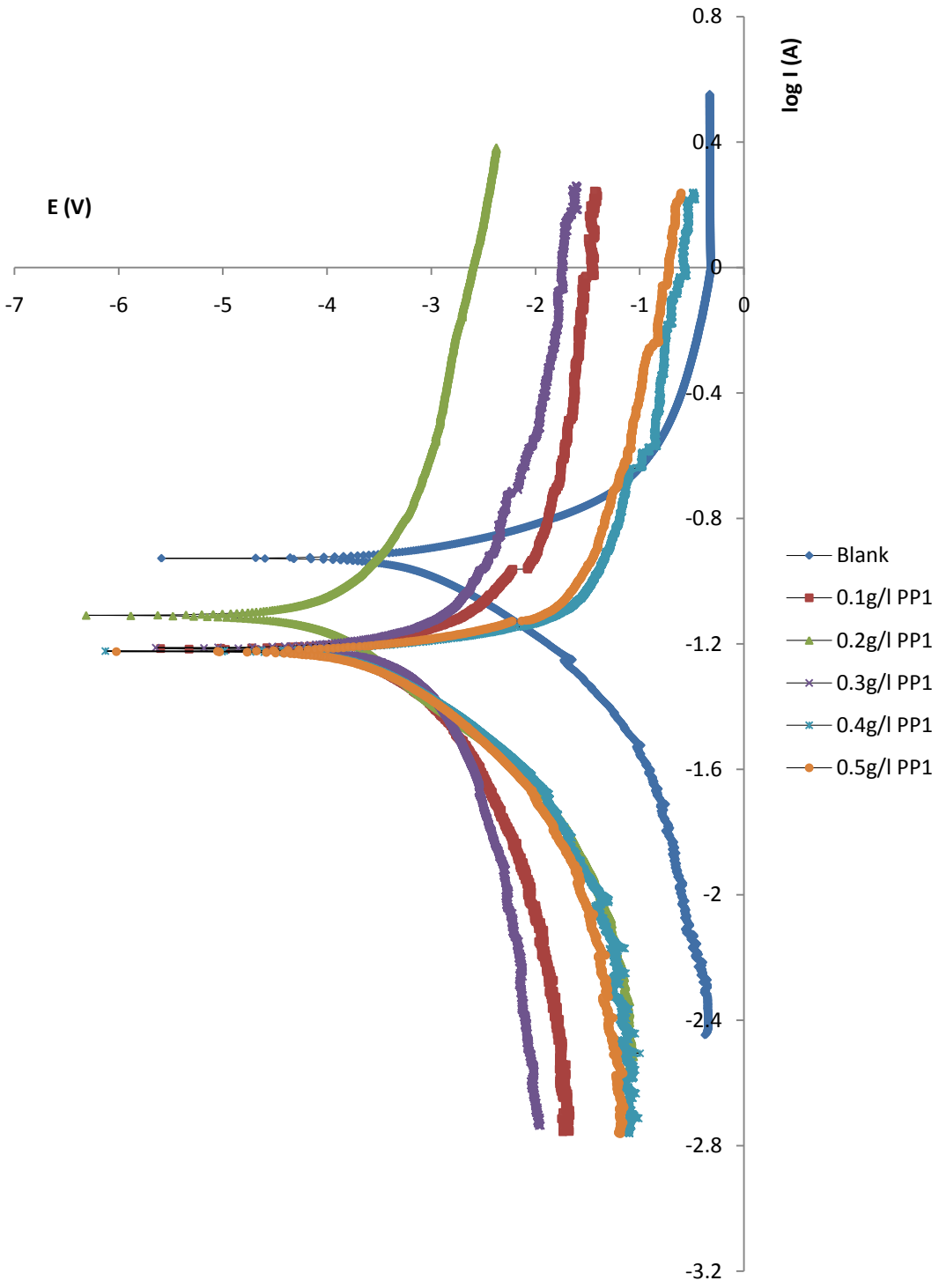


Fig. 4.64: Polarization Curve for the Corrosion of Aluminium in 1.0 M HCl in the Presence and Absence of Various Concentrations of PP1 at 303K

Table 4.15: Tafel Polarization Parameters Obtained at Various Concentration of Inhibitors on Mild Steel in Acidic Media

		HCl			H_2SO_4		
Inhibitor	Conc.(g/l)	E_{corr}(mV)	Icorr (µA)	IE %	E_{corr}(mV)	I_{corr} (µA)	IE %
	Blank	-864.95	1179.0	-	-1004.4	1642.2	-
	0.1	-869.38	516.46	56.19	-876.45	679.96	58.59
	0.2	-934.37	343.09	70.89	-995.08	489.53	70.19
PP	0.3	-952.04	286.53	75.69	-1013.2	473.24	71.18
	0.4	-1109.5	187.68	84.08	-935.00	372.01	77.34
	0.5	-1223.4	128.56	89.09	-966.65	304.67	81.44
	0.1	-940.2	654.25	44.50	-1045.6	1104.30	32.75
	0.2	-924.05	583.39	50.51	-1052.0	1004.20	38.85
PA	0.3	-932.84	480.84	59.21	-888.29	918.70	44.05
	0.4	-926.85	475.14	59.69	-948.84	834.23	49.20
	0.5	-933.07	394.61	66.53	-1003.4	722.32	56.01
	0.1	-986.68	511.00	56.65	-966.43	725.40	55.82
	0.2	-934.37	343.09	70.89	-1024.7	556.52	66.11
BS	0.3	-882.40	286.53	75.69	-1015.0	482.35	70.62
	0.4	-1212.4	151.07	87.18	-1222.6	361.28	78.01
	0.5	-961.36	136.12	88.45	-995.55	295.60	82.00
	0.1	-940.20	654.25	44.50	-926.15	1069.8	34.85
	0.2	-869.38	516.46	56.19	-956.73	861.27	47.55
PP1	0.3	-808.70	372.83	68.37	-1003.4	722.32	56.01
	0.4	-932.58	331.41	71.89	-932.84	480.84	70.71
	0.5	-882.40	286.53	75.69	-935.0	372.01	77.34

Table 4.16: Linear Polarization Resistant Data for BS, PA, PP and PP1 in Various Acidic Media

	C (g/L)	R_p (Ω/cm^2) (Fe in HCl)	R_p (Ω/cm^2) (Fe in H_2SO_4)	R_p (Ω/cm^2) (Al in HCl)	%I (Fe/HCl)	%I (Fe/ H_2SO_4)	%I (Al/ HCl)
	Blank	17.105	14.103	46.087	-	-	-
BS	**0.1**	51.383	28.146	69.748	66.71	49.89	33.91
	0.2	85.63	34.285	119.77	80.02	58.87	61.51
	0.3	66.049	44.451	134.51	74.10	68.27	65.73
	0.4	134.51	261.18	349.79	87.28	94.60	86.82
	0.5	826.5	174.68	759.63	97.93	91.93	93.93
PA	**0.1**	35.223	20.513	119.77	51.44	31.25	61.51
	0.2	36.638	23.263	121.34	53.31	39.38	62.01
	0.3	41.322	25.873	131.69	58.61	45.49	65.00
	0.4	46.247	27.016	134.51	63.01	47.80	65.73
	0.5	54.897	30.085	141.322	68.84	53.12	67.38
PP	**0.1**	41.87	30.219	119.61	59.15	53.33	61.46
	0.2	85.63	32.369	134.51	80.02	56.43	65.73
	0.3	66.049	32.779	519.14	74.10	56.98	91.12
	0.4	568.03	37.228	568.03	96.99	62.12	91.88
	0.5	98.119	39.533	759.63	82.57	64.33	93.93
PP1	**0.1**	35.223	19.27	98.119	51.44	26.81	53.02
	0.2	41.87	24.257	119.61	59.15	41.86	61.46
	0.3	58.157	30.085	131.69	70.59	53.12	65.00
	0.4	61.59	32.779	134.51	72.23	56.98	65.73
	0.5	66.049	41.322	568.03	74.10	65.87	91.88

The standard Gibbs'free energy calculated for the different adsorption isotherms at the various temperatures for the plant extracts are also presented in appendice I- VI.

Figure 4.65 – 4.70 also shows a comparative study of the inhibition efficiencies obtained from the various experimental methods (Gravimetric method GM, Linear polarization resistance LPR, and Potentiodynamic polarization PDP). This shows that the IE% of the acid/inhibitor environment increases with an increase in the inhibitor concentrations.

4.6 Infrared Spectroscopic Study

IR analysis was carried out on the powder of the extracts as well as the corrosion products (in the presence and absence of the inhibitors). Figures 4.71 - 4.82 show the spectra of the products of the scrap of the mild steel and aluminium after immersion for 7 days in 1.0 M HCl and 0.5 M H_2SO_4 containing 0.5g/l of the various inhibitors. From various peaks it could be seen that there are shift in the absorption band in the presence of the extracts, which indicate that the mechanism of absorption of the extracts on the metals is through a physical absorption.

4.7 Scanning Electron Microscopy Study

Surface morphologies of mild steel and aluminium in solutions of 1.0 M HCl and 0.5 M H_2SO_4 were studied using scanning electron microscopy. Plate 4.1 - 4.5 show the micrographs of polished aluminium and mild steel sheet, corroded mild steel and aluminium at x 5000 magnification in the presence and absence of the various inhibitors

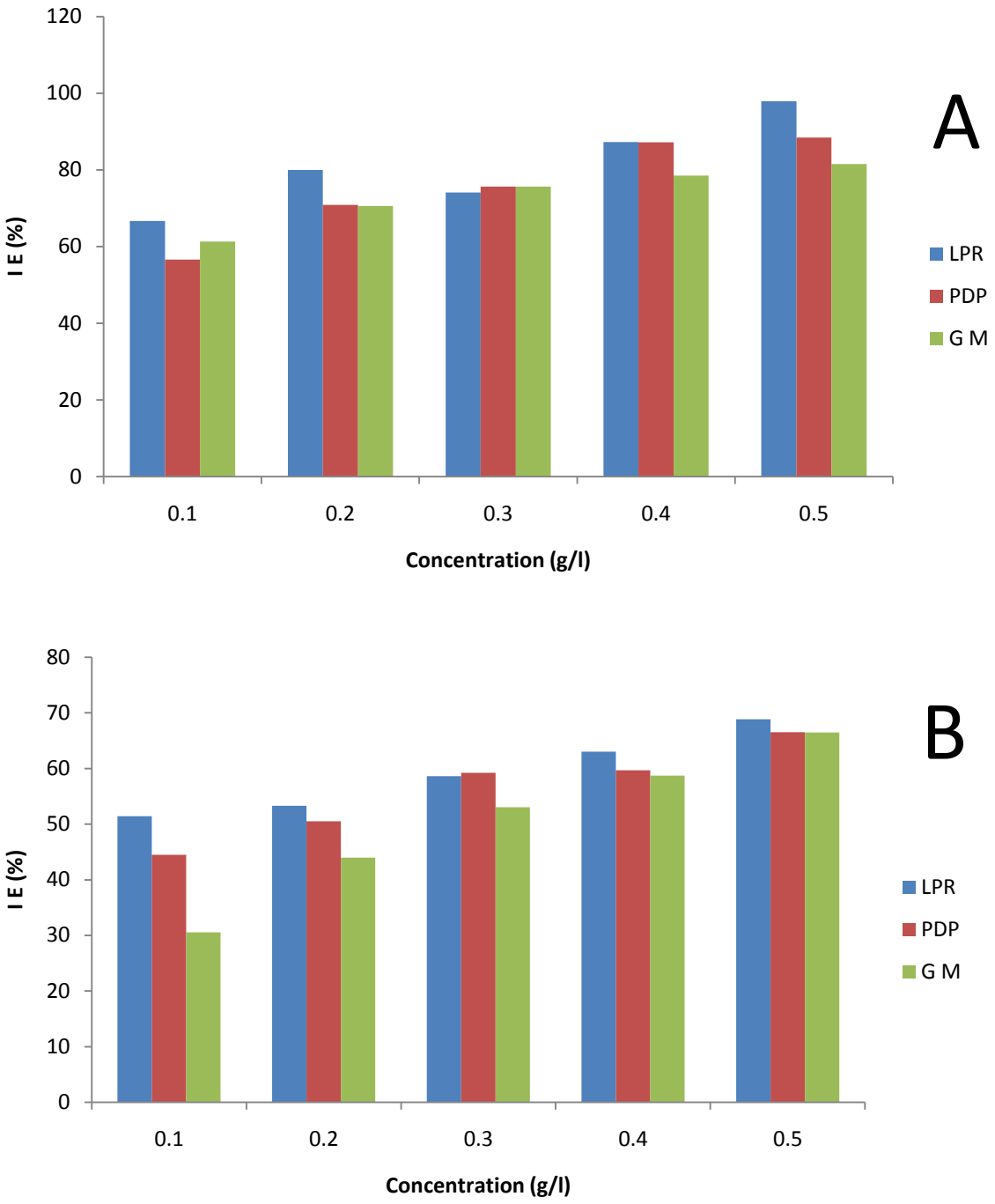


Fig. 4.65: **Comparative Chart of Inhibitor Efficiency (IE) for Mild Steel - 1 M HCl Solution of A) *Boscia senegalensis* and B) *Phyllanthus amarus* Concentration Obtained by Different Techniques**

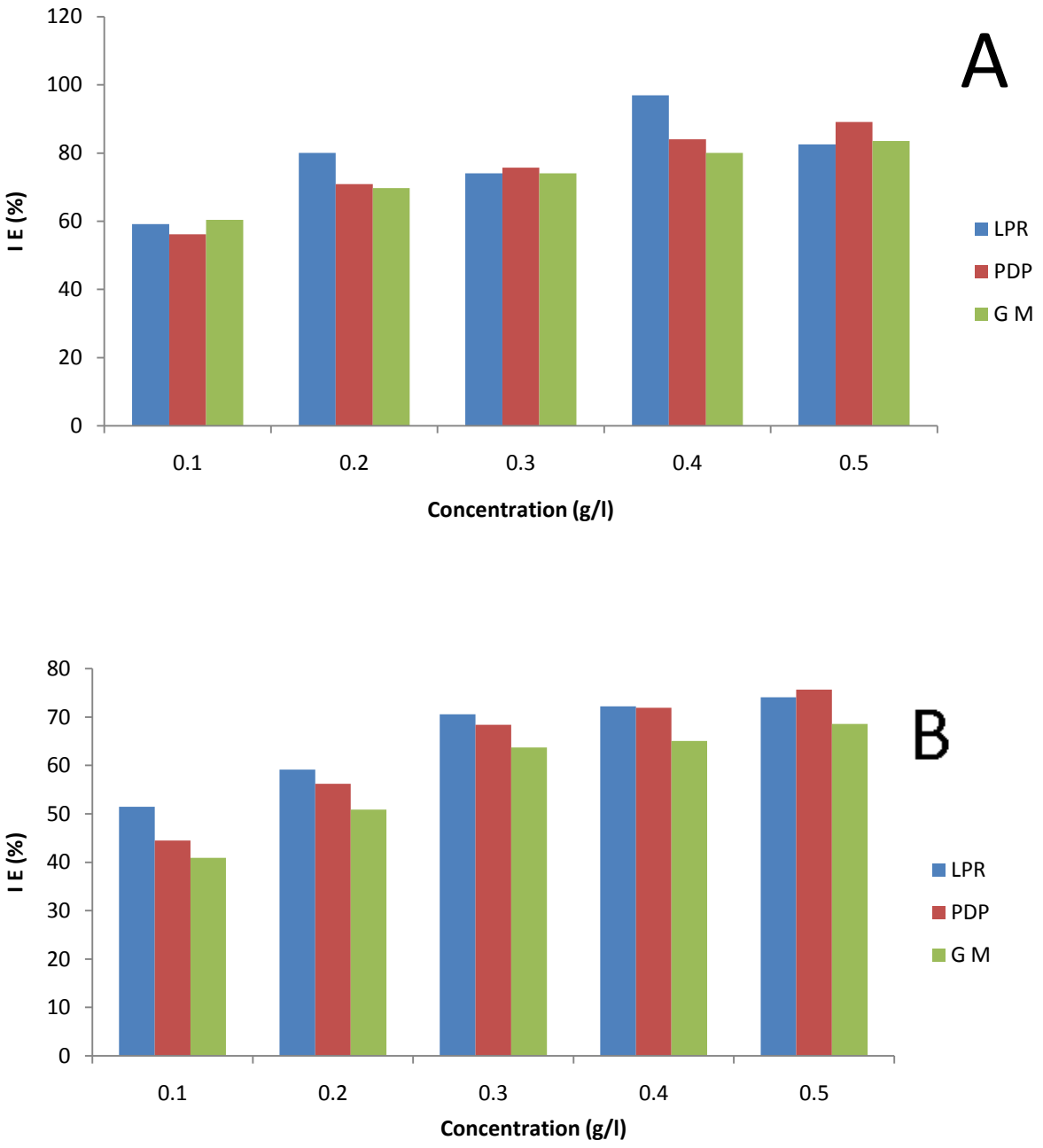


Fig. 4. 66: **Comparative Chart of Inhibitor Efficiency (IE) for Mild Steel - 1 M HCl Solution of A) *Paulina pinnata* and B) *Parinari polyandra* Concentration Obtained by Different Techniques**

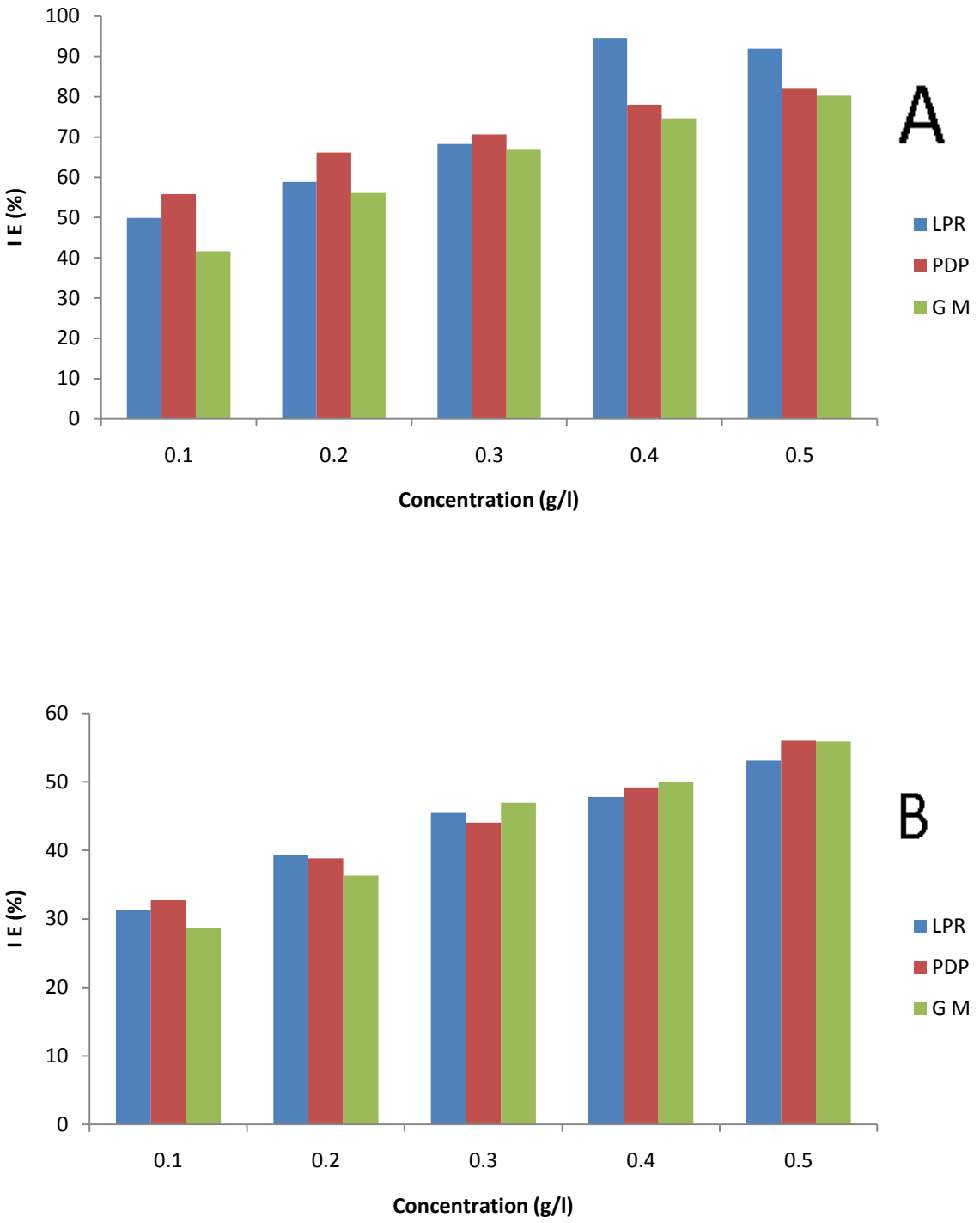


Fig. 4.67: **Comparative Chart of Inhibitor Efficiency (IE) for Mild Steel - 0.5 M H_2SO_4 Solution of A) *Boscia senegalensis* and B) *Phyllanthus amarus* Concentration Obtained by Different Techniques**

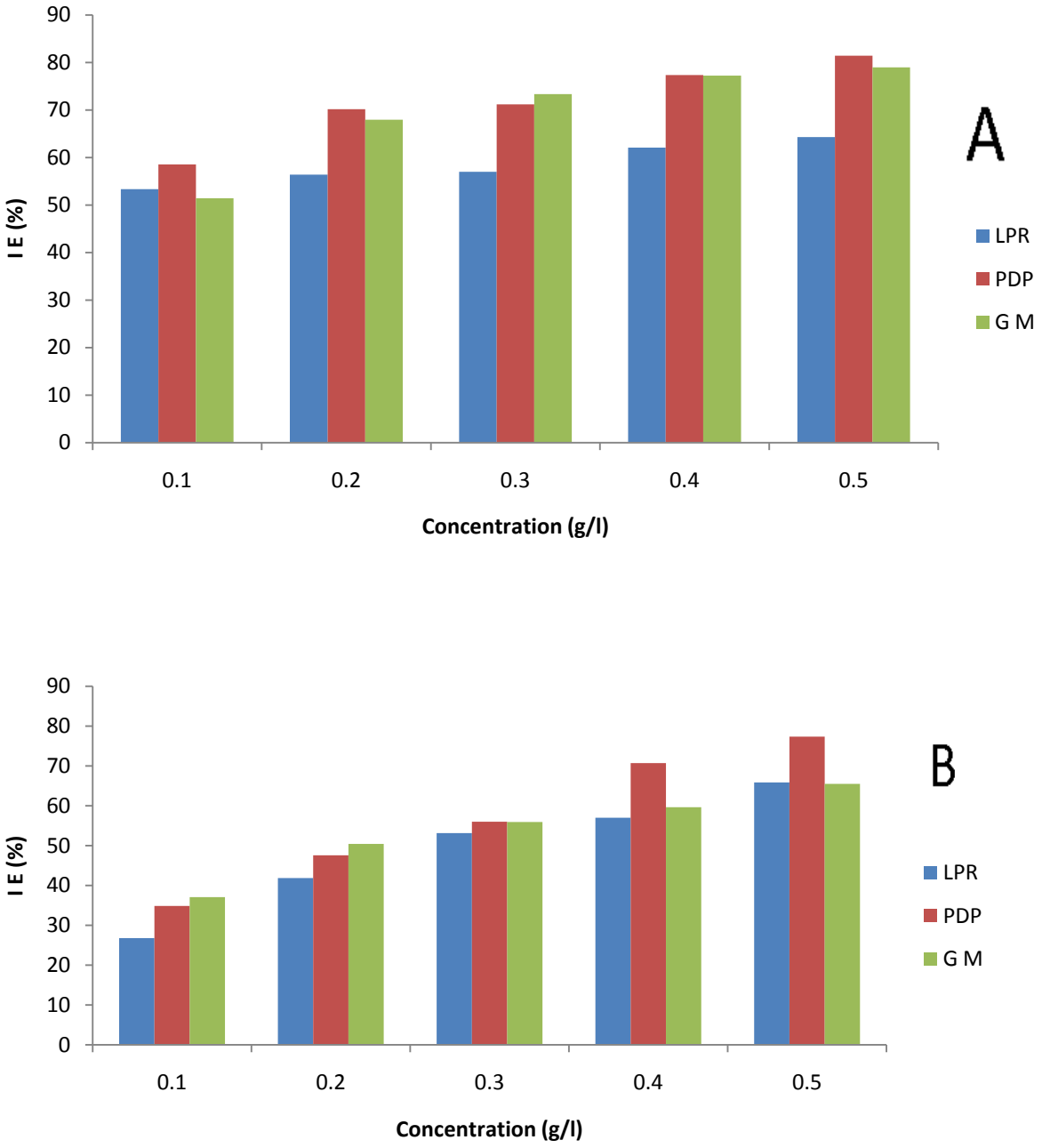


Fig. 4. 68: **Comparative Chart of Inhibitor Efficiency (IE) for Mild Steel - 0.5 M H_2SO_4 Solution of A) *Paulina pinnata* and B) *Parinari polyandra* Concentration Obtained by Different Techniques**

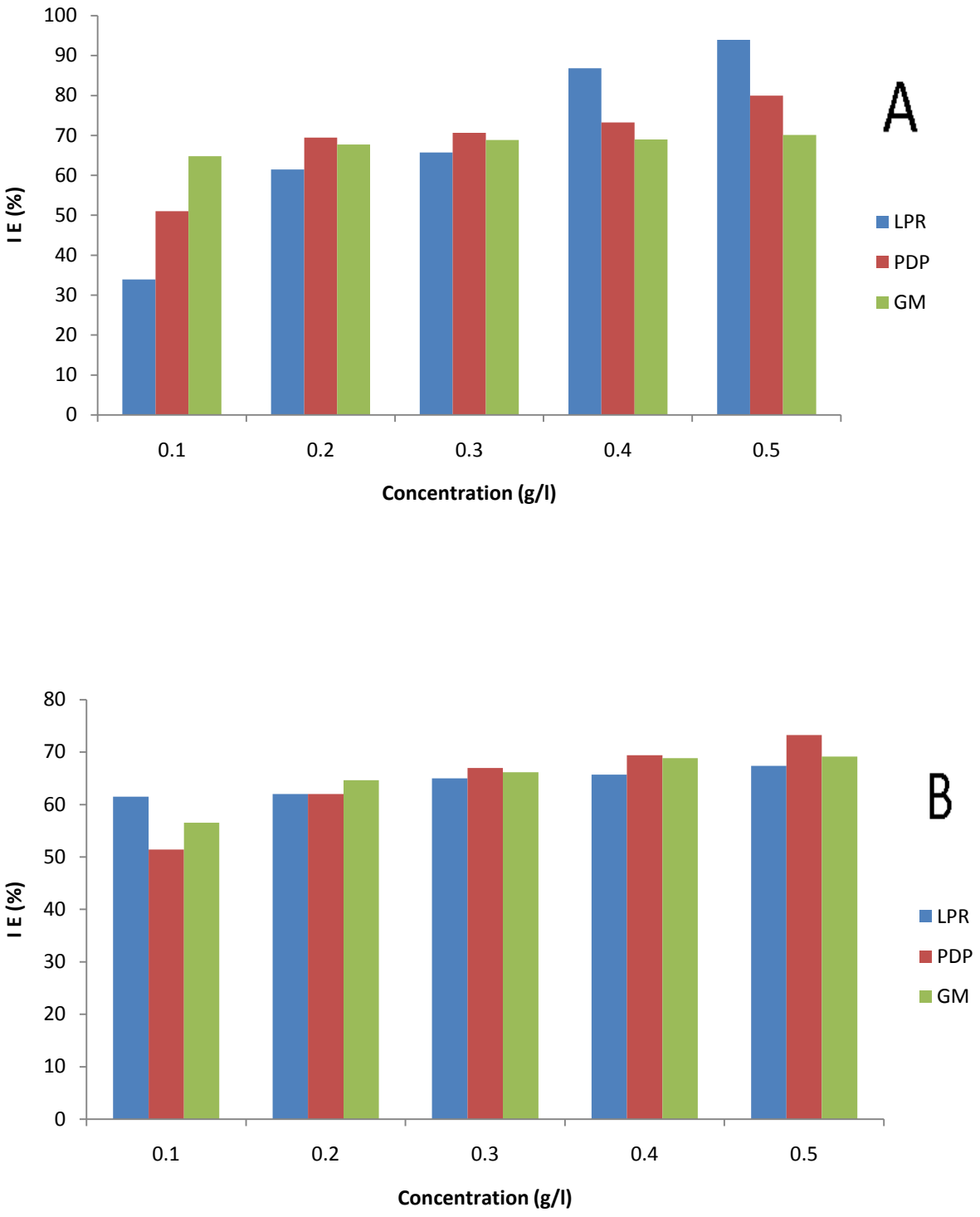


Fig. 4.69: Comparative Chart of Inhibitor Efficiency (IE) for Aluminium - 1 M HCl Solution of A) *Boscia senegalensis* and B) *Phyllanthus amarus* Concentration Obtained by Different Techniques

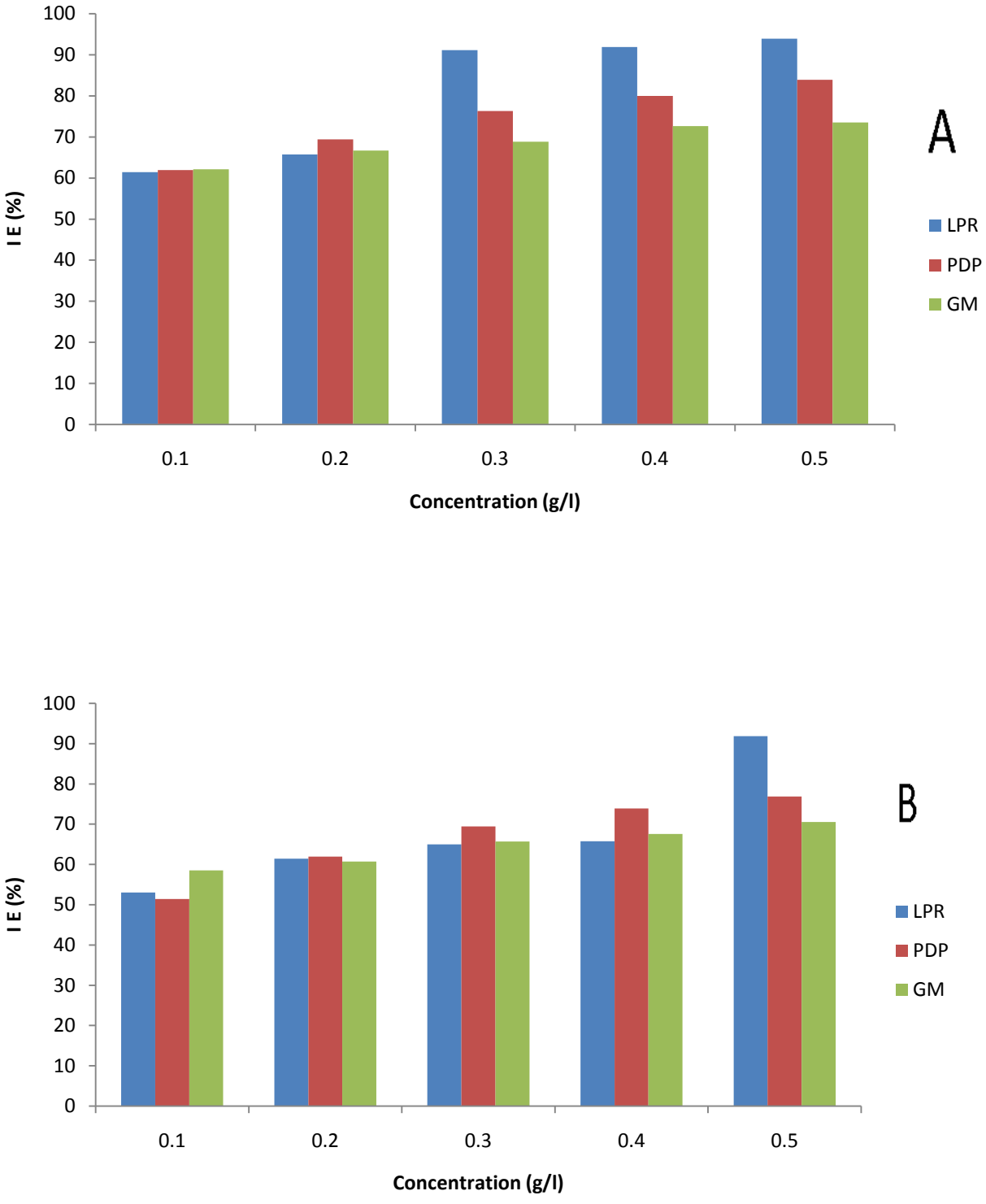


Fig. 4.70: Comparative Chart of Inhibitor Efficiency (IE) for Aluminium - 1 M HCl Solution of A) *Paulina pinnata* and B) *Parinari polyandra* Concentration Obtained by Different Techniques

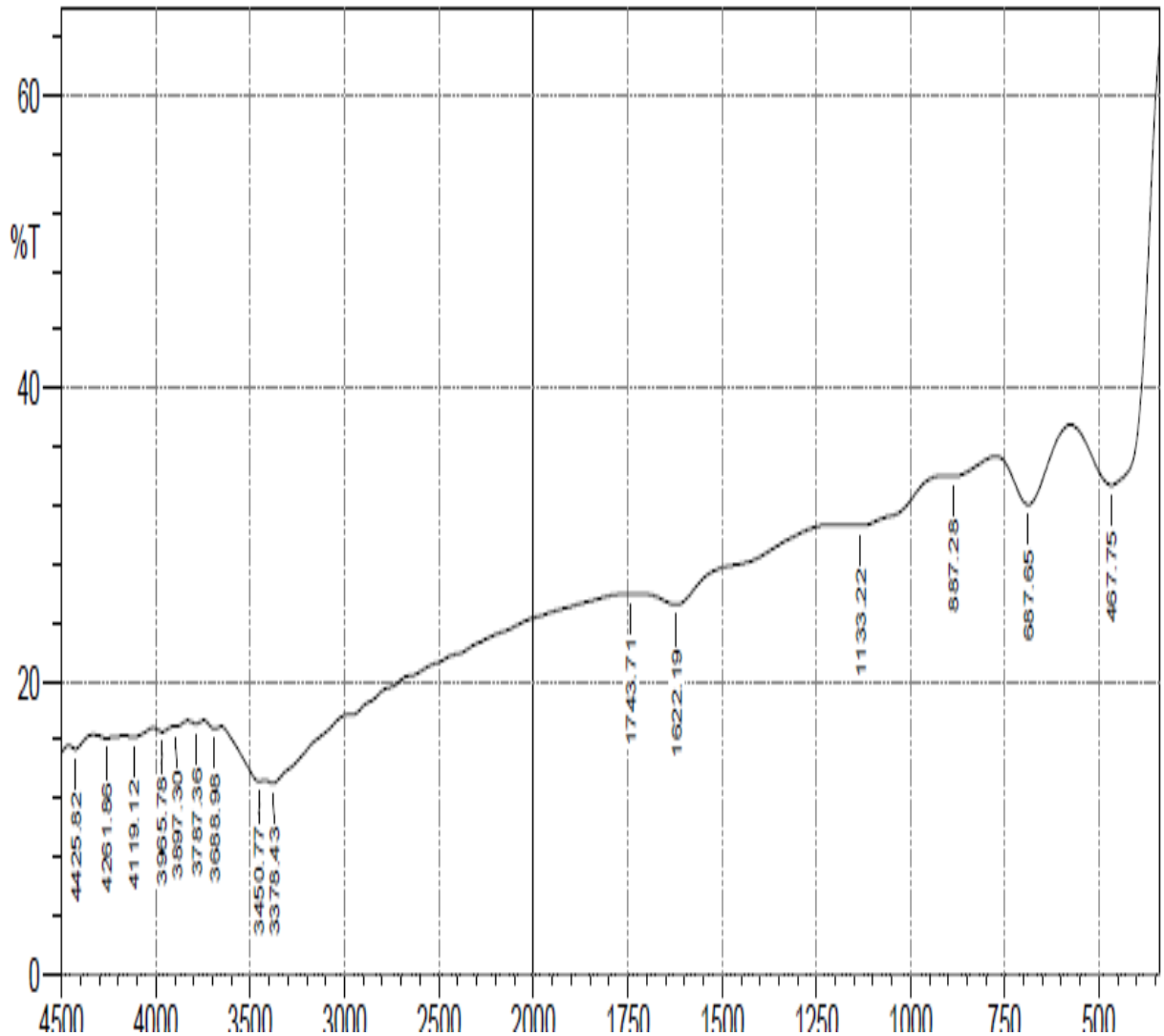
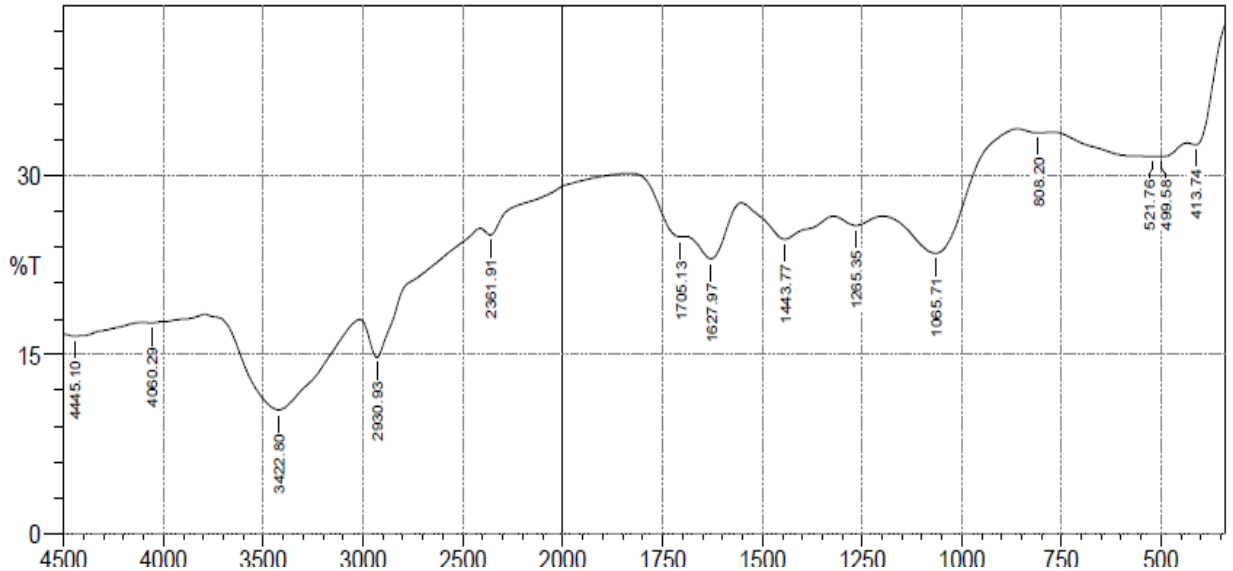
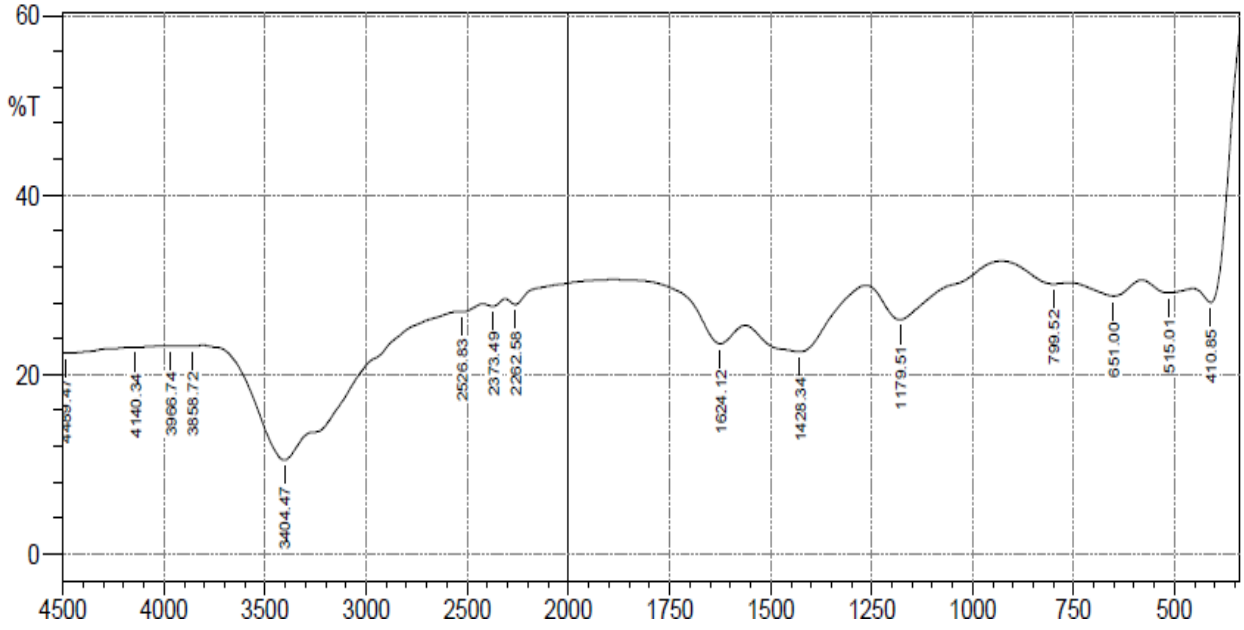


Fig. 4.71: FTIR Spectrum of the Corrosion Product from the Corrosion of Mild Steel in 1.0 M HCl

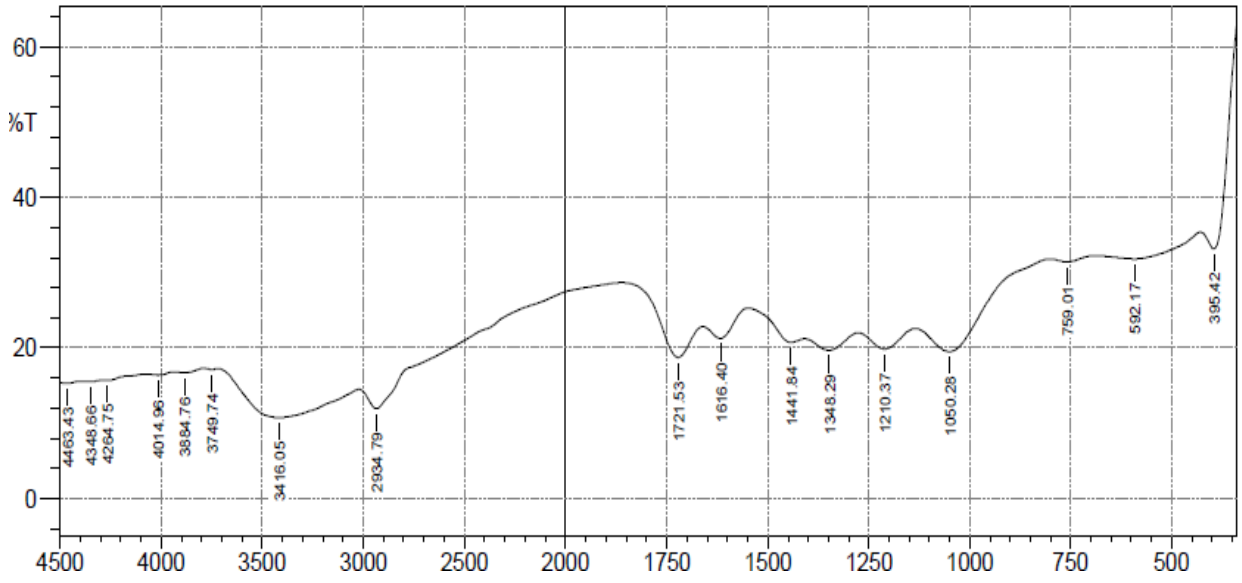


(a)

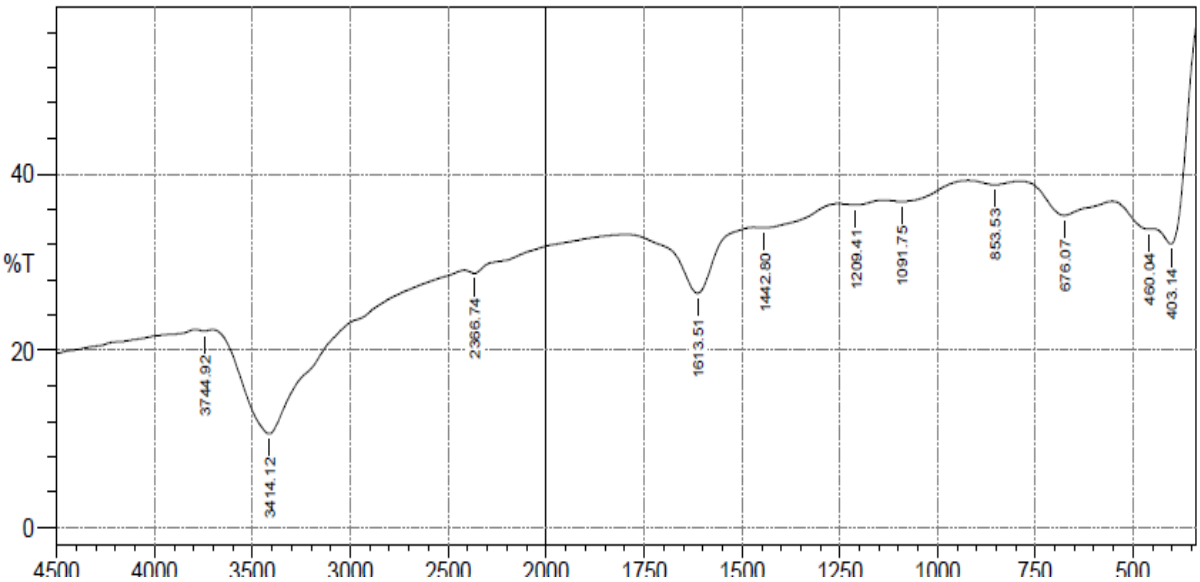


(b)

Fig. 4.72: FTIR Spectra of (a) BS alone (b) Corrosion Product from the Corrosion of Mild Steel when 0.5g/l of BS was used as an Inhibitor in 1.0 M HCl

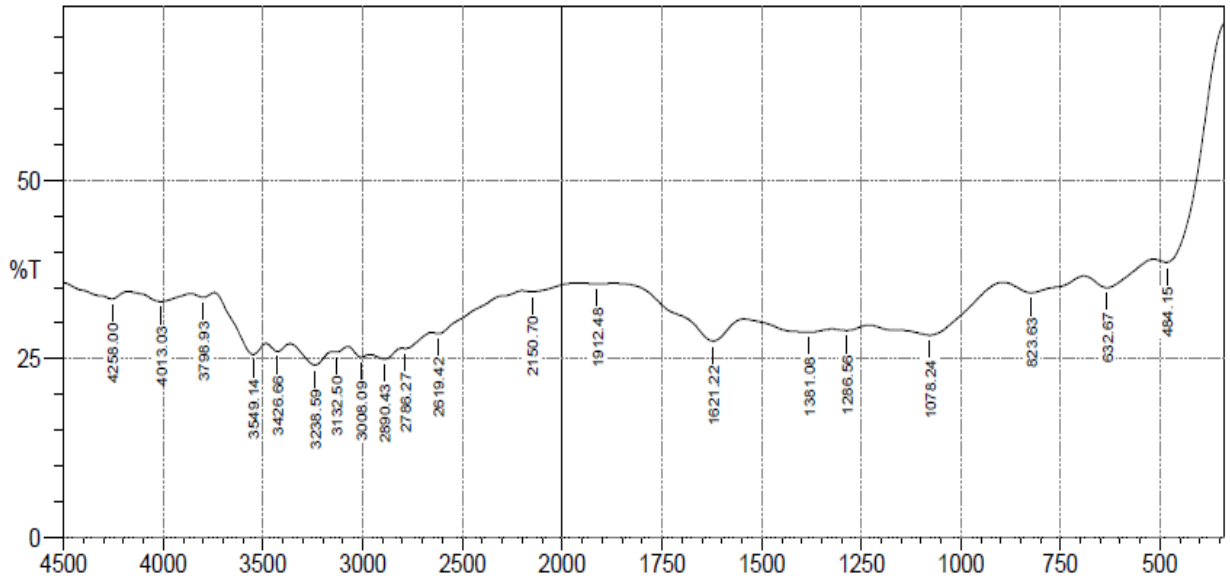


(a)

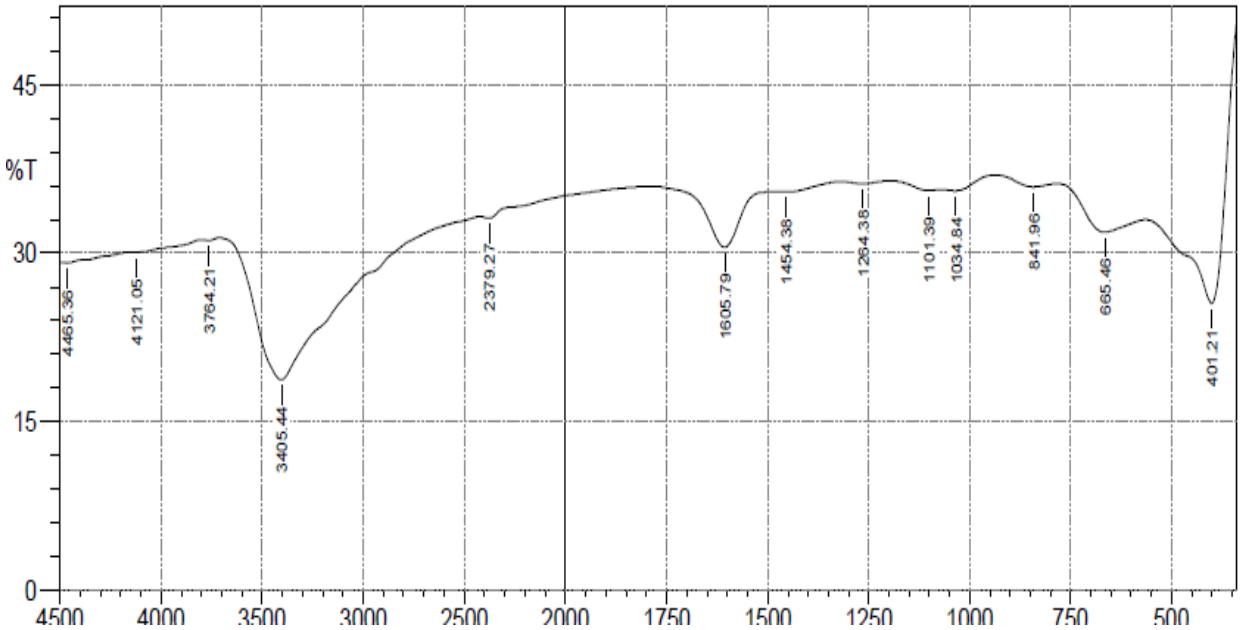


(b)

Fig. 4.73: FTIR Spectra of (a) PA alone (b) Corrosion Product from the Corrosion of Mild Steel when 0.5g/l of PA was used as an Inhibitor in 1.0 M HCl



(a)



(b)

Fig.4.74: FTIR Spectra of (a) PP alone (b) Corrosion Product from the Corrosion of Mild Steel when 0.5g/l of PP was used as an Inhibitor in 1.0 M HCl

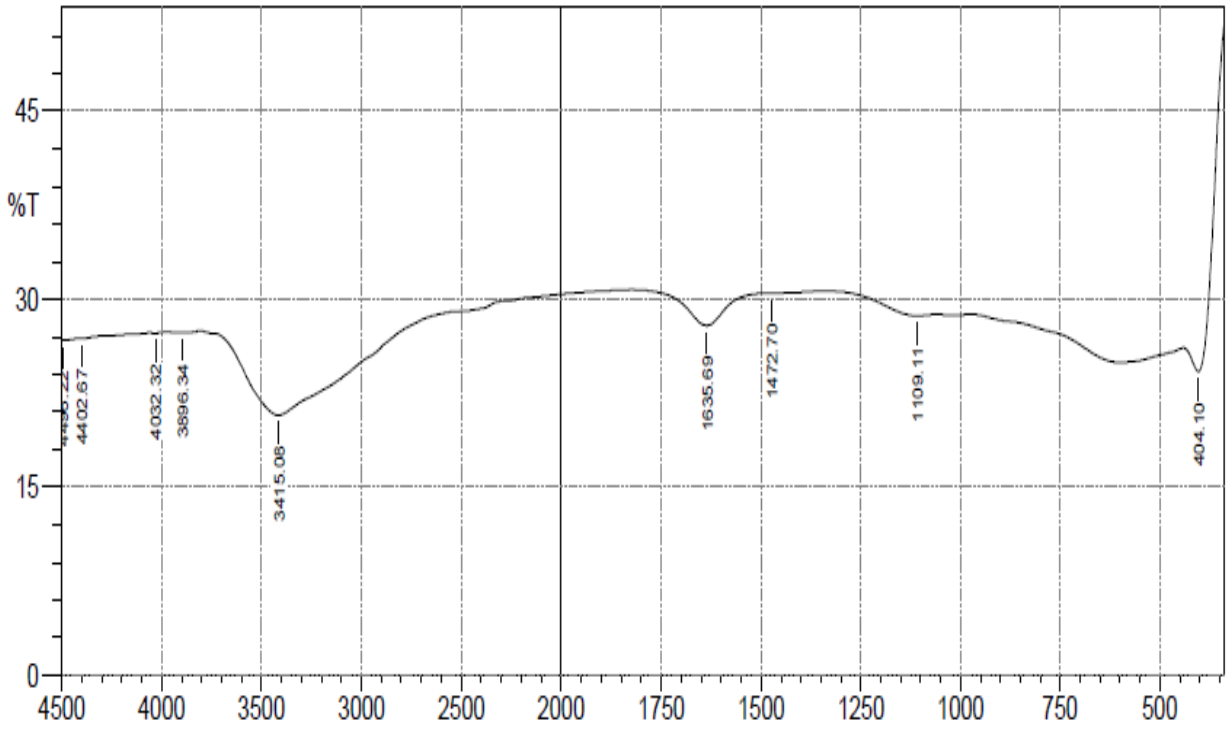
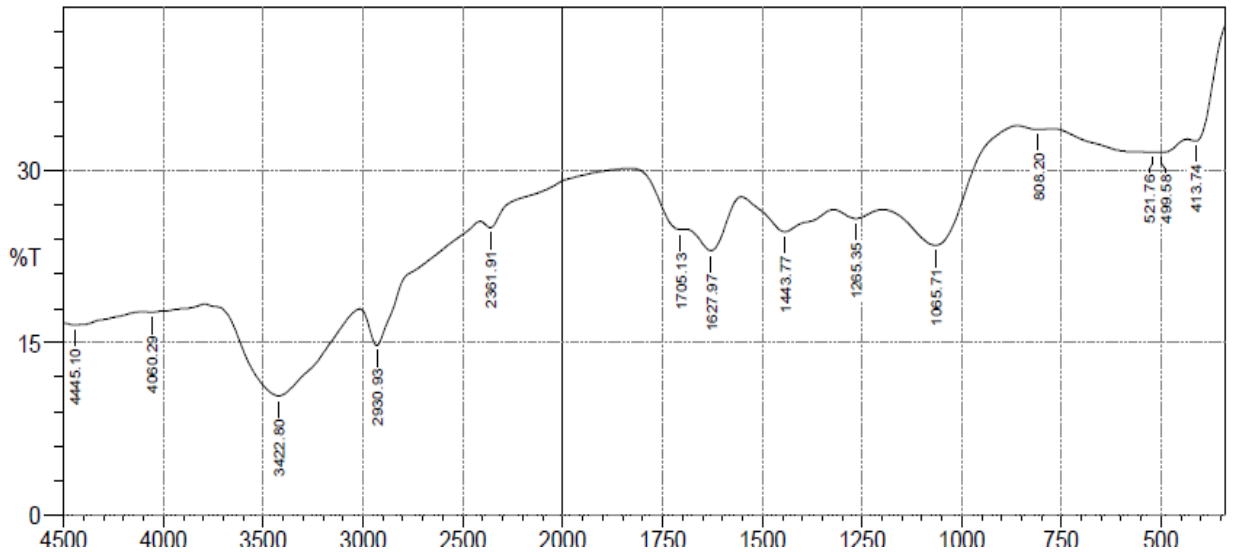
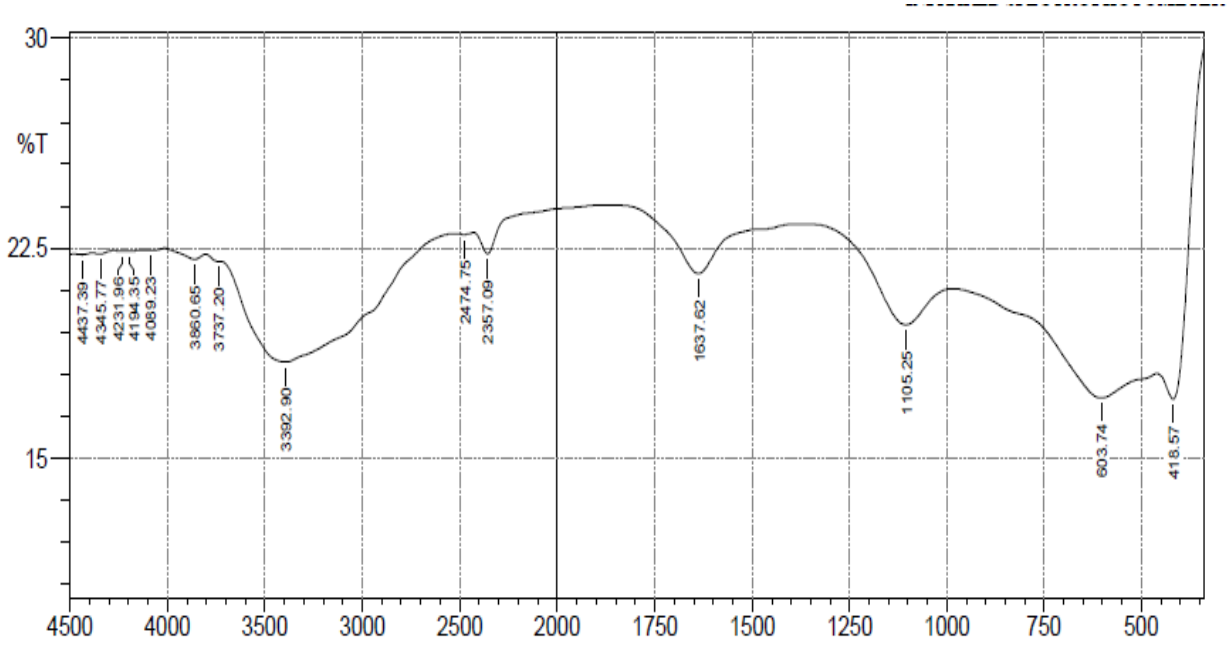


Fig. 4.75: FTIR Spectrum of the Corrosion Product from the Corrosion of Aluminium in 1.0 M HCl

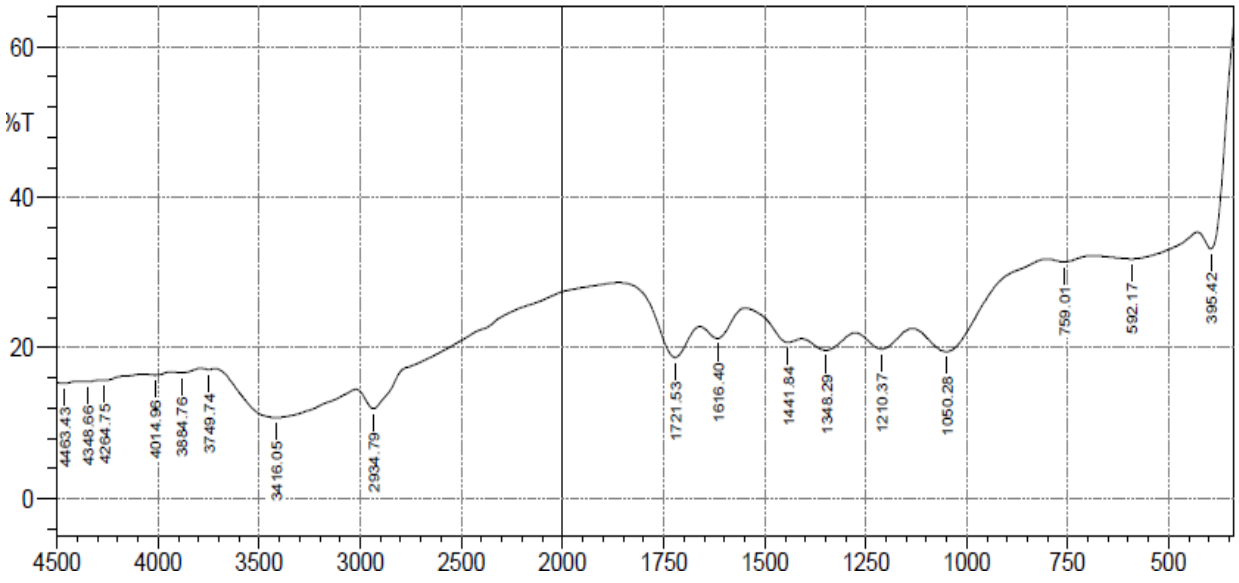


(a)

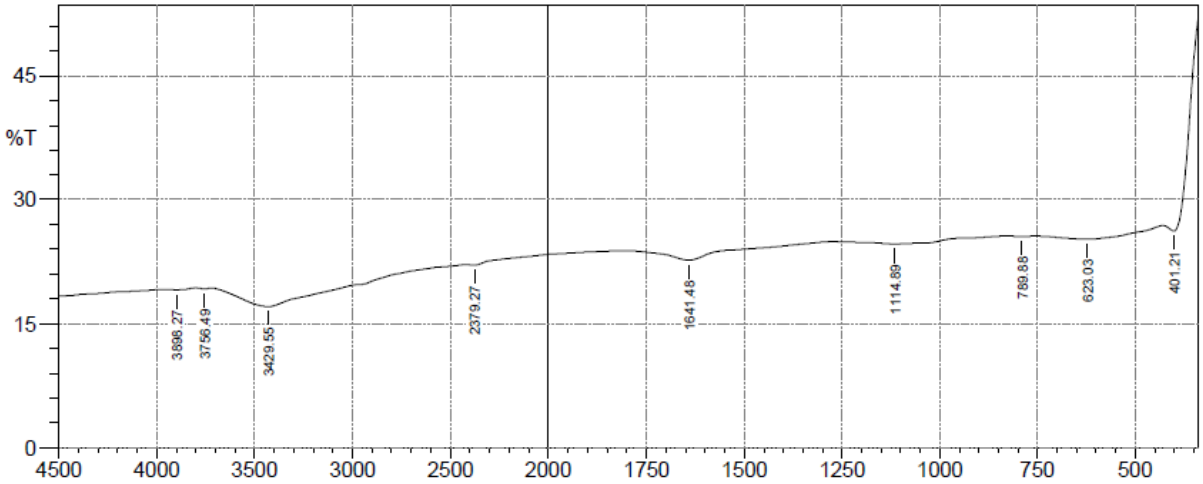


(b)

Fig.4.76: FTIR Spectra of (a) BS alone (b) Corrosion Product from the Corrosion of Aluminium when 0.5g/l of BS was used as an Inhibitor in 1.0 M HCl

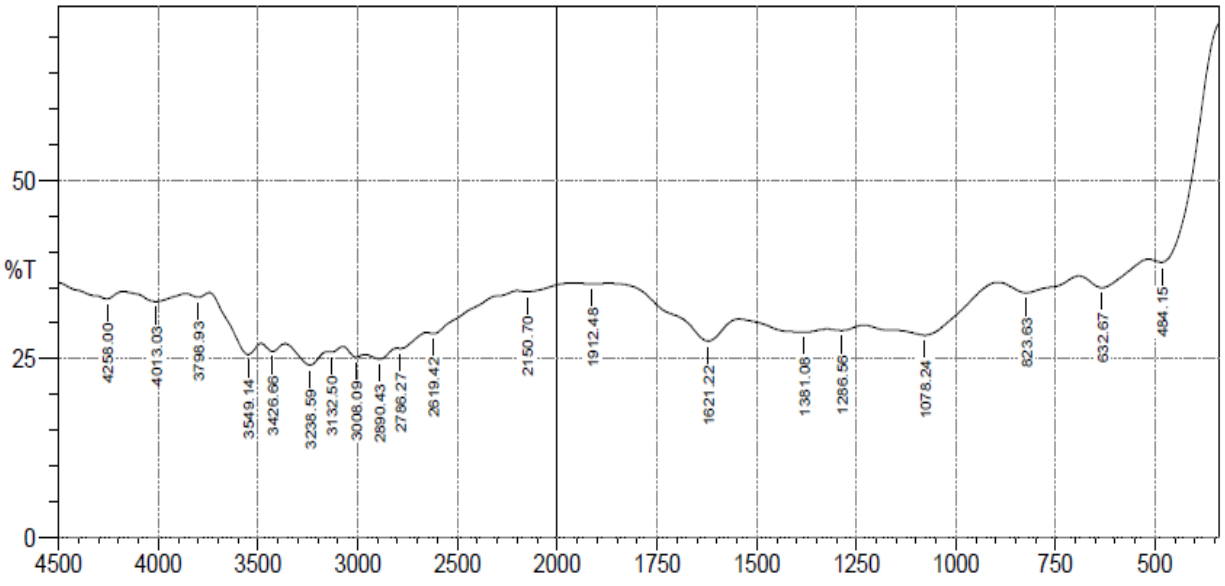


(a)

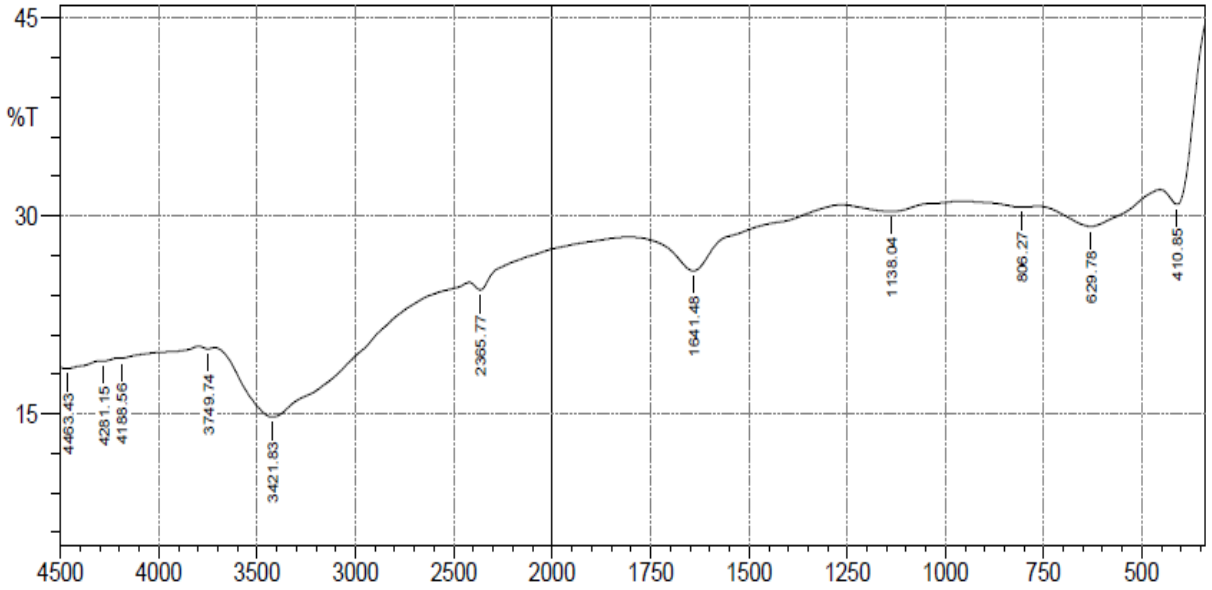


(b)

Fig. 4.77: FTIR Spectra of (a) PA alone (b) Corrosion Product from the Corrosion of Aluminium when 0.5g/l of PA was used as an Inhibitor in 1.0 M HCl



(a)



(b)

Fig. 4.78: FTIR Spectra of (a) PP alone (b) Corrosion Product from the Corrosion of Aluminium when 0.5g/l of PP was used as an Inhibitor in 1.0 M HCl

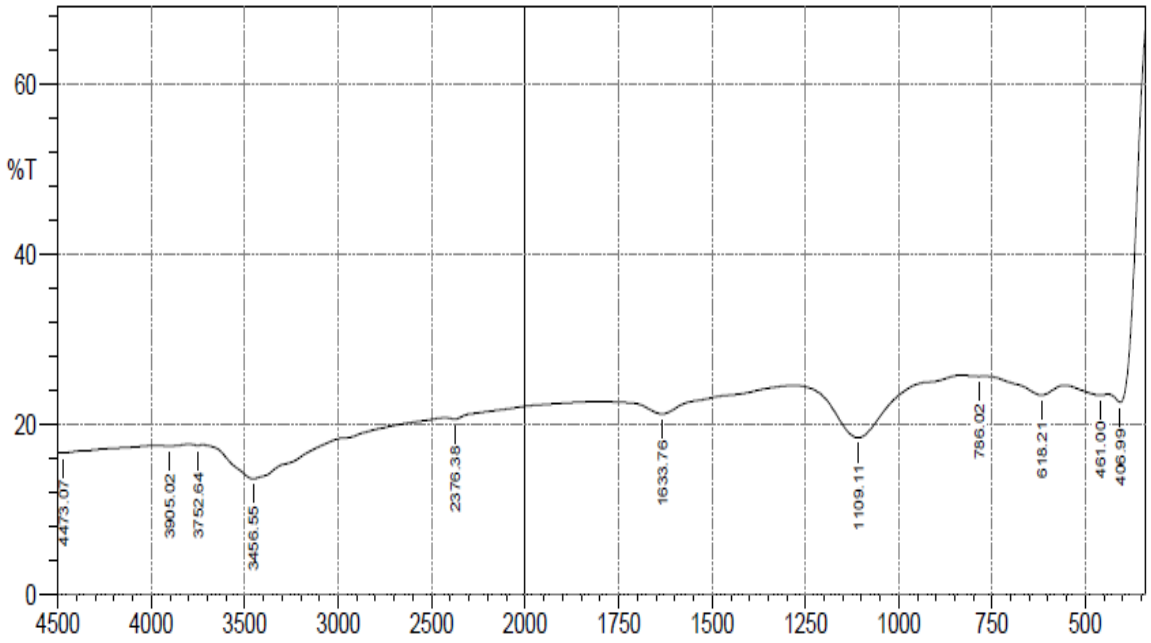
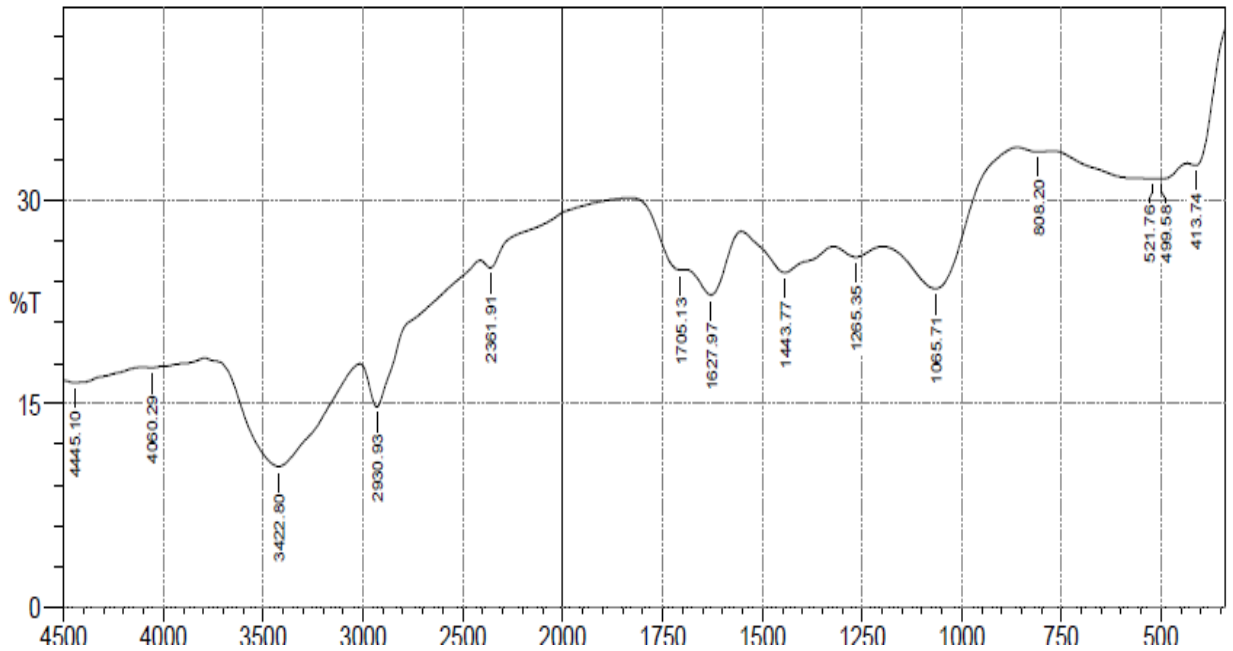
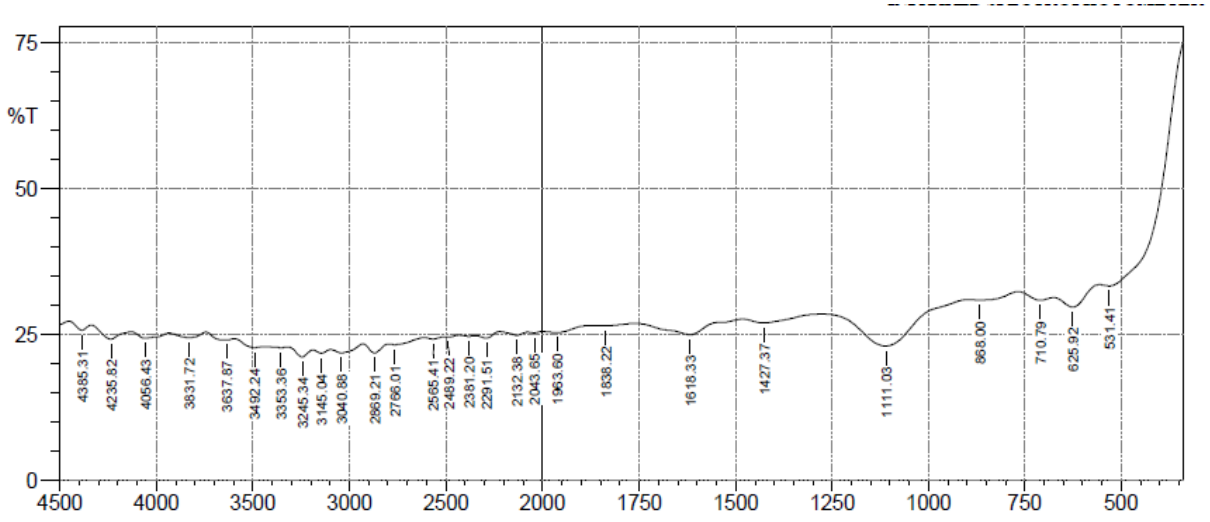


Fig.4.79: FTIR Spectrum of the Corrosion Product from the Corrosion of Mild Steel in 0.5 M H_2SO_4

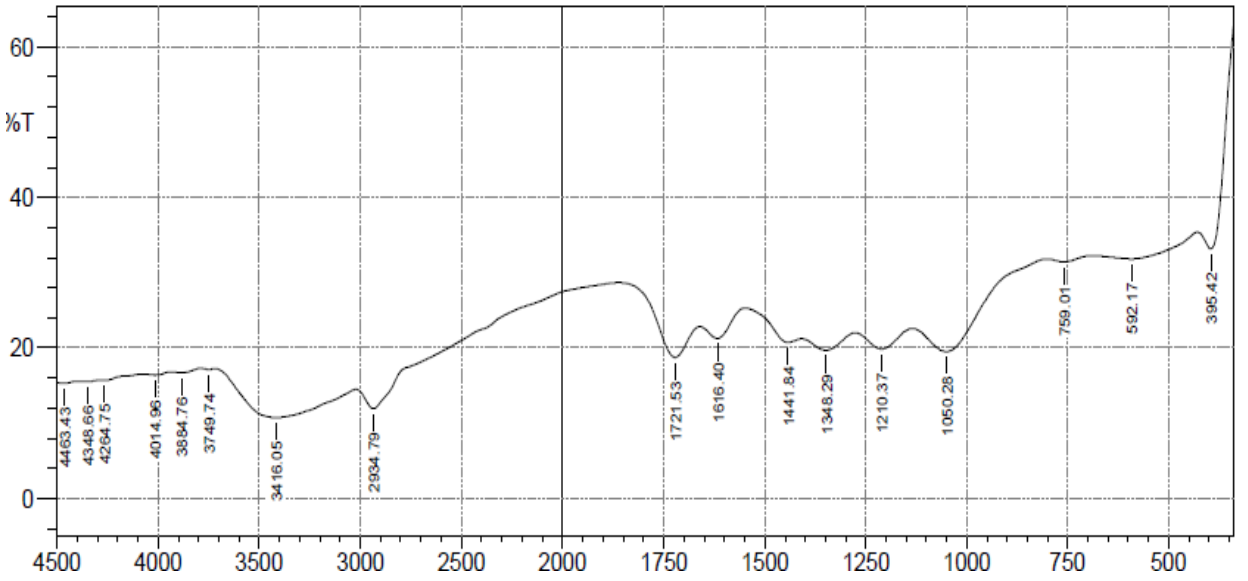


(a)

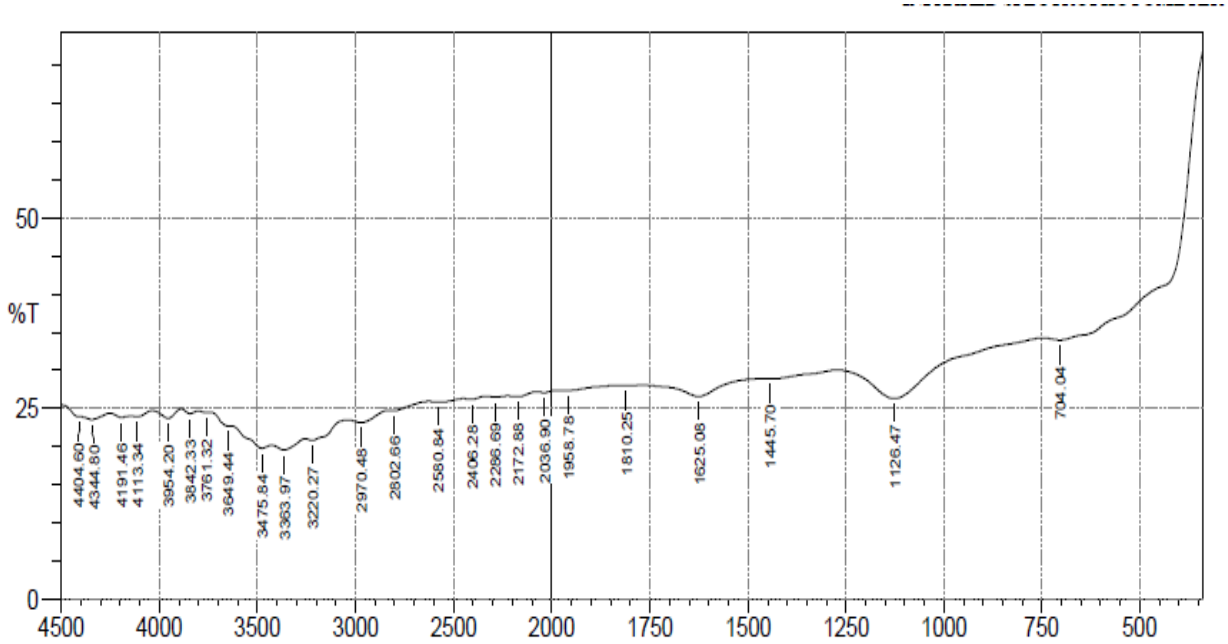


(b)

Fig.4.80: FTIR Spectra of (a) BS alone (b) Corrosion Product from the Corrosion of Aluminium when 0.5g/l of BS was used as an Inhibitor in 0.5 M H_2SO_4

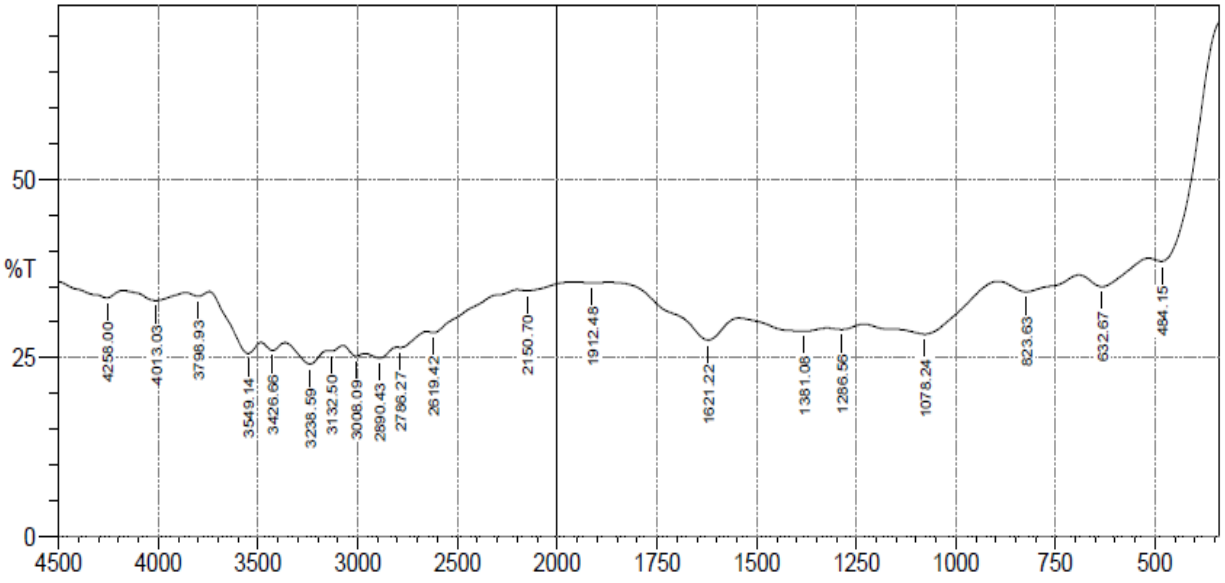


(a)

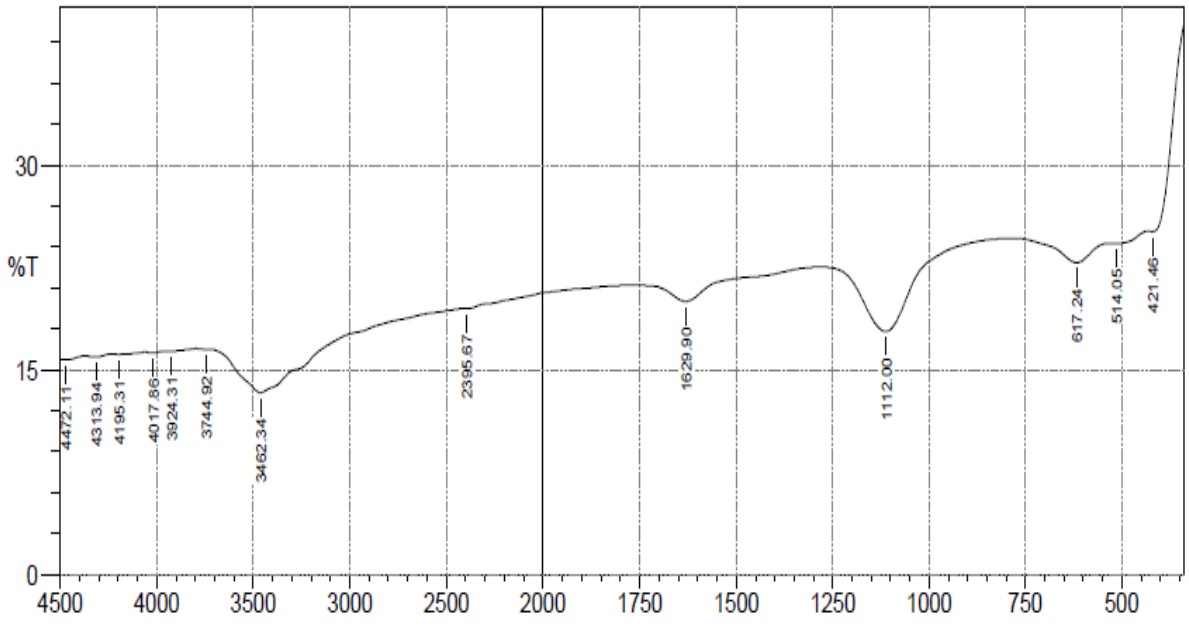


(b)

Fig. 4.81: FTIR Spectra of (a) PA alone (b) Corrosion Product from the Corrosion of Aluminium when 0.5g/l of PA was used as an Inhibitor in 0.5 M H_2SO_4



(a)



(b)

Fig.4.82: FTIR Spectra of (a) PP alone (b) Corrosion Product from the Corrosion of Aluminium when 0.5g/l of PP was used as an Inhibitor in 0.5 M H_2SO_4

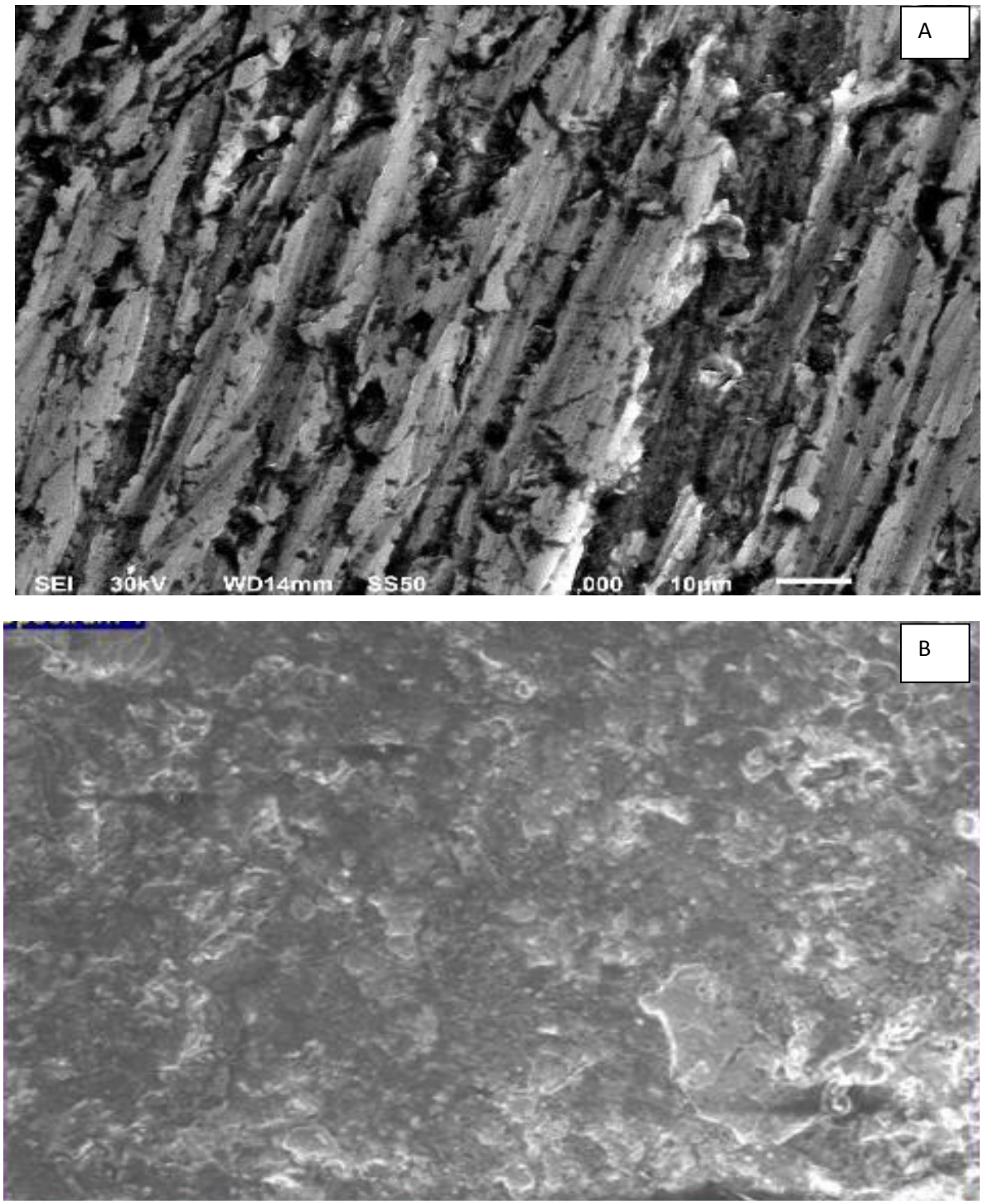


Plate 4.1: SEM Micrographs of Polished A) Aluminium Sheet and B) Mild Steel alone

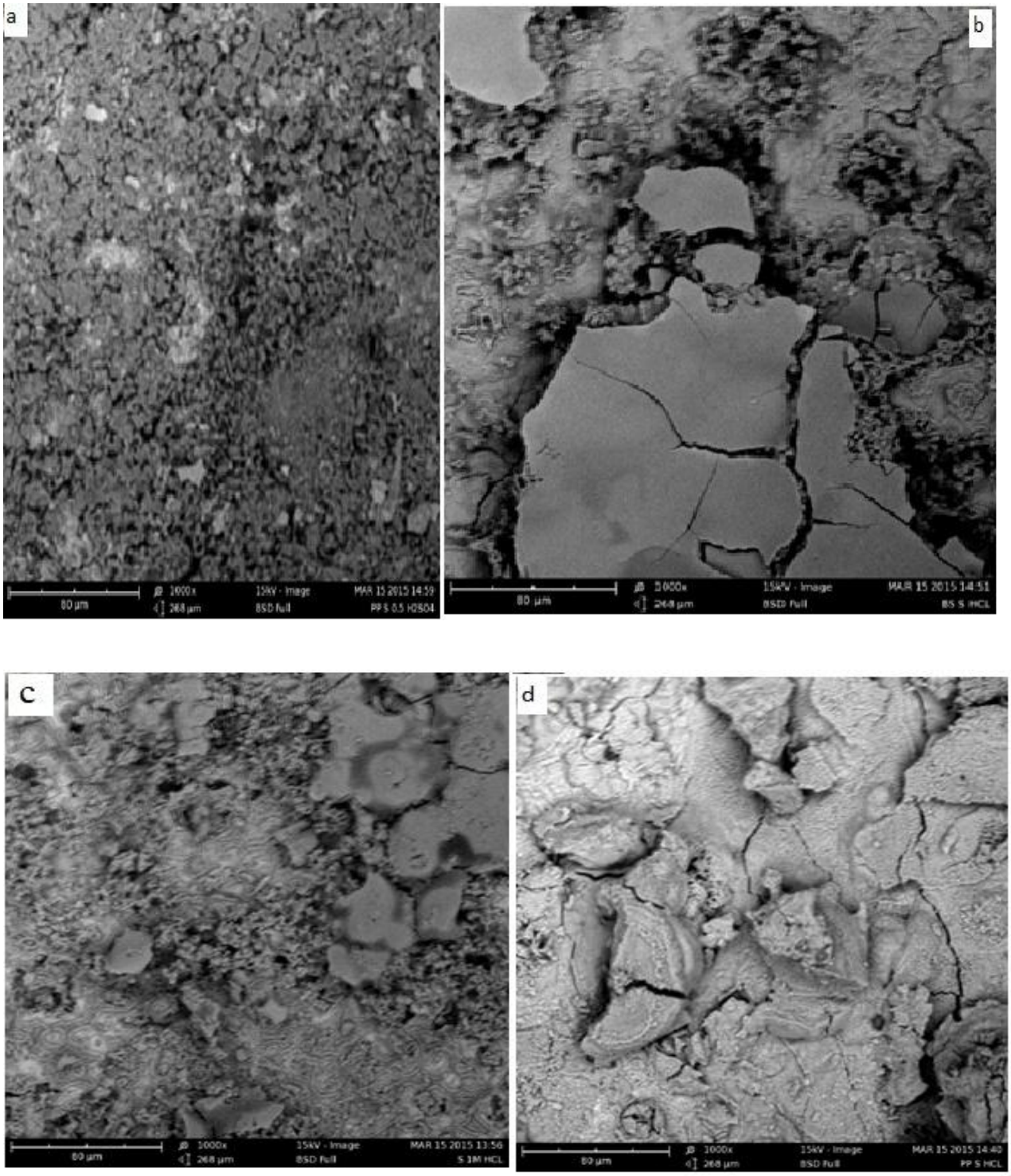


Plate 4.2: SEM Micrographs of Mild Steel Corroded in 1.0 M HCl Solution for 7days (a)Mild Steel alone and in the Presence of (b) *Boscia senegalensis* (c) *Phyllanthus amarus* (d) *Paullina pinnata* (x 5000)

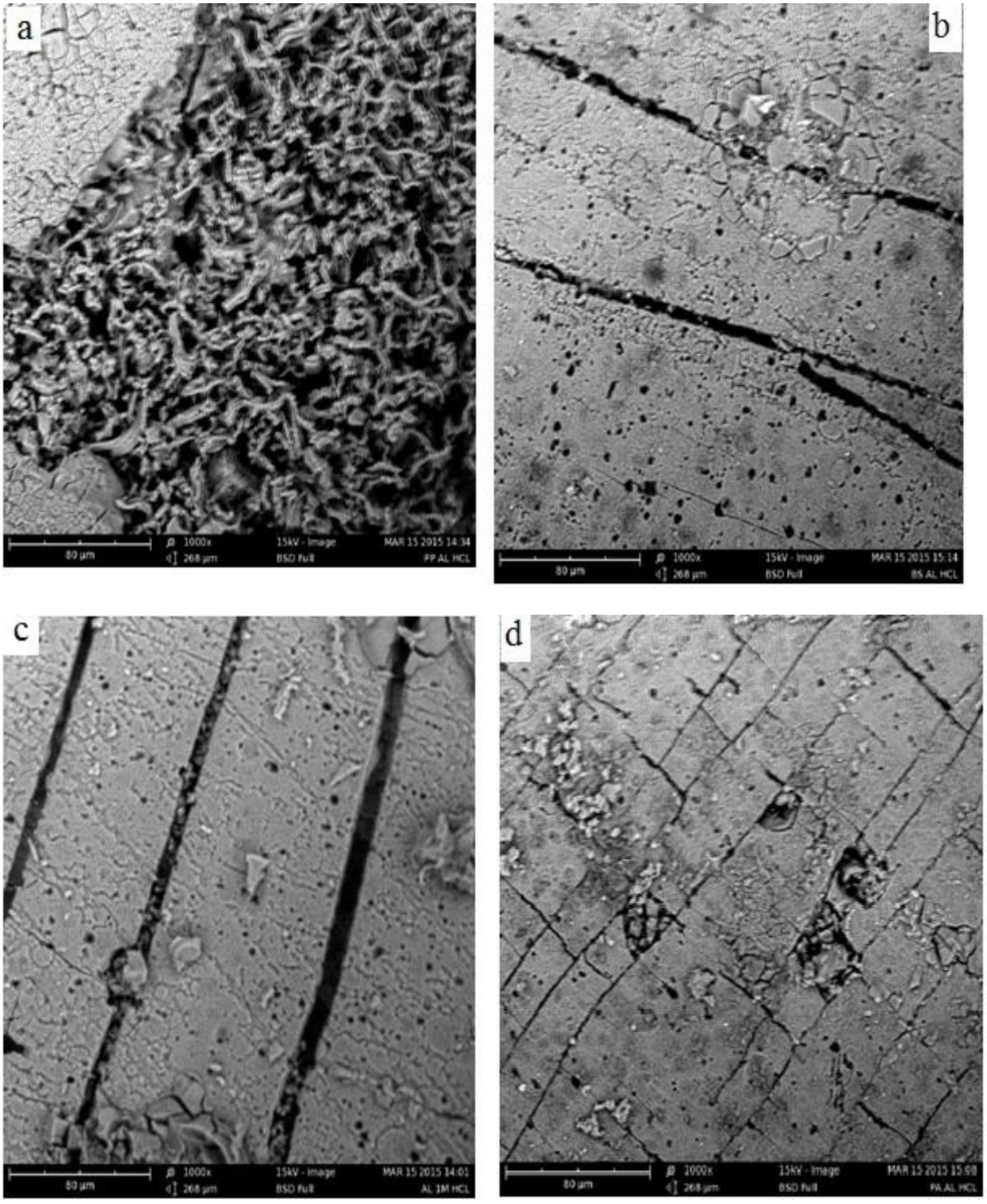


Plate 4.3: SEM Micrographs of Aluminium Corroded in 1.0 M HCl Solution for 7days (a) Aluminium alone and in the Presence of (b) *Boscia senegalensis* (c) *Phyllanthus amarus* (d) *Paullina pinnata* (x 5000)

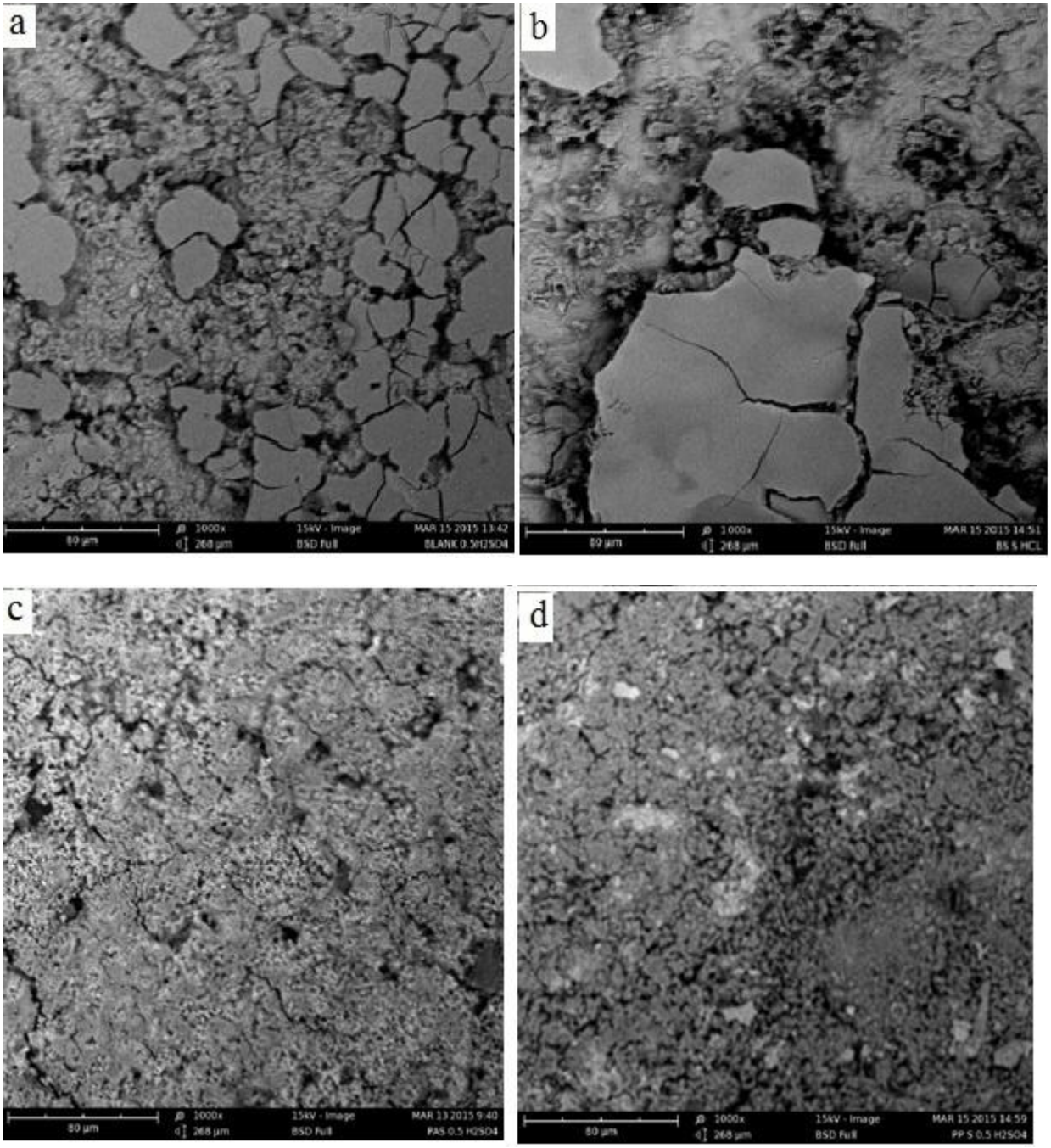


Plate 4.4: SEM Micrographs of Mild Steel Corroded in 0.5 M H_2SO_4 Solution for 7days (a) Mild Steel alone and in the Presence of (b) *Boscia senegalensis* (c) *Phyllanthus amarus* (d) *Paullina pinnata* (x 5000)

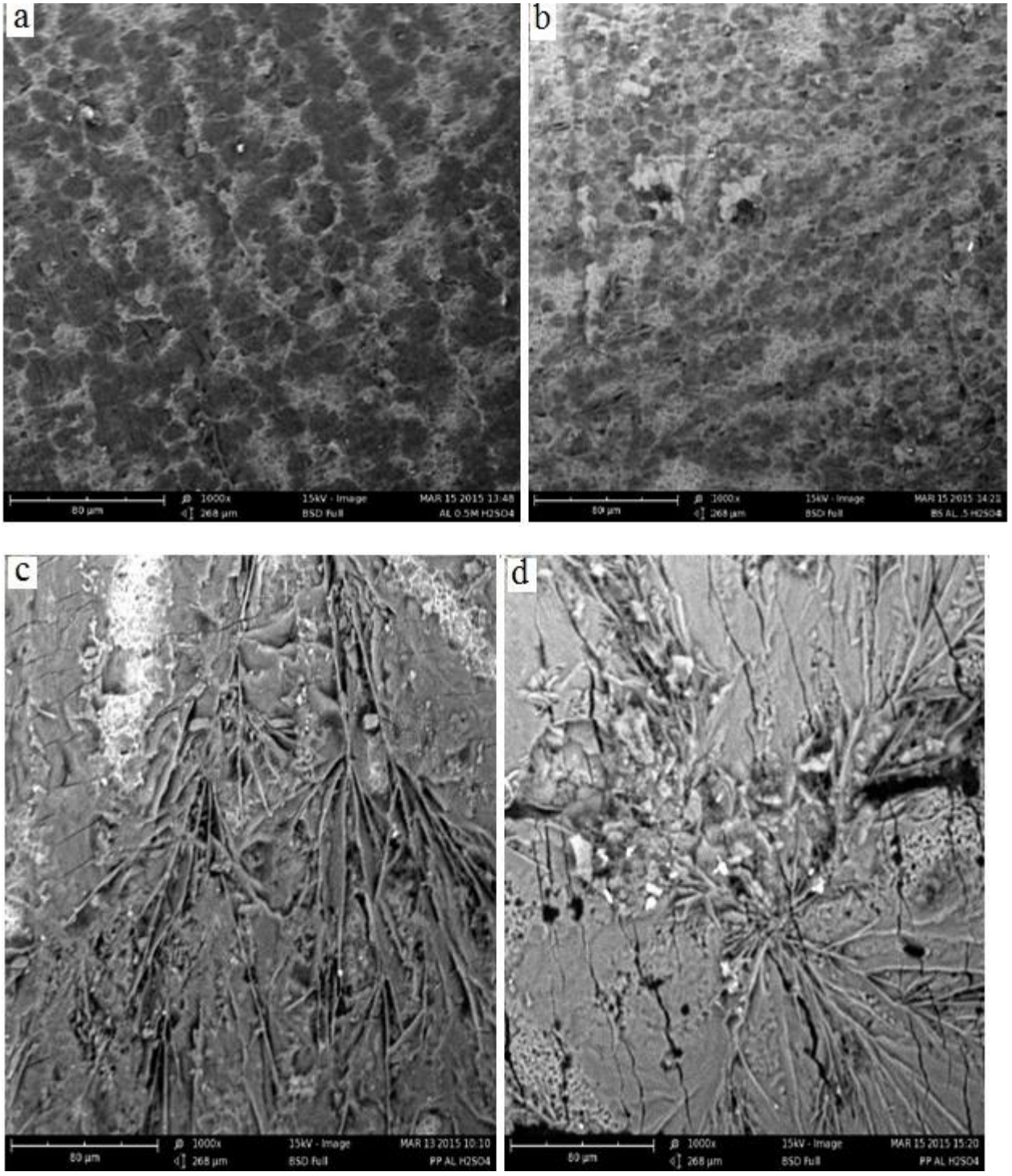


Plate 4.5: SEM Micrographs of Aluminium Corroded in 0.5 M H_2SO_4 Solution for 7days (a) Aluminium alone and in the Presence of (b) *Boscia senegalensis* (c) *Phyllanthus amarus* (d) *Paullina pinnata* (x 5000)

4.8 Computational and Theoretical Modelling

4.8.1 Quantum chemical calculations

Quantum chemical calculations give insights to the molecular level, electron distribution of the different organic constituents present in the plant extracts as well as to understudy the nature of their interactions with the metal surfaces. Geometric optimization of isolated compounds from the extracts was established including the distribution of frontier molecular orbitals, with a view to establish the active sites as well as local reactivity of the molecules. The simulations were performed by means of the density functional theory (DFT) electronic structure program DMol^3 available in Material Studio 7.0 (Accelrys Inc., San Diego, CA, USA) (Delley, 1990, 2000; Xia et al., 2008; Khaled, 2010a, 2010b). Electronic structures parameters for the simulation include spin unrestricted polarization using the DND basis set and the Perdew-Wang local-correlation density functional.

Figures 4.83 – 4.86 illustrate the optimize structure, the highest occupied molecular orbital (HOMO) and lowest unoccupied molecular orbital (LUMO), of various selected constituent in the plant extracts with a view of establishing there inhibitive capacity respectively. The corresponding quantum chemical parameters are presented on Tables 4.17 and 4.18.

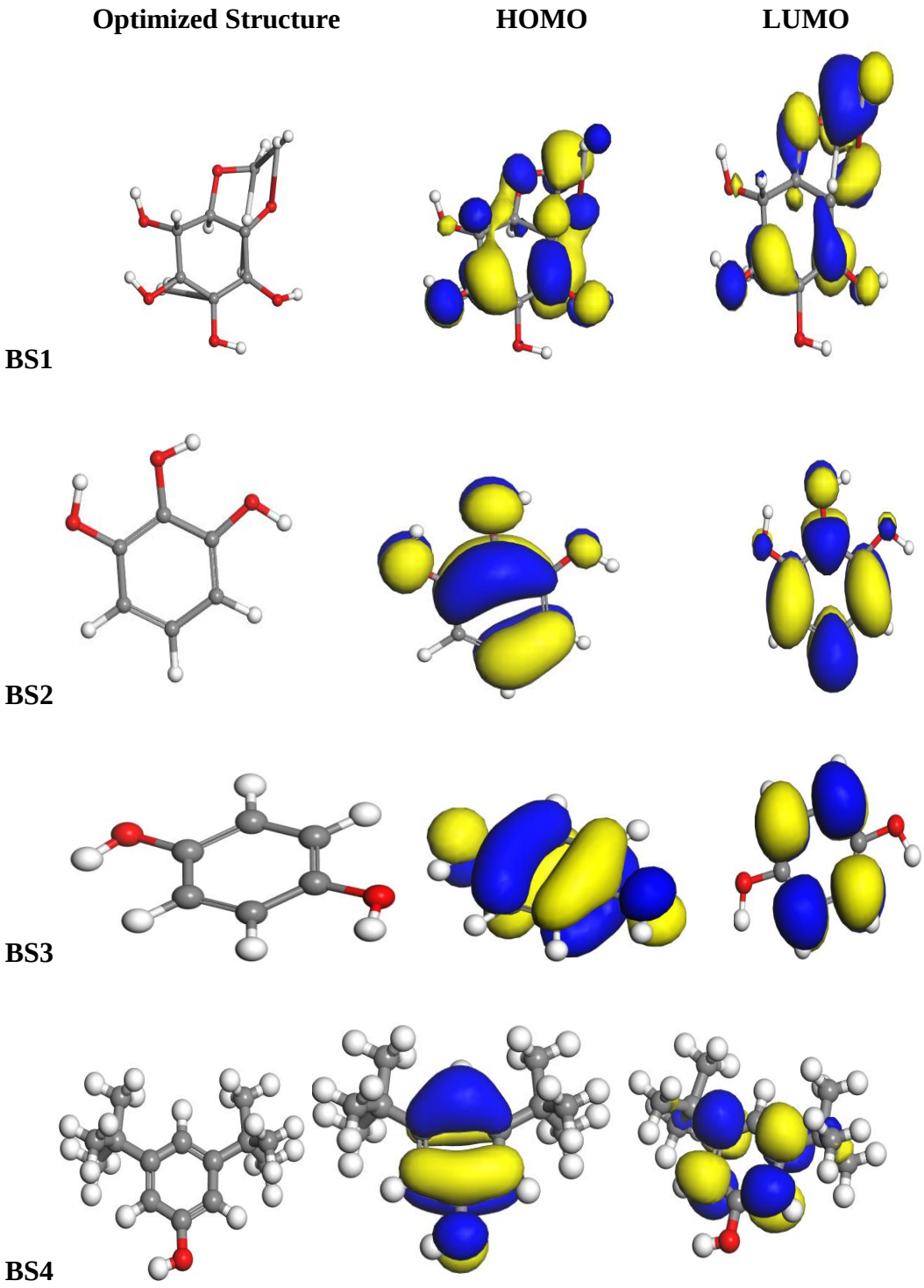


Fig. 4.83: HOMO – LUMO Orbital Diagram of some Constituents of *Boscia senegalensis* Extract (atom legend: White = H; Light gray = C; Red = O; Blue = N). The blue and yellow isosurfaces depict the electron density difference, the blue regions show electron accumulation, while the yellow regions show the electron loss

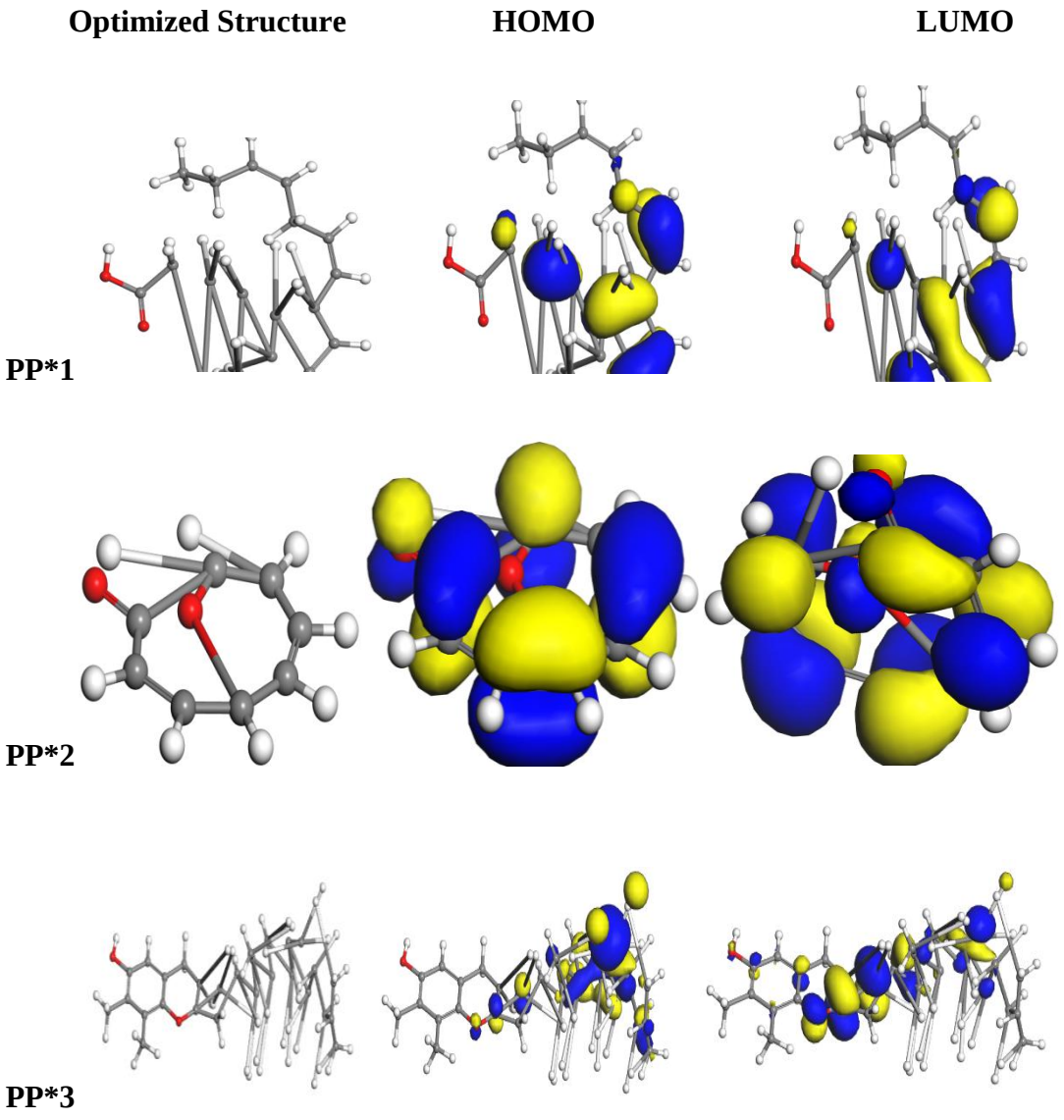


Fig. 4.84: HOMO – LUMO Orbital Diagram of some Constituents of *Parinari polyandra* Extract (atom legend: White = H; Light gray = C; Red = O; Blue = N)

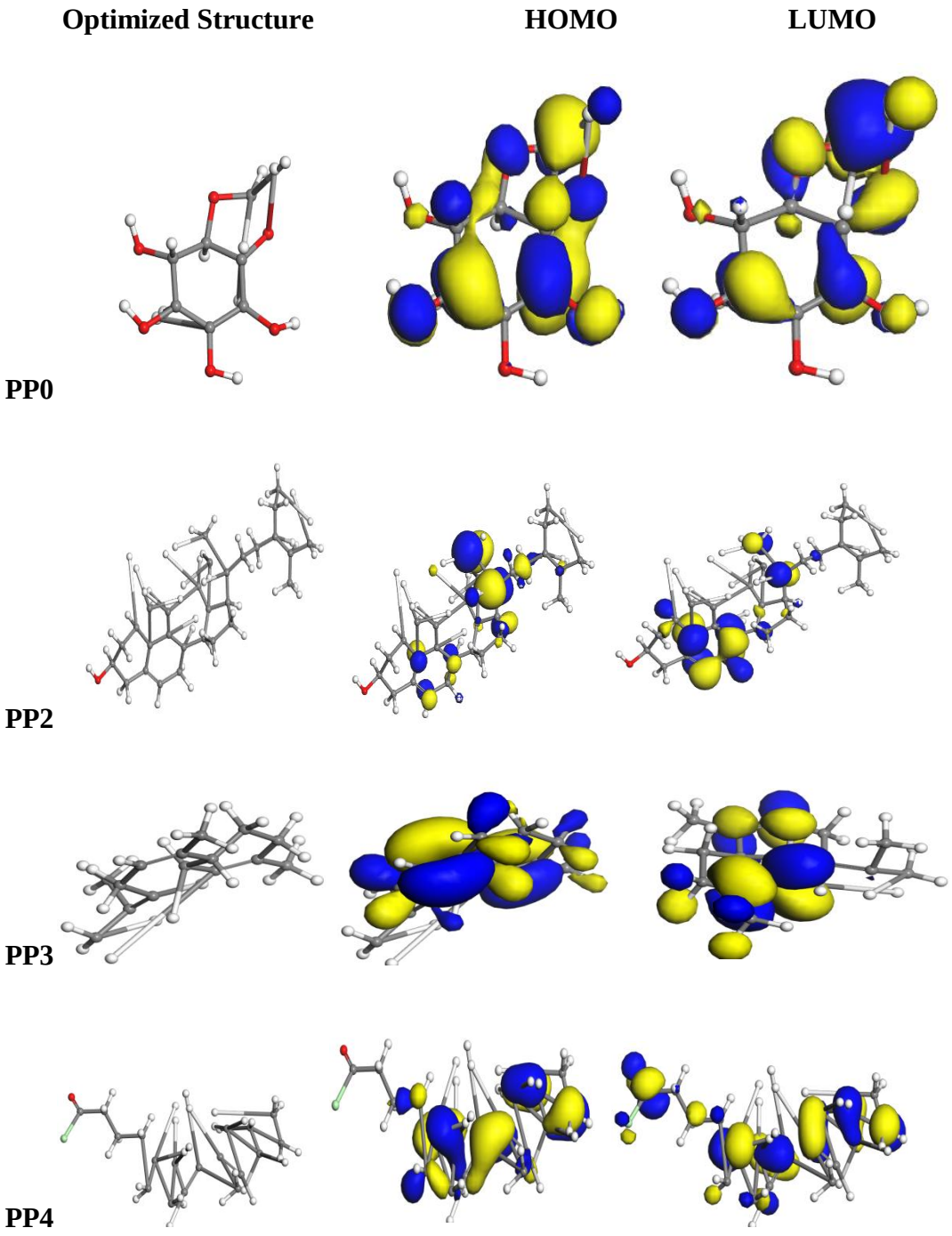


Fig. 4.85: HOMO – LUMO Orbital Diagram of some Constituents of *Paulina pinnata* Extract (atom legend: White = H; Light gray = C; Red = O; Blue = N)

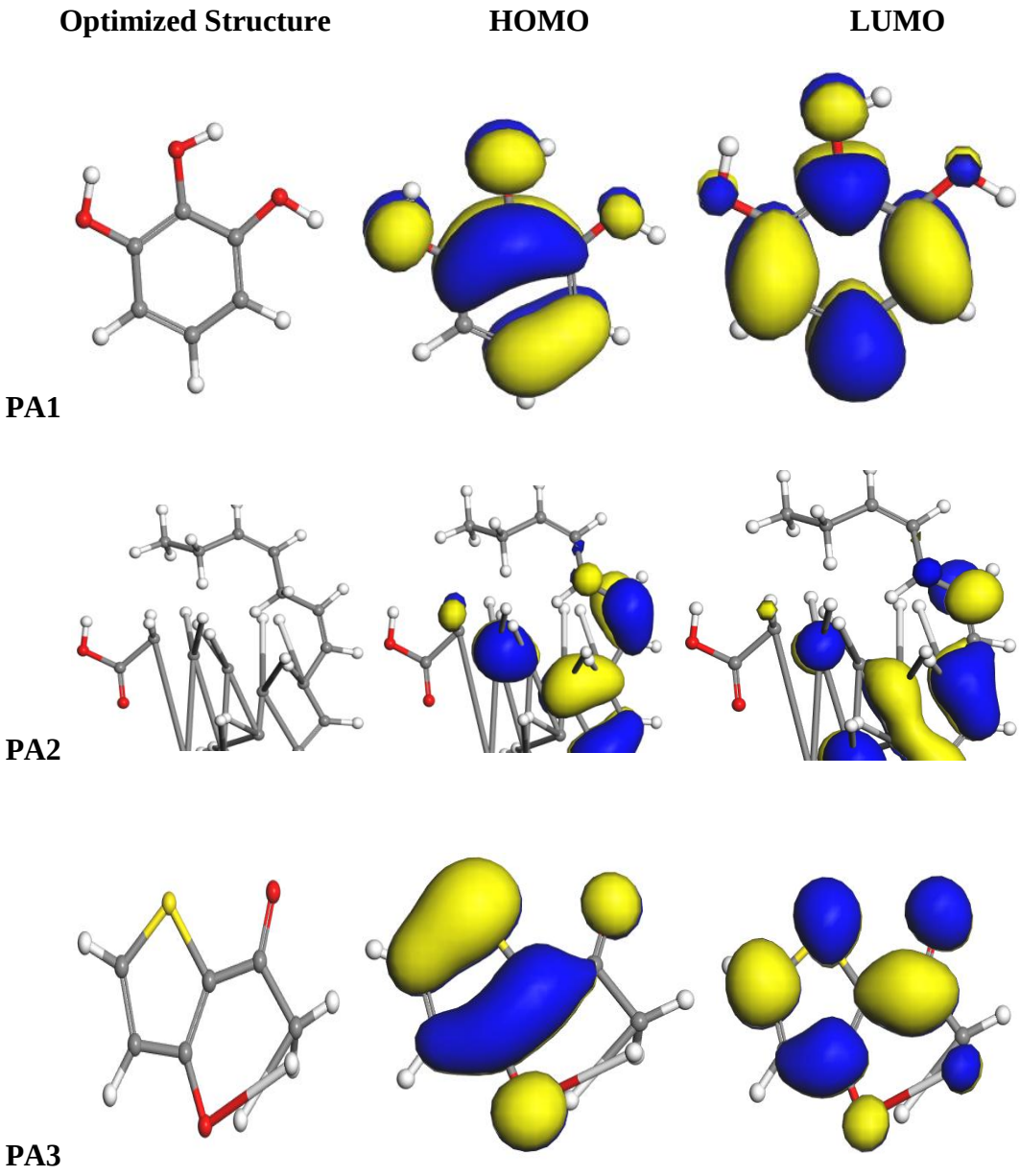


Fig. 4.86: HOMO – LUMO Orbital Diagram of some Constituents of *Phyllanthus amarus* Extract (atom legend: White = H; Light gray = C; Red = O; Blue = N)

Table. 4.17: Computed Quantum Chemical Parameters of the Studied Compound.

Molecule	E_{HOMO}(eV)	E_{LUMO}(eV)	ΔE(eV)
PA1	-0.1848	-0.0172	0.1676
PA2	-0.1812	-0.1095	0.0717
PA3	-0.2148	-0.0947	0.1201
BS1	-0.1218	-0.1128	0.009
BS2	-0.1848	-0.0172	0.1676
BS3	-0.1779	-0.0385	0.1394
BS4	-0.1915	-0.0323	0.1592
PP0	-0.1218	-0.1128	0.009
PP2	-0.1208	-0.1180	0.0028
PP3	-0.1901	-0.0104	0.1797
PP4	-0.1758	-0.0931	0.0827
PP*1	-0.1812	-0.1095	0.0717
PP*2	-0.1728	-0.0645	0.1083
PP*3	-0.1393	-0.1289	0.0104

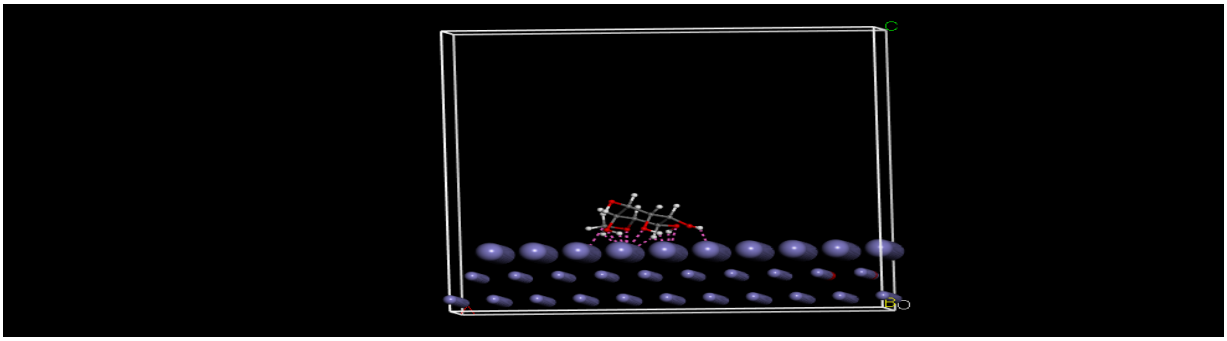
Table 4.18: Fukui Indices Calculated with DND.

Molecule	Nucleophilic (f^+)		Electrophilic (f^-)	
	Mulliken		**Mulliken**	
	Atom	Value	Atom	Value
PA1	C(6)	0.087	O(8)	0.109
PA2	C(6)	0.097	C(5)	0.099
PA3	S(5)	0.173	O(9)	0.179
BS1	C(4)	0.112	C(13)	0.107
BS2	C(6)	0.087	O(8)	0.109
BS3	H(11)	0.104	O(7)	0.118
BS4	C(4)	0.096	O(7)	0.135
PP0	C(4)	0.112	C(13)	0.107
PP2	C(34)	0.062	C(34)	0.061
PP3	C(3)	0.100	C(9)	0.084
PP4	O(1)	0.086	C(18)	0.073
PP*1	C(6)	0.097	C(5)	0.099
PP*2	C(2)	0.085	C(4)	0.104
PP*3	H(65)	0.079	H(65)	0.078

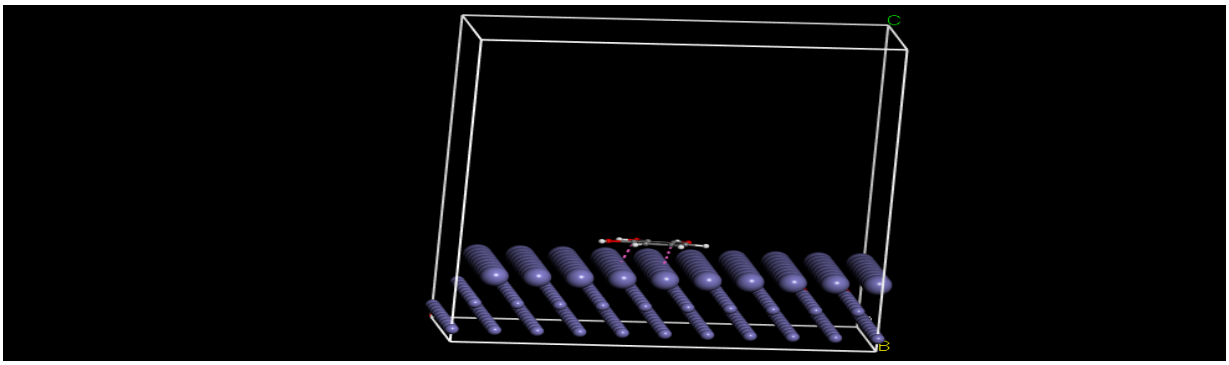
4.8.2 Molecular dynamics

Figures 4.87 – 4.94 show representative snapshots of the crosssection of the lowest energy adsorption configurations for the single molecules on Fe (110) and Al (110) surface respectively.

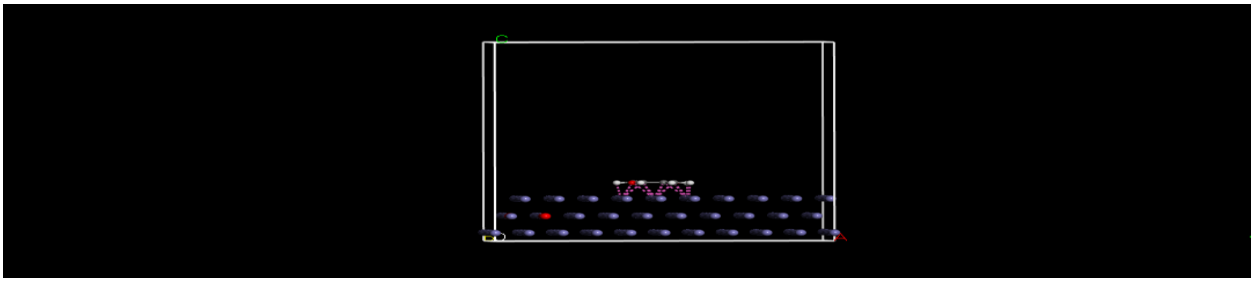
Table 4.19 presents the binding energy of mild steel and aluminium with the isolated compounds from each extracts. The results obtained were all negative signifying strong affinity.



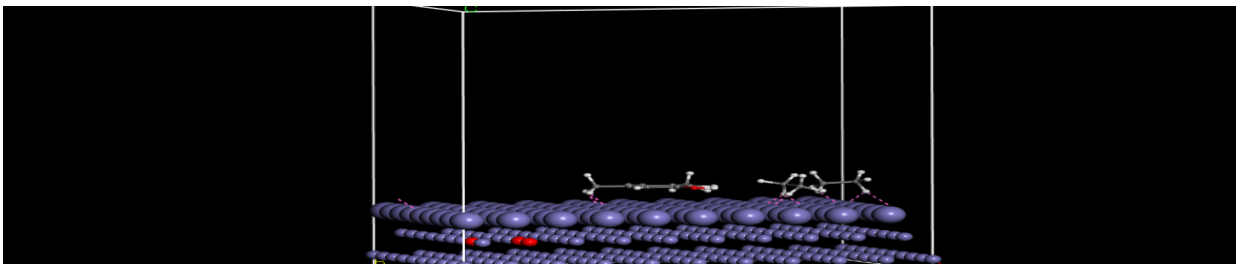
BS1 (Methyllinositol)



BS2 (1, 2, 3-Benzaetriol)

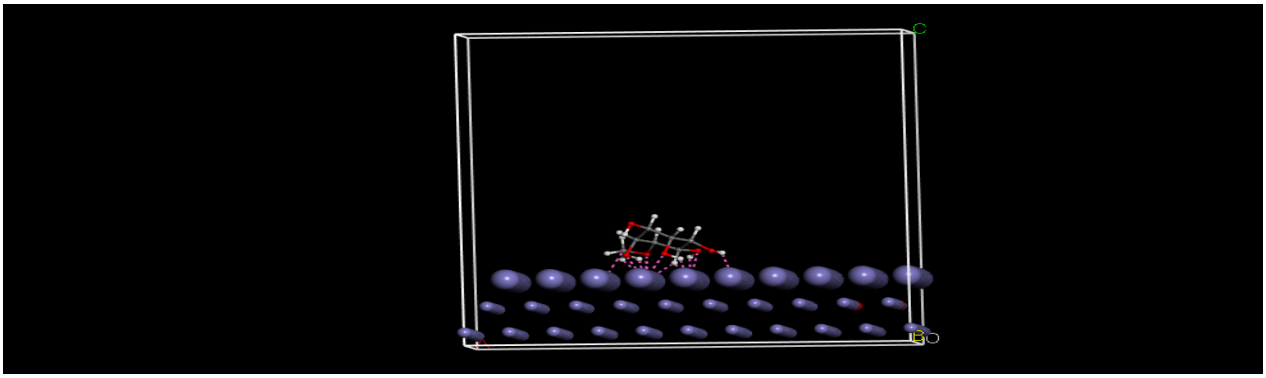


BS3 (Hydroquinone)

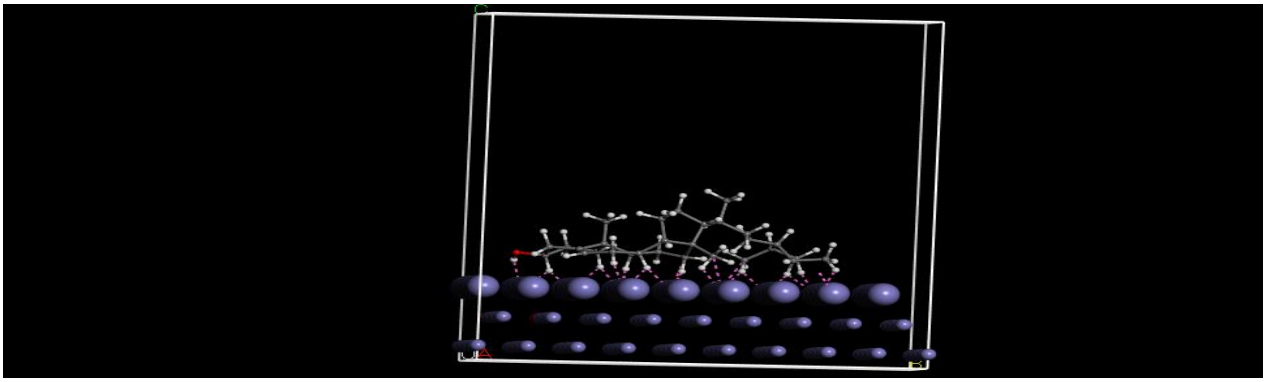


BS4 (3, 5-bis(1, 1-dimethylethyl)-phenol)

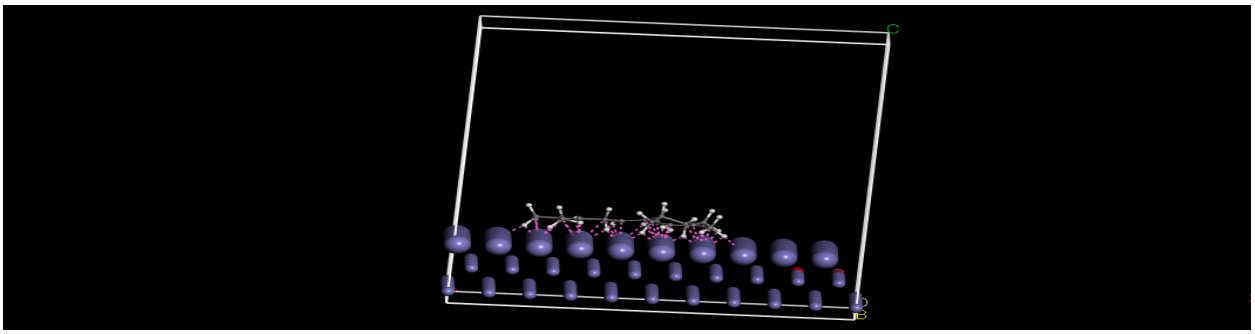
Fig. 4.87: Adsorption of Single Molecules of BS1, BS2, BS3 and BS4 on a Fe (110) Surface



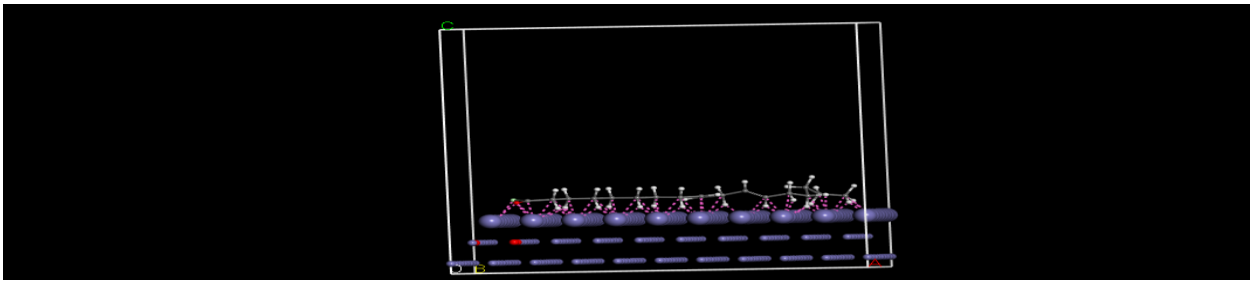
PP0 (Methyllinositol)



PP2 (β-sitosterol)

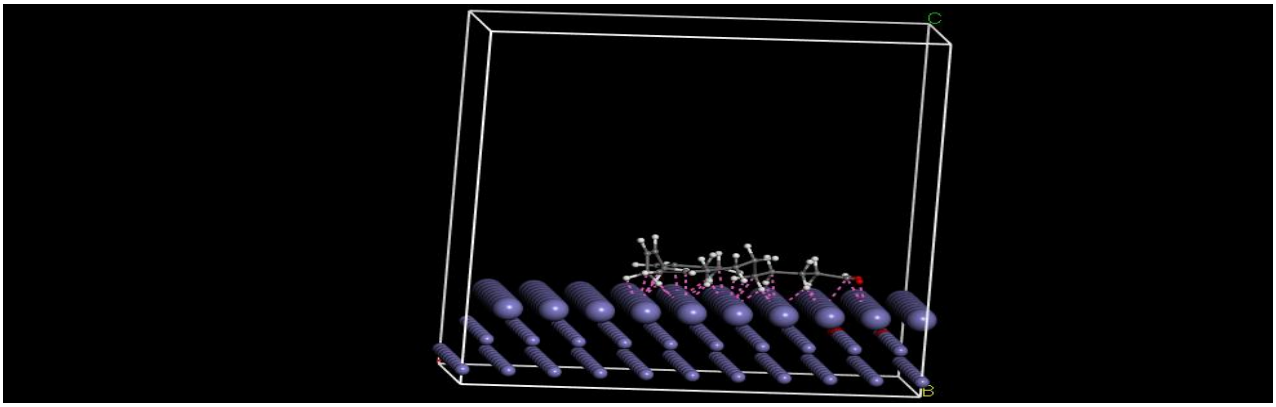


PP3 (Cis-alpha-bisabolene)

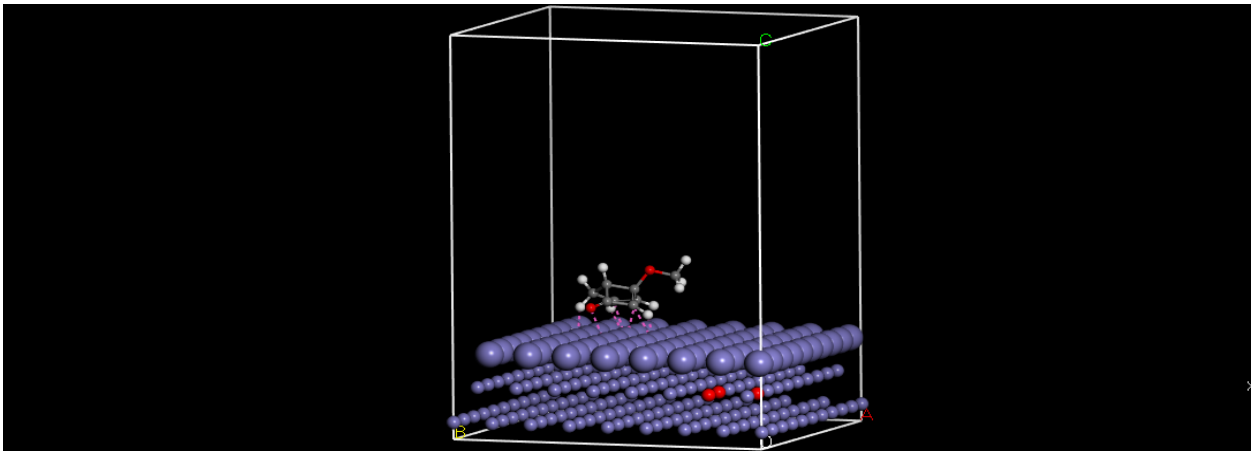


PP4 (Squalene)

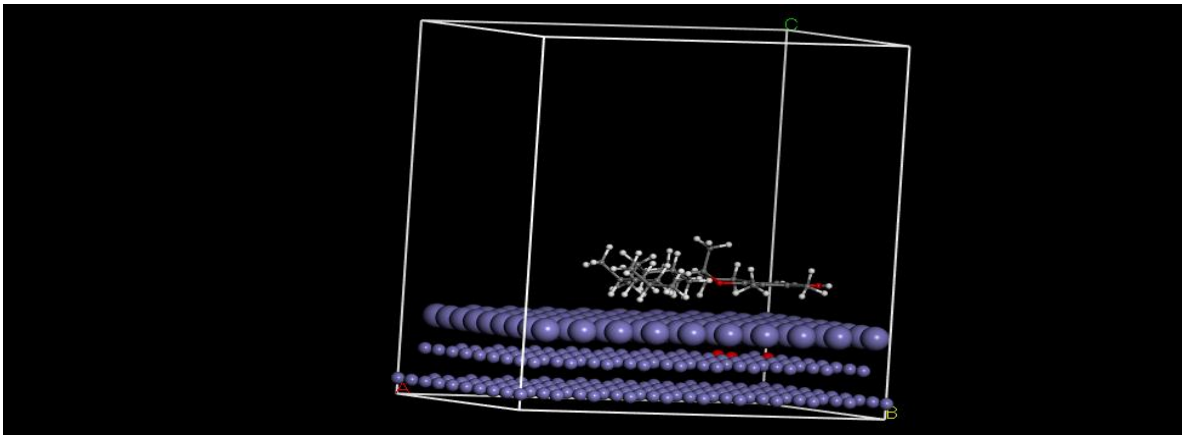
Fig. 4.88: Adsorption of Single Molecules of PP0, PP4, PP2 and PP3 on a Fe (110) Surface



PP*1 (linolenic acid)

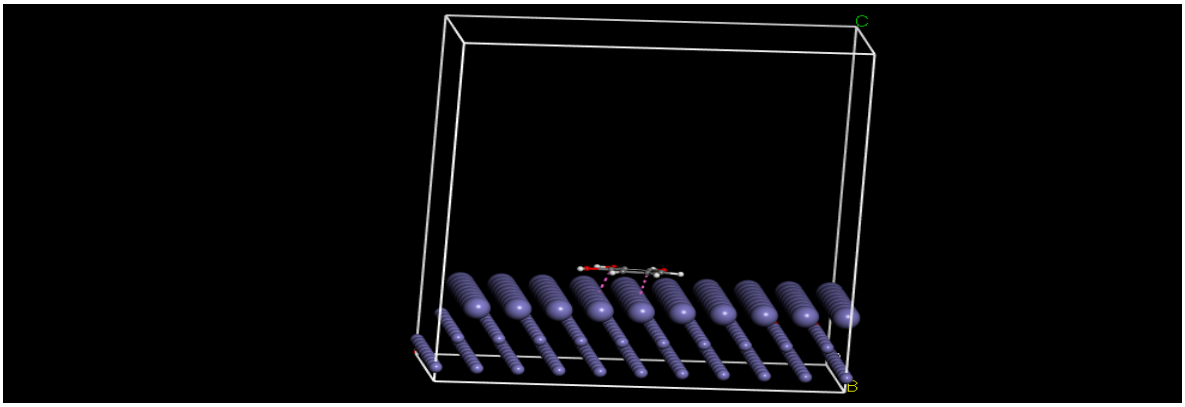


PP*2 (9-oxabicyclo[3,3,1]nona-3, 6-dien-2-one)

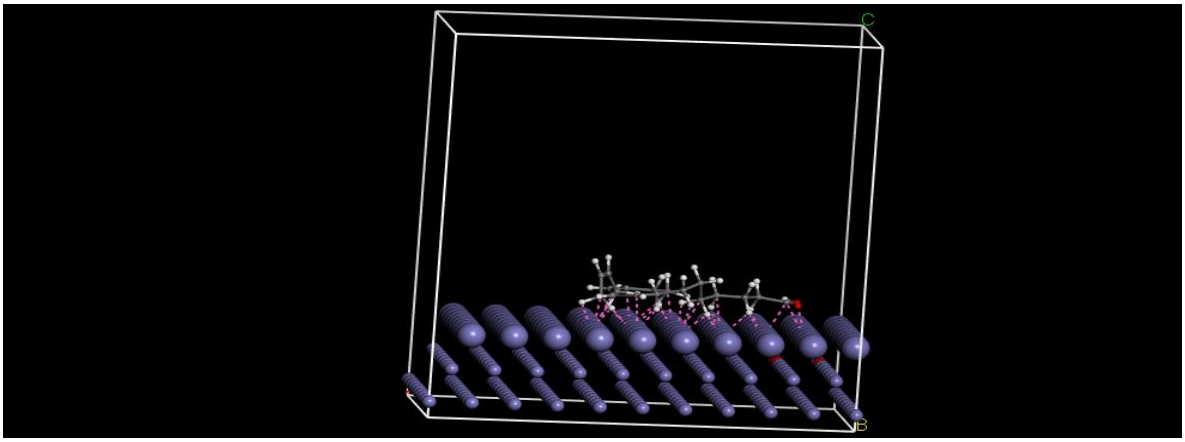


PP*3 (Gama Tocophenol)

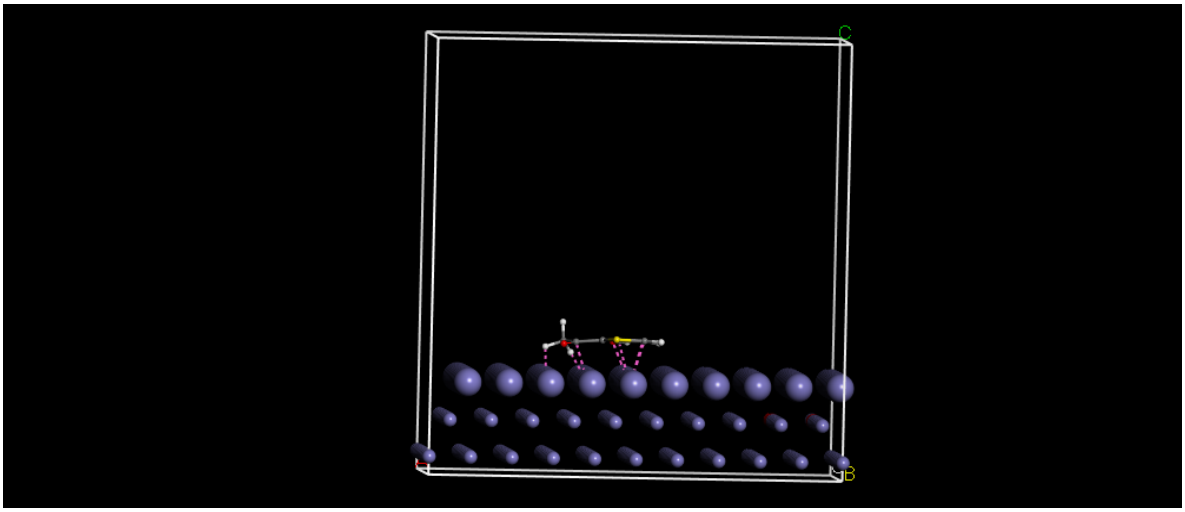
Fig. 4.89: Adsorption of Single Molecules of PP*1, PP*2 and PP*3 on a Fe (110) Surface



PA1 (1, 2, 3-benzaetriol)

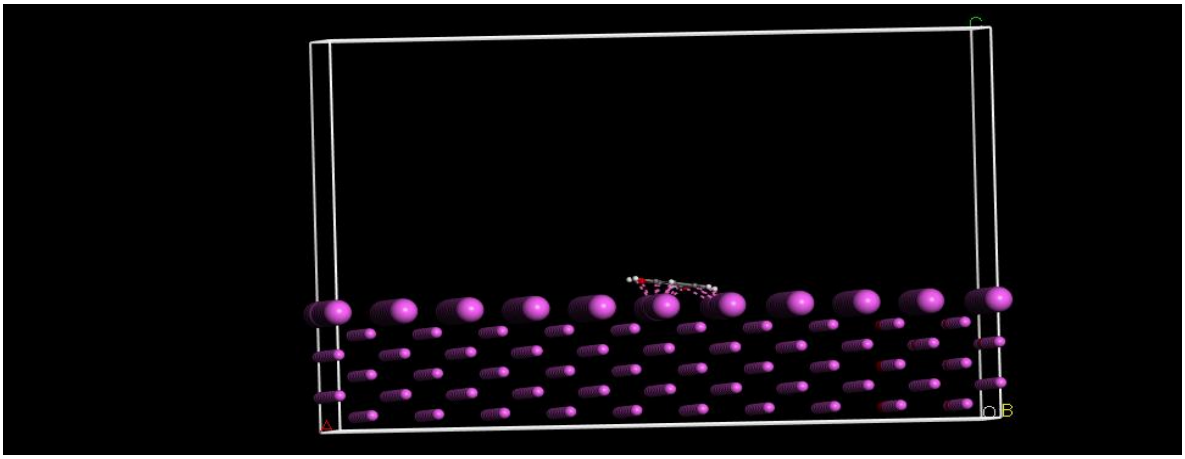


PA2 (linolenic acid)

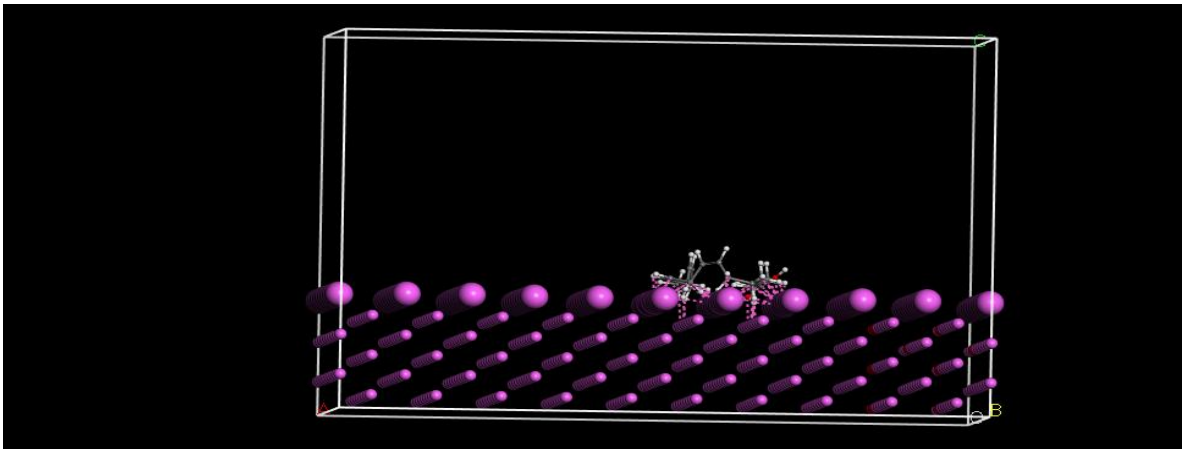


PA3 (ethanone)

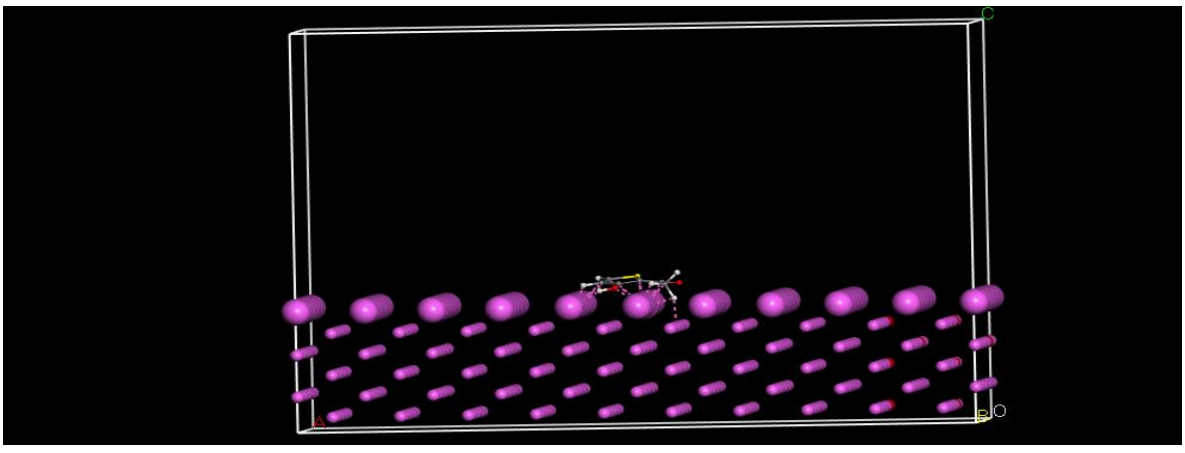
Fig. 4.90: Adsorption of Single Molecules of PA1, PA2 and PA3 on a Fe (110) Surface



PA1

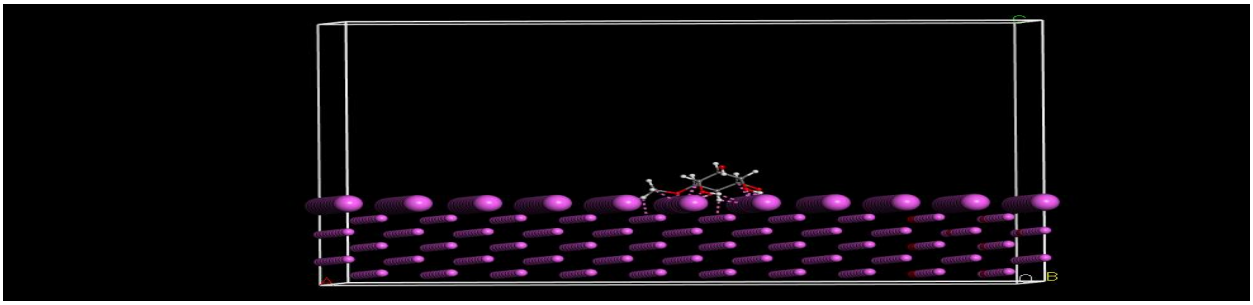


PA2

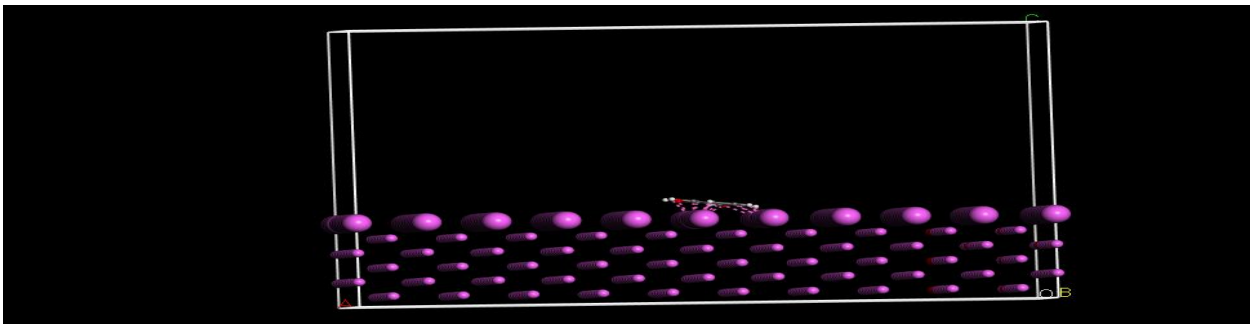


PA3

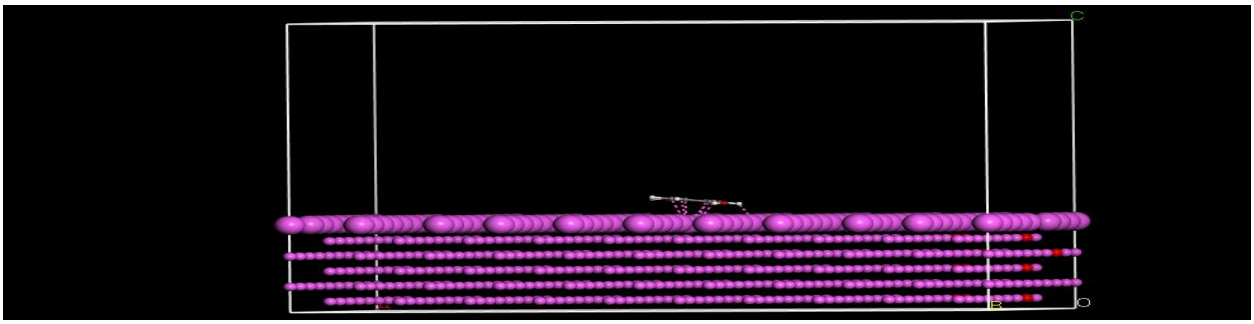
Fig. 4.91: Adsorption of Single Molecules of PA1, PA2 and PA3 on an Al (110) Surface



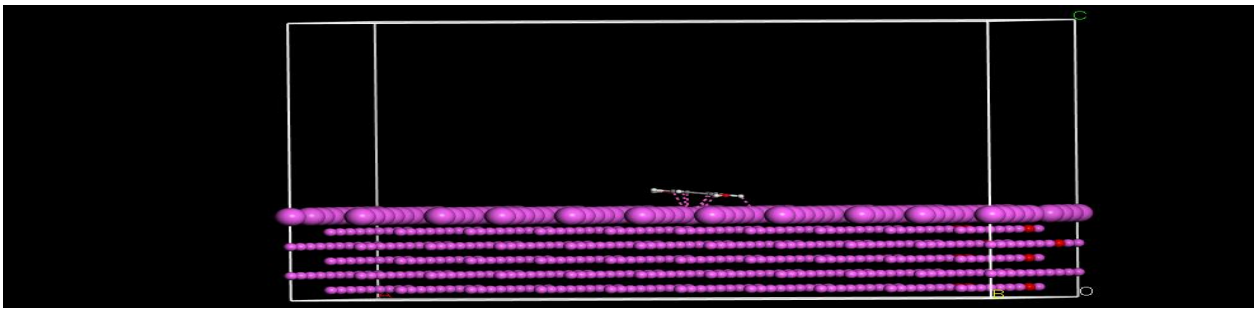
BS1



BS2



BS3

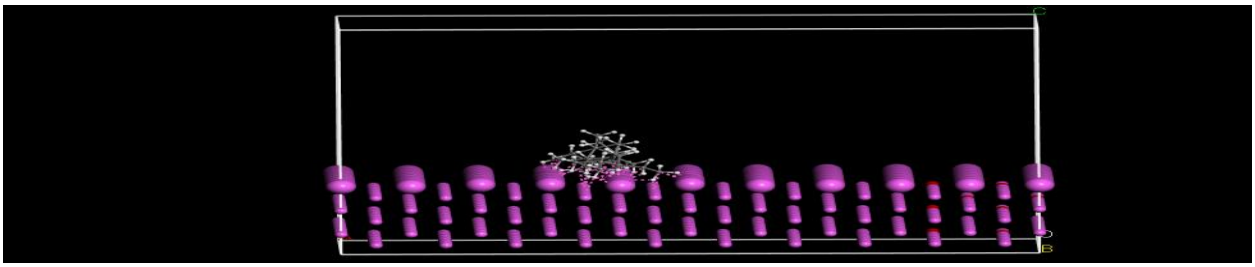


BS4

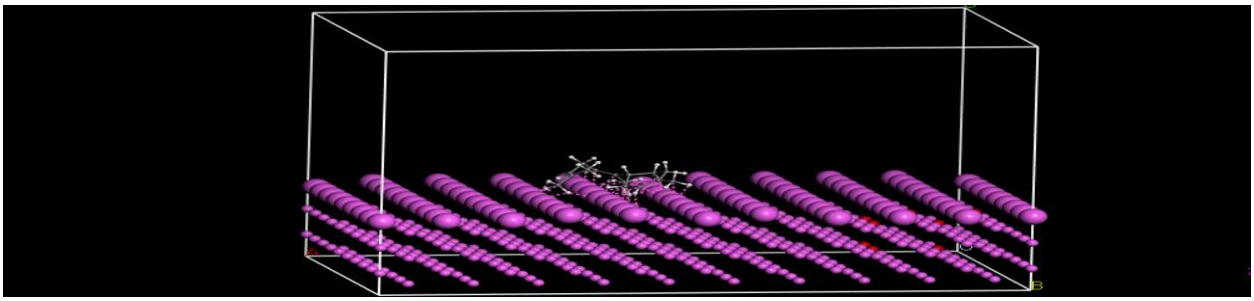
Fig. 4.92: Adsorption of Single Molecules of BS1, BS2, BS3 and BS4 on an Al (110) Surface



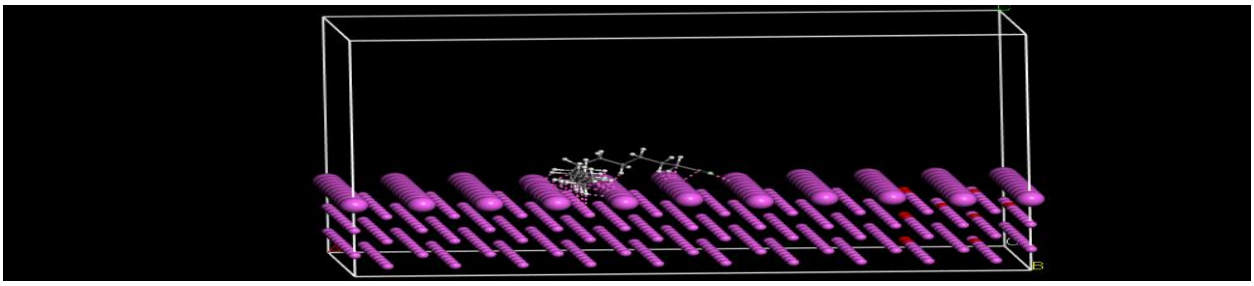
PP0



PP2

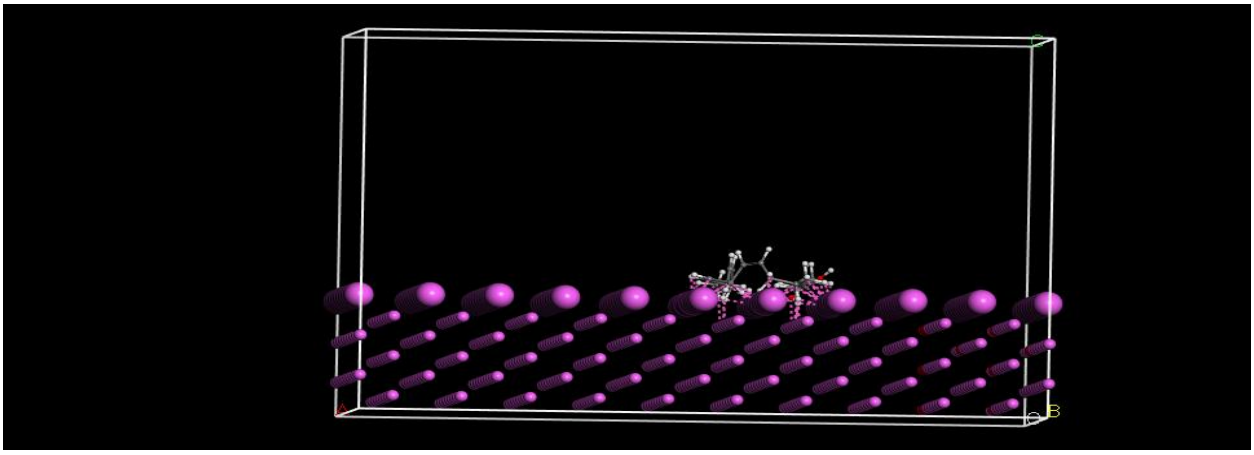


PP3

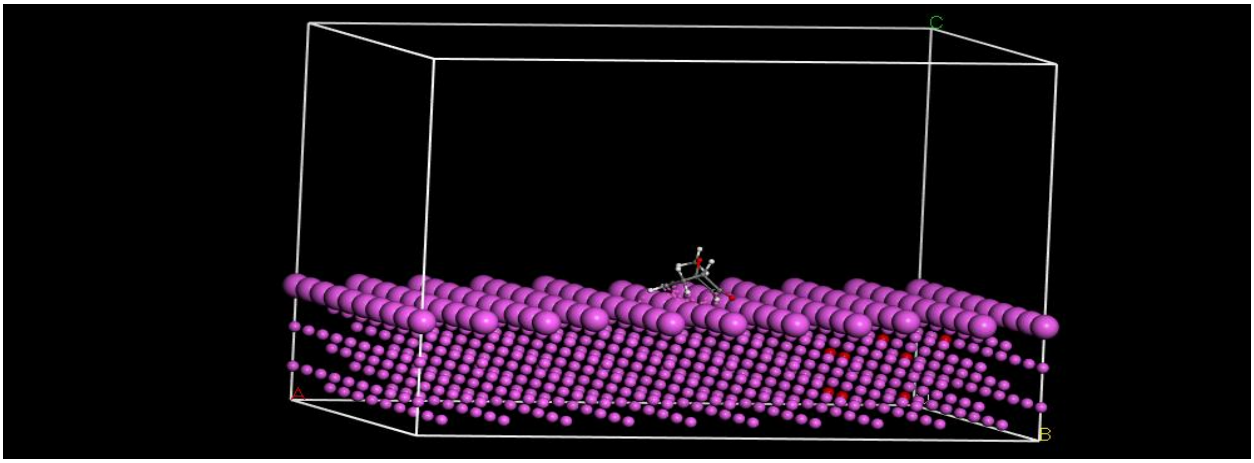


PP4

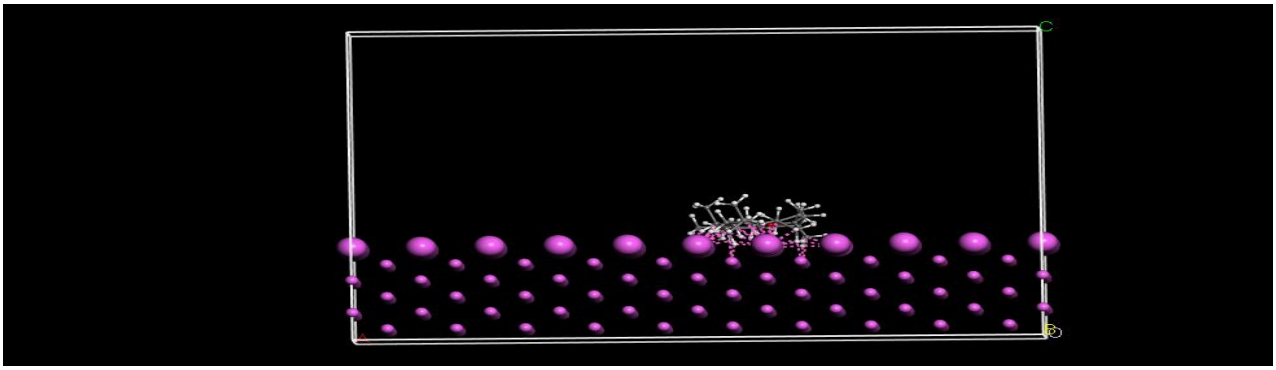
Fig. 4.93: Adsorption of Single Molecules of PP0, PP2, PP3 and PP4 on an Al (110) Surface



PP*1



PP*2



PP*3

Fig. 4.94: Adsorption of Single Molecules of PP*1, PP*2 and PP*3 on an Al (110) Surface

Table 4.19: Calculated Binding Energies of the Adsorption of Various Molecules of the Extracts using Forcite Quench Molecular Dynamics

Structures	Molecular Weight (g/mol)	Fe/Molecule Binding energy (kcal/mol)	(kJ/mol)	Al/Molecule Binding energy (kcal/mol)	(kJ/mol)
	126.11	-63.21	-264.65	-25.29	-105.88
	278.44	-169.56	-709.91	-77.11	-322.84
	142.17	-70.19	-293.87	-31.39	-131.42
	194.18	-79.70	-333.69	-35.86	-150.14
	414.72	-182.13	-762.54	-66.59	-278.80
	204	-136.74	-572.50	-52.12	-218.22
	298	-181.12	-758.31	-79.82	-334.19
	194.18	-79.70	-333.69	-35.86	-150.15
	126.11	-63.21	-264.65	-25.29	-105.88

	110	-57.79	-241.96	-24.90	-104.25
	186	-117.38	-491.45	-56.41	-236.18
	278.44	-169.56	-709.91	-77.11	-322.84
	416.69	-233.77	-978.75	-92.87	-388.83

CHAPTER FIVE

5.0 DISCUSSION

5.1 Gas Chromatography-Mass Spectra

The corrosion of mild steel and aluminium in HCl and H_2SO_4 solution containing the extracts are inhibited due to the adsorption of phytochemicals present in the extracts through their lone pair of electrons and π-electrons with the *d*-orbitals on the mild steel surface (Eddy *et al*., 2009 and Oguzie, 2008). The functional groups with S, O or N and π-electrons of the organic compounds are usually regarded as the reaction center for the establishment of the adsorption process. Gas chromatography–mass spectrometry (GC–MS) as presented in Tables 4.2 – 4.5, show the analysis of the extracts that led to the identification of thirteen components from all the extracts with close similarity to well known and established corrosion inhibitors. It is interesting to see here that all the identified compounds from plant extracts contained oxygen and/or π-electrons in their molecules. Moreover, from previous studies on the phytochemical constituents of the extracts it was established that the extracts used in this study also contain a mixture of organic compounds with O, N or π-electrons in their molecules. Also some compounds have been reported from the extracts of *Paullinia pinnata* such as: methyllinositol, β- sitosterol and Friedelin (Zafel *et al*., 2007; Gupta *et al*., 2011; Klass *et al*., 1992; and Mahato and Kundu, 1994). Hence, the corrosion inhibition of mild steel and aluminium through the extracts may be attributed to the adsorption of the phytochemical containing O, N or π-electrons in their molecules as these atoms are regarded as centers of adsorption onto the metal surface.

However, the highly complex chemical compositions of the extracts make it rather difficult to assign the inhibitive effect to a particular compound present in the extracts.

5.2 Corrosion Studies

5.2.1 Effect of concentration of extracts on the corrosion of mild steel and aluminium

From the plots shown in (Figures 4.1 - 4.12) it can be seen that the weight loss of mild steel and aluminium decreases with increase in the concentration of the plant extracts but increases with increasing period of contact. This indicates that the corrosion rate of mild steel and aluminium in HCl and H_2SO_4 solutions increased with increase in period of contact but decreased with increase in concentration of the extracts. It is also observed that the corrosion rate of aluminium in HCl was higher than that obtained in the presence of H_2SO_4. The observed difference in this behavior of mild steel and aluminium in different acid media is as a result of the relative positions of the metals in the electrochemical series. The electrochemical series provide a guide on the corrosion resistance of specific metals and its alloys. Since aluminium is has a more negative potential than mild steel, it should corrode more readily than mild steel. This may be responsible for the higher corrosion rate for aluminium compared to those of mild steel in HCl solutions as observed in Tables 4.6 and 4.8. The metals in H_2SO_4 have higher corrosion rate because of it corrosive nature as compare to HCl.

Aluminium has been reported to have high resistance to corrosion due to the formation of oxide film on the surface which usually protects it in air or neutral solutions (Eddy *et al*., 2015). On immersion in alkaline and acidic media, this film is preserved for long periods of time (Pourbaix, 1974). The potentials of zero charge for aluminium oxide

occurs from pH 9.0 to 9.1 chloride or any aggressive anion is likely to be adsorbed at pH values < 9.0 (Cabot *et al*., 1991; Emregul, 2006). This lead to localization of the corrosion attack by preferential adsorption at weak sites on the passive film. The lower corrosion rate observed in H_2SO_4 solutions is an indication that these media do not completely dissolve the passive oxide film on the aluminium surface, to prevent the corrosion process.

Basically, solubility of the corrosion products is another factor which is responsible for the different behaviours of mild steel and aluminium in these two acid media. A soluble corrosion product signifies more dissolution of the metal in the acid medium resulting in higher corrosion rates and lower inhibition efficiency.

As shown in Figures 4.1 - 4.12 and Tables 4.6 - 4.9, the results obtain indicate that the corrosion rate of mild steel and aluminium decreases with increase in the concentration of the extracts while the inhibition efficiency increases with increasing concentration of the extract. The results indicate that the extracts are adsorbed on aluminium and mild steel in both acid media except at higher temperature where the inhibitor act as catalyst in aluminium in H_2SO_4. The inhibition efficiency of an adsorption inhibitor tends to increase with increase in the concentration of the inhibitor (Eddy *et al*., 2010; Oguzie, 2008 and Lashgari *et al*., 2010). The inhibition efficiencies of the investigated extracts decreased with an increase in temperature indicating that the adsorption of the extracts supports the mechanism of physical adsorption. In physical adsorption mechanism, the inhibition efficiency is expected to decrease with increasing temperature but for a chemical adsorption mechanism, the inhibition efficiency increases with increasing temperature (Eddy and Mamza, 2009; Ihebrodike *et al*., 2012)

As presented in Tables 4.6 - 4.9 it is evident that both aluminium and mild steel can retained more than 46% degree of surface covered, the plot of the weight loss from various inhibitors also shows that after 168 hours of immersion, PP can retain more than 60% of its inhibition potentials while the other inhibitors (PA, BS and PP1) can retain more than 40% of their respective inhibition potentials in mild steel. It is observed that the inhibition efficiency first decreased with time until a critical value of 62% was attained after which it started to decrease. These trends suggest that at first, there was equilibrium between the adsorption and desorption processes and after the critical zone, adsorption facilitated the formation of a protective layer and thus protected the metals against further corrosion attack. In general, the chemical stability of a metal exposed to a solution is a function of the potential of the metal with respect to the pH of the solution. This is also explains in the difference in weight losses hence corrosion rates of mild steel and aluminium in the acid media. The IE% of the extracts in both acidic media increase with increase in concentrations in the following order PP > BS > PP1> PA. While in the case of aluminium, the IE% increased with concentrations of the extracts in the order PP >PP1 > BS > PA although negative inhibition efficiencies were obtained at higher temperature in H_2SO_4.

Chen *et al.* (2000), reported negative inhibition efficiencies in the application of immidazole at high temperature/pressure corrosion inhibition of mild steel in brine. It was also reported that negative inhibition efficiency were obtained for 0.01M sodium nitrite as corrosion inhibitor for concrete in marine environment. Higher inhibition efficiencies signify higher degree of surface coverage on the metal surface as well as better stability of the corrosion products formed. The driving force for the corrosion of a metal is the

thermodynamic instability of the metal in its surrounding environment. A metal tend to corrode faster when its dissolution potential is negative. In the absence of any additive, the oxidation of the metal is the primary anodic reaction. The fact that some of the inhibitor at higher temperature in H_2SO_4 for aluminium, function as catalysts with negative inhibition efficiencies could implies that their corrosion products were not thermodynamically stable leading to their solubilities and formation of species that actually enhanced the anodic oxidation or dissolution of the aluminium electrode instead of inhibiting it.

5.2.2 Effect of temperature

The effect of temperature on the corrosion of aluminium and mild steel in the absence and presence of various concentrations of plant extracts was investigated using the Arrhenius transition state equations. From Figures 4.13 – 4.20, it shows that the presence of inhibitor increases the activation energy of the system, thereby increasing the adsorption affinity of inhibitor-metal and difficult for desorption to take place (Oguzie *et al*., 2012c).

The chemically stable surface - active inhibitors increase the energy of activation and decrease the surface area available for corrosion. From Tables 4.10 - 4.12, it is seen that the value of activation energy (E_a) for the corrosion of the metals in the acid solutions in the presence of the inhibitor are higher than that in the absence of the inhibitor. Also, the extent of increase in E_a is proportional to the inhibitor concentration, indicating that the energy barrier for the corrosion reaction increases with the increase in the concentration of inhibitor. The increase in E_a may be considered to be due to the physical adsorption of the inhibitor, which results in the increase in surface coverage with increase in the concentration of the inhibitor. The values at different temperatures also indicate that the

inhibition efficiency decreases with the increase in temperature. This may be due to the decrease in the adsorption of the inhibitor on the metal surface as the temperature increases and a corresponding increase in corrosion rate due to the greater area of metal being exposed to the acid (Eddy *et al*., 2010; Oguzie *et al*., 2012b; Ihebrodike *et al*., 2012). The mechanism of physical adsorption is favoured, if values of E_a is less than 80kJmol^{-1} as distinct from the mechanism of chemical adsorption where E_a values are expected to be greater than 80kJmol^{-1} (Eddy *et al*., 2010; and Ihebrodike *et al*., 2012). The adsorption of the extracts on metal surfaces is consistent with the mechanism of charge transfer from the inhibitors' molecule to the metal surface, which represents physiosorption.

The effect of temperature on the inhibition of any metal by inhibitors is highly a complex system, because many changes may occur on the metal surface including etching, desorption of the inhibitor, and the inhibitor may undergo decomposition and/or rearrangement (Obot *et al*., 2012, 2009b; Oguzie *et al*., 2012c).

It is evident from Tables 4.6 - 4.9 that the corrosion rate in the acid solutions and in the presence of the inhibitors increased as the temperature of the system increased from 303K to 333K. All the inhibitors maintained their inhibiting effects at all temperatures in the acid media for mild steel systems except for aluminium system which at higher temperature, the inhibitors function as catalyst in H_2SO_4. The corrosion rate were found to be highest at the highest temperature, these is because a rise in temperature exponentially accelerates the rates of corrosion processes in the media where hydrogen gas evolution accompanies corrosion process, resulting in higher dissolution rates of the metals. Higher rates of hydrogen evolution increasingly agitate the metal/corrodent interface and could hinder inhibitor adsorption or perturb the inhibitor which has been adsorbed on the surface

of the metal, especially when interaction between the metal and the inhibitor is relatively very weak (Oguzie, 2012a, b). As a result, the efficiency of considerable number of inhibitors is significantly reduced when the temperature of the system is increased; this trend is often attributed to physical adsorption rather than chemical adsorption of the inhibiting species on the corroding metal surface (Eddy *et al*., 2010; Oguzie *et al.*, 2012c; Adejor *et al.*, 2012).

As shown in Figures 4.21 - 4.28 the Arrhenius transition plots for the corrosion of aluminium and mild steel in HCl and H_2SO_4 containing inhibitor. It is seen that adsorption of the inhibitor is more enhanced as the concentration of inhibitor increases. The activation parameters presented in Table 4.13 and 4.14, the enthalpies of activation of the corrosion process are positive which reflect endothermic nature of dissolution process. Moreover, the average difference value of (E_a - ΔH_a) is 2.636 which is approximately equal to the average value of RT (2.6438). Therefore, it is indicated that the corrosion process is a unimolecular reaction (Dahmani *et al*., 2010 and Lebrini *et al*., 2011).

The entropy of activation in the presence and absence of the inhibitor also has negative values which indicates that the activated complex in the rate-determining-step represents an association rather than dissociation, implying that a decrease in disordering took place on going from the reactant to the activated complex (Lebrini *et al*., 2010).

5.2.3 Thermodynamic or adsorption study

In a reaction process, assuming a direct relationship between the inhibition efficiency and the degree of surface coverage at different concentrations of inhibitor, data obtained from weight loss studies are used to determine the fit to some well-known

adsorption isotherms which include the Langmuir, Freundlich, Temkim, Flory-Huggins, and the kinetic-thermodynamic model (El-Awardy *et al*., 1992). The generalized form of the adsorption isotherms is of the form given in equation 5.1. (El-Awady *et al*., 1992; Oguzie *et al*., 2012b).

$$f(\theta, x)\exp(-\alpha\theta) = kC \qquad 5.1$$

where f(θ, x) is the configuration factor, which is dependent on the physical model adopted and the assumptions made to derive the isotherms, x is the size ratio which represents the relative size of the adsorbed molecule to the solvent molecule, α is the molecular interaction parameter which accounts for the lateral interaction between the adsorbed species (Shibli and Saji, 2005), C is the inhibitor concentration and k is the adsorption equilibrium constant. As shown in Figures 4.29 - 4.52 for the various adsorption isotherms. Basically, organic corrosion inhibitors are known to decrease metal dissolution via adsorption on the metal / corrodent interface to form a protective film which separates the metal surface from the corrosive medium. The adsorption route is usually regarded as a substitution process between the organic inhibitor in the aqueous solution ($Inh_{(sol)}$) and water molecules adsorbed at the metal surface ($H_2O_{(ads)}$) as follows (Oguzie *et al*., 2007; and Ameer *et al*., 2002).

$$Inh_{soln} + \square H_2O_{ads} \rightleftharpoons Inh_{ads} + \square H_2O_{soln} \qquad 5.2$$

where □ represents the number of water molecules replaced by one molecule of adsorbed inhibitor. The adsorption bond strength is dependent on the composition of the metal and corrodent, inhibitors components, concentration as well as temperature. By considering of some of these variables useful information regarding the adsorption mechanism are established. Although the complex nature of the corrosion inhibition process is not in

doubt, basic information on the interaction between the inhibitor and the metal surface can be provided by the adsorption isotherm. It is observed that the calculated values of the adsorption equilibrium constants k_{ads} were very high expecially for the temkim adsorption isotherm, which indicates a high adsorption ability of the extracts on both the aluminium and mild steel at the various temperatures.

From the results obtained from various plots, the free energies are found to be negatively less than the threshold value of -40kJmol^{-1}, required for the mechanism of chemical adsorption to take place. Therefore, the adsorption of the investigated extracts on both aluminium and mild steel surface is spontaneous and is consistent with the mechanism of physical adsorption (Eddy *et al*., 2015 and Oguzie *et al*., 2012c).

For corrosion inhibition studies, a large number of experimental adsorption data has been reported supporting Langmuir isotherm (i.e. R^2 close to unity). Similar linear fit were obtained for the extracts on aluminium at the various temperatures, whereas, the mild steel were found to be linearly fit at the various temperature for Freundlich adsorption isotherm. However, the linear fit is expected to intercept either the y-axis or the x-axis and the slope close to unity; however a contrary output of isotherm prediction was obtained. Similar results have been reported by Döner *et al*. (2011). This anomaly may be attributed to interactions between the adsorbate species on the metal surface as well as changes in the heat of adsorption with increasing surface coverage, e.g. factor that might not have been taken into consideration in the isotherm. Basically a number of modifications to the Langmuir isotherm have been proposed which included the interaction term (Villamil *et al*., 1999). Nevertheless, the possibility of adapting the isotherm for physical or chemical adsorption may account for its widespread applicability.

Adsorption of uncharged molecules on any heterogeneous surface is approximately described by the Temkim adsorption isotherm by ($\theta = 1/f \ln k_{ads}C$), where θ represent the linear function of lnC (Fuchs-Godec and Zerjav, 2009). The term contain a correction factor ($f=-2\alpha$) which clearly takes into consideration the interaction between the adsorbate – adsorbent molecule. This makes the isotherm quite suitable for systems where chemical interaction of inhibiting species with the metal surface is more pronounced for the extracts on mild steel surface in H_2SO_4 at a higher temperature. Whereas all the tested isotherms quantitatively describe the result obtained from experiment. Langmuir, Freundlich and Temkim isotherms provided the exact interpretation from the regression coefficient, the free energy and the k_{ads} data.

5.3 Infrared Spectroscopic Study

From Figures 4.71 - 4.82 and Appendices VI - XIV, it can be observed that most of the peaks for the extracts were also noticed in the surface films of the inhibitors on the metal surface, suggesting that most of the functional groups within the extracts are also present in the surface film. This further confirms the fact that the extracts were actually adsorbed on the metal surfaces. Moreover, some of the peaks for the adsorbed film diminished or even vanished indicating that the functional groups responsible for these adsorption could have been used for the formation of inhibitor-metal complex which further protected the metal from corrosion. Figures 4.71, 4.75 and 4.79 show the IR spectrum of the corrosion products of mild steel and aluminium in absence of inhibitors. From the spectrum, it can be seen that the corrosion products without the inhibitor are not IR active. Therefore there was no adsorption.

As shown in Figure 4.72(a-b) for the corrosion product of mild steel when BS was used as an inhibitor. The results showed that, the aromatic stretch at 808cm^{-1} shifted to 800cm^{-1}, C-O stretch at 1065cm^{-1} shifted to 1180cm^{-1}, C-C stretch in ring at 1443cm^{-1} shifted to 1428cm^{-1}, N-H bend at 1628cm^{-1} shifted to 1624cm^{-1} and O-H stretch at 2931cm^{-1} and 3423cm^{-1} were shifted to 2527cm^{-1} and 3405cm^{-1}. The shift in the frequencies indicates that there is interaction between the mild steel and the inhibitor (Eddy *et al*., 2010). On the other hand, C-N stretch at 1265cm^{-1} and C=O stretch at 1705cm^{-1} were missing suggesting that these bond were used for adsorption of the inhibitor onto the surface of the mild steel.

Examination of the IR spectrum of PA and that of the corrosion product as shown in Figure 4.73(a-b) show that =C-H bend in an alkene at 759cm^{-1} was shifted to 854cm^{-1}, C-O stretch at 1050cm^{-1} and 1210cm^{-1} were shifted to 1092cm^{-1} and 1209cm^{-1} , C-C stretch in ring at 1442cm^{-1} was shifted to 1443cm^{-1}, N-H bend at 1616cm^{-1} was shifted to 1614cm^{-1} and O-H stretch at 3416cm^{-1} was shifted to 3405cm^{-1}. This shift in frequencies indicates that there is interaction between the mild steel and the inhibitor (Eddy *et al*., 2010). Also, C=O stretch at 1722cm^{-1} and O-H stretch at 2935cm^{-1} were missing suggesting that these bond were used for adsorption of the inhibitor onto the surface of the mild steel.

The FTIR spectrum of PP and that of the corrosion product of mild steel as shown in Figure 4.74(a-b) indicated that some peaks were shifted. From the results obtained, the Aromatic stretch at 824cm^{-1} was shifted to 841cm^{-1}, C-O stretch at 1078cm^{-1} was shifted to 1034cm^{-1}, C-N stretch at 1287cm^{-1} was shifted to 1264cm^{-1}, N-H bend at 1621cm^{-1} was shifted to 1606cm^{-1} and O-H stretch at 3427cm^{-1} was shifted to 3405cm^{-1}. Functional groups that were absent in the spectra of the corrosion products in the presence of the inhibitor suggest that they might have been used for adsorption on the metal surface. The shift in the frequencies indicates

that there is interaction between the mild steel and the inhibitor (Eddy *et al*., 2010). Also new bond was formed at 1454cm^{-1} indicating chemical interaction, a character official to chemisorptions (Oguzie *et al*., 2012c; Obot *et al*, 2009a, 2009b).

As presented in the spectra of BS and that of the corrosion product in aluminium Figure 4.76(a-b). From the results obtained, there were shift in adsorption peaks of some functional groups indicating that there is interaction between the metal surface and the inhibitor (Eddy *et al*., 2010). On the other hand, C-N stretch at 1265cm^{-1},Aromatic C-H stretch at 808cm^{-1}, C-C stretch at 1443cm^{-1} and C=O stretch at 1705cm^{-1} were missing suggesting that these bond were used for adsorption of the inhibitor onto the surface of the metal.

The FTIR spectrum of PA and that of the corrosion product in aluminium as shown in Figure 4.77(a-b). From the results, =C-H bend in an alkene at 759cm^{-1} shifted to 790cm^{-1}, C-O stretch at 1050cm^{-1} was shifted to 1115cm^{-1}, N-H bend at 1616cm^{-1} was shifted to 1642cm^{-1} and O-H stretch at 3416cm^{-1} shifted to 3430cm^{-1} (Eddy *et al*., 2010). The missing functional groups include C-O stretch at 1210cm^{-1}, C-C stretch in ring at 1442cm^{-1}, O-H stretch at 2935cm^{-1} and C=O stretch at 1722cm^{-1} which suggest that these bond were used for adsorption of the inhibitor onto the surface of the metal.

For PP, examination of the spectra of its powder with the corrosion product in the presence of aluminium Figure 4.78(a-b) show that, aromatic C-H at 824cm^{-1} shifted to 806cm^{-1}, C-N stretch at 1287cm^{-1} was shifted to 1138cm^{-1}, N-H bend at 1621cm^{-1} was shifted to 1642cm^{-1} and O-H stretch at 3427cm^{-1} shifted to 3422cm^{-1}. The shift in the frequencies indicates that there is interaction between the metal and the inhibitor. There was indication of

C-O stretch at 1078cm^{-1} functional group missing suggesting that the bond was used for adsorption of the inhibitor onto the metal surface (Eddy *et al*., 2010).

Spectra of BS as shown in Figure 4.80a, and that of the corrosion product Figure 4.80b. From the results obtained, Aromatic C-H at 808cm^{-1} shifted to 868cm^{-1}, C-O stretch at 1066cm^{-1} was shifted to 1111cm^{-1}, C-C stretch in ring at 1443cm^{-1} was shifted to 1427cm^{-1} and O-H stretch at 3423cm^{-1} shifted to 3492cm^{-1}. The shift in the frequencies indicates that there is interaction between the aluminium and the inhibitor (Eddy *et al*., 2010). Furthermore, C-N stretch at 1265cm^{-1}, N-H stretch at 1628cm^{-1}, and C=O stretch at 1705cm^{-1} were missing suggesting that these bond were used for adsorption of the inhibitor onto the surface of the aluminium. Finally new bonds of O-H were formed at 3245cm^{-1}, 3353cm^{-1} and 3145cm^{-1}, indicating chemical interaction, a character typical of chemiosorption (Reinhard and Rammet, 1985; Obot *et al*, 2009a, 2009b).

The FTIR spectrum of PA as well as the corrosion product of aluminium in H_2SO_4 as shown in Figure 4.81(a-b), some absorption peaks were found to have shifted which include: =C-H bend at 759cm^{-1} shifted to 704cm^{-1}, C-O stretch at 1050cm^{-1} was shifted to 1127cm^{-1}, C-C stretch in ring at 1442cm^{-1} shifted to 1446cm^{-1} and O-H stretch at 2935cm^{-1} and 3416cm^{-1} shifted to 2581cm^{-1} and 3476cm^{-1} respectively. The shift in the frequencies indicates that there is interaction between the aluminium and the inhibitor (Eddy *et al*., 2010). On the other hand, C-O stretch at 1210cm^{-1} and C=O stretch at 1722cm^{-1} were missing suggesting that these bond were used for adsorption of the inhibitor onto the surface of the aluminium.

The FTIR spectrum of PP as shown in Figure 4.82a, Figure 4.82b show the FTIR spectrum of the corrosion product of aluminium when PP was used as an inhibitor in H_2SO_4.

Absorption peaks of some prominent functional group were found to have shifted in the spectra of the corrosion product. The shift in the frequencies indicates that there is interaction between the aluminium and the inhibitor (Eddy *et al*., 2010). Also, aromatic C-H at 824cm^{-1}, C-N stretch at 1287cm^{-1}, O-H stretch at 2619cm^{-1}, 2786cm^{-1}, 2890cm^{-1}, and 3239cm^{-1} were missing suggesting that these bond were used for adsorption of the inhibitor onto the surface of the aluminium.

5.4 Scanning Electron Microscopy Study

The surface morphologies of mild steel and aluminium in solutions of HCl and H_2SO_4 were studied using scanning electron microscopy. Plate 4.1 a and b show the aluminum and mild steel samples before immersion seems smooth and appears some abrading scratches on the surface.

From Plates 4.2a and 4.3a, flakes showing corrosion products of mild steel and aluminium in the absence of the inhibitor as corroded in HCl, indicate that the surfaces were severely damaged but in the presence of the inhibitor on mild steel (Plates 4.2b-d)), the damaging effect of the acid on the metal sample is greatly reduced giving rise to more ordered corrosion products as surface coatings. Also the surface of the aluminium electrode (Plate 4.3 b-d) was modified by the inhibitor through the formation of a thin protective layer (Oguzie, 2012a). A severely corroded surface morphology is observed after immersion in the uninhibited systems, due to the corrosive attack of the acids solution as shown in the Plate 4.2a and 4.3a. Corrosion was relatively general with no evidence of localized attack. With the addition of extracts (Plate 4.2b-d and Plate 4.3b-d), the corrosion damage is visibly reduced, and there is slight evidence of the adsorbate presence on the metal surface. Moreover, the corrosion product layer on the metal surface in uninhibited 0.5

M H_2SO_4 is clearly very loose and porous and would thus offer insignificant corrosion protection. On the other hand, a distinct, compact, and highly ordered corrosion product layer is obvious in the presence of the extracts, which possibly account for the high inhibition efficiency of the extracts in 0.5 M H_2SO_4 even at short immersion periods. The morphology of the mild steel surface in uninhibited 1.0 M HCl reveals blisters of soluble corrosion products, with inherent fractures. Addition of the extracts into the acid solutions hindered formation of the corrosion product blisters, leaving a comparatively smoother and more protective corrosion product layer, which is not, however, as compact as that formed by the extracts in 0.5 M H_2SO_4. The difference in inhibition efficiency of the extracts in 1.0 M HCl and 0.5 M H_2SO_4 at short immersion periods is therefore interconnected with the extent to which the extracts modified the morphology of the corrosion product layer in the respective acid media.

The results obtained from the scanning electron micrographs of the inhibitor are consistent with those obtained from the FTIR spectra of the corrosion products of the metals and impedance spectra of mild steel and aluminium in the presence of these inhibitors, showing that these compounds inhibited the corrosion of mild steel and aluminium to varying degrees through the mechanism of physical adsorption (Enenebeaku, 2011; Oguzie *et al.,* 2012a).

5.5 Linear Polarization Measurements

Polarization measurements are suitable for monitoring the progress and meachanism of the anodic and cathodic partial reactions as well as identifying the effect of the additive on either partial reaction. Potentiondynamic and Linear polarization experiments were thus carried out to understudy the effect of adsorbed extracts on the kinetics of the anodic and

cathodic processes. The corrosion current is a function of the reactivity of a metal in an aqueous environment. The higher the values of i_{corr}, the higher the dissolution of the metal and vice versa. Typical Linear polarization curves(Tafel plots) for mild steel and aluminium in 1.0 M solutions of HCl, and 0.5 M H_2SO_4 in the absence and presence of various concentration of the inhibitors are shown in Figures 4.53 - 4.64 while the electrochemical parameters derived from the polarization curves and inhibition efficiencies are summarized on Tables 4.15 and 4.16. A typical Tafel plots will show Tafel region, plateau region and high polarization region. The plots revealed high dominance of the Tafel region and thus a wide potential range. Addition of additives could be to affect the anodic as well as the cathodic partial reactions by, shifting the corrosion potential (E_{corr}) slightly toward more positive (anodic) values and reducing the anodic and cathodic current densities and the corresponding corrosion current density (i_{corr}). This is an indication of a mixed-type corrosion inhibition mechanism. From the polarization curves however, it is obvious that the plant extracts exerts a more significant inhibiting effect on the cathodic hydrogen ion reduction reaction in 1.0 M HCl, whereas the inhibiting effect is more pronounced on the anodic metal dissolution reaction in 0.5 M H_2SO_4. The IE% data obtained (Tables 4.15 and 4.16) follows the same trend as those of gravimetric method, confirming the corrosion inhibiting efficacy of the extracts. This is consistent with report of Oguzie *et al.* 2012a and Khadom *et al*., 2009.

The computed data for the IE using gravmetric (GM), Linear polarization resistance (LPR) and Potentiodynamic polarization (PDP) as depicted in Figure 4.65 - 4.70, shows that the IE% increases with an increase in inhibitor concentration as a result, the surface area covered by these inhibitor increased. It was also found that there was good agreement

between the experimental techniques employed as the regression coefficient gave values great than 0.9 (Li *et al*., 2010; Kumar, 2008; Mansfeld, 1984).

The formed ferrous hydroxide and aluminium hydroxide on iron and aluminium respectively reacts with more oxygen to form the top layer of corrosion product, Fe_3O_4 (magnetite) and Al_2O_3. The presence of such oxide partially protects the steel and aluminium surface from further dissolutions and leads in turn to the appearance of a passive region on the polarization potential-current behavior. The passive region dissolves under the influence of chloride and sulphate ions attack and pitting corrosion occurs as indicated by the rapid increases in the current values for steel and aluminium with increasing potential and by the appearance of the wide hysteresis loop in the area between the forward and backward directions for potential in the anodic branch shown in the polarization curves. This effect was also found to increase the values for the cathodic and anodic Tafel slopes (βc and βc) and highly increases the polarization resistance, Rp as shown in Table 4.16.

5.6 Computational and Theoretical Modelling

5.6.1 Quantum chemical calculations

Figures 4.83 – 4.86 illustrate the optimized structure, highest occupied molecular orbital (HOMO), lowest unoccupied molecular orbital (LUMO) of various constituents from the extracts. The regions of high HOMO density are the sites at which electrophiles attack and represent the active centers, with the utmost ability to bond to the metal surface, whereas the LUMO orbital can accept the electrons in the d-orbital of mild steel and 3p orbital of the aluminium using anti-bonding orbital to form back bonds (Martinez and

Stagljar, 2003 and Khaled, 2010b). The eigen values of the HOMO (E_{HOMO}) and LUMO (E_{LUMO}) as well as the energy gap $\Delta E = E_{LUMO–HOMO}$ are presented in Table 4.17. High values of E_{HOMO} indicate the disposition of the molecule to donate electrons to an appropriate acceptor with vacant molecular orbitals, whereas low values of ΔE would enhance inhibition efficiencies because the energy to remove an electron from the last occupied orbital will be minimized (Rodriquez-Valdez *et al*., 2005). The local reactivity of each molecule was analyzed by means of the Fukui indices (FI) to assess reactive regions in terms of nucleophilic and electrophilic behavior as presented in Table 4.18. The f^- measures reactivity with respect to electrophilic attack or the propensity of the molecule to release electrons, whereas f^+ is a measure of reactivity relating to nucleophilic attack or tendency of the molecule attract electrons.

5.6.2 Molecular dynamics simulation

Adsorption of various constituent of the plant extract molecules on the mild steel and aluminium surfaces were analyzed at a molecular level by molecular dynamics simulations, using Forcite quench molecular dynamics to sample many different low energy configurations and to identify the low energy minima (Casewit *et al.*, 1992a, 1999b; Oguzie *et al*., 2012a). The structures were optimized with COMPASS forcefield and were used for the simulation. Solvent and charge effects were neglected in all the simulations and calculations were performed at the metal/vacuum interface in vaccum slab. Although this is clearly an oversimplification of the actual situation, it is adequate to qualitatively illustrate the differences in the adsorption behaviour of the molecules and provide sufficient insight to the study objectives.

Figures 4.87 - 4.90 show representative snapshots of the cross section of the lowest energy adsorption configurations for the single molecules on the Fe (110) surface from the

simulations, while Figures 4.91 – 4.94 show the representative snapshots for the single molecules on the Al (110) surface. The molecules can be seen to maintain a flat-lying adsorption orientation on the metal surfaces thereby maximizing contact and enhancing the degree of surface coverage. This parallel adsorption orientation also facilitates interaction of π - electrons and the hetero-atoms (Cl, N and O) in the molecules with the metal surfaces.

Results of the binding energy (E_{bind}) between the metal surface and the inhibitor molecules are presented on Tables 4.19. In each case, the potential energies were calculated by averaging the energies of the five structures of lowest energy. As can be seen from the data, the binding energies are all negative suggesting stable adsorption of the structures, however, the magnitude of the calculated binding energies is < 100 kcal mol^{-1} in some cases despite the fact that the simulations did not take into consideration the specific covalent interactions between the molecules and the Fe surface. This value has been reported by Akalezi *et al.* (2012) to be in the range of physiosorptive interactions. From Table 4.14, it is observed that the binding energies for the extracts constituents molecules on Fe (110) slab are of higher magnitude (-57.79 to -233.77 kcal/mol) than those obtained for Al (110) slab (-24.90 to -92.87 kcal/mol). This implies that the molecules are more strongly adsorbed on surface of Fe than Al.

CHAPTER SIX

6.0 SUMMARY, CONCLUSIONS AND RECOMMENDATIONS

6.1 Summary

The extracts show presence of some phytochemicals that might be responsible for their inhibitory properties. This study indicated that extracts of PP, PA, BS and PP1 effectively inhibit mild steel and aluminium corrosion in both 1 M HCl and 0.5 M H_2SO_4. The inhibition efficiencies were found to increase with increasing concentrations of the inhibitors. The inhibition efficiencies of the extracts for the corrosion of mild steel in 0.1 M HCl and 0.5 M H_2SO_4 solutions decreased in the order: PP> PA> PP1> BS (in HCl) and BS> PP> PP1> PA (in H_2SO_4). For aluminium the inhibition efficiencies decreased in the order: PP> PP1> BS> PA (in HCl) and PP> BS> PP1> PA (H_2SO_4). No evidence of corrosion inhibition by the extracts in H_2SO_4 in aluminium as they rather enhanced the dissolution of aluminium thereby function as corrosion catalysts. It was also observed that the inhibition efficiencies decreased with inmersion time for all the systems as temperature increases. Polarization measurements show that it functioned via mixed-type mechanism, inhibiting the rates of both the anodic metal dissolution and cathode hydrogen ion reduction reactions. Furthermore, the inhibition efficiencies of the plant extracts obtained from gravmetric and polarization studies were observed to be similar and in good agreement. From the activation energies (E_a), heats of adsorption (Q_{ads}) and standard free energies of adsorption (ΔG_{ads}) obtained from the study, it is evident that the inhibitors are adsorbed on the steel and aluminium surfaces through both physical and chemical interactions suggesting that both molecular as well as protonated species in the plant extracts were responsible for the observed inhibitory actions of the compounds in the different acid media. Adsorption characteristics of the plant extracts fitted both the Langmuir and

Freundlich isotherms. Linear polarization, SEM, and FTIR results all indicate that the corrosion reaction was inhibited by adsorption of the extract organic matter on the corroding mild steel surface. The trends of inhibition efficiency with temperature as well as values of activation parameters for corrosion and corrosion inhibition processes point toward significant physiosorption of the extract constituents on the mild steel surface. While DFT-based quantum chemical computations of parameters associated with the electronic structures of the constituent from the ethanol extract confirmed their inhibiting potential, which was further corroborated by molecular dynamics modeling of the adsorption of the single molecules on the metal surface.

6.2 Conclusions

The following conclusions are derived from the investigation:

(i) It has been established in this study that the extracts of *Boscia senegalensis*, *Phyllanthus amarus*, *Paullina pinnata*, and *Parinari polyandra* exerted an inhibiting effect on the acid corrosion of mild steel and aluminium.

(ii) It has been established in this study that the rate of corrosion decreases with increase in concentrations of inhibitors, equally the corrosion rate increased with temperature, and the corrosion rate of mild steel was found to be more pronounced than that of aluminium in the studied media.

(iii) The corrosion inhibition efficiency of the extract increased with increase in concentration, while the corrosion rate was found to decrease with increase in concentration of inhibitor.

(iv) The extract maintained remarkable corrosion inhibition efficiency even with prolonged exposure time.

(v) The adsorption of the extracts on the mild steel and aluminium surface in 1.0 M HCl and 0.5 M H_2SO_4 solutions respectively obeys Langmuir and Freundlich isotherm.

(vi) The presence of this extracts in the acid media increases the activation energy of corrosion process which indicates physical adsorption.

(vii) The results obtained from linear polarization and gravimetric measurements are in good agreement.

(viii) DFT-based quantum chemical computations of parameters associated with the electronic structures of specific components of the extract confirmed their inherent affinity toward adsorption on the metal surface and hence inhibit the corrosion reaction.

6.3 Recommendations

Further studies on the following will give detailed information on the inhibitory property of the plants extract:

i. Having confirmed the corrosion inhibition effectiveness of this extracts, and their various constituents, further studies can be done on derivatives of such compounds as corrosion inhibitors in coatings on metallic surfaces.

ii. The use of Electrochemical Impedance Spectrometry (EIS) and Electrochemical Noise (ES) are recommended.

iii. Corrosion inhibition studies by these plants should be carried out under service conditions to simulate operational conditions including the effects of flow,

pressure, a wider temperature range and pH of the aqueous systems in order to explore the possibility of using them as inhibitor formulations in the industries

References

Abdallah, M. (2004a). Guar gum as corrosion inhibitor for carbon steel in sulphuric acid solutions. *Portugaliae Electrochimica Acta,* **22:**161-175.

Abdallah, M. (2004b). Antibacterial drugs as corrosion inhibitors for aluminium in HCl solution. *Corrosion Science,* **46:** 1981-1996.

Abdeli, M., Ahmadi, N. P. and Khosroshahi, R. A. (2009). Nile blue and indigo carmine organic dyes as corrosion inhibitor of mild steel in hydrochloric acid. *Journal of Solid State Electrochemistry*, **14(7):** 1317-1324.

Abiola, K. O., Oforka, N. C, Ebenso, E. E. and Nwinuka, N. M. (2007). Ecofriendly corrosion inhibitors: Inhibitive action of Delonix regia extract for the corrosion of aluminium in acidic medium. *Anti-Corrosion Methods and Materials,* **54(4):** 219 - 224.

Achebe, C. H., Nneke, U. C. and Anisiji, O. E. (2012). Analysis of oil pipeline failures in the oil and gas industries in the Niger Delta area of Nigeria. Proceedings of the International MultiConference of Engineers and Computer Scientists, IMECS. **2:** 14 – 16.

Adejo, S. O., Ekwenchi, M. M., Momoh, F. and Odiniya, E. (2012). Adsorption characterization of ethanol extract of leaves of *Portulaca oleracea* as green corrosion inhibitor for corrosion of mild steel in sulphuric acid medium. *International Journal of Modern Chemistry*, **1(3):** 125-134.

Ajayi, E.O. (2003). Predictive model for evaluating corrosion rate of mild steel in six environments. LAUTECH, *Journal of Engineering and Technology*,**1:**75-81.

Akalezi, C. O., Enenebaku, C. K. and Oguzie, E. E. (2012). Application of aqueous extracts of coffee senna for control of mild steel corrosion in acidic environments. *International Journal of Industrial Chemistry,* **3**:13-25.

Akpan, I. A. (1994). Kinetic study of corrosion of aluminium and steel in acidic medium and their inhibition by thiosemicarbozone derivatives. Unpublished M.Sc. Thesis. University of Calabar. Calabar.

Aksot, A. A. and Bilgic, S. (1992). The effect of amino acids on the corrosion of nickel in H_2SO_4. *Corrosion Science*, **33**:379-387.

American Society for Testing Materials (ASTM) G96-90. (2001). Standard Guide for On-Line Monitoring of Corrosion in Plant Equipment (Electrical and Electrochemical Methods). Annual Book of ASTM Standards, Vol. 03.02, ASTM, Philadelphia, PA.

Arora, P., Kumar, S., Sharma, M. K. and Mathur, S. P. (2007). Corrosion inhibition by capparis deciduas in acidic media. *Electronic Journal of Chemistry,* **4(4):**450-456.

Ashassi-Sorkhabi, H., Ghasemi, Z. and Seifzadeh, D. (2005a). The inhibition effect of some amino acids towards the corrosion of aluminium in 1 M HCl + 1 M H_2SO_4 solution. *Applied Surface Science,* **249:**408-418.

Ashassi-Sorkhabi, H., Majidi, M. R. and Seyyedi, K. (2004). Investigation of inhibition effect of some amino acids against steel corrosion in HCl solution. *Applied Surface Science,* **225:**176–185.

Ashassi-Sorkhabi, H., Shabani, B., Aligholipour, B., and Seifzadeh, D. (2006). The effect of some Schiff bases on the corrosion of aluminium in hydrochloric acid solution. *Applied Surface Science,* **252:**4039–4047.

Atkins, P. (2002). *Physical Chemistry,* 7th edition. Oxford: Oxford press.

Baboian, R., Bellante, E. L. and Cliver, E. B. (1990). The Statue of Liberty Restauration. Houston, Tex., NACE International.

Badawy, W. A., Ismail, K. M., Ahlam, H. and Fathi, M. (2006). Corrosion control of Cu–Ni alloys in neutral chloride solutions by amino acids, *Electrochimica Acta*, **51**:4182–4189.

Barouni, K., Bazzi, L., Salghi, R., Mihit, M., Hammouti, B., Albourine, A. and El Issami, S. (2008). Some amino acids as corrosion inhibitors for copper in nitric acid solution. *Materials Letters,* **62:**3325–3327.

Bendahou, M.A., Benadellah, M. B. E. and Hammouti, B. B. (2006). A study of rosemary oil as a green corrosion inhibitor for steel in 2M H_3PO_4. *Pigment and Resin Technology,* **35(2):**95-10.

Bouyanzer, A and Hammouti, B. (2004). A study of anti-corrosion effects of Artemisia oil on steel. *Pigment and Resin Technology,* **33(5):**287-292.

Bilgic, L. and Caliskan, N. (2001). An investigation of some Schiff bases as corrosion inhibitors for austenite chromium-nikel steel in H2SO4. *Journal of Applied Electrochemistry,* **31:**79 -83.

Cabot, P. L., Centellas, F. A., Garrido, J. A., Perez, E. and Vidal, H. (1991). "Electrochemical Study of Aluminium Corrosion in Acid Chloride Solutions". *Electrochimica Acta.,* **36**: 171-187.

Cardoso, S. P., Hollauer, E., Borges, L. E. P. and Gomes, J. A. C. P. (2006). QSPR prediction analysis of corrosion inhibitors in hydrochloric acid on 22%-Cr stainless steel. *Journal of Brazilian Chemical Society*, **17:** 1241-1249.

Cardoso, S. P., Gomes, J. A. C. P., Borges, L. E. P. and Hollauer, E. (2007). Predictive QSPR analysis of corrosion inhibitors for super 13% Cr steel in hydrochloric acid. *Brazilain Journal of Chemical Engineering*, **24 :** 547–559.

Casewit, C. J., Colwell, K. S. and Rappé, A. K. (1992a). Application of a universal force field to organic molecules. *Journal of the American Chemical Society*, **114**:10035–10046.

Casewit, C. J., Colwell, K. S. and Rappé, A. K. (1992b). Application of a universal force field to main group compounds. *Journal of the American Chemical Society*, **114**:10046–10053.

Chetounani, A., Hammouti, B. and Benkaddour, M. (2004). Corrosion inhibition of iron in hydrochloric acid solution by jojoba oil. *Pigment and Resin Technology*, **33(1):**26-31.

Chi, M. and Zhao, Y. P. (2009). Adsorption of formaldehyde molecule on the intrinsic and Al-doped grapheme: A first principle study. *Computional Materials Science*, **48**:1085–1090.

Clark, D. S. and Varney, W. R. (1987). Physical Metallurgy for Engineers. Canada: Van Nostrand Reinhold ltd.

Dahmani, M.; Et-Touhami, A.; Al-Deyab, S. S.; Hammouti, B. and Bouyanzer, A. (2010). Corrosion Inhibition of C38 Steel in 1M HCl: A Comparative Study of Black Pepper Extract and Its Isolated Piperine, *International Journal of Electrochemical Science*, **5**, 1060 - 1069.

Dai, W. and Zhang, Y. Y. (2012). Molecular dynamics simulation of the adsorption behaviour of amino acid corrosion inhibitor on Cu (1 0 0) surface. *Applied Mechanics and Materials*, **121-126:** 226 - 230.

Dean, S.W. (2003). Corrosion monitoring for industrial processes. In: D.S Cramer, B.S Covino (eds.), Corrosion: Fundamentals, Testing and Protection. **13A**: 533-541.

Delley, B. (1990). An All-Electron Numerical Method for Solving the Local Density Functional for Polyatomic Molecules. *Journal of Chemical Physics*, **92**:508–517.

Delley, B. (2000). From molecules to solids with the DMol3 approach. *Journal of Chemical Physics*, **113**:7756–7764.

Denny, J. (2004). Principles and Preventions of Corrosion, Upper Saddle River, New Jersey Prentice Hall. ISBN 0-13-359993-0.

Döner, A., Solmaz, R., Özcan, M. and Kardas, G. (2011). Experimental and theoretical studies of thiazoles as corrosion inhibitors for mild steel in sulphuric acid solution. *Corrosion Science*, **53**: 2902–2913.

Ebenso, E. E., Eddy, N. O. and Odiongenyi, A. O. (2008). Corrosion inhibitive properties and adsorption behaviour of ethanol extract of *Piper guinensis* as a green corrosion inhibitor for mild steel in H_2SO_4. *African Journal of Pure & Applied Chemistry* **4(11)**: 107-115.

Ebenso, E. E. and Ekpe, U. J. (1996). Kinetic study of corrosion and corrosion inhibition of mild steel in H_2SO_4 using Carica papaya leaves extract. *West African Journal of Boilogical Applied Chemistry*, **41:**21-27.

Ebenso, E. E., Ekpe, U. J. and Ibok, U. J. (1998). Studies on the inhibition of mild steel corrosion by some plant extracts in acidic medium. *Discovery and Innovation*, **10:**52-59.

Ebenso, E. E., Ibok, U. J., Ekpe, U. J., Umoren, S., Ekarete J., Abiola, O. K., Oforka, N. C., and Martinez S. (2004). Corrosion inhibition studies of some plant extracts on aluminiumin acidic medium. *Transaction Of SAEST*, **39(4):**117-123.

Eddy. N. O., Momoh, Y. H., and Oguzie, E. E. (2015). Theoreticaland experimental studies on the corrosion inhibition potentials of some purines for aluminium in 0.1 M HCl. Journal of Advanced Research, **6:** 203-217.

Eddy, N. O. (2008). Inhibition of the corrosion of mild steel in H_2SO_4 by some antibiotics. Ph. D Thesis, University of Calabar, Calabar.

Eddy, N. O. (2009a). Ethanol Extract of *Phyllanthus Amarus* as a Green Inhibitor for the Corrosion of Mild Steel in H_2SO_4. *Portugaliae Electrochimica Acta*, **27**(5):579-589.

Eddy, N. O. (2009b). Inhibitive and adsorption properties of ethanol extract of *Colocasia esculenta* leaves for the corrosion of mild steel in H_2SO_4. *International Journal of Physical Sci*ence, **4(3)**: 1-7.

Eddy, N. O. and Ebenso, E. E. (2008). Adsorption and inhibitive properties of ethanol extract of *Musa sapientum* peels as a green corrosion inhibitor for mild steel in H_2SO_4. *African Journal of Pure and Applied Chem*istry, **2(6):** 1-9.

Eddy, N. O. and Ebenso, E. E. (2010). Corrosion inhibition and adsorption properties of ethanol extract of *Gongronema latifolium* on mild steel in H_2SO_4. *Pigment and Resin Technology*, **42**(7): 1029-1032.

Eddy, N. O. and Ita, B. I. (2010). Experimental and theoretical studies on the inhibition potentials of some derivatives of cyclopenta-1,3-diene for the corrosion of mild steel in HCl solutions. *International Journal of Quantum Chemistry*, **DOI:** 104152/pea.200904443.

Eddy, N. O. and Mamza, P. A. P. (2009). Inhibitive and adsorption properties of ethanol extract of seeds and leaves of *Azadirachta indica*. *Portugaliae Electrochimica Acta*, **27**(2): 20-28.

Eddy, N. O. and Odoemelam, S. A. (2009); Inhibition of the corrosion of mild steel in H_2SO_4 by ethanol extract of *Aloe vera*. *Resin and Pigment Technology*, **38**(2): 111-115.

Eddy, N. O., Ebenso, E. E. and Ibok, U. J. (2010). Adsorption, synergistic inhibitive effect and quantum chemical studies of ampicillin (AMP) and halides for the corrosion of mild steel in H_2SO_4. *Journal of Applied Electrochem*istry, **40**: 445-456.

Eddy, N. O., Odoemelam, S. A. and Ibiam (2009a). Adsorption and inhibitive properties of ethanol extract of *Costus afer* on the inhibition of the corrosion of mild steel in H_2SO_4. *Journal of Surface Science Technology*, **25** (3-4):1-14.

Eddy, N. O., Ibok, U. J. and Ebenso, E. E. (2009b). Adsorption, synergistic inhibitive effect and quantum chemical studies on ampicillin and halides for the corrosion of mild Steel, *Journal of Applied Electrochemistry*, **DOI:** 10.1007/s10800-009-0015- z

Eddy, N. O., Odoemelam S. A. and Odiongenyi, A. O. (2009c). Joint effect of halides and ethanol extract of *Lasianthera Africana* on the inhibition of the corrosion of mild steel in H_2SO_4. *Journal of Applied Electrochemistry*, **39**(6): 849 – 857.

Eddy, N. O., Ekwumemgbo, P. A. and Mamza, P. A. P. (2009d). Ethanol extract of *Terminalia catappa* as a green inhibitor for the corrosion of mild steel in H_2SO_4. *Green Chemistry Letters and Review*, **2**(4): 223-231.

Eddy, N. O., Odoemelam, S. A. and Odiongenyi, A. O. (2009e). Inhibitive, adsorption and synergistic studies on ethanol extract of *Gnetum africana* as green corrosion inhibitor for mild steel in H_2SO_4. *Green Chemistry Letters and Review*, **2** (2):111-119.

Eddy, N.O. and Odoemelam, S. A. (2008a). Effect of pyridoxal hydrochloride-2,4-dinitrophenyl hydrazone on the corrosion of mild steel in HCl. *Journal of Surface Science Technology*, **24(1-2):** 1-14.

Eddy, N. O. and Odoemelam, S. A. (2008b). Norfloxacin and sparfloaxin as corrosion inhibitors for zinc. Effect of concentrations and temperature. *Journal of Material Science,* **4:**87.

Ekpe, U. J., Ebenso, E. E. and Ibok, U. J. (1994). Inhibitory action of Azadiracchta indica leaves extract on the corrosion of mild steel in H_2SO_4. *Journal of West African Science Association,* **37:**13-30.

El Ashry, E. H., El Nemr, A., Essawy, S. A. and Ragab, S. (2006a). Corrosion inhibitors Part II: quantum chemical studies on the corrosion inhibitions of steel in acidic medium by some triazole, oxadiazole and thiadiazole derivatives. *Electrochimica Acta,* **51:**3957–3968.

El Ashry, E. H., El Nemr, A., Essawy, S. A. and Ragab, S. (2006b). Corrosion inhibitors part III : quantum chemical studies on the efficiencies of some aromatic hydrazides and Schiff bases as corrosion inhibitors of steel in acidic medium. ARKIVOC **11:**205–220.

El-Etre, A. Y. (1998). Natural honey as corrosion inhibitor for metals and alloy: Copper in neutral aqueous solution. *Corrosion Science,* **40(11):**1845-1850.

El-Etre, A. Y. (2003). Inhibition of aluminum corrosion using Opuntia extract. *Corrosion Science,* **45:**2485-2495.

El-Etre, A. Y. (2006). Khillah extract as inhibitor for acid corrosion of SX 326 steel. *Applied Surface Science,* **252:**8521-8525.

El-Etre, A. Y. and Abdallah, M. (2002). Natural honey as corrosion inhibitor for metals and alloys II C-steel in high saline water. *Corrosion Science,* **42:** 731-738.

Elayyoubi, S. B., Hammouti, S., Kertit, H. O. and Maarouf, E. B. (2004). Corrosion inhibition of mild steel in hydrochloric acid solutions by malonitrile compounds. *Review and Method Paris,* **2:**153-157.

El-Rabiee, M. M., Helal, N. H., Abd El-Hafez, G. M. and Badawy, G. A. (2008). Corrosion control of vanadium in aqueous solutions by amino acids. *Journal of Alloys and Compounds,* **459**: 466–471.

Emregul, K. C. and Hayvali, M. (2006). Studies on the effect of a newly synthesized Schiff base compound from phenazone and vanillin on the corrosion of steel in 2M HCl. *Corrosion Science,* **48:** 797-812.

Enenebeaku, C. K. (2011). Electrochemical studies of the inhibitory effects of selected plant extracts on the acid corrosion of mild steel. Ph.D Thesis. Federal University of Technology, Owerri.

Fuchs-Godec, R. and Zerjav, G. (2009). Inhibition properties of triton X100 on ferritic stainless steel in sulphuric acid at increasing temperature. *Acta Chimica Slovenica*, **56**:78-85.

Gao, G. and Liang, C. (2007). Electrochemical and DFT studies of □-amino alcohols as corrosion inhibitors for brass. *Electrochimica Acta,* **52:** 4554-4559.

Ghasemi, Z. and Tizpar, A. (2006). The inhibition effect of some amino acids towards Pb–Sb–Se–As alloy corrosion in sulfuric acid solution, *Applied Surface Science*, **252**: 3667–3672.

Gopi, D., Govindaraju, K. M., Manimozhi, S., Ramesh, S. and Rajeswari, S. (2007). Inhibitors with biocidal functionalities to mitigate corrosion on mild steel in natural aqueous environment. *Journal of Applied Electrochemistry*, **37**(6): 681-689.

Gupta, R., Sharma, K., Dobhal, M. P., Sharma, M. C., and Gupta, R. S. (2011). Antidiabetic and antioxidant potential of β -sitosterol instreptozotocin-induced experimental hyperglycemia. *Journal of Diabetes*. **3:**29 – 37.

Hazwan-Hussin, M. and Jain-Kassim, M. (2010). The corrosion inhibition and adsorption behavior of Uncaria gambir extract on mild steel in 1 M HCl. Material Chemistry and Physics xxx, xxx-xxx. doi: 10.1016/j.matchemphys.2010.10.032. Article in press.

Hosseini, M. G., Khalilpur, H., Ershad, S. and Saghatforoush, L. (2009). Protection of mild steel corrosion with new thia-derivative salens in 0.5 M H_2SO_4 solution. *Journal of Applied Electrochemistry*, **40**(2): 215-223.

Hosseini, S. M. A., Eftekhar, S. and Amiri, M. (2007). Polarization behavior of stainless steel type 302 in HCl solution of benzotriazole. *Asian Journal of Chemistry,* **19(4):**2574-2580.

Ita, B. I. (2004a). 4-Formylmorpholine hydrazone and 4-formymorpholine: New corrosion inhibitors for mild steel in 0.1M hydrochloric acid solution. *Proccurement of the Chemical Society of Nigeria.*

Ita, B. I. (2004b). A study of corrosion inhibition of mild steel in 0.1M hydrochloric acid by O-vanilin hydrazone. *Bulletine of Electrochemistry,* **20(8):**363-370.

Ita, I. B. and Offiong, O. E. (1997). The inhibition of mild steel corrosion in hydrochloric acid by 2, 2'-pyridil and 2, 2'-pyridon. *Materials Chemistry and Physics,* **51:**203-210.

Jones, D. A. (1982). Forms of corrosion, recognition and prevention Dillon, C.P. edited. NACE, Houston. Reprinted by permission of the National Association of Corrosion Engineers.

Ihebrodike, M. M.; Michael, C. N., Kelechukwu, B. O.; Lebe, A. N.; Maduabuchi, A. C.; Francis, C. E.; and Emeka, O.O. (2012). Experimental and theoretical assessment of the inhibiting action of Aspilia Africana extract on corrosion aluminium alloy AA3003 in hydrochloric acid. *Journal Material Science*, **47:**2559-2572.

Kelly, L. G., Scully, J. R., Shoessmith, D. W and Buchheit, R. G. (2003). Electrochemical techniques in corrosion science. NewYork. Morcell Dekker.

Khadom, A. A., Yaro, A. S., Altaie, A. S. and Khadum, A. A. H. (2009). Electrochemical, activations and adsorption studies for the corrosion inhibition of low carbon steel in acidic media. *Portugaliae Electrochimica Acta*, **27(6):** 699-712.

Khaled, K. F. (2010a).Studies of iron corrosion inhibition using chemical, electrochemical and computer simulation techniques. *Electrochimica Acta*, **55:** 6523−6532.

Khaled, K. F. (2010b). Corrosion of copper in nitric acid solutions using some amino acids: A combined experimental and theoretical study. *Corrosion Science*, 52:3225–3234.

Khavasfar, A. and Iran, M. (2006). Study of organic corrosion inhibition on CO_2 corrosion of mild steel by electrochemical measurements. Paper presented at the 5^{th} Internal surface engineering congress. Seattle, Washington. May 16, 2006.

Kiani, M. A. Mousavi, M. F., Ghasemi, S. Shamsipur, M. and Kazemi, S. H. (2008). Inhibitory effect of some amino acids on corrosion of Pb–Ca–Sn alloy in sulfuric acid solution, *Corrosion Science*, **50**:1035–1045.

Klass, J., Tinto, W. F., McLean, S., and Reynolds, W. F. (1992). Friedelane triterpenoids from Peritassa compta: Complete ^{1}H-NMR and ^{13}C-NMR assignments by 2D NMR spectroscopy. Journal of Natural Products. **55:**1626 – 1630.

Kliskic, M., Radoservic, J., Gudic, S. and Katalinic, V. (2000). Aqueous extract of Rosmmarius officinalis L. as inhibitor of Al-Mg alloy corrosion in chloride solution. *Journal of Applied Electrochemistry,* **30:**823-830.

Krajewka, D., Dabrowska, M., Jackonny, P. and Rozonski, A. (2002). Purole analysis of chloramphenicle: Synthesis and antimicrobial activity. *Acta Pol. Pharm.* **59:**127-132.

Kumar, A. (2008). Corrosion inhibition of mild steel in hydrochloric acid by sodium laury sulphate. *Electronic Journal of Chemistry,* **5(2):** 275-280.

Lashgari, M., Arshadi, M. R. and Biglar, M. J. (2010). Experimental and theoretical studies of media effects on copper corrosion in acidic environments containing 2-amino-5-mercapto-1,3,4-thiadiazole. *Iranian Chemical Soc*iety, **7:** 478-486.

Lebrini, M. Robert, F. , Lecante, A. and Ross, C. (2010). Corrosion Inhibition of C38 Steel in 1M Hydrochloric Acid Medium by Alkaloids Extract from, *Journal of Material Engineering Performance*, **22**: 3792–3800.

Li, W., Hu, L., Tao, Z., Tian, H. and Hou, B. (2011). Experimental and quantum chemical studies on two triazole derivatives as corrosion inhibitors for mild steel in acid media. *Materials and Corros*ion, 62: n/a. doi: 10.1002/maco.201005965.

Li, Y., Umoren, S. A. and Wang, F. H. (2010). Electrochemical study of corrosion inhibition and adsorption behaviour for pure iron by polyacrylamide in H_2SO_4: Synergistic effect of iodide ions. *Corrosion Science*, **52**: 1777–1786.

Mansfeld, F. (1987). Corrosion mechanisms. New York: Dekker M.

Mahato, S. B, and Kundu, A. P. (1994). 13 C NMR Spectra of pentacyclic triterpenoids – a compilation and some salient features. *Phytochemistry*, 37:1517–1575.

Matheswaran, P. and Ramasamy, A. K. (2010). Influence of benzotriazole on corrosion inhibition of mild steel in citric acid medium. *Electronanalytical Journal of Chemistry*, **7**(3)**:** 1090-1094.

Martinez, S. (2003). Inhibitory mechanism of mimosa tannin using molecular modeling and substitutional adsorption isotherms. *Materials Chemistry and Physics*, 77(1):97-102.

Mercer,A. P. (1990). Chemical inhibitors for corrosion control. Glubley edited. London: *Royal Society Of Chemistry.*

Monica, W. A., Dubey, A. and Arwind, D. (2005). Inhibiting effect of N-acetyl N,N,Ntrimethylammonium bromide on corrosion of mild steel in acidic medium. *Portugallise Electrochemica Acta*. **23(4):**445-455.

Moniz, B. J. (1986). Process industries corrosion Moniz, B.J. and Pollock edited. NACE. Houston. Reprinted by permission of the National Association of Corrosion Engineers.

Moore, J. J. (1990). Chemical metallurgy. 2nd edition. London. Butterworths.

Morgan, W. M. (1984) .Outline of paint technology. England: Charles Griffins Ltd.

Moretti, G., Guidi, F., and Grion, G. (2004). Tryptamine as a green iron corrosion inhibitor in 0.5 M deaerated sulphuric acid, *Corrosion Science*, **46**:387–403.

Muralidharan, S., Chandrasekar, R. and Iyer, S. V. K. (2000). Effect of piperidones on hydrogen permeation and inhibition of mild steel in acidic solutions. *Proccurement of Indian Academy of Science.* **112(2):** 127-136.

National Association of Corrosion Engineers. (1999). Techniques for monitoring corrosion and related parameters in field applications, NACE, 3T199, NACE International, Houston, TX.

Noor, E. A. (2009). Potential of aqueous extract of Hibiscus sabdariffa leaves for inhibiting the corrosion of aluminum in alkaline solutions. *Journal of Applied Electrochemistry*, **39**: 1465-1475.

Nwosu, O. F. Nnanna, L. A. and Okeoma, K. B. (2013): Corrosion Inhibition for Mild Steel in 0.5 M H_2SO_4 solution using *Achyranthes aspera L*. leaf extract. *African Journal of Pure and Applied Chemistry*, **7**(2): 56-60.

Obot, I. B., Ebenso, E. E., Akpan, I. A., Z. M. Gasem, Z. M. and Afolabi, A. S. (2012). Thermodynamic and density functional theory investigation of sulphathiazole as green corrosion inhibitor at mild steel/hydrochloric acid interface. *International Journal of Electrochemical Science*, **7:** 1978 – 1996.

Obot, I. B., Obi-Egbedi, N. O. and Umoren, S. A. (2009a). Experimental and theoretical investigation of clotrimazole as corrosion inhibitor for aluminium in hydrochloric acid and effect of iodide ion addition. *Der Pharma Chemica*, **1(1):** 151-166.

Obot, I. B., Umoren, S. A., Ebenso, E. E. and Obi-Egbedi, N. O. (2009b). The Inhibition of aluminium corrosion in hydrochloric acid solution by exudate gum from Raphia hookeri. *Desalination,* **250**: 225–236.

Odiongenyi, A. O., Odoemelam, S. A. and Eddy, N. O. (2009). Corrosion inhibition and adsorption properties of ethanol extract of *Vernonia Amygdalina* for the corrosion of mild steel in H_2SO_4. *Portugaliae Electrochimica Acta* **27**(1): 33-45.

Odoemelam, S. A., Ibiam, N. A. and Eddy, N. O. (2009). Adsorption and inhibitive effects of ethanol extracts of *Costus afer* on the corrosion of mild steel in H_2SO_4. *Journal of Surface Science and Technology*, **25(3-4):**1-14.

Ogoko, E. C., Odoemelam, S. A., Ita, B. I. and Eddy, N. O. (2009). Adsorption and inhibitive properties of clarithromycin for the corrosion of zinc in 0.01 to 0.05M H_2SO_4. *Portugaliae Electrochimica Acta,* **27(6):** 713-724.

Oguzie, E. E. (2008). Corrosion Inhibitive Effect and Adsorption Behaviour of *Hibiscus Sabdariffa* Extract on Mild Steel in Acidic Media. *Portugaliae Electrochimica Acta* **26**: 303-314.

Oguzie, E. E., Onuoha, G. N. and Ejike, E. N. (2007).Effect of Gongronema latifolium extract on aluminium corrosion in acidic and alkaline media. *Pigment and Resin Technolgy*, **36**(1):44 - 49.

Oguzie, E. E. (2005). Inhibition of acid corrosion of mild steel by Telfaria occidentalis extract. *Pigment and Resin Technology,* **34(6):** 321-326.

Oguzie, E. E. (2006). Studies on the inhibition effect of Occinum vivridis extract on acid corrosion of mild steel. *Material Chemistry and Physics,* **99(2-3):**441-446.

Oguzie, E. E. (2007). Corrosion inhibition of aluminum in acidic and alkaline media on Sanseviera triasciata extract. *Corrosion Science*, **49:** 1527-1539.

Oguzie, E. E. and Ebenso, E. E., (2005). Corrosion inhibition of mild steel in acidic media by some organic dyes. *Materials Letters,* **59:**2163–2165.

Oguzie, E. E., Adindu, C. B., Enenebeaku, C. K., Ogukwe, C. E., Chidiebere, M. A. and Oguzie, L. L. (2012a). Natural products for materials protection: Mechanism of corrosion inhibition of mild steel by acid extracts of Piper guineense. *Journal of Physical Chemistry,* dx.doi.org/10.1021/jp300791s

Oguzie, E. E., Mejeha, I. M., Nwandu, M. C., Okeoma, K. B., Nnanna, L. A., Chidiebere, M. A. and Eze, F. C. (2012b). Experimental and theoretical assessment of the inhibiting action of *Aspilia africana* extract on corrosion of aluminium alloy AA3003 in hydrochloric acid. *Journal of Materials Science,* **47:** 2559-2572.

Oguzie, E. E., Ogukwe, C. E., Ogbulie, J. N., Nwanebu, F. C., Adindu, C. B., Udeze, I. O., Oguzie, K. L., and Eze, F. C. (2012c). Broad spectrum corrosion inhibition: corrosion and microbial (SBR) growth inhibiting effects of *Piper guineense* extract. *Journal of Material Science*, **47**: 3592-3601.

Oguzie, E. E., Onuchukwu, A. I., Okafor, P. C. and Ebenso, E. E. (2006). Corrosion inhibition and adsorption behavior of Occimum basiclicum extract on aluminum. *Pigment and Resin technology,* **35(2):**63-70.

Oguzie, E. E., Unaegbu, C., Ogukwe, C. N., Okolue, B. N. and Onuchukwu, A. I. (2004). Inhibition of mild steel corrosion in sulphuric acid using indigo dye and synergistic halide additives. *Materials Chemistry and Physics*, **84(2-3):**363-368.

Okafor, P. C. and Ebenso, E. E. (2007). Inhibitive action of *Carica papaya* extracts on the corrosion of mild steel in acidic media and their adsorption characteristics. *Pigment and Resin Technology*, **36(3):** 134-140.

Okafor, P. C., Ekpe, U. J., Ebenso, E. E., Umoren, E. S. and Leizou, K. E. (2005). Inhibition of mild steel corrosion in acidic medium of sativum. *Bulletin of Electrochemistry*, **21(8):**347-352.

Okafor, P. C., Ikpi, M. I., Uwah, I. E., Ebenso, E. E., Ekpe, U. J. and Umoren, S. A. (2008). Inhibitory action of Phyllanthus amarus on the corrosion of mild steel in acidic medium. *Corrosion Science*, doi:10.1016/j.

Okafor, P. C., Ebiekpe, V. E., Azike, C. F., Egbung, G. E., Brisibe, E. A. and Ebenso, E. E. (2012). Inhibitory action of Artemisia annua extracts and artemisinin on the corrosion of mild steel in H_2SO_4 solution. Bulletin of Electrochemistry, **22(9):** 234-242.

Okafor, P. C., Osabor, V. and Ebenso, E. E. (2007). Eco friendly corrosion inhibitors: Inhibitive action of ethanol extracts of Garcinia Kola for the corrosion of aluminium in acidic medium. *Pigment and Resin Technology*, **36(5):**299-305.

Olasehinde, E. F., Olusegun, S. J., Adesina, A. S., Omogbehin, S. A. and Momoh-Yahaya, H. (2012). Inhibitory action of *Nicotiana tabacum* extracts on the corrosion of mild steel in HCl: Adsorption and Thermodynamics Study. *Nature and Science*, **10**(12): 21-34.

Oldfield, J. W. (1988). Electrochemical theory of galvanic corrosion. In: Hack, H. P. (Ed.). *Galvanic Corrosion*. Philadelphia, Penn., American Society for Testing of Materials, 5–22.

Olivares-Xometl, O., Likhanova, N. V., Dom´ınguez-Aguilar, M. A., Arce, E., Dorantesc, H. and Arellanes-Lozada, P. (2008). Synthesis and corrosion inhibition of amino acids alkylamides for mild steel in acidic environment, *Materials Chemistry and Physics*, **110**: 344-351.

Onuegbu, T. U.; Umoh, E. T. and Ehiedu, C. N. (2013). Emilia Sonchifolia Extract as Green Corrosion Inhibitor for Mild Steel in Acid Medium using Weight Loss Method, *Journal of Natural Science and Reserved*, **3**(9),52-55.

Pourbaix, J. L. (1981). Atias of electrochemical equilibrium in aqueous solution. NACE, London.

Pourbaix, M. (1974). Atlas of Electrochemical Equilibria in Aqueous Solutions. 2nd edition, National Association of Corrosion Engineers, Houston TX.

Patel, N. S.; Jauhariand1, S. ;.Mehta, G. N.; Al-Deyab, S. S.; Warad, I. and Hammouti B.(2013). Mild Steel Corrosion Inhibition by Various Plant Extracts in 0.5 M Sulphuric acid , *International Journal of Electrochemical Science*, **8**, 2635 – 2655.

Popova, A., Sokolova, E., Raicheva, S. and Christov, M. (2003). AC and DC study of the temperature effect on mild steel corrosion in acid media in the presence of benzimidazole derivatives. *Corrosion Science,* **45(1):** 33-58.

Quraishi, M. A., Ahamad, I., Sudhish, A. K. S., Lal, K. S. B. and Singh, V. (2008). N-(Piperidinomethyl)-3-[(pyridylidene)amino]isatin: A new and effective acid corrosion inhibitor for mild steel, *Materials Chemistry and Physics*, **112**: 1035–1039.

Qureshi, A. A. and Eswar, K. K. (2010). Phytochemical constituents and pharmacological activities of Trachyspermum ammi, *Plant Archives*, 10: 955-959.

Rajendran, S., Joany, M. R., Apparao, B. V. and Palaniswamy, N. (2005). Synergistic effect of calcium gluconate and Zn^{2+}on the inhibition of corrosion of mild steel in neutral aqueous environment. *Transaction of the SEAST,* **35(3, 4):**113-117.

Rodriguez-Valdez, L. M, Martinez-Villafane, A., Martinez, L., Glossman-Mitnik, D. (2005). Computational simulation of the molecular structure and properties of heterocyclic organic compounds with possible corrosion inhibition properties. *Journal of Molecular Structure (THEOCHEM)*, **713:** 65–70.

Saratha, R. and Vasudha, V. G. (2010). Emblica officinalis (Indian gooseberry) leaves extract as corrosion inhibitor for mild steel in 1N HCl medium. *E-Journal of Chemistry* , **7**(3) : 677 □ 684.

Sastri, V. S. (1998). Corrosion Inhibitors: Principles and Applications. New York: John Wiley & Sons Ltd. West Sussex.

Sastri, V. S. (2011). Green Corrosion Inhibitors: Theory and Practice. John Wiley & Sons, Inc., Hoboken, New Jersey.

Selvi, S. T., Raman, V., and Rajendran, N. (2003).Corrosion inhibition of mild steel by benzotriazole derivatives in acidic medium. *Journal of Applied Electrochemistry,* **33(12):** 1175-1182.

Sethuran, M. G. and Raja, P. B. (2005). Corrosion inhibition of mild steel by Datura metel in acidic medium. *Pigment and Resin Technol*ogy, **34(6):**327-331.

Shibli, S. M. A. and Saji, V. S. (2005). Co-inhibition characteristics of sodium tungstate with potassium iodate on mild steel corrosion. *Corrosion Science,* **47(9):** 2213-2224.

Silva, A. B. Agostinho, S. M. l., Barcia, O. E., Cordeiro, G. G. O. and D'Elia, E. (2006). The effect of cysteine on the corrosion of 304L stainless steel in sulphuric acid, *Corrosion Science,* **48**:3668–3674.

Singh, A., Singh, V. K. and Quraishi, M. A. (2010). Inhibition effect of environmentally benign Kuchla (Strychnos nuxvomica) seed extract on corrosion of mild steel in hydrochloric acid solution. *Rasayan Journal of Chemistry*, **3**(4) 811-824

Spah, M., Spah, D. C., Deshwal, B., Lee, S., Chae, Y., Park, J. W. (2009). Thermodynamic studies on corrosion inhibition of aqueous solutions of amino/carboxylic acids toward copper by EMF measurement. *Corrosion Science*, **51**:1293–1298.

Tavassoli-Salardini, P. (2004). Inhibition of corrosion of mild steel in aqueous solution. Ph.D. Thesis. University of Sydney.

Umoren, S. A. and Ebenso, E. E. (2007). The synergistic effect of polyacrylamide and iodided ions on the corrosion of mild steel in H_2SO_4. *Materials Chemistry and Physics*, **106:** 387-393.

Umoren, S. A. and Ebenso, E. E. (2008). Studies of anti-corrosive effect of Raphia hockeri exudates gum-halide mixtures for aluminium corrosion in acidic medium. *Pigment and Resin Technol*ogy, **37(3):**173-182.

Umoren, S. A., Ebenso, E. E., Okafor, P. C., Ekpe, U. J. and Ogbobe, O. (2006a). Effect of halides on the corrosion inhibition of mild steel in alkaline medium using polyvinyl alcohol. *Journal of Applied Polymer Science*, **103:** 2810-2816.

Umoren, S. A., Ogbobe, O., Ebenso, E. E., and Ekpe, U. J. (2006b). Effect of halides on the corrosion inhibition of mild steel in acidic medium using polyvinyl alcohol. *Pigment & Resin Technology,* **35(5):** 284-292.

Umoren, S. A., Obot, I. B. and Ebenso, E. E. (2008a). Corrosion inhibition of aluminium using exudate gum from Pacchylobus edulis in the presence of halide ions in HCl. *Electronic Journal of Chemistry,* **5(2):**355-364.

Umoren, S. A., Ogbobe, O., Igwe, I. E. and Ebenso, E. E. (2008b). Inhibition of mild steel corrosion in acidic medium using synthetic and naturally occurring polymers and synergistic halide additives. *Corrosion Science doi:* 10.1016/j.

Umoren, S. A., Obot, I. B. and Igwe, I. O. (2009). Synergistic inhibition between polyvinylpyrollidone and iodide ions on corrosion of aluminium in HCl. *The Open Corrosion Journal*, **2:** 1-7.

Upadhyay, S. K., Tehlan, S. and Mathur, P. (2007). Synthesis, Spectral and oxidase studies of a new diamide copper(II) complex with pendant benzimidazolyl groups. *Spectrochimica Acta part A*, **66:** 347-352.

Uwah, I. E., Ugi, B. U., Okafor, P. C. and Ikeuba, A. I. (2013). Comparative study of the corrosion inhibition and adsorption characteristics of ethanol extracts of *Andrographis paniculata*(King bitters) and *Vernonia amygdalina* (Bitter leaf) on Mild steel in HCl solution. *International Journal of Applied Chemistry*, **9** (1): 73 – 88

Van, A. C. and Orden, A. C. (1998). Applications and problem solving using the polarization technique, Corrosion, Paper No. 301, NACE International, Houston, TX.

Villamil, R. F. V., Corio, P., Agostinho, S. M. L. and Rubim, J. C. (1999). Effect of sodium dodecylsulphate on copper corrosion in sulphuric acid media in the absence and presence of benzotriazole. *Journal of Electroanalytical Chemistry,* **472(2):** 112-119.

Xia, S., Qiu, M., Yu, L., Liu, F. and Zhao, H. (2008). Molecular dynamics and density functional theory study of relationship between structure of imidazoline derivatives and inhibition performance. *Corrosion Science,* **50:** 2021-2029.

Yurt, A. Bereket, G. and Ogretir, C. (2005). Quantum chemical studies on inhibition effect of amino acids and hydroxy carboxylic acids on pitting corrosion of aluminium alloy 7075 in NaCl solution, *Journal of Molecular Structure*: THEOCHEM **725**: 215–221.

Zafer, U., Nazlı, B., ElÇin, T., Ömer, K., İhsan, Y., and Süheyla, K. (2007). Flavonoid glycosides and methylinositol from Ebenus haussknechtii. *Natural Product Reserved.* **20(11):**999 –1007.

Zerfaoui, M. Ouddac, H. Hammouti, B. Kertit, S. and Benkaddourb, M. (2004). Inhibition of corrosion of iron in citric acid media by amino acids, *Progress in Organic Coatings*, **51**:134–138.

Zhang, D. Cai, Q., He, X., Gao, L. and Zhou, G. (2008). Inhibition effect of some amino acids on copper corrosion in HCl solution, *Materials Chemistry and Physics*. **112**:353–358.

Zuchi, F. and Omar, I.H. (1985). Plant extracts as corrosion inhibitors of mild steel in HCl solution. *Surface Technology,* **24(4):**391-399.

Zuchi, F., Trabanelli, G. and Gullari, G. (1978). Inhibitory action of some organic sulphides. *Electrochemica Material,* **34:**407-419.

APPENDICES

Appendix I: Adsorption Isotherm Parameters Obtained from the Corrosion Data of Mild Steel in 1.0 M HCl Containing Various Concentration of Inhibitors

Isotherm	Inhibitor	333K					323K				
		intercept	Slope	R^2	ΔG ($kJmol^{-1}$)		intercept	Slope	R^2	ΔG ($kJmol^{-1}$)	
	PP	0.28	-0.129	0.078	-9.34		0.225	-0.01	0.035	-9.40	
Langmuir	**PA**	0.369	0.386	0.697	-8.77		0.313	0.459	0.775	-8.85	
	BS	0.441	0.289	0.537	-8.31		-0.111	-0.062	0.044	-11.47	
	PP1	-0.051	0.614	0.998	-11.45		-0.103	0.368	0.988	-11.42	
	PP	-0.28	1.129	0.865	-9.34		-0.225	1.01	0.996	-9.40	
Freundlich	**PA**	-0.369	0.613	0.853	-8.77		-0.313	0.54	0.827	-8.88	
	BS	-0.441	0.71	0.875	-8.31		0.111	1.062	0.93	-11.47	
	PP1	-0.062	0.604	0.998	-10.73	a	-0.099	0.353	0.98	-10.18	a
	PP	0.314	0.295	0.86	-17.88	-3.90	0.371	0.333	0.928	-17.71	-3.46
Temkin	**PA**	0.362	0.276	0.782	-19.47	-4.17	0.43	0.311	0.724	-19.32	-3.70
	BS	0.259	0.187	0.93	-19.98	-6.16	0.727	0.629	0.972	-17.96	-1.83
	PP1	0.141	0.15	0.898	-17.12	-7.68	0.587	0.453	0.999	-18.77	2.54
	PP	-0.471	-1.695	0.345	-8.12		-0.24	-0.096	0.095	-9.30	
Florry-Huggin	**PA**	-0.02	1.239	0.221	-10.99		0.092	1.084	0.218	-11.36	
	BS	-0.112	2.237	0.296	-10.41		0.047	-0.132	0.036	-11.08	
	PP1	-1.633	24.89	0.764	-0.71		0.206	0.863	0.77	-12.06	

Appendix II: Adsorption Parameters Obtained from the Corrosion Data of Mild Steel in 1.0 M HCl Containing Various Concentrations of Inhibitors

Isotherm	Inhibitor	313K					303K				
		Intercept	Slope	R^2	ΔG ($kJmol^{-1}$)		intercept	Slope	R^2	ΔG ($kJmol^{-1}$)	
	PP	-0.046	0.12	0.112	-10.73		0.019	0.8	0.999	-10.01	
Langmuir	**PA**	0.373	0.701	0.948	-8.22		0.263	0.626	0.958	-8.59	
	BS	-0.145	0.107	0.136	-11.32		0.032	0.823	0.999	-9.93	
	PP1	0	0.363	0.996	-10.45		0.06	0.329	0.996	-9.77	
	PP	0.046	0.879	0.87	-10.73		-0.019	0.199	0.995	-10.01	
Freundlich	**PA**	-0.373	0.298	0.769	-8.22		0.033	0.475	0.996	-10.31	
	BS	0.145	0.892	0.916	-11.32		-0.032	0.176	0.993	-9.93	
	PP1	-0.051	0.355	0.998	-10.15	a	-0.033	0.323	0.99	-9.93	a
	PP	0.787	0.682	0.862	-17.41	-1.69	0.926	0.326	0.99	-25.67	-3.53
Temkin	**PA**	0.407	0.203	0.704	-22.44	-5.67	0.798	0.5	0.992	-20.39	-3.8
	BS	0.885	0.71	0.981	-17.95	-1.62	0.902	0.287	0.998	-17.37	-1.59
	PP1	0.809	0.437	0.943	-21.54	-2.64	0.819	0.413	0.967	-21.61	-2.79
	PP	0.116	-0.003	0.023	-11.15		1.309	1.439	0.947	-17.71	
Flory-Huggin	**PA**	0.504	3.134	0.452	-13.47		0.647	1.173	0.966	-13.87	
	BS	0.265	0.192	0.129	-12.04		1.525	1.819	0.995	-18.97	
	PP1	0.826	1.4	0.86	-15.40		0.94	1.553	0.929	-15.57	

Appendix III: Adsorption Isotherm Parameters Obtained from the Corrosion Data of Mild Steel in 0.5 M H_2SO_4 Containing Various Concentration of Inhibitors

Isotherm	Inhibitor	333K					323K				
		intercept	Slope	R^2	ΔG ($kJmol^{-1}$)		intercept	Slope	R^2	ΔG ($kJmol^{-1}$)	
	PP	0.247	-0.182	0.481	-9.55		0.344	0.204	0.761	-8.66	
Langmuir	PA	0.418	0.418	0.775	-8.46		0.297	0.656	0.992	-8.95	
	BS	0.539	0.463	0.898	-7.68		0.267	0.325	0.768	-9.14	
	PP1	-0.385	-2.823	0.813	-13.58		0.065	0.095	0.299	-10.39	
	PP	-0.247	1.182	0.975	-9.55		-0.344	0.795	0.979	-8.66	
Freundlich	PA	-0.418	0.581	0.869	-8.46		-0.297	0.344	0.972	-8.95	
	BS	-0.539	0.536	0.922	-7.68		-0.267	0.675	0.934	-9.14	
	PP1	0.385	3.823	0.888	-13.58	a	-0.065	0.904	0.974	-10.39	a
	PP	0.312	0.294	0.928	-17.88	-3.92	0.33	0.273	0.924	-18.27	-4.22
Temkin	PA	0.326	0.24	0.818	-19.79	-4.80	0.459	0.233	0.99	-22.91	-4.92
	BS	0.248	0.173	0.871	-20.24	-6.66	0.418	0.315	0.918	-19.01	-3.66
	PP1	0.108	0.116	0.907	-17.05	-9.93	0.555	0.462	0.992	-18.21	-2.49
	PP	-0.444	-1.345	0.623	-8.29		-0.133	1.103	0.497	-9.97	
Flory-Huggin	PA	0.001	1.939	0.346	-11.13		0.846	4.446	0.976	-16.02	
	BS	0.006	3.925	0.586	-11.16		0.091	1.429	0.5	-11.35	
	PP1	-2.048	-42.79	0.574	-11.94		0.048	0.382	0.361	-11.08	

Appendix IV: Adsorption Isotherm Parameters Obtained from the Corrosion Data of Mild Steel in 0.5 M H_2SO_4 Containing Various Concentration of Inhibitors

Isotherm	Inhibitor	313K					303K				
		intercept	Slope	R^2	ΔG ($kJmol^{-1}$)		intercept	Slope	R^2	ΔG ($kJmol^{-1}$)	
	PP	0.034	0.162	0.175	-10.25		0.005	0.738	0.992	-10.09	
Langmuir	**PA**	0.336	0.784	0.997	-8.44		0.126	0.577	0.992	-9.39	
	BS	-0.083	0.078	0.233	-10.91		-0.0035	0.587	0.999	-10.32	
	PP1	0.092	0.606	0.994	-9.90		0.078	0.659	0.995	-9.67	
	PP	-0.034	0.837	0.849	-10.25		-0.005	0.266	0.945	-10.09	
Freundlich	**PA**	-0.336	0.215	0.973	-8.44		0.126	0.577	0.992	-9.39	
	BS	0.083	0.921	0.976	-10.91		0.035	0.412	0.998	-10.32	
	PP1	-0.092	0.393	0.986	-9.90	a	-0.078	0.34	0.982	-9.67	a
	PP	0.673	0.572	0.852	-17.47	-2.01	0.929	0.395	0.967	-23.81	-2.92
Temkin	**PA**	0.445	0.168	0.954	-26.34	-6.85	0.664	0.392	0.973	-19.98	-2.94
	BS	0.773	0.648	0.99	-17.59	-1.78	0.964	0.556	0.996	-20.16	-2.07
	PP1	0.722	0.402	0.996	-21.18	-2.86	0.764	0.389	0.991	-21.49	-2.96
	PP	0.073	0.065	0.04	-10.89		1.171	1.384	0.976	-16.91	
Flory-Huggin	**PA**	1.343	6.564	0.92	-18.50		0.68	1.842	0.925	-14.06	
	BS	0.175	0.2	0.317	-11.50		0.783	0.854	0.966	-14.66	
	PP1	0.807	1.831	0.989	-15.29		0.938	1.838	0.976	-15.56	

Appendix V: Adsorption Isotherm Parameters Obtained from the Corrosion Data of Aluminium in 1.0 M HCl Containing Various Concentration of Inhibitors

Isotherm	Inhibitor	333K					323K				
		Intercept	Slope	R^2	ΔG (kJmol^{-1})		Intercept	Slope	R^2	ΔG (kJmol^{-1})	
	PP	0.321	0.735	0.951	-9.07		0.269	0.693	0.982	-9.12	
Langmuir	PA	0.319	0.748	0.996	-9.09		0.327	0.815	0.998	-8.77	
	BS	0.504	0.62	0.983	-7.91		0.322	0.906	0.997	-8.80	
	PP1	0.242	0.963	0.986	-9.58		0.113	0.597	0.967	-10.09	
	PP	-0.321	0.264	0.718	-9.07		-0.269	0.306	0.915	-9.12	
Freundlich	PA	-0.319	0.251	0.967	-9.09		-0.327	0.184	0.971	-8.77	
	BS	-0.079	0.689	0.951	-10.62		-0.127	0.498	0.824	-10.00	
	PP1	0.01	0.865	0.914	-11.19	a	-0.084	0.505	0.926	-10.27	a
	PP	0.462	0.209	0.66	-25.21	-5.51	0.508	0.251	0.865	-23.28	-4.59
Temkin	PA	0.455	0.188	0.973	-26.55	-6.13	0.458	0.151	0.967	-29.59	-7.63
	BS	0.28	0.151	0.965	-22.98	-7.63	0.473	0.09	0.755	-12.86	-12.79
	PP1	0.383	0.346	0.845	-18.2	-3.33	0.442	0.229	0.968	-22.72	-5.03
	PP	0.602	2.71	0.411	-14.96		0.757	3.151	0.724	-15.47	
Florry	PA	1.207	5.89	0.953	-18.82		1.669	7.558	0.947	-21.11	
	BS	0.536	7.303	0.909	-14.54		2.458	9.485	0.688	-25.99	
	PP1	-0.287	0.653	0.99	-9.29		0.769	4.357	0.928	-15.54	

Appendix VI: Adsorption Isotherm Parameters Obtained from the Corrosion Data of Aluminium in 1.0M HCl Containing Various Concentration of Inhibitors

Isotherm	Inhibitor	313K					303K				
		Intercept	Slope	R^2	ΔG (kJmol^{-1})		Intercept	Slope	R^2	ΔG (kJmol^{-1})	
Langmuir	**PP**	0.08	0.621	0.997	-9.97		0.101	0.893	0.999	-9.53	
	PA	0.201	0.88	0.998	-8.24		0.114	0.875	0.998	-9.46	
	BS	0.259	0.86	0.997	-8.9		0.139	0.953	0.999	-9.31	
	PP1	0.188	0.553	0.978	-9.34		0.192	0.454	0.95	-9.01	
Freundlich	**PP**	-0.08	0.378	0.993	-9.97		-0.101	0.107	0.986	-9.53	
	PA	-0.201	0.119	0.911	-8.24		0.033	0.524	0.997	-10.31	
	BS	-0.159	0.384	0.591	-9.5		-0.15	0.334	0.415	-9.25	
	PP1	-0.083	0.429	0.839	-9.96	a	-0.095	0.322	0.723	-9.57	a
Temkin	**PP**	0.749	0.409	0.998	-21.42	-2.82	0.746	0.125	0.951	-36.23	-6.94
	PA	0.621	0.145	0.896	-36.1	-7.94	0.756	0.18	0.954	-34.49	-6.4
	BS	0.543	0.146	0.906	-32.75	-7.89	0.723	0.072	0.962	-68.37	-15.99
	PP1	0.744	0.19	0.98	-33.95	-6.06	0.747	0.173	0.938	-35.18	-6.66
Florry	**PP**	0.845	1.762	0.995	-15.52		2.357	3.803	0.964	-23.79	
	PA	2.189	5.6	0.846	-23.57		2.212	3.941	0.955	-22.95	
	BS	1.96	6.426	0.858	-22.2		5.164	9.551	0.963	-40.08	
	PP1	2.029	3.751	0.959	-22.61		2.123	3.804	0.904	-22.44	

Appendix VII: Frequencies and Peaks of IR Adsorption by *Boscia senegalensis* and the Corrosion Product of Mild Steel in HCl

BS-Steel in HCl					
Plant Sample				**Corrosion Product**	
Frequency of IR	**Area**	**Assignment**	**Frequency of IR**	**Area**	**Assignment**
808.20	41.03	C-H‘oop’ Aromatic	799.52	84.56	C-H‘oop’ Aromatic
1065.71	188.11	C-O Stretch	1179.51	178.54	C-O Stretch
1265.35	70.67	C-N Stretch (amide)	-	-	-
1442.80	135.26	C-C stretch (in ring)	1428.34	179.19	C-C stretch (in ring)
1627.97	85.42	N-H Bend	1624.12	180.40	N-H Bend
1705.13	76.222	C=O Stretch	-	-	-
2930.93	413.89	O-H Stretch	2526.83	73.90	O-H Stretch
3422.80	663.28	O-H Stretch	3404.47	905.91	O-H Stretch

Appendix VIII: Frequencies and Peaks of IR Adsorption by *Phyllanthus amarus* and the Corrosion Product of Mild Steel in HCl

PA-Steel in HCl					
Plant Sample				**Corrosion Product**	
Frequency of IR	**Area**	**Assignment**	**Frequency of IR**	**Area**	**Assignment**
759.01	55.71	=C-H Bend	853.53	53.64	=C-H Bend
1050.28	199.48	C-O Stretch	1091.75	91.33	C-O Stretch
1210.37	94.66	C-O Stretch	1209.41	49.57	C-O Stretch
1441.84	89.52	C-C stretch (in ring)	1442.8	98.72	C-C stretch (in ring)
1616.40	71.77	N-H bend	1613.51	164.17	N-H bend
1721.53	125.97	C=O Stretch	-	-	-
2934.79	790.05	O-H Stretch	-	-	-
3416.05	624.96	O-H Stretch	3414.12	881.09	O-H Stretch

Appendix IX: Frequencies and Peaks of IR Adsorption by *Paulina pinnata* and the Corrosion Product of Mild Steel in HCl

PP-Steel in HCl					
Plant Sample				**Corrosion Product**	
Frequency of IR	**Area**	**Assignment**	**Frequency of IR**	**Area**	**Assignment**
823.63	91.55	C-H'oop'	841.96	67.08	CH'oop'
1078.24	172.98	C-O Stretch	1034.84	58.42	C-O Stretch
1286.56	49.46	C-N Stretch	1264.38	53.47	C-N Stretch
1621.22	162.67	N-H bend	1605.79	143.38	N-H bend
2619.42	226.15	O-H stretch	1454.38	70.91	C-H bend
2786.27	82.92	O-H stretch	-	-	-
2890.43	94.37	O-H stretch	-	-	-
3008.09	64.80	O-H stretch	-	-	-
3132.50	45.99	O-H stretch	-	-	-
3238.59	124.09	O-H stretch	-	-	-
3426.66	68.82	O-H stretch	3405.44	729.05	O-H stretch

Appendix X: Frequencies and Peaks of IR Adsorption by *Boscia senegalensis* and the Corrosion Product of Aluminium in HCl

BS-Al in HCl					
Plant Sample				**Corrosion Product**	
Frequency of IR	**Area**	**Assignment**	**Frequency of IR**	**Area**	**Assignment**
808.20	41.035	C-H 'oop' Aromatic	-	-	-
1065.71	188.1167	C-O Stretch	1105.25	268.53	C-O Stretch
1265.35	70.6734	C-N Stretch (amide)	-	-	-
1442.80	135.2602	C-C stretch (in ring)	-	-	-
1627.97	85.4204	N-H Bend	1637.62	311.37	N-H Bend
1705.13	76.2227	C=O Stretch	-	-	-
2930.93	413.8916	O-H Stretch	3392.90	824.07	O-H Stretch
3422.80	663.2868	O-H Stretch	3737.20	48.65	O-H Stretch

Appendix XI: Frequencies and Peaks of IR Adsorption by *Phyllanthus amarus* and the Corrosion Product of Aluminium in HCl

PA-Al in HCl					
Plant Sample				**Corrosion Product**	
Frequency of IR	**Area**	**Assignment**	**Frequency of IR**	**Area**	**Assignment**
759.01	55.71	=C-H Bend	789.88	45.67	=C-H Bend
1050.28	199.48	C-O Stretch	1114.89	264.66	C-O Stretch
1210.37	94.66	C-O Stretch	-	-	-
1441.84	89.52	C-C stretch (in ring)	-	-	-
1616.40	71.77	N-H bend	1641.48	331.588	N-H bend
1721.53	125.97	C=O Stretch	-	-	-
2934.79	790.05	O-H Stretch	-	-	-
3416.05	624.96	O-H Stretch	3429.55	919.494	O-H Stretch

Appendix XII: Frequencies and Peaks of IR Adsorption by *Paulina pinnata* and the Corrosion Product of Aluminium in HCl

PP – Al in HCl					
Plant Sample				**Corrosion Product**	
Frequency of IR	**Area**	**Assignment**	**Frequency of IR**	**Area**	**Assignment**
823.63	91.55	C-H'oop'	806.27	97.91	C-H'oop'
1078.24	172.98	C-O Stretch	-	-	-
1286.56	49.46	C-N Stretch	1138.04	156.74	C-N Stretch
1621.22	162.67	N-H bend	1641.48	293.07	N-H bend
2619.42	226.15	O-H stretch	-	-	-
2786.27	82.92	O-H stretch	-	-	-
2890.43	94.37	O-H stretch	-	-	-
3008.09	64.80	O-H stretch	-	-	-
3132.50	45.99	O-H stretch	-	-	-
3238.59	124.09	O-H stretch	-	-	-
3426.66	68.82	O-H stretch	3421.81	922.85	O-H stretch

Appendix XIII: Frequencies and Peaks of IR Adsorption by *Boscia senegalensis* and the Corrosion Product of Aluminium in H_2SO_4

BS-Al in H_2SO_4					
Plant Sample				**Corrosion Product**	
Frequency of IR	**Area**	**Assignment**	**Frequency of IR**	**Area**	**Assignment**
808.20	41.04	C-H 'oop' Aromatic	868	65.192	C-H 'oop' Aromat
1065.71	188.12	C-O Stretch	1111.03	214.52	C-O Stretch
1265.35	70.67	C-N Stretch (amide)	-	-	-
1442.80	135.26	C-C stretch (in ring)	1427.37	114.64	C-C stretch ring
1627.97	85.42	N-H Bend	-	-	-
1705.13	76.22	C=O Stretch	-	-	-
3422.80	663.29	O-H Stretch	3492.24	97.85	O-H Stretch
			3245.34	84.56	O-H Stretch
			3353.36	78.58	O-H Stretch
			3145.04	58.86	O-H Stretch

Appendix XIV: Frequencies and Peaks of IR Adsorption by *Phyllanthus amarus* and the Corrosion Product of Aluminium in H_2SO_4

PA-Al in H_2SO_4					
Plant Sample				**Corrosion Product**	
Frequency of IR	**Area**	**Assignment**	**Frequency of IR**	**Area**	**Assignment**
759.01	55.71	=C-H Bend	704.04	163.23	=C-H Bend
1050.28	199.48	C-O Stretch	1126.47	270.05	C-O Stretch
1210.37	94.66	C-O Stretch	-	-	-
1441.84	89.52	C-C stretch (in ring)	1445.7	102.62	C-C stretch (in ring)
1616.40	71.77	N-H bend	1625.08	167.13	N-H bend
1721.53	125.97	C=O Stretch	-	-	-
2934.79	790.05	O-H Stretch	2580.84	103.26	O-H Stretch
3416.05	624.96	O-H Stretch	3475.84	140.82	O-H Stretch

Appendix XV: Frequencies and Peaks of IR Adsorption by *Paulina pinnata* and the Corrosion Product of Aluminium in H_2SO_4

PP-Al in H_2SO_4					
Plant Sample				**Corrosion Product**	
Frequency of IR	**Area**	**Assignment**	**Frequency of IR**	**Area**	**Assignment**
823.63	91.55	C-H'oop'	-	-	-
1078.24	172.98	C-O Stretch	1112.00	327.94	C-O Stretch
1286.56	49.46	C-N Stretch (amide)	-	-	-
1621.22	162.67	N-H bend	1629.9	327.44	N-H bend
2619.42	226.15	O-H stretch	-	-	-
2786.27	82.92	O-H stretch	-	-	-
2890.43	94.37	O-H stretch	-	-	-
3008.09	64.80	O-H stretch	-	-	-
3132.50	45.99	O-H stretch	-	-	-
3238.59	124.09	O-H stretch	-	-	-
3426.66	68.82	O-H stretch	3462.34	1020.13	O-H stretch